Laboratory Medicine

May 2024 Vol 55 No 3 Pgs 251–394

labmedicine.com

Laboratory Medicine (ISSN 0007-5027), is published 6 times per year (bimonthly). Periodicals Postage paid at Chicago, IL and additional mailing offices. POSTMASTER: Send address changes to *Laboratory Medicine*, Journals Customer Service Department, Oxford University Press, 2001 Evans Road, Cary, NC 27513-2009.

SUBSCRIPTION INFORMATION: Annually for North America, $182 (electronic) or $241 (electronic and print); single issues for individuals are $32 and for institutions $71. Annually for Rest of World, £118/€167 (electronic) or £154/€220 (electronic and print); single issues for individuals are £21/€30 and for institutions £44/€63. All inquiries about subscriptions should be sent to Journals Customer Service Department, Oxford Journals, Great Clarendon Street, Oxford OX2 6DP, UK, Tel: +44 (0) 1865-35-3907, e-mail: jnls.cust.serv@oup.com. In the Americas, please contact Journals Customer Service Department, Oxford Journals, 4000 CentreGreen Way, Suite 310, Cary, NC 27513, USA. Tel: 800-852-7323 (toll-free in USA/Canada) or 919-677-0977, e-mail: jnlorders@oup.com.

MEMBERSHIP INFORMATION: The ASCP membership fees for pathologists are as follows: fellow membership is $399; fellow membership plus 1-year unlimited online CE is $529; 2-year fellow membership is $749; and 2-year fellow membership plus 2-year unlimited online CE is $1009. The ASCP membership fees for laboratory professionals are as follows: young professional membership is $59; annual membership is $119; annual membership plus 1-year unlimited online CE is $158; 3-year membership is $389. All inquiries about membership should be sent to American Society for Clinical Pathology, 33 West Monroe Street, Suite 1600, Chicago, IL 60603, Tel: 312-541-4999, e-mail: ascp@ascp.org.

CLAIMS: Publisher must be notified of claims within four months of dispatch/ order date (whichever is later). Subscriptions in the EEC may be subject to European VAT. Claims should be made to Laboratory Medicine, Journals Customer Service Department, Oxford University Press, 4000 CentreGreen Way, Suite 310, Cary, NC 27513, USA, Tel: 800-852-7323 (toll-free in USA/Canada) or 919-677-0977, e-mail: jnlorders@oup.com.

Laboratory Medicine is published bimonthly by Oxford University Press (OUP), on behalf of the ASCP, a not-for-profit corporation organized exclusively for educational, scientific, and charitable purposes. Devoted to the continuing education of laboratory professionals, *Laboratory Medicine* features articles on the scientific, technical, managerial, and educational aspects ofthe clinical laboratory. Publication of an article, column, or other item does not constitute an endorsement by the ASCP of the thoughts expressed or the techniques, organizations, or products described therein. *Laboratory Medicine* is indexed in the following: MEDLINE/PubMed, Science Citation Index, Current Contents—Clinical Medicine, and the Cumulative Index to Nursing and Allied Health Literature.

Printed in the USA

ASCP
Laboratory Medicine
33 West Monroe Street, Suite 1600
Chicago, IL 60603
T: 312-541-4999
F: 312-541-4750

Laboratory Medicine

May 2024
Vol 55, No 3
Pgs 251-394

OVERVIEW

SPECIAL REPORT

SCIENCE

CASE STUDY

CORRECTION

ON THE COVER: Four articles in this issue of *Laboratory Medicine* focus on ways the clinical laboratory influences the treatment of pregnant patients. Mohideen and colleagues compared the results of thyroid function tests in fasting and nonfasting pregnant patients, finding that postprandial thyroid-stimulating hormone results were lower compared to fasting results. Tang et al established trimester-specific reference intervals for homocysteine and suggested a correlation of biomarker levels with pregnancy complications and perinatal outcomes. Yang and coworkers examined the frequencies of false-positive results in 3 commercially available syphilis serology screening tests in pregnant and nonpregnant women, finding that false-positive rates were low but significantly different across the 3 methods. Finally, dos Santos and colleagues compared the efficiencies of 3 methods for processing umbilical cord blood for storage. These 4 studies illustrate the importance of clinical laboratories in the health care of pregnant patients.

OVERVIEW

Trend towards reduction of transfusion reactions using prestorage leukocyte-reduced and pooled whole blood–derived platelets and cost savings compared with poststorage whole blood–derived random platelets as evidenced by real-time hemovigilance

Nick Park, MD,[1] Mayrin Correa Medina, MD, PhD,[1] Fernando Martinez, MD, MScPH,[1] Marla Throssel, MS,[1] Amitava Dasgupta, PhD,[2] Adriana Knopfelmacher, MD,[1] Colleen Villamin, MSN,[1] Sandra Rivas, MS,[1] Nancy Tomczak, BSN,[1] Saahith Garg,[3] Lorraine Layton, MSN,[1] Kimberly Klein, MD[1]

[1]Department of Laboratory Medicine, The University of Texas MD Anderson Cancer Center, Houston, TX, US; [2]Department of Pathology and Laboratory Medicine University of Kansas Medical Center, Kansas City, KS, US; [3]Department of Biochemistry, University of Texas Health Science Center at Houston, Houston, TX, US. Corresponding author: Kimberly Klein; KKlein@mdanderson.org

Key words: acrodose; platelets; transfusion reaction; hemovigilance; oncology patients; prestorage

Abbreviations: WBD, whole blood–derived; RDP, conventionally produced poststorage WBD platelets; FNHTR, febrile nonhemolytic transfusion reactions; TACO, transfusion-associated circulatory overload; HVU, hemovigilance unit; EHR, electronic health record; NHSN, National Healthcare Safely Network; APP, advanced practice provider

Laboratory Medicine 2024;55:251-254; https://doi.org/10.1093/labmed/lmad106

ABSTRACT

Background: Due to chemotherapy-induced neutropenia or hematologic malignancies, immunocompromised cancer patients may have higher incidence of febrile nonhemolytic transfusion reactions compared with the general population and frequently require platelet transfusions. This quality improvement project compared the safety of transfusion using prestorage leukocyte-reduced and pooled whole blood–derived platelets (Acrodose/WBD) with conventionally produced poststorage WBD platelets (RDP) using an active hemovigilance system.

Methods: Every patient receiving a blood product at the hospital was virtually monitored in real time by trained nurses from a remote hemovigilance unit. These nurses monitor a digital dashboard, which populates a watch list of patients from the time blood product administration is initiated until 12 hours posttransfusion. Over the course of 6 months, 371 patients receiving 792 RDP transfusions and 423 patients receiving 780 Acrodose/WBD platelets transfusions were monitored for transfusion reactions.

Results: We identified 26 transfusion reactions in RDP but only 12 transfusion reactions in the Acrodose/WBD platelet group.

Conclusion: Acrodose platelet transfusion was associated with fewer transfusion reactions, which resulted in significant cost savings.

Introduction

Platelet transfusion is sometimes incorporated in routine blood transfusion strategies in different clinical settings, including stopping bleeding or prophylactic strategy to prevent bleeding during a procedure. Platelet transfusion is useful in severely thrombocytopenic patients receiving chemotherapy or undergoing surgery or invasive exploration. Despite published guidelines from national professional societies or other recognized organizations, there is no clinical consensus for platelet transfusion. As a result, protocols not only vary from one nation to another but also between hospitals in the same nation, including the United States.[1] Platelets for the purpose of transfusion can be prepared either by separation of units of platelet concentrates from whole blood using either the buffy coat or the platelet-rich plasma method, which can be pooled before administration, or by apheresis from a single donor. The Pall Acrodose system allows whole blood–derived (WBD) platelets to be pooled safely using a closed system without altering the platelet quality after transfusion.[2] More recently, Terumo announced IMUGARD whole blood, which also allows for WBD platelets to be pooled safely using a closed system and extends the shelf-life of WBD platelets from 5 to 7 days.[3] In routine

circumstances, WBD platelets and apheresis platelets can be used interchangeably, although platelets prepared from pooled whole blood are more cost-effective.[4]

Cancer patients undergoing chemotherapy or stem cell transplant frequently require platelet transfusions to prevent bleeding complications related to hypoproliferative thrombocytopenia. There are updated guidelines that provide evidence-based recommendations about preparation of platelet products and transfusion thresholds for patients with cancer.[4] Benefits from the leukoreduction of platelet products include prevention of refractoriness from human leukocyte antigen alloimmunization, reduction of cytomegalovirus transmission, and decreased incidence of transfusion reactions.[5-7] More specifically, prestorage leukoreduction of platelets has been shown to decrease the rate of febrile nonhemolytic transfusion reactions (FNHTRs),[8] allergic reactions,[9] and cardiopulmonary complications such as transfusion-associated circulatory overload (TACO).[10] In the opinion of Bianchi et al,[11] leukoreduction significantly improves the safety of transfusion.

Estimates of transfusion reactions vary, but active hemovigilance systems have consistently demonstrated higher rates of transfusion reactions compared with passive systems.[12] To enhance patient safety at the institution, real-time hemovigilance was implemented to monitor every patient receiving a blood transfusion.[13] The purpose of this retrospective study is to report the incidence and types of transfusion reactions seen in cancer patients receiving prestorage vs poststorage WBD platelets while being monitored by a real-time hemovigilance program.

Methods

The quality improvement project was conducted at the University of Texas MD Anderson Cancer Center located in Houston, TX, US. The MD Anderson Cancer Center is a 678-bed hospital and ambulatory care center that exclusively treats adult and pediatric cancer patients. Our cancer center dispenses over 34,000 platelet transfusions annually. This project was approved by the Quality Improvement Advisory Board and Institutional Review Board of the MD Anderson Cancer Center.

Platelet Components

Prestorage leukocyte-reduced pooled WBD platelets (Acrodose, Haemonetics) were produced and supplied by Carter Blood Care. Acrodose platelets were pooled from 5 WBD platelet concentrates and became available to the institution in March 2021. We pooled poststorage leukocyte-reduced WBD platelets (RDP) in the hospital blood bank prior to release and leukocyte-reduced at bedside using the PXL8 filter (Haemonetics). Blood shortages necessitated pooling WBD RDP from 4 WBD platelet concentrates to maintain a stable inventory. Three WBD RDP platelet concentrates (low dose) were pooled for RDP for certain circumstances: patient age (<18 years), patient weight (<50 kg), or during periods of critical platelet shortages (**TABLE 1**). All platelet products transfused at our institution received Cesium[137] irradiation to eliminate the possibility of transfusion-associated graft-vs-host disease, a risk for the immunocompromised population.

TABLE 1. Blood product characteristics

	Prestorage leukocyte-reduced	Units of pooled WBD platelet per dose	Filter required
Random donor platelet	No	3 or 4	Yes
Acrodose/WBD	Yes	5	No

WBD, whole blood–derived.

Patients and Clinical Data

All patients receiving a blood product at MD Anderson Cancer Center are virtually monitored by trained nurses from a remote hemovigilance unit (HVU) as described previously.[13] Briefly, HVU nurses monitor a digital dashboard that populates a watch list of patients from the time of initiation of transfusion until 12 hours posttransfusion. An algorithm integrated with the electronic health record (EHR) analyzes various data elements to calculate a transfusion reaction risk score based on criteria from the National Healthcare Safety Network (NHSN) Hemovigilance Module.[14] When a patient is suspected of having a transfusion reaction, HVU nurses communicate with the nurse administering the transfusion and frequently deploy a transfusion medicine advanced practice provider (APP). The APPs are available around the clock and are specially trained to recognize and manage transfusion reactions. The APPs perform patient bedside evaluations, order pertinent laboratory testing, and medically manage the patient's symptoms in collaboration with the patient's primary care team. Additionally, the APP serves a regulatory function, as they are responsible for documenting applicable clinical information related to each suspected transfusion reaction in the EHR and perform a bedside clerical check.

Evaluation of Transfusion Reactions

A transfusion medicine physician evaluates transfusion reaction reports within 24 hours of the event as per protocol. Following guidelines from the NHSN Hemovigilance Module, each transfusion reaction is classified according to the reaction-specific case definition, severity, and imputability or designated as unrelated to the transfusion. Laboratory evaluation of transfusion reactions includes a clerical check, visual inspection for hemolysis, and direct antiglobulin test on a posttransfusion blood specimen. Bacterial cultures from the platelet bag or segment are obtained when available, except for cases presenting with localized cutaneous allergic symptoms.

Statistical Analysis

The Fisher exact test and χ^2 tests were performed to compare the rates of transfusion reactions between Acrodose/WBD products and RDP. The reaction rate for each platelet product was calculated as [the number of transfusion reactions classified by transfusion medicine physician] divided by [number of transfusions] × 100.

Results

Between March 2021 and August 2021 (6 months), 371 patients received 792 RDP transfusions and 423 patients received 780 Acrodose/WBD transfusions. The average volume of transfusion was 199 mL for RDP compared with 260 mL for the Acrodose/WBC group. Most patients were treated for leukemia: 78.7% in the RDP group and 74.8% in the Acrodose group (**TABLE 2**). Acute myeloid leukemia was the major diagnosis of patients in both groups (48.5% in the RDP group and 40.0% in the Acrodose/WBD group).

Transfusion Reaction Incidence

The transfusion medicine attending physician, using NHSN criteria, identified 26 transfusion reactions in the RDP group: 15 FNHTRs, 6 allergic, and 5 TACO (**TABLE 3**). The incidence rates for each type of reaction to RDP were 1.89% (FNHTR), 0.76% (allergic), and 0.63% (TACO). In contrast, only 12 transfusion reactions occurred in the Acrodose/WBD group: 6 FNHTRs, 2 allergic, and 4 TACO. The incidence rates of reactions to Acrodose/WBD platelets were 0.77% (FNHTR), 0.26% (allergic), and 0.51% (TACO). No other type of transfusion reaction was observed in our patient population following transfusion.

TABLE 2. Patient diagnoses

Diagnosis	RDP	Acrodose/WBD
Leukemia		
B-cell acute lymphoblastic	33	40
T-cell acute lymphoblastic	9	16
Acute myeloblastic	180	169
Myelodysplastiic syndrome	28	40
Myelofibrosis	10	13
Multiple myeloma	17	18
Chronic lymphocytic	5	5
Chronic myelogenous	6	5
Other	4	6
Total	292	312
Lymphoma		
Hodgkin's	10	10
Non-Hodgkin's	36	41
T-cell	12	12
Burkitt	0	1
Diffuse large B-cell	15	17
Mantle cell	4	6
Other	5	5
Total	46	51
Solid tumor	25	47
Aplastic anemia	3	7
Hemophagocytic lymphohistiocytosis	0	3
Miscellaneous	5	3
Total	371	423

RDP, conventionally produced poststorage WBD platelets; WBD, whole blood–derived.

The overall rate of FNHTR and allergic reactions in cancer patients who received RDP was 2.65% (21/792). In comparison, the overall rate of FNHTR and allergic reactions in the Acrodose/WBD group was lower at 1.03% (8/780). Using the χ^2 test, we found the incidence of FNHTR was significantly lower in the Acrodose/WBD group than in the RDP group at the 95% confidence interval ($\chi^2 = 3.772$, $P = .026$ [one-tailed]). Results of the Fisher exact test indicated differences were also significant at the 95% confidence level ($P = .0412$) using a one-tailed test. Although allergic reactions tended to be lower in Acrodose/WBD group, the differences were not statistically significant using the Fisher exact test. However, the χ^2 value was 1.949 ($P = .0813$), which was significant only at the 90% confidence interval using a one-tailed test. The rate of TACO was similar between the RDP (0.63%) and Acrodose/WBD (0.51%) groups.

Discussion

To our knowledge, there is no published report that compares platelet transfusion safety using RDP and AcrodoseWBD groups. Dalal et al[15] compared clinical utility but not safety of platelet transfusion using platelets obtained by apheresis and Acrodose/WBD platelets. The authors concluded that Acrodose/WBD platelets induced a more robust response and increased the time to next transfusion compared with single donor platelets among all patients, including acute leukemia patients. Unfortunately, that same effect was absent in bone marrow transplant patients (**TABLE 4**).

Our study, to our knowledge, is the first quality improvement project in oncology patients comparing platelet transfusion safety using RDP and Acrodose/WBD groups. This project demonstrates that both types of platelet transfusions were relatively safe; however, prestorage leukocyte-reduced WBD platelets tend to have a lower incidence of FNHTR and allergic transfusion reactions than poststorage leukocyte-reduced random donor platelets in an oncologic cohort when using real-time hemovigilance. Although no difference was detected in cardiopulmonary complications between the RDP and Acrodose/WBD groups, any potential benefit of prestorage leukocyte reduction may have been offset by larger transfused volumes (260 vs 199 mL) in those patients receiving Acrodose/WBD platelets, as we have previously demonstrated the mean volume of blood components before a TACO event in our institution was 626.6 mL.[16] Prior exposure to anthracycline chemotherapy resulting in cardiotoxicity, especially for patients with relapsed or refractory acute myeloblastic leukemia, may also be a factor.

Although the project did not include a detailed cost analysis, preliminary assessment indicates that each FNHTR incidence costs roughly

TABLE 3. Transfusion reactions

Reaction type	RDP	Acrodose	Fisher exact test *P* value	χ^2 test *P* value
FNHTR	15	6	$P = .0412$, one tailed (significant at 95% confidence interval)	$P = .026$, one tailed (significant to 95% confidence interval)
Allergic reaction	6	2	$P = .149$, not significant	$P = .081$, significant only at 90% confidence interval, one tailed
TACO	5	4	Not different	Not different
TRALI	0	0	Not applicable	Not applicable
Total transfusions	792	780	Not applicable	Not applicable
Average volume (mL)	199	260		

FNHTR, febrile nonhemolytic transfusion reactions; TACO, transfusion-associated circulatory overload; TRALI, transfusion-related acute lung injury.

TABLE 4. Transfusion effectiveness in AML patients

	RDP	Acrodose/WBD
Patients	57	53
Transfusions	90	67
Transfusion mCCI ≥ 5000	57	39
Percentage of mCCI ≥ 5000	63	58
Average CCI	9246	7167
Median CCI	8023	5760
Median TTNT (days)	2.03	2.02

AML, acute myeloblastic leukemia; CCI, Charlson comorbidity index; RDP, conventionally produced poststorage whole blood–derived platelets; TTNT, time to next transfusion; WBD, whole blood–derived.

$3000. This approximated cost stems from the observed additional personnel expenditures; unnecessary diagnostic and laboratory testing, replacement blood cost, and unnecessary outpatient admissions. The lower Charlson comorbidity index for Acrodose/WBD was not factored into cost, as the time to next transfusion was not affected. Thus, we surmise that an Acrodose/WBD transfusion may be more cost-effective than conventional RDP. Project findings revealed only 6 FNHTRs in the Acrodose/WBD group, costing the hospital roughly $18,000. In contrast, RDP resulted in 15 incidences, costing the hospital $45,000. Clinicians at the institution perform approximately 34,000 platelet transfusions annually and switching from RDP to Acrodose/WBD should be associated with substantial cost savings. However, more data and detailed cost analysis are needed to confirm this.

Conclusion

This quality improvement project, based on 371 patients receiving 792 RDP transfusions and 423 patients receiving 780 Acrodose/WBD transfusions, indicates that Acrodose/WBD transfusions were associated with fewer adverse effects than RDP transfusions. Increased use of Acrodose/WBD platelets has the potential to improve transfusion safety, enhance patient experience, and provide cost savings.

Conflict of Interest Disclosure

The authors have nothing to disclose.

REFERENCES

1. Capraru A, Jalowiec KA, Medri C, Daskalakis M, Zeerleder SS, Mansouri Taleghani B. Platelet transfusion—insights from current practice to future development. *J Clin Med.* 2021;10(9):1990. doi:10.3390/jcm10091990
2. Sawant RB, Marathe AN. Pooled platelet product using the Acrodose plus system: evaluation of feasibility, safety and efficacy. *Transfus Apher Sci.* 2013;49(3):535-538. doi:10.1016/j.transci.2013.09.001
3. US Department of Health and Human Services Food and Drug Administration Center for Biologics Evaluation and Research. Bacterial Risk Control Strategies for Blood Collection Establishments and Transfusion Services to Enhance the Safety and Availability of Platelets for Transfusion. 2020. Accessed October 15, 2023. https://www.fda.gov/regulatory-information/search-fda-guidance-documents/bacterial-risk-control-strategies-blood-collection-establishments-and-transfusion-services-enhance
4. Schiffer CA, Bohlke K, Delaney M, et al. Platelet transfusion for patients with cancer: American Society of Clinical Oncology clinical practice guideline update. *J Clin Oncol.* 2018;36(3):283-299. doi:10.1200/JCO.2017.76.1734
5. Bowden RA, Slichter SJ, Sayers M, et al. A comparison of filtered leukocyte-reduced and cytomegalovirus (CMV) seronegative blood products for the prevention of transfusion associated CMV infection after marrow transplant. *Blood.* 1995;86(9):3598-3603. doi:10.1182/blood.V86.9.3598.bloodjournal8693598
6. Heddle NM, Blajchman MA, Meyer RM, et al. A randomized controlled trial comparing the frequency of acute reactions to plasma-removed platelets and prestorage WBC-reduced platelets. *Transfusion.* 2002;42(5):556-566. doi:10.1046/j.1537-2995.2002.00094.x
7. Bilgin YM, van de Watering LM, Brand A. Clinical effects of leukoreduction of blood transfusions. *Neth J Med.* 2011;69(10):441-450.
8. Paglino JC, Pomper GJ, Fisch GS, Champion MH, Snyder EL. Reduction of febrile but not allergic reactions to RBCs and platelets after conversion to universal prestorage leukoreduction. *Transfusion.* 2004;44(1):16-24. doi:10.1046/j.0041-1132.2004.00608.x
9. Chien S-H, Tsai Y-C, Lu S-H, Chen Y-J, Chen W-C, Liu C-Y. A comparison of transfusion reactions between prestorage and postage leukoreduced apheresis platelets: a propensity-score matching analysis. *Hemasphere*. 2023;7(S3):e43622b3-e4363077. doi:10.1097/01.hs9.0000973204.43622.b3
10. Blumberg N, Heal JM, Gettings KF, et al. An association between decreased cardiopulmonary complications (transfusion-related acute lung injury and transfusion-associated circulatory overload) and implementation of universal leukoreduction of blood transfusions. *Transfusion.* 2010;50(12):2738-2744. doi:10.1111/j.1537-2995.2010.02748.x
11. Bianchi M, Vaglio S, Pupella S, et al. Leucoreduction of blood components: an effective way to increase blood safety? *Blood Transfus*. 2016;14(3):214-227. doi:10.2450/2015.0154-15
12. Hendrickson JE, Roubinian NH, Chowdhury D, et al.; National Heart, Lung, and Blood Institute (NHLBI) Recipient Epidemiology and Donor Evaluation Study (REDS-III). Incidence of transfusion reactions: a multicenter study utilizing systematic active surveillance and expert adjudication. *Transfusion.* 2016;56(10):2587-2596. doi:10.1111/trf.13730
13. Villamin C, Bates T, Mescher B, et al. Digitally enabled hemovigilance allows real time response to transfusion reactions. *Transfusion.* 2022;62(5):1010-1018. doi:10.1111/trf.16882
14. NHSN Network Biovigilance Component Hemovigilance Module Surveillance Protocol v2.8: Division of Healthcare Quality Promotion National Center for Emerging and Zoonotic Infectious Diseases Centers for Disease Control and Prevention. 2009. Accessed June 2022. https://www.cdc.gov/nhsn/pdfs/biovigilance/bv-hv-protocol-current.pdf.
15. Dalal N, Cheema N, Klein LM. Single donor versus Acrodose platelets in oncology patients: a single institutional experience. *Blood.* 2014;124(21):4298-4298. doi:10.1182/blood.v124.21.4298.4298
16. Maldonado M, Villamin CE, Murphy LE, et al. Oncology patients who develop transfusion-associated circulatory overload: an observational study. *Lab Med*. 2022;53(4):344-348. doi:10.1093/labmed/lmab119

SCIENCE

Evaluating direct amplification from viral transport medium for SARS-CoV-2 detection, strain typing, and angiotensin-converting enzyme genotyping and expression assays

Kala F. Schilter, PhD,[1] Shivani Kapoor, MS,[1] Brandon A. Smith, BA,[1] Ayofemi Saleem, BS,[1] Samantha J. Scott, MS, MB(ASCP),[1] Dana Batchelor, BS,[1] Kathryn A. Stoll, HT(ASCP),[1] Qian Nie, PhD,[1] Honey V. Reddi, PhD, FACMG[1]

[1]Precision Medicine Laboratory, Department of Pathology and Laboratory Medicine, Medical College of Wisconsin, Milwaukee, WI, US. Corresponding author: Honey V, Reddi, PhD, FACMG; hreddi@mcw.edu

Key words: direct amplification; PCR; next-generation sequencing; gene expression

Abbreviations: ACE, angiotensin-converting enzyme; PCR, polymerase chain reaction; NAAT, nucleic acid amplification test; VTM, viral transport medium; TNA, total nucleic acid; cDNA, complementary DNA; NGS, next-generation sequencing

Laboratory Medicine 2024;55:267-270; https://doi.org/10.1093/labmed/lmad075

ABSTRACT

Objective: The aim of this study was to compare the performance of direct amplification of viral nucleic acid from transport medium to extracted nucleic acid for polymerase chain reaction (PCR), sequencing, and genotyping applications.

Methods: XpressAmp lysate and extracted total nucleic acid from viral transport medium containing nasopharyngeal specimens were evaluated across different molecular applications to determine performance characteristics.

Results: SARS-CoV-2 quantitative PCR and angiotensin-converting enzyme (*ACE*) genotyping assays worked well with XpressAmp lysate, almost equal with or better than extracted nucleic acid in some specimens. However, XpressAmp completely failed to perform in next-generation sequencing for strain typing. Both protocols failed to detect *ACE2* expression in viral transport medium.

Conclusion: Direct amplification of viral nucleic acid from viral transport medium containing nasopharyngeal specimen works well for molecular assays with low thresholds of quality; however, it does have limitations with assays that require high quality nucleic acid for input. Use of the XpressAmp protocol significantly improves turnaround time and allows for easy ramp-up of PCR and genotyping assays.

The COVID-19 pandemic stimulated the need to develop high-throughput, fast-turnaround assays for the detection and strain typing of the SARS-CoV-2 virus in human specimens. Additionally, research on correlatives was being carried out to address the variations observed globally in terms of susceptibility to SARS-CoV-2 infection across ethnicity, sex, and age. Studies were being done to evaluate expression of the angiotensin-converting enzyme 2 (*ACE2*), which is believed to be the host receptor for SARS-CoV-2 infection.[1,2] Additionally, the ACE that shares 42% of amino acid identity with ACE2[3] and characterized by a genetic deletion/insertion polymorphism in intron 16 was shown to be in involved in the modulation of *ACE2* expression levels, particularly the D allele of *ACE* being associated with reduced expression of *ACE2*.[4] The literature also suggests that the deletion/insertion polymorphism shows an important geographical variation across ethnicities,[5] which when reviewed in the context of differences in global prevalence of COVID-19 infection,[2] indicates the potential for *ACE* to serve as a confounder for COVID-19.[4]

Studies in our laboratory focused on establishing molecular tests addressing the various correlates associated with virus infection: a nucleic acid amplification test (NAAT) for detection of SARS-CoV-2, next-generation sequencing (NGS) for strain typing, and genotyping for *ACE* polymorphisms and evaluation of *ACE2* expression in nasopharyngeal and anterior nasal specimens collected in viral transport medium (VTM). Extraction methods were validated for DNA and RNA isolation from VTM for downstream molecular testing. With a goal to reduce turnaround time for result reporting, we also evaluated a direct amplification kit (XpressAmp, Promega) on nasopharyngeal specimens for molecular testing. This report outlines the results from our comparative study and demonstrates the strengths and limitations of direct amplification for specific molecular applications.

Materials and Methods

SARS-CoV-2 positive and negative specimens from symptomatic and asymptomatic individuals received for routine testing were processed in 2 ways. One method involved directly subjecting VTM containing nasopharyngeal/anterior nasal swabs to processing using the XpressAmp Direct Amplification Reagents kit (Promega) according to manufacturer's instructions. The other method required extracting total nucleic acid (TNA) using established procedures (Kingfisher, Thermo Fisher Scientific) for performance evaluation in multiple assays such as SARS-CoV-2 NAAT, *ACE* genotyping PCR,[6] *ACE2* gene expression, and SARS-CoV-2 strain typing (**TABLE 1**)

For the XpressAmp procedure, briefly, prior to any downstream molecular procedure, Direct Amp Lysis Buffer was prepared with 1% 1-thioglycerol by adding 1 µL of 1-thioglycerol for every 100 µL of Direct Amp Lysis Buffer required. Each VTM sample was combined with the prepared Direct Amp Lysis Buffer in a 1:1 ratio based on how much input lysate was needed downstream. Sample lysates were mixed and incubated at room temperature for 10 minutes. Different volumes of the final lysates (4 µL for NAAT, 3 µL for *ACE* genotyping, 2 to 5 µL for *ACE2* gene expression; 8 µL lysate was reverse transcribed and 5 µL of the complementary DNA [cDNA] product was used for strain typing) were then used for the evaluation of performance in various established downstream applications, as listed in **FIGURE 1A**.

Total nucleic acid was extracted from 200 µL of VTM using the Kingfisher MagMax Viral/Pathogen Isolation Kit (Part #A48310, Thermo Fisher Scientific) into an elution volume of 50 µL. Different volumes of extracted TNA were used for downstream processing: 5 µL for NAAT, 2 to 3 µL for *ACE* genotyping, 2 to 5 µL for *ACE2* gene expression; 8 µL lysate was reverse transcribed and 5 µL of the cDNA product was used for strain typing.

Data from both processes were analyzed and compared to determine performance characteristics, including accuracy, efficiency and hands-on time. This study was done over a period of time, as assay needs arose, and therefore, different specimen cohorts were used for evaluating the performance of XpressAmp vs extracted TNA for downstream processes. This study was performed as part of a process improvement initiative and approved by the Medical College of Wisconsin Institutional Review Board (PRO38057).

Results

The XpressAmp direct lysis protocol was successful for SARS-CoV-2 amplification across the 35 specimens tested (N1 Cq range 26.34-41.61, N2 Cq range 23.56-43.18), in most cases performing equivalent to or better than extracted total nucleic acid (N1 Cq range 25.1-35.58, N2 Cq range 25.11-38.28) (**FIGURE 1B**), with 100% accuracy. Genotyping for *ACE* polymorphisms was extremely effective, with the XpressAmp kit producing high-quality data in all 30 initial specimens tested with 100% accuracy (**FIGURE 1C**), resulting in the analytical validation and incorporation of this protocol for clinical use, with subsequent testing of ~300 specimens (**FIGURE 1A**).

When evaluated for the detection of *ACE2* expression levels in VTM, both the XpressAmp and extracted nucleic acid specimens failed to perform as expected, suggesting a limitation of the specimen type, as the nasopharyngeal collection would not contain the same concentration of nucleic acid as blood samples. Because neither extraction method worked (**FIGURE 1A**), this test was later developed using blood as a specimen type (data not provided).

Strain typing for SARS-CoV-2 includes a 2-step process, a NAAT assay, based on the results of which only specimens with a Cq of <30 are sequenced for clade assignment using the ARTIC protocol (https://artic.network/ncov-2019). The Cq cut-off was based on initial studies that showed RNA extracted from specimens with a Cq >30 failed to sequence, with the ideal Cq range being 18-28 (data not provided). Using this cut-off, 8 of the 15 samples with NAAT results in the range of 25-30 Cq were processed for strain typing. Despite passing library preparation quality control, all 8 samples failed in read depth, coverage, lineage, and clade identification when compared with the same specimens with extracted nucleic acid that successfully passed analysis and enabled clade designation. This result indicated the presence of potential inhibitors in the XpressAmp lysate or that sequencing for strain typing required high-quality nucleic acid. Another point of consideration could be that the XpressAmp kit was designed for 1-step RT-quantitative PCR and not a 2-step process as that required for strain typing. **TABLE 1** summarizes the comparative performance of both methods evaluated.

TABLE 1. Summary of assays evaluated and performance of the two extraction methods

Assay	Primer/probes used		Vendor (part No.)	XpressAmp	Extracted TNA
SARS-CoV-2 NAAT	CDC approved	2019-nCoV EUA Kit, 500 rxn primers/probe set	IDT (10006606)	Yes	Yes
ACE genotyping	Forward primer	5′-CTG GAG ACC ACT CCC ATC CTT TCT-3′	IDT[6]	Yes	Yes
	Reverse primer	5′-GAT GTG GCC ATC ACA TTC GTC AGA T-3′	IDT[6]		
ACE2 expression	ACE2, exons 14-15 probe	5′-/56-FAM/ ACTCCAGTC/ZEN/ GGTACTCCATCCCA/31ABkFQ/-3′	IDT (Hs.PT.58.27645939)	No	No
	ACE2, exons 14-15 primer	5′-GCCACTGCTCAACTACmG-3′			
	ACE2, exons 14-15 primer	5′-GCTTATCCTCACTTTGATGCmG-3′			
	Internal control HPRT1 probe	5′-/56-FAM/AGCCTAAGA/ZEN/ TGAGAGTTCAAGTTGAGTTTGG/31ABkFQ/-3′	IDT (Hs.PT.58v.45621572)		
	HPRT1, exons 8-9 primer	5′-TTGTTGTAGGATATGCCCTTGA-3′			
	HPRT1, exons 8-9 primer	5′-GCGATGTCAATAGGACTCCAG-3′			
SARS-CoV-2 strain typing	Artic protocol	https://artic.network/ncov-2019	IDT (10011442)	No	Yes

NAAT, nucleic acid amplification test; TNA, total nucleic acid.

FIGURE 1. **A, Schematic of study design. The total number of specimens used to evaluate each downstream methodology after XpressAmp or TNA extraction are listed above each process; the number of specimens listed in green next to specific evaluation methods indicate the number of specimens processed post evaluation for methods that worked successfully; the red X indicates methods where the XpressAmp or TNA extraction did not work, the green check mark indicates that extracted methods worked for associated processes but were not used subsequently due to performance limitations or lack of efficiency or throughput. B, Representative snapshots of SARS-CoV-2 detection using XpressAmp and extracted nucleic acid for 2 different specimens. C, Representative gel picture of the expected *ACE* genotyping results using XpressAmp. ACE, angiotensin-converting enzyme; NAAT, nucleic acid amplification test; NGS, next-generation sequencing; RT-PCR, reverse transcription-polymerase chain reaction; VTM, viral transport medium.**

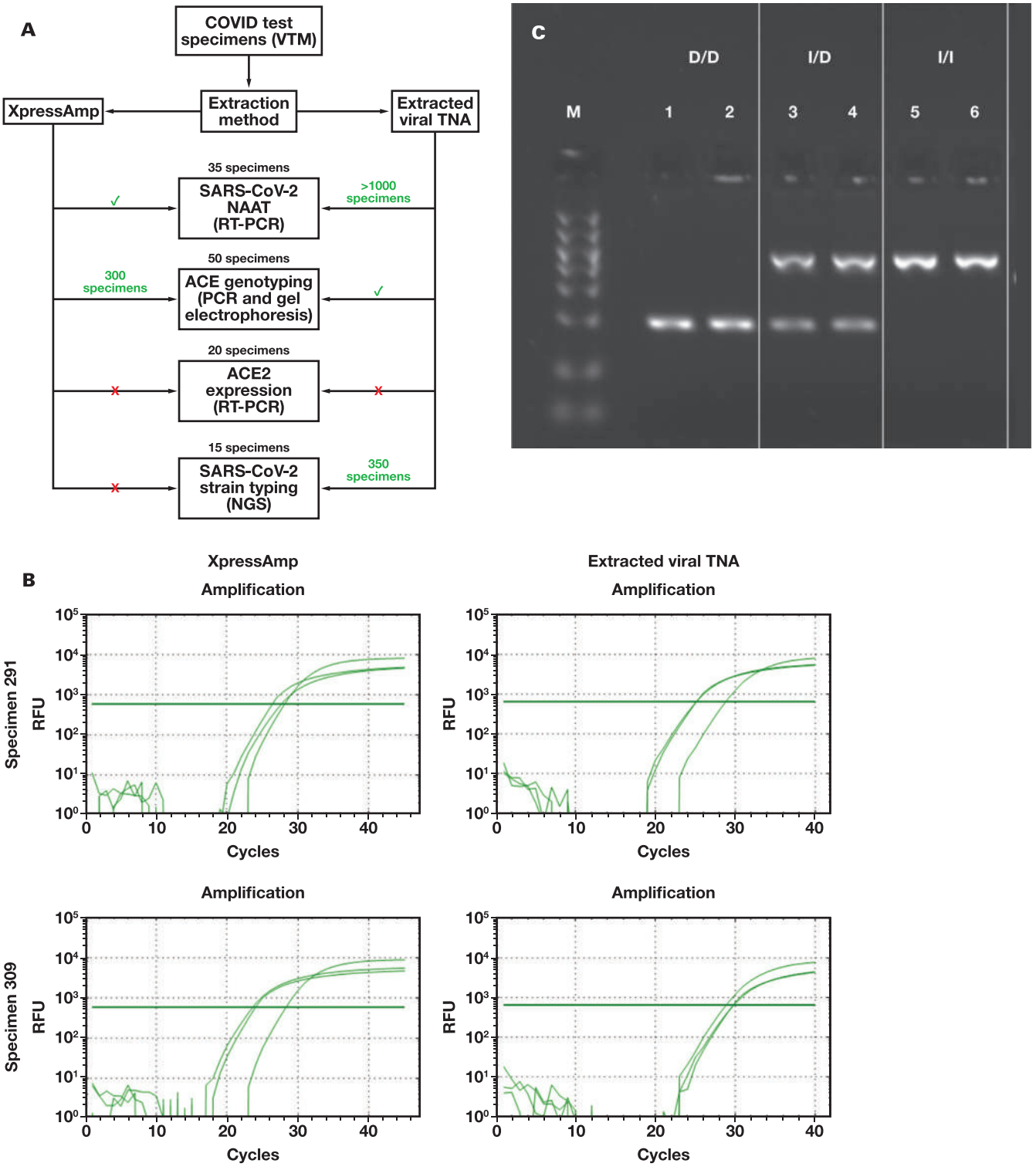

Discussion

There are always challenges in direct PCR amplification, with both sample and lysis buffer components affecting the reaction efficiency and sensitivity. The Direct Amp Lysis Buffer used in our assay worked well for SARS-CoV-2 amplification across all 35 specimens tested with 100% accuracy, although the PCR products failed to sequence for strain typing and clade assignment, suggesting that quality of the nucleic acid generated by the kit was not high enough for an NGS-based test. Optimal and high-quality amplification of the *ACE* polymorphisms further demonstrated the applicability of this protocol for PCR-based applications such as genotyping. The failure of the XpressAmp kit to detect expression of ACE2 in VTM must be evaluated in the context of comparability with our established protocol using nucleic acid extracted from VTM. Use of high-quality RNA from VTM also failed to amplify with the ACE2 expression protocol, suggesting that the failure of XpressAmp was not due to an inherent limitation but rather due to the limitation of the specimen type used. Although RNA extracted from blood worked well with our ACE2 expression PCR assay, we could not evaluate the performance of the XpressAmp on blood as it was developed primarily for use with VTM.

In conclusion, this study demonstrates the successful use of the XpressAmp kit for direct evaluation of nasopharyngeal and anterior nasal specimens in TM for SARS-CoV-2 detection and *ACE* genotyping, suggesting that this protocol specimen works well for molecular assays with targeted amplification and less stringent thresholds of nucleic acid quality. The XpressAmp kit demonstrated some limitations with assays that require high-quality nucleic acid for input and broader more sensitive detection, such as gene expression assays and NGS. Use of the XpressAmp protocol does significantly improve turnaround time and allows for easy ramp-up of PCR and genotyping assays.

Conflict of Interest Disclosure

The authors have nothing to disclose.

REFERENCES

1. Hu B, Guo H, Zhou P, Shi ZL. Characteristics of SARS-CoV-2 and COVID-19. *Nat Rev Microbiol.* 2021;19(3):141-154. doi:10.1038/s41579-020-00459-7
2. Kuba K, Imai Y, Penninger JM. Angiotensin-converting enzyme 2 in lung diseases. *Curr Opin Pharmacol.* 2006;6(3):271-276. doi:10.1016/j.coph.2006.03.001
3. Donoghue M, Hsieh F, Baronas E, et al. A novel angiotensin-converting enzyme-related carboxypeptidase (ACE2) converts angiotensin I to angiotensin 1-9. *Circ Res.* 2000;87(5):E1-E9. doi:10.1161/01.res.87.5.e1
4. Delanghe JR, Speeckaert MM, De Buyzere ML. The host's angiotensin-converting enzyme polymorphism may explain epidemiological findings in COVID-19 infections. *Clin Chim Acta.* 2020;505:192-193. doi:10.1016/j.cca.2020.03.031
5. Saab YB, Gard PR, Overall AD. The geographic distribution of the ACE II genotype: a novel finding. *Genet Res.* 2007;89(4):259-267. doi:10.1017/S0016672307009019
6. Yoshida H, Mitarai T, Kawamura T, et al. Role of the deletion of polymorphism of the angiotensin converting enzyme gene in the progression and therapeutic responsiveness of IgA nephropathy. *J Clin Invest.* 1995;96(5):2162-2169. doi:10.1172/JCI118270

SPECIAL REPORT

Leading medical laboratory professionals toward change readiness: a correlational study

Taryn L. Waraksa-Deutsch, DHSc, SCT(ASCP)[1,2]

[1]Division of Cytopathology, Fox Chase Cancer Center, Philadelphia, PA, US; [2]Department of Health Science, Bay Path University, Longmeadow, MA, US. Corresponding author: Taryn L. Waraksa-Deutsch; taryn.waraksa@fccc.edu

Key words: laboratory medicine; leadership; change readiness; continuous improvement

Abbreviations: MLQ, Multifactor Leadership Questionnaire; TCM, 3-component model; TL, transformational leadership; CTC, commitment to change; H, hypothesis; ACC, affective commitment to change; CCC, continuance commitment to change; NCC, normative commitment to change; PAB, passive-avoidant behavior; LF, laissez-faire leadership; MBE-P, management by exception-passive; MBE-A, MBE-active; CR, contingent reward; II, idealized influence; IC, individualized consideration; IM, inspirational motivation; IS, intellectual stimulation; ASCP, American Society for Clinical Pathology; ASC, American Society of Cytopathology; IIA, II-attributed; IIB, II-behavior; EE, extra effort; EFF, efficiency; SAT, satisfaction; MANOVA, multivariate analysis of variance

Laboratory Medicine 2024;55:255-266; https://doi.org/10.1093/labmed/lmad091

ABSTRACT

Background: To remain effective in the dynamic health care landscape, the laboratory must embrace the continuous improvement mindset to support a culture of change, and leadership must facilitate the change process, mitigating perceived barriers of change readiness in followers.

Methods: This quantitative study was designed to determine whether there is an association between leadership style (Multifactor Leadership Questionnaire [MLQ]) and change readiness (3-component model [TCM] commitment to change/Employee Commitment Survey, and whether leadership style predicts change readiness. Laboratory professionals (n = 718) were recruited through national societies to complete a combined MLQ-TCM survey instrument. Multivariate analysis of variance, Pearson correlations, and multiple regression analyses were performed.

Results: A significant correlation between leadership style and change readiness (transformational leadership [TL] and affective commitment to change, $r(716) = .12$, $P = .002$; passive-avoidant behavior and continuance commitment to change, $r(716) = .25$, $P < .001$) and between leadership style and leadership outcomes (TL and effectiveness, $r(716) = .90$, $P < .001$) was identified. Transformational leadership was a significant predictor of change readiness ($\beta = .17$, $P < .05$).

Conclusion: It is recommended that laboratory leaders use transformational leadership or situational leadership to improve followers' affective commitment to change and reduce followers' continuance commitment to change, thus improving commitment to continuous improvement. Leaders should also limit passive-avoidant behavior.

Introduction

At the forefront of laboratory research is innovation and technology, whereas the foci of laboratory medicine as a profession includes training, professional development, staffing shortages, and burnout prevention or response. However, leadership within the profession and its impact on process outcomes through continuous improvement has not been proficiently examined. In other occupations, leadership style and methods have been thoroughly examined for their impact on organizational outcomes.[1] As demonstrated by the response to the COVID-19 pandemic, a significant construct of professional preparedness desired in laboratory professionals is change readiness. Change readiness is defined as a measure of confidence that a person, team, or organization is committed, capable, and culturally inclined to embrace a proposed project or initiative that would lead to the desired target of change.[2]

Continuous improvement, as a form of change, is necessary to remain effective and evolve in health care. Antony et al[3] share 3 main barriers to successful continuous improvement projects: resistance to change, lack of leadership support and commitment, and incompetent teams; whereas Erlingsdottir et al[4] suggest that leaders can enable effective continuous improvement implementation by coaching the process, promoting autonomy, and providing the necessary resources. Leadership should help employees understand that a culture of continuous improvement can help reduce errors and avoid personal blame, and by appreciating and adopting the continuous improvement mindset, employees are doing their part for themselves, their organization, and their patients.[5] Leaders must identify and effectively use appropriate change management tools to reduce employee resistance to change and promote readiness and adaptability, yet it is not clear whether leadership styles or methods are associated with change readiness in laboratory medicine.

Purpose of the Study

This correlational study was designed to determine whether there is an association between leadership style as a change management tool and change readiness via commitment to change (CTC) in laboratory medicine, affecting laboratory professionals as both leaders and followers. There are limited data available regarding medical laboratory professionals' perceptions of change and whether resistance and readiness are related to leadership style, communication issues, lack of resources and commitment, or a combination of various factors.[6] Although studies have demonstrated an association between transformational leadership (TL) and continuous improvement initiatives through harnessing CTC across multiple sectors, there is no evidence that this relationship exists in laboratory medicine.

Hypotheses

Two hypotheses were made for this study. Hypothesis 1 (H1) is that there is a significant association between leadership style (defined by the MLQ) and change readiness (measured by the 3-component model [TCM] of CTC/Employee Commitment Survey). Hypothesis 2 (H2) is that leadership style (defined by the MLQ) is a significant predictor of change readiness (measured by the TCM).

Change Readiness via CTC

Weiner's theory of organizational readiness for change posits that 2 collective affective states are related to change readiness: change efficacy and CTC.[7] Herscovitch and Meyer define CTC as an individual's mindset that binds them to the pathway or course of action an organization takes to achieve an improvement or change initiative.[8] The TCM of CTC consists of 3 levels (affective, continuance, and normative commitment to change).[9] Bouckenooghe et al[9] opine that CTC behavior is driven by beliefs, such as inherent benefits or intrinsic motivation to remain with the organization throughout the change process (affective commitment to change, ACC), the risk analysis or perception of costs associated with change (continuance commitment to change, CCC), and a moral obligation or duty to support the change (normative commitment to change, NCC). ACC is most often correlated with positive work performance, mentorship, and reduced burnout; CCC is stress-inducing and depletes energy, leading to employee burnout and turnover; and NCC is influenced by externally-driven CCC and internally-motivated ACC, with higher levels of NCC correlated with increased stress and emotional exhaustion.[9-11]

Full Range of Leadership

Bass' full range leadership model conceptualizes that all leaders exhibit five leadership styles to some extent: laissez-faire leadership (LF), management by exception-passive (MBE-P), management by exception-active (MBE-A), contingent reward (CR), and the four Is of TL. The optimal leadership profile, as posited by Bass and Riggio,[12] features LF as the least-used style and TL as the most frequently displayed style. Passive-avoidant behavior (PAB) is defined by nonaction or passivity where leaders remove themselves from their responsibilities (LF) or only act after a complaint is received (MBE-P), contributing to a blame culture.[1,12,13] Lutz Allen et al[14] determined that LF is negatively associated with building a psychological climate for both change readiness and organizational creativity due to a lack of leadership communication and unwillingness to facilitate an environment of transformational change. Although MBE-P is considered a form of transactional leadership according to Bass and Riggio,[12] the style falls under PAB within leadership measurement instruments for its inaction or passivity.

Transactional leadership focuses on contractual relationships, structured management, formal delegation, and reinforcement systems that revolve around rewards and penalties.[12,15] Perceptions of risk and safety drive commitment to organizational goals, enabling success preventative MBE-A leadership.[12] MBE is a corrective transaction and it is therefore deemed less effective than CR and TL due to a lack of motivation involved.[12,16,17] CR motivates employees by rewarding behavior with social and economic incentives, but transactional leadership may not be able to sustain CTC in long-term continuous improvement initiatives as well as TL due to changes in reward attractiveness.[12,18]

As the theoretical framework driving this study, TL is well recognized and accepted as an effective leadership strategy across the world.[12] TL is known for its adaptability and empowerment, inspiring a shared vision to engage followers in their personal and professional growth while collectively working toward the organization's mission and strategic initiatives.[1] Ledlow and Stephens posit that the most effective transformational leaders in health care use transactional and TL simultaneously as an adaptive style to address the unique needs of their followers and the ongoing changes within the health care system.[1] The effectiveness of TL is based on the impact the leader has on the follower across 4 psychological mechanisms or competencies: idealized influence (II), individualized consideration (IC), inspirational motivation (IM), and intellectual stimulation (IS).[12]

Methods

Participants, Sampling, and Data Collection

During an 8-week period in October and November of 2022, a survey was distributed online via SurveyMonkey to the American Society for Clinical Pathology (ASCP) and the American Society of Cytopathology (ASC) online listservs. All currently employed or retired medical laboratory professionals and pathologists, including supervisors, managers, and midlevel directors, within the United States were eligible for this study due to their relative experience working under some form of higher leadership.[12] All medical laboratory professionals aged 18 years or older of any gender, educational background, length of experience, certification status, laboratory discipline, and setting were eligible to participate. International laboratory professionals who are proficient in written English language and work within the United States were also included in the study to better understand a potential association between leadership style and change readiness within ever-diversifying US health care organizations regardless of ethnicity, race, or nationality and to close the literature gap regarding laboratory medicine leadership in the United States. Membership in professional societies was not a requirement, but sampling procedures actively recruited members of the ASCP and ASC. Medical laboratory students and pathology residents without previous or current employment within a laboratory were excluded. Medical laboratory professionals who do not work in the United States were excluded due to the study's intended understanding of leadership and change readiness in United States health care. Laboratory professionals who are not proficient in the written English language were excluded from the study, as the survey and related study documents were only offered in English. Although unanticipated, all professional or laboratory leaders who did not report to a higher level

of leadership were excluded because the survey instrument used in this study was intended to measure an association between leadership style and subordinate change readiness.

Instrumentation

Two previously validated measures, the MLQ 5X Short and the TCM Employee Commitment Survey, were combined in a 74-item survey and distributed online via SurveyMonkey to measure leadership style and change readiness (see Supplemental Materials). Following the consent statement and demographic questions, the combined MLQ-TCM survey presented statements to which the participant responded based on their degree of frequency or level of agreement/disagreement on a 5-point Likert scale.

Multifactor Leadership Questionnaire

The MLQ 5X Short measures scales of TL, transactional leadership, and PAB in the form of 45-items, with 36 items on leadership style and 9 items on leadership outcomes.[12] The MLQ Rater Form asks subordinates to rate a leader's behavior. As a 9-subscale questionnaire, the MLQ examines 4 subscales associated with the 4 psychologic mechanisms of TL: IC, II (II-attributed [IIA] and II-behavior [IIB]), IM, and IS; 2 facets of transactional leadership: CR and MBE-A; and 2 subscales of PAB or nonleadership styles: MBE-P and LF. The ninth subscale measured the leadership outcomes of efficiency (EFF), extra effort (EE), and satisfaction (SAT). The MLQ has been psychometrically validated across various sectors, making it 1 of the most frequently used leadership questionnaires in research for its internal reliability, convergent validity, and discriminant validity.[12,19,20] The MLQ does not have to remain a stand-alone measure, as the instrument was previously paired with the Implementation Leadership Scale, demonstrating acceptable internal consistency across all subscales, an excellent fit via confirmatory factor analysis, and convergent validity via moderate to high correlations between the MLQ and Implementation Leadership Scale.[19]

TCM of Employee Commitment Survey

The TCM of commitment was originally established by Meyer and Allen in 1991 and later revised in 2004 as an 18-item Employee Commitment Survey with 6 items assessing each of the 3 well-validated subscales or levels of commitment.[21] The TCM survey can be used to measure other foci of commitment, such as CTC, without negatively affecting reliability or validity, which spurred a CTC extension of the TCM.[8] This extension of the revised survey was used in this project to measure an employee's CTC within their organization on 3 levels: ACC, NCC, and CCC. Herscovitch and Meyer[8] determined that the CTC extension of the TCM yielded alpha coefficients of .94, .94, and .86 for ACC, CCC, and NCC, respectively, which is greater than the original TCM with an average internal reliability of .82, .73, and .76 for affective, continuance, and normative commitment to the organization, respectively.

Data Analysis

Data was analyzed via SPSS version 29 for Windows 11. Cronbach's alpha coefficient was performed to determine the internal reliability of the combined MLQ-TCM.[8] The MLQ-TCM responses were scored according to item, subscale, and scale, yielding 9 overarching results for each participant: 3 leadership scores (TL, transactional leadership, and PAB), 3 leadership outcomes (EFF, EE, and SAT), and 3 CTC scores (ACC, CCC, and NCC).[12,21] Response frequencies and percentages for each survey item and the mean and standard deviation for each item and item subscale for the overall study sample were calculated. A 1-way multivariate analysis of variance (MANOVA) was also performed to assess the differences of demographic categorical data on change readiness via CTC scales.

A Pearson product-moment correlation coefficient (Pearson's *r*) was used to assess the strength and direction of potential associations between the scale and subscale averages of both survey elements.[22] The parametric correlation was used to determine the strength and direction between each of the 3 leadership styles (transformational, transactional, and PAB) as independent variables and each of the 3 types of CTC (affective, normative, and continuance) as dependent variables. Because an association was identified between leadership style and change readiness via CTC, a multiple regression analysis was performed to determine which leadership style, if any, is a significant antecedent or predictor of change readiness.[22,23] Analyzing 2-tailed hypotheses, an alpha level of .05 ($P \leq .05$) was deemed statistically significant.[22]

Ethical Approval

This study was approved by a private university's institutional review board on September 23, 2022 (IRB # 2022_Waraksa).

Results

Demographic Characteristics of the Study Sample

On survey closure, 991 individual responses were recorded. A CONSORT diagram was used to depict the flow of participant eligibility (**FIGURE 1**). Twelve recruited participants (1.2%) did not provide consent to participate in the research study and were therefore excluded. Of the 979 laboratory professionals (98.8%) who consented to the study, 5 participants (0.5%) reported that they did not work within or retire from a laboratory within the United States or United States Territories and were excluded. Of those 974 participants (99.5%) who work within or have retired from the United States, 4 participants (0.4%) reported that they are students and were deemed ineligible to participate in the study. A total of 970 eligible participants (99.6%) reported that they are currently employed or retired from a laboratory within the United States, proficient in reading the English language, and 18 years of age or older. Of the 970 eligible participants, 252 laboratory professionals (26.0%) did not respond to any of the MLQ-TCM instrument questions beyond the demographic questions and were consequently excluded from analysis due to an incomplete survey response. Therefore, 718 participants with completed survey responses were included in the analysis as the final study sample size.

Detailed participant demographic characteristics can be found within **TABLE 1**. Of the 718 study participants, most of the sample identified as Caucasian (White) (75.9%), female (78.4%), and between the ages of 30 and 39 (34.0%) or 40 and 49 (25.6%). As for education and work experience, most of the study participants reported that they work full-time (87.5%), have earned either a bachelor's degree (56.4%) or a master's degree (21.4%), have at least 10 years of experience in the laboratory (61.5%), and work in a hospital-based laboratory (77.0%). Additionally, the majority of the participants reported a laboratory discipline of medical laboratory science (MLT/MLS) (62.4%) and a role of technician/technologist (43.9%), lead technician/technologist (17%), or supervisor/manager (20.8%) (**FIGURES 2** and **3**, respectively).

FIGURE 1. CONSORT flow diagram.

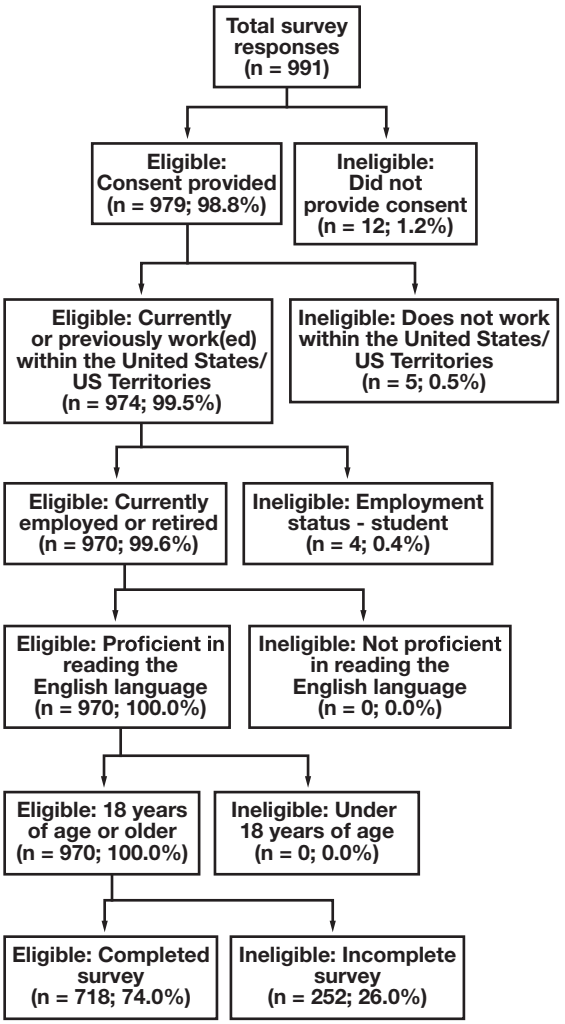

Descriptive Results

Multivariate Analysis of Variance

There was homogeneity of variance-covariance matrices as assessed by Box's test of equality of covariance matrices ($P > .001$) and homogeneity of variance as assessed by Levene's test of homogeneity of variance ($P > .05$). Due to unequal sample sizes between categorical levels, Pillai's trace multivariate statistical findings are presented.[23] The difference between gender identity on the combined change readiness scores was statistically significant, $F(9, 2142) = 4.107$, $P < .001$; Pillai's V = .051; partial $\eta^2 = .021$; and Tukey post hoc tests showed that for ACC, females had higher mean scores than males ($P < .001$), whereas males had higher NCC mean scores than females ($P = .003$). The differences between highest level of education on change readiness were also statistically significant, $F(15, 2136) = 2.579$, $P < .001$; Pillai's V = .053; partial $\eta^2 = .021$; and participants who earned a bachelor's or master's degree had a higher mean score for ACC than those with an associate's degree ($P = .007$ and $P < .001$, respectively). No statistically significant difference was identified between level of education and CCC or NCC mean scores. Differences between laboratory role on change readiness were significant, $F(18, 2133) = 3.024$, $P < .001$; Pillai's V = .075; partial $\eta^2 = .031$; and both laboratory director/administrator and supervisor/manager had significantly higher mean scores for ACC than laboratory assistants ($P = .012$ and $P = .004$, respectively). Supervisor/manager roles also had significantly higher mean ACC scores than technicians/technologists ($P < .01$). Technician/technologists had higher mean CCC scores than supervisor/managers and laboratory directors/administrators ($P < .001$ and $P = .043$, respectively). No significant differences were identified between laboratory role and mean NCC scores.

Results for H1: Correlation

H1 states that there is a significant association between leadership style (defined by the MLQ) and change readiness (measured by the TCM of CTC/Employee Commitment Survey).

$H1_0$ states that there is not a significant association between leadership style (defined by the MLQ) and change readiness (measured by the TCM) of CTC/Employee Commitment Survey).

The Cronbach's alpha coefficient measured .903, indicating a high level of internal consistency for the combined MLQ-TCM instrument within this specific sample.[23] Pearson product-moment correlations examined potential associations between overall leadership style scales, detailed leadership style subscales, leadership outcomes, and the 3 CTC scales (ACC, CCC, and NCC) (**TABLE 2**).

Leadership Style Subscale by Leadership Style Scale Correlation

MLQ scale intercorrelations demonstrate significant strong correlations both within subscales and across broad scales. IIA is not only significantly and strong positively correlated with all other TL subscales; that is, IIA and IC ($r[716] = .88$, $P < .001$), but with the overall TL scale as well ($r[716] = .94$, $P < .001$). The TL subscales have moderate to strong positive correlations with overall transactional leadership. For example, IIA is strongly and positively correlated with transactional leadership, $r(716) = .70$, $P < .001$. All transformational and transactional leadership subscales, except MBE-A, have significant strongly negative correlations with PAB. An example of this case is IIA and PAB, $r(716) = -.75$, $P < .001$. Despite CR falling under the category of transactional leadership, the association is stronger under TL than transactional leadership, $r(716) = .90$, $P < .001$ and $r(716) = .80$, $P < .001$, respectively. Both subscales of PAB have significant and strongly positive correlations with PAB and strong negative associations with TL. For example, MBE-P and PAB ($r[716] = .96$, $P < .001$) and LF and TL ($r[716] = -.76$, $P < .001$). Both subscales are moderately and negatively associated with transactional leadership.

Leadership Style by Outcomes Correlation

The overall TL average and transformational subscales are strongly and positively associated with the 3 leadership outcomes of EE, EFF, and SAT. All TL subscales are strongly and positively associated with the 3 leadership outcomes. For example, IIA is strongly and positively correlated with all leadership outcomes: EE, $r(716) = .84$, $P < .001$; EFF, $r(716) = .89$, $P < .001$; and SAT, $r(716) = .89$, $P < .001$. The overall transactional leadership average and CR subscale are strongly and positively associated with the 3 leadership outcomes; however, no statistically significant correlation was identified between MBE-A and leadership outcomes. Both PAB and its 2 subscales, MBE-P and LF, are moderate-strongly and negatively correlated with the 3 leadership outcomes.

TABLE 1. Demographic characteristics of survey sample

Characteristic	No. (%)	Characteristic	No. (%)
Gender		Laboratory discipline	
Female	563 (78.4)	Cytology (CT/SCT)	43 (6.0)
Male	144 (20.1)	Medical Laboratory Science (MLT/MLS)	448 (62.4)
Nonbinary	2 (0.3)	Phlebotomy (PBT)	37 (5.2)
Prefer not to answer	9 (1.3)	Molecular Biology (MB/SMB)	18 (2.5)
Age, y		Cytogenetics (CG)	28 (3.9)
18-29	103 (14.3)	Microbiology (M/SM)	14 (1.9)
30-39	244 (34.0)	Surgical Pathology/Histology (PA/HTL/HT)	33 (4.6)
40-49	184 (25.6)	Blood Banking/Chemistry/Hematology	28 (3.9)
50-59	105 (14.6)	Pathologist/Professor/ Researcher	45 (6.3)
60+	74 (10.3)	Other (including multiple disciplines)	24 (3.3)
Prefer not to answer	8 (1.1)	Laboratory role	
Ethnicity		Laboratory Assistant	23 (3.2)
Caucasian (White)	545 (75.9)	Technician/Technologist	315 (43.9)
African-American	39 (5.4)	Technician/Technologist—Lead	122 (17.0)
Latino or Hispanic	26 (3.6)	Supervisor/Manager	149 (20.8)
Asian	43 (6.0)	Laboratory Director/Administrator	41 (5.7)
Native American	3 (0.4)	Pathologist	35 (4.9)
Native Hawaiian/Pacific Islander	2 (0.3)	Other (PA, LIS, Quality, Education, etc)	33 (4.6)
Other/unknown/prefer not to say	25 (3.5)	Experience, y	
Multiple reported ethnicities	35 (4.9)	<1	16 (2.2)
Employment		1-3	80 (11.1)
Full-time	628 (87.5)	4-9	180 (25.1)
Part-time	40 (5.6)	10-19	243 (33.8)
Per diem	34 (4.7)	20+	199 (27.7)
Retired	16 (2.2)	Laboratory type	
Education		Independent private or reference	71 (9.9)
High school diploma	16 (2.2)	Hospital-based	553 (77.0)
Associate's degree	76 (10.6)	Clinical outpatient	37 (5.2)
Bachelor's degree	405 (56.4)	Research/Public health	17 (2.4)
Master's degree	154 (21.4)	Academic facility	38 (5.3)
Doctoral degree	63 (8.8)		
Prefer not to say	4 (0.6)		

Leadership Style by Change Readiness Correlation

A significant weak positive correlation was identified between TL and ACC, $r(716) = .12$, $P = .002$; and a significant moderate negative correlation was identified between TL and CCC, $r(716) = -.28$, $P < .001$. All TL subscales (IIA, IIB, IM, IS, and IC) were also positively associated with ACC and negatively associated with CCC. A significant yet minimal positive correlation was identified between transactional leadership and ACC, $r(716) = .07$, $P = .050$; and a significant weak negative correlation was identified between transactional leadership and CCC, $r(716) = -.14$, $P < .001$. Significant correlations were identified for both transactional leadership subscales CR and MBE-A. A significant weak positive correlation was identified between CR and ACC, $r(716) = .11$, $P = .004$, and a significant moderate negative correlation was identified between CR and CCC, $r(716) = -.30$, $P < .001$. MBE-A differed from the remainder of the leadership subscales in that a significant albeit weak positive correlation was identified in NCC, $r(716) = .08$, $P = .027$. Between MBE-A and CCC, a significant weak positive correlation was identified, $r(716) = .14$, $P < .001$. No significant correlation was identified between MBE-A and ACC.

A significant yet minimal negative correlation was identified between PAB and ACC, $r(716) = -.08$, $P = .041$, and a significant moderate correlation was identified between PAB and CCC, $r(716) = .25$, $P < .001$, with similar patterns in PAB's subscales. Statistically significant correlations were identified between leadership style and both ACC and CCC; however, no statistically significant correlations were identified between leadership style and NCC. Therefore, there is a significant association between leadership style and change readiness, and we reject the null hypothesis. Leadership subscale and CTC correlations generally follow the same pattern as overall leadership scale and CTC results. This further supports the significant association identified between leadership style and change readiness.

FIGURE 2. **Sample laboratory disciplines/ASCP certifications. Note: "Other" laboratory disciplines include Flow Cytometry (SCYM); administration, such as those certified as Diplomats in Laboratory Management (DLM); generalists; and those certified in multiple disciplines.**

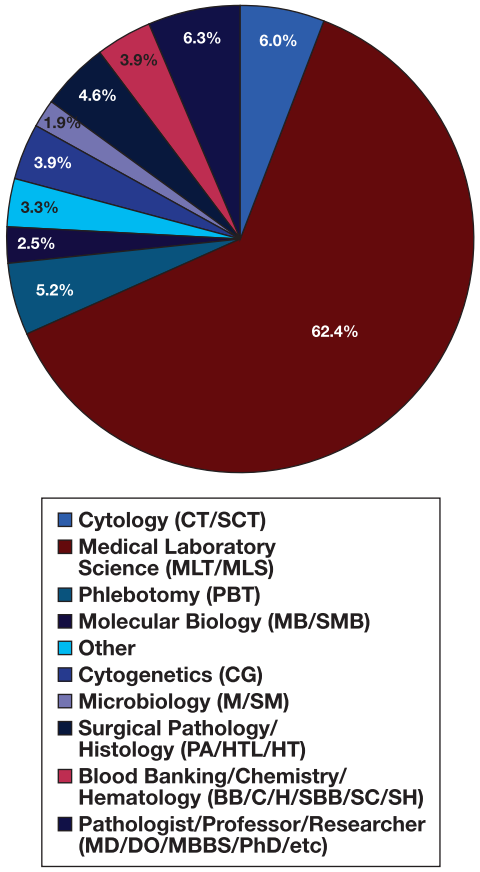

FIGURE 3. **Sample reported laboratory roles. Note: "Other" roles include pathologist assistant, LIS analyst, quality specialist, educator/professor, and consultant.**

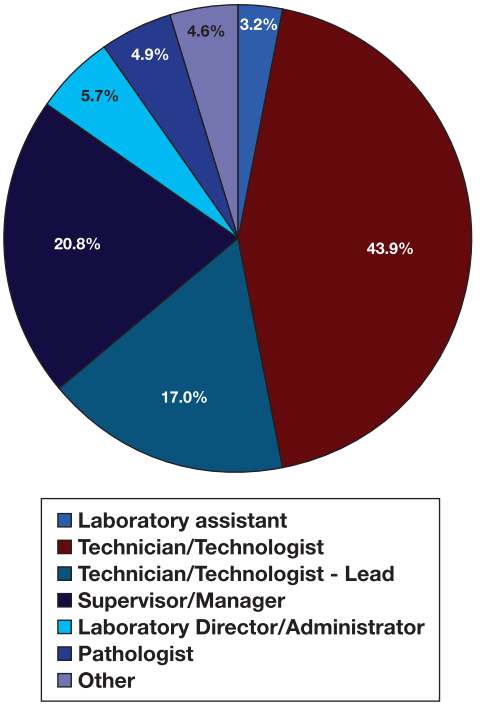

Results for H2: Regression

The H2 states that leadership style (defined by the MLQ) is a significant predictor of change readiness (measured by the TCM of CTC/Employee Commitment Survey).

$H2_0$ states that leadership style (defined by the MLQ) is not a significant predictor of change readiness (measured by measured by the TCM of CTC/Employee Commitment Survey).

Three multiple regressions were performed to predict change readiness via ACC, CCC, and NCC from transformational, transactional, and passive-avoidant leadership styles. There was independence of residuals as assessed by a Durbin-Watson statistic of 1.936, 1.990, and 1.955, respectively. To determine linearity, scatterplots of CTC scales against leadership styles with a superimposed regression line were plotted (**FIGURE 4**).

There was homoscedasticity as assessed by visual inspection of a plot of standardized residuals vs standardized predicted values. Residuals were normally distributed as assessed by visual inspection of a normal probability plot; however, partial regression plots of NCC and leadership styles with superimposed regression lines did not exhibit linearity. Seven participants were outliers on the ACC scale with an average range of 1.83 to 2.50, 1 outlier with a CCC scale average of 1.33, and 4 outliers on the NCC scale with an average range of 1.17 and 5.00. They were not removed from the analysis despite the possibility of not representing the target population. Regression coefficients and standard errors can be found in **TABLE 3**.

The first prediction equation was ACC = 4.07 + (0.093 × TL score) − (0.020 × transactional leadership score) + (0.022 × PAB score). The multiple regression model statistically significantly predicted ACC, F(3, 714) = 3.51, P = .015, accounting for 2.0% of the variation in ACC with adjusted R^2 = 0.01. Only TL added statistically significantly to the prediction (P < .05). For CCC, the prediction equation was: CCC = 3.26 − (0.235 × TL score) + (0.141 × transactional leadership score) + (0.047 × PAB score). The multiple regression model statistically significantly predicted CCC F(3, 714) = 23.72, P < .001, accounting for 9.1% of the variation in CCC with adjusted R^2 = 0.09. Transformational and transactional leadership styles added statistically significantly to the prediction (P < .01). For NCC, the prediction equation was: NCC = 3.04 + (0.059 × TL score) + (0.024 × transactional leadership score) + (0.060 × PAB score). Leadership style did not statistically significantly predict change readiness via NCC as there is no linear relationship, F(3, 714) = 1.77, P = .151, accounting for 0.7% of the variation in NCC with adjusted R^2 = 0.003, which is virtually no size effect according to Cohen.[24] Despite no significant relationship between leadership style and NCC, there were significant relationships between leadership style and both ACC and CCC. Leadership style is therefore a significant predictor of change readiness, and we reject the null hypothesis.

Discussion

Regarding MANOVA findings, gender identity, education level, and laboratory role had significant yet minimal differences between average reported change readiness scores. For ACC, females had higher mean scores than males, whereas males had higher NCC mean scores than

TABLE 2. Correlation: leadership style subscales by commitment to change scales (n = 718)

Variables		Transformational					Transactional		Passive-avoidant		Outcomes			Leadership style			Commitment to change		
		IIA	IIB	IM	IS	IC	CR	MBE-A	MBE-P	LF	EE	EFF	SAT	TL	Trans.	PAB	ACC	CCC	NCC
Idealized influence-attributed	Pearson correlation	1.000	.835[a]	.844[a]	.848[a]	.858[a]	.852[a]	.081[b]	−.735[a]	−.755[a]	.835[a]	.885[a]	.890[a]	.943[a]	.698[a]	−.781[a]	.116[a]	−.240[a]	.061
	Sig (2-tailed)		< .001	< .001	< .001	< .001	< .001	.029	< .001	< .001	< .001	< .001	< .001	< .001	< .001	< .001	.002	< .001	.100
Idealized influence-behavioral	Pearson correlation	.835[a]	1.000	.855[a]	.825[a]	.788[a]	.826[a]	.101[a]	−.681[a]	−.671[a]	.764[a]	.804[a]	.796[a]	.923[a]	.690[a]	−.708[a]	.114[a]	−.274[a]	.058
	Sig (2-tailed)	< .001		< .001	< .001	< .001	< .001	.007	< .001	< .001	< .001	< .001	< .001	< .001	< .001	< .001	.002	< .001	.123
Inspirational motivation	Pearson correlation	.844[a]	.855[a]	1.000	.830[a]	.803[a]	.832[a]	.031	−.704[a]	−.690[a]	.766[a]	.816[a]	.812[a]	.929[a]	.653[a]	−.731[a]	.095[b]	−.260[a]	.031
	Sig (2-tailed)	< .001	< .001		< .001	< .001	< .001	.406	< .001	< .001	< .001	< .001	< .001	< .001	< .001	< .001	.011	< .001	.409
Intellectual stimulation	Pearson correlation	.848[a]	.825[a]	.830[a]	1.000	.859[a]	.847[a]	.071	−.701[a]	−.704[a]	.792[a]	.840[a]	.833[a]	.936[a]	.689[a]	−.737[a]	.116[a]	−.272[a]	.044
	Sig (2-tailed)	< .001	< .001	< .001		< .001	< .001	.058	< .001	< .001	< .001	< .001	< .001	< .001	< .001	< .001	.002	< .001	.239
Individualized consideration	Pearson correlation	.858[a]	.788[a]	.803[a]	.859[a]	1.000	.849[a]	.068	−.669[a]	−.697[a]	.812[a]	.863[a]	.853[a]	.926[a]	.689[a]	−.716[a]	.101[a]	−.267[a]	.005
	Sig (2-tailed)	< .001	< .001	< .001	< .001		< .001	.067	< .001	< .001	< .001	< .001	< .001	< .001	< .001	< .001	.007	< .001	.889
Contingent reward	Pearson correlation	.852[a]	.826[a]	.832[a]	.847[a]	.849[a]	1.000	.063	−.693[a]	−.715[a]	.790[a]	.860[a]	.846[a]	.903[a]	.801[a]	−.738[a]	.107[a]	−.297[a]	−.005
	Sig (2-tailed)	< .001	< .001	< .001	< .001	< .001		.090	< .001	< .001	< .001	< .001	< .001	< .001	< .001	< .001	.004	< .001	.890
Management by exception-active	Pearson correlation	.081[b]	.101[a]	.031	.071	.068	.063	1.000	−.002	−.069	.050	.049	.020	.076[b]	.649[a]	−.037	−.014	.143[a]	.083[b]
	Sig (2-tailed)	.029	.007	.406	.058	.067	.090		.952	.064	.177	.187	.598	.043	< .001	.323	.700	< .001	.027
Management by exception-passive	Pearson correlation	−.735[a]	−.681[a]	−.704[a]	−.701[a]	−.669[a]	−.693[a]	−.002	1.000	.820[a]	−.670[a]	−.766[a]	−.756[a]	−.749[a]	−.530[a]	.955[a]	−.078[b]	.242[a]	.002
	Sig (2-tailed)	< .001	< .001	< .001	< .001	< .001	< .001	.952		< .001	< .001	< .001	< .001	< .001	< .001	< .001	.037	< .001	.967
Laissez-faire leadership	Pearson correlation	−.755[a]	−.671[a]	−.690[a]	−.704[a]	−.697[a]	−.715[a]	−.069	.820[a]	1.000	−.682[a]	−.795[a]	−.790[a]	−.756[a]	−.587[a]	.953[a]	−.068	.230[a]	.018
	Sig (2-tailed)	< .001	< .001	< .001	< .001	< .001	< .001	.064	< .001		< .001	< .001	< .001	< .001	< .001	< .001	.069	< .001	.628
Extra effort	Pearson correlation	.835[a]	.764[a]	.766[a]	.792[a]	.812[a]	.790[a]	.050	−.670[a]	−.682[a]	1.000	.844[a]	.835[a]	.853[a]	.633[a]	−.709[a]	.085[b]	−.231[a]	.055
	Sig (2-tailed)	< .001	< .001	< .001	< .001	< .001	< .001	.177	< .001	< .001		< .001	< .001	< .001	< .001	< .001	.022	< .001	.141
Effectiveness	Pearson correlation	.885[a]	.804[a]	.816[a]	.840[a]	.863[a]	.860[a]	.049	−.766[a]	−.795[a]	.844[a]	1.000	.929[a]	.904[a]	.685[a]	−.818[a]	.075[b]	−.279[a]	.017
	Sig (2-tailed)	< .001	< .001	< .001	< .001	< .001	< .001	.187	< .001	< .001	< .001		< .001	< .001	< .001	< .001	.045	< .001	.657
Satisfaction	Pearson correlation	.890[a]	.796[a]	.812[a]	.833[a]	.853[a]	.846[a]	.020	−.756[a]	−.790[a]	.835[a]	.929[a]	1.000	.899[a]	.657[a]	−.810[a]	.050	−.258[a]	−.011
	Sig (2-tailed)	< .001	< .001	< .001	< .001	< .001	< .001	.598	< .001	< .001	< .001	< .001		< .001	< .001	< .001	.182	< .001	.762
Transformational leadership	Pearson correlation	.943[a]	.923[a]	.929[a]	.936[a]	.926[a]	.903[a]	.076[b]	−.749[a]	−.756[a]	.853[a]	.904[a]	.899[a]	1.000	.734[a]	−.789[a]	.117[a]	−.282[a]	.043
	Sig (2-tailed)	< .001	< .001	< .001	< .001	< .001	< .001	.043	< .001	< .001	< .001	< .001	< .001		< .001	< .001	.002	< .001	.254
Transactional leadership	Pearson correlation	.698[a]	.690[a]	.653[a]	.689[a]	.689[a]	.801[a]	.649[a]	−.530[a]	−.587[a]	.633[a]	.685[a]	.657[a]	.734[a]	1.000	−.585[a]	.073[b]	−.141[a]	.046
	Sig (2-tailed)	< .001	< .001	< .001	< .001	< .001	< .001	< .001	< .001	< .001	< .001	< .001	< .001	< .001		< .001	.050	< .001	.222
Passive-avoidant behavior	Pearson correlation	−.781[a]	−.708[a]	−.731[a]	−.737[a]	−.716[a]	−.738[a]	−.037	.955[a]	.953[a]	−.709[a]	−.818[a]	−.810[a]	−.789[a]	−.585[a]	1.000	−.076[b]	.247[a]	.010
	Sig (2-tailed)	< .001	< .001	< .001	< .001	< .001	< .001	.323	< .001	< .001	< .001	< .001	< .001	< .001	< .001		.041	< .001	.786
Affective commitment to change	Pearson correlation	.116[a]	.114[a]	.095[b]	.116[a]	.101[a]	.107[a]	−.014	−.078[b]	−.068	.085[b]	.075[b]	.050	.117[a]	.073[b]	−.076[b]	1.000	−.329[a]	.309[a]
	Sig (2-tailed)	.002	.002	.011	.002	.007	.004	.700	.037	.069	.022	.045	.182	.002	.050	.041		< .001	< .001
Continuance commitment to change	Pearson correlation	−.240[a]	−.274[a]	−.260[a]	−.272[a]	−.267[a]	−.297[a]	.143[a]	.242[a]	.230[a]	−.231[a]	−.279[a]	−.258[a]	−.282[a]	−.141[a]	.247[a]	−.329[a]	1.000	.153[a]
	Sig (2-tailed)	< .001	< .001	< .001	< .001	< .001	< .001	< .001	< .001	< .001	< .001	< .001	< .001	< .001	< .001	< .001	< .001		< .001
Normative commitment to change	Pearson correlation	.061	.058	.031	.044	.005	−.005	.083[b]	.002	.018	.055	.017	−.011	.043	.046	.010	.309[a]	.153[a]	1.000
	Sig (2-tailed)	.100	.123	.409	.239	.889	.890	.027	.967	.628	.141	.657	.762	.254	.222	.786	< .001	< .001	

ACC, affective commitment to change; CTC, commitment to change; CCC, continuance commitment to change; CR, contingent reward; EE, extra effort; EFF, efficiency; IC, individualized consideration; II, idealized influence; IIA, II-attributed; IIB, II-behavior; IM, inspirational motivation; IS, intellectual stimulation; LF, laissez-faire leadership; MBE, management by exception; MBE-A, MBE-active; MBE-P, MBE-passive; SAT, satisfaction; TL, transformational leadership.

[a]*Correlation is significant at the .01 level (2-tailed).*

[b]*Correlation is significant at the .05 level (2-tailed).*

FIGURE 4. Multiple regression scatterplots. A, Affective commitment to change average by transformational leadership average (R^2 = 0.014). B, Affective commitment to change average by transactional leadership average (R^2 = 0.005). C, Affective commitment to change average by passive-avoidant behavior average (R^2 = 0.006). D, Continuance commitment to change average by transformational leadership average (R^2 = 0.079). E, Continuance commitment to change average by transactional leadership average (R^2 = 0.020). F, Continuance commitment to change average by passive-avoidant behavior average (R^2 = 0.061). G, Normative commitment to change average by transformational leadership average (R^2 = 0.002). H, Normative commitment to change average by transactional leadership average (R^2 = 0.002). I, Normative commitment to change average by passive-avoidant behavior average (R^2 = 1.032E-4).

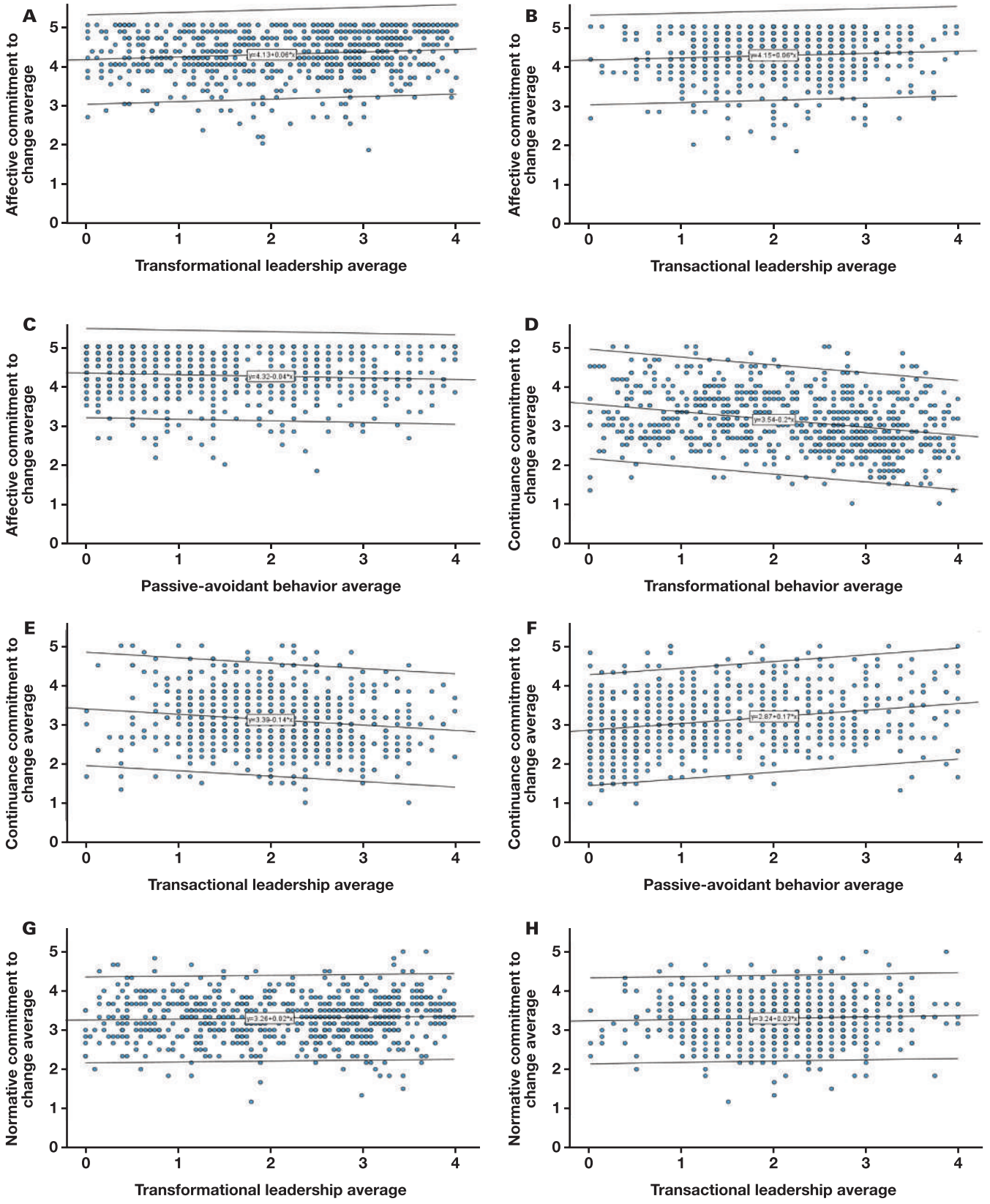

FIGURE 4. (cont)

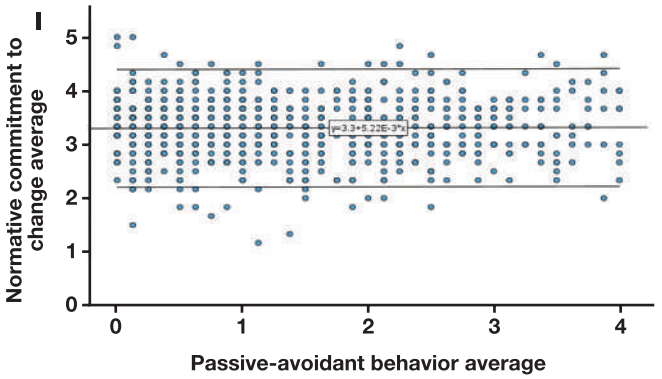

females, suggesting that females might be more intrinsically and autonomously motivated to commit to change based on self-determination theory when they perceive the leader to be supportive.[25] Gender-related differences associated with self-determination theory can also justify that males experienced more of a moral obligation or controlled motivation to commit to change than females.[25]

Participants who earned a bachelor's or master's degree had a higher mean score for ACC than those with an associate's degree, indicating that pursuing a higher level of education might also be associated with intrinsic motivation. Higher levels of education promote autonomy-supportive teaching, which promotes intrinsic motivation in students.[26] Similarly, there may be an association between higher levels of intrinsic motivation and climbing a career ladder. Regarding laboratory role and ACC, both laboratory director/administrator and supervisor/manager roles had significantly higher mean scores for ACC than laboratory assistants, and supervisor/manager roles also had significantly higher mean ACC scores than technician/technologist. Where technician/technologists had higher mean CCC scores than supervisor/managers and laboratory director/administrators, this suggests that technicians and technologists may perceive there is too much at risk (loss of benefits, income, etc) to not accept the impending change compared with higher-level management who may be more secure in their positions.[27,28] Lack of significant differences between laboratory role and mean NCC scores may indicate that, regardless of laboratory role, there is an inherent moral obligation to commit to change in the laboratory due to the nature of the profession.[27]

Discussion of H1: Correlation

The positive correlation between TL and ACC suggests that followers may have higher levels of intrinsic motivation under transformational leaders, regardless of their dominant subscale. The opposite is also true, that TL and its 5 subscales are negatively correlated with CCC. The negative correlation is higher between IIB and CCC than the other subscales, suggesting that followers who perceive their leaders to exhibit higher levels of IIB are less likely to commit out of fear or negative feelings of risk. Lack of significant correlation between TL with associated subscales and NCC suggests that regardless of perceived TL level, it was not associated with higher or lower NCC. Additionally, the strong positive correlations between TL and the 3 leadership outcomes of EE, EFF, and SAT suggest that leaders who use TL have improved motivational skills, effective organizational interactions, and work with others in a satisfactory manner. These findings support the premise that TL improves job satisfaction, interpersonal interactions, and follower inspiration.[12]

Of the transactional leadership subscales, it is likely that CR is positively correlated with ACC and negatively correlated with CCC because leaders who express this subscale often use situational leadership where they vacillate between transactional and TL when appropriate.[1,29] CR, like TL, was strongly and positively associated with leadership outcomes, which is likely also related to the use of situational leadership. The positive correlation between MBE-A and CCC is likely due to overlapping characteristics in leaders who express both MBE-A and MBE-P, the latter of which is characterized as a PAB.[12] This is also supported by the fact that MBE leadership behaviors are corrective in nature and are associated with lower motivation.[12,16,17]

PAB's negative correlation with ACC and positive correlation with CCC indicate that followers who perceive their leaders to exhibit nonleadership behavior are not intrinsically motivated to commit to change and instead commit only because they feel that that the cost of abandoning the organization is not worth the risk of not acceding the change. PAB is moderate-strongly and negatively correlated with the 3 leadership outcomes, suggesting that leaders who use PAB are more likely to produce negative outcomes, fail to inspire extra effort, be viewed as effective, or deliver satisfactory results.

The lack of significant correlation between leadership style and NCC suggests that a follower's moral obligation to commit to change is unrelated to leadership style in the laboratory. However, both transformational and transactional leadership are positively correlated with ACC and negatively correlated with CCC, and PAB follows the opposite pattern. Medical laboratory followers under leaders who use any of the TL style subscales or the transactional leadership subscale of CR are more likely to report higher levels of intrinsic motivation to commit to change. In contrast, followers under leaders who exhibit MBE-A and PAB are more likely to report that they commit to change as a result of perceived cost.

Discussion of H2: Regression

The multiple regression model significantly predicted ACC with only TL serving as a statistically significant predictor. Therefore, use of TL can positively predict higher levels of ACC in followers while having no causal or predictive relationship with CCC or NCC. This finding supports the premise of TL theory, in which leaders use this style to promote inspiration, intrinsic motivation, leadership attachment, and value alignment in their followers.[1,12] The multiple regression model also significantly predicted CCC. Both transformational and transactional leadership styles added to the prediction in that use of TL results in lower levels of CCC, higher levels of transactional leadership without TL predicts higher levels of CCC, and lower values in TL predicts higher levels of CCC. The absence of a linear relationship between leadership style and change readiness via NCC explains the lack of correlation and predictive relationship between the 2 variables. This is likely due to the moral obligation or sense of duty that laboratory professionals and pathologists feel as health care providers to commit and remain loyal to organizational changes that promote quality.[27] Despite the absence of a relationship between leadership style and NCC, there were significant predictor relationships between leadership style and both ACC and CCC, which carry implications for practice.

Study Limitations

A methodological limitation of the study is the survey length, according to Portney and Watkins.[22] Although the average completion time for

TABLE 3. Multiple regression analysis

Change readiness	*B*	95% CI for *B*		SE B	*β*	*P* value	R^2	ΔR^2
		LL	UL					
Affective commitment to change								
Model							.02	.01
Constant	4.074	3.84	4.31	.12		< .001		
Transformational	.093[a]	.01	.17	.04	.17	.020		
Transactional	−.020	−.10	.06	.04	−.03	.634		
Passive-avoidant	.022	−.04	.09	.03	.04	.500		
Continuance commitment to change								
Model							.09	.09
Constant	3.261	2.97	3.55	.15		< .001		
Transformational	−.235[b]	−.33	−.14	.05	−.33	< .001		
Transactional	.141[b]	.01	.24	.05	.14	.006		
Passive-avoidant	.047	.03	.12	.04	.07	.237		
Normative commitment to change								
Model							.01	.003
Constant	3.043	2.81	3.27	.12		< .001		
Transformational	.059	−.02	.13	.04	.11	.127		
Transactional	.024	−.06	.10	.04	.03	.554		
Passive-avoidant	.060	.00	.12	.03	.12	.055		

B, *unstandardized regression coefficient; LL, lower limit; Model, "Enter" method in SPSS Statistics; UL, upper limit.*
[a]P < *.05.*
[b]P < *.001.*

this research survey was less than 8 minutes, it is likely that the 74-item survey was too long, resulting in a 73% completion rate. Other than limiting the number of demographic questions, removal of any of the scale items for the MLQ or the TCM could invalidate the results of the intended measures. Another limitation of the study is recruitment procedures. Although the survey was sent via email to ASCP and ASC members, it is possible that society members have restricted their communication preferences to limit survey emails. Additionally, the survey could have been sent to other medical laboratory and pathology professional societies. This approach could have increased recruitment for laboratory disciplines that had lower response rates, such as flow cytometry and microbiology, compared with medical laboratory science. Regarding participant demographics, a limitation is the lack of racial, ethnic, and gender diversity within the study sample. The survey was designed to promote equity in eligibility, and recruitment procedures did not demonstrate bias toward any 1 characteristic; however, there was an overwhelming representation of respondents reporting a Caucasian (White) ethnicity and a limited representation of respondents who identified as nonbinary or transgender. Although this finding was unexpected, recruitment procedures should have addressed potential barriers to better understand diversity, equity, and inclusion-related gaps in leadership and change readiness.

It is possible that extraneous factors affected leadership and commitment ratings. Highly motivated followers may perceive their leaders as transformational and overinflate their leaders' TL scores rather than taking the survey through a more objective lens. Conversely, followers who are unsatisfied with their overall job, organizational culture, or senior leadership beyond their immediate manager may describe higher PAB in their direct leader rather than attributing other factors influencing their perspective. Similar external factors may influence their reported CTC, and the participant's perspective of change may serve as a limiting feature. For example, some followers may perceive a change as minor, such as offering a new test or implementing new equipment, or major, such as a shift change or a hospital acquisition or merger. A change in leadership might also affect the follower's responses, especially if leadership styles differ, therefore influencing change readiness responses. Previous negative experiences of change may alter change readiness responses even if more recent experiences were positive. To reduce variation, the CTC survey prompt should have specified "experiences regarding change … under your current leader."

Implications for Practice

Leaders in laboratory medicine should immediately reflect on their current leadership style and determine whether behaviors incite intended commitment effects in their followers. Based on the findings of this study, it is recommended that laboratory leaders use TL and contingent reward styles to improve ACC and either transformational or transactional leadership to reduce CCC in their followers. If TL is the dominant leadership style but ACC is low and CCC is high, consider increasing IIB to reduce levels of CCC. If use of transactional leadership is necessary to offer structured management, formal delegation, and reinforcement systems, this style is still appropriate and effective at reducing CCC.[12,15] However, consider situational leadership as the primary style where, depending on the situation, followers have the opportunity to develop higher levels of ACC under TL.[1,12] The use of situational leadership may also improve leadership outcomes in the laboratory, as both TL and transactional leadership, including the CR subscale, are strongly and positively correlated with leadership outcomes of EE, EFF, and SAT.

Although LF did not serve as a predictor of CCC, its strong positive correlation with CCC suggests that use of the leadership style must be avoided to reduce the negative impact of CCC on their employees. Senior leadership must address LF in their subordinate managers as early as possible to reduce its potential downstream effects. It is also the responsibility of the follower to provide the leader with feedback of their experiences both individually and as a team, thus communicating potential gaps between leadership style and change readiness. Just as the MLQ can be used as both a leader self-assessment and as a follower's assessment of the leader, the combined survey instrument may be used as an annual feedback tool. This combined survey instrument can also be used as the laboratory or health care organization anticipates additional changes, such as enrolling in a continuous improvement program or pivoting to meet new regulations.

Using TL to promote ACC and reduce CCC can mitigate barriers associated with change readiness, therefore promoting commitment to quality initiatives that promote high-value, patient-centered care. Laboratory teams that are affectively and intrinsically committed to change are more likely to embrace improvements within the laboratory and their organization that produce quality results for the patients.[30-32] These improvements include engaged and accountable employees and increased efficiency by reducing turnaround time and errors or process variations in the total testing process.[33,34] Consequently, clinicians and patients alike will benefit from improved accuracy and timeliness result delivery, leading to faster clinical decision-making and ideally, better patient outcomes.[12,34-36]

As health care organizations have a synergistic effect, improvements in change readiness within the laboratory will likely benefit other departments or disciplines within the organization.[30,37] Interdisciplinary collaboration is better facilitated with motivated teams who have streamlined processes, and the laboratory that intrinsically commits to quality sets a precedent for other departments to follow.[30,37] Although different organizational departments and health care disciplines may have unique demands when it comes to leadership, it would be helpful to observe leaders in laboratory medicine who use TL or a combination of both transformational and transactional leadership to incite change readiness via ACC and reduce levels of CCC. Other departments or health care disciplines can trial TL styles to determine whether there is an immediate benefit in their follower's CTC.

Future Research

As the first laboratory medicine study to examine the variables of leadership style and change readiness using the combined MLQ-TCM instrument, this study effectively established both associations and predictive relationships; however, a few notable gaps remain, encouraging additional research. Although the study involved a robust sample, it may prove worthwhile to replicate or modify the study to capture more data on marginalized populations or disciplines that were not sufficiently represented within this study. As all health disciplines must effectively collaborate to provide high-value, patient-centric care, this study should also be replicated across other health disciplines to determine consistency of findings and tailor leadership styles to specific disciplines, if applicable.

Additionally, future research should explore mediating factors between leadership style and change readiness. The association between laboratory passive behavior and CCC should be examined more closely. Nonleadership and CCC or total lack of commitment may have a snowball effect, negatively affecting other departments and, subsequently, patient care. Promoters of nonleadership and barriers of effectively using transformational, transactional, or situational leadership should be examined to determine whether internal factors within the leader or external restraints, such as insufficient resources in the laboratory, mediate this association. Because of the sensitive nature of NCC, with higher levels of NCC correlated with increased stress and emotional exhaustion, it is imperative to identify both internal and external factors outside of leadership style that may contribute to increased NCC and subsequent burnout in laboratory medicine.[10] Most importantly, this study was completed during and within the early aftermath of the COVID-19 pandemic, and researchers must explore the long-term effects of the pandemic on leadership style and change readiness via CTC. It is recommended that the study be repeated within the next decade to explore differences in pandemic and postpandemic results within the laboratory. It is also important to understand how the COVID-19 pandemic affected leadership and CTC across multiple fields, including other health care disciplines and non–health care sectors.

Conclusions

This quantitative study determined that leadership style is correlated with both change readiness via CTC and leadership outcomes in laboratory medicine. All subscales of TL along with the CR subscale of transactional leadership are positively correlated with ACC and negatively correlated with CCC. The reverse is also true, with PAB being negatively correlated with ACC and positively correlated with CCC. TL and transactional leadership are also strongly and positively correlated with the leadership outcomes of EE, EFF, and SAT, whereas PAB is strongly and negatively correlated with these outcomes. This study also determined that leadership style is a predictor of ACC and CCC but not NCC, and leaders should use TL to improve ACC and either TL or situational leadership to reduce CCC. Although the use of situational leadership can reduce CCC, it is likely that this leadership style will also increase follower's ACC given that the situation calls for TL behavior. To inspire followers to embrace a change culture and be intrinsically motivated to support the continuous improvement mindset, it is recommended that leaders effectively use TL and contingent reward leadership. PAB serves as a barrier to intrinsic CTC and is associated with an intensified follower commitment out of stress or fear, further contributing to the field's ever-increasing level of laboratory professional burnout and resistance to change. For the growth and well-being of the field and to remain competitive in the dynamic health care landscape, PAB should be limited or avoided, and TL along with contingent reward leadership should be embraced by leaders of laboratory medicine.

Acknowledgments

I thank my doctoral committee members, Casey Mace Firebaugh and Terry DeVito (Bay Path University), for their help in designing the study, reviewing the findings, and guiding the editing process. I also thank Joseph Clarici, Hormoz Ehya, and my cytology colleagues (Fox Chase Cancer Center), Tatiana Zorina (Thomas Jefferson University), the American Society for Clinical Pathology, and the American Society of Cytopathology for their ongoing support.

Conflict of Interest Disclosure

The author has nothing to disclose.

REFERENCES

1. Ledlow GR, Stephens JH. *Leadership for Health Professionals: Theory, Skills, and Applications*. Jones & Bartlett Learning; 2018.
2. Combe M. Change readiness: focusing change management where it counts. PMI White Paper. 2014. Accessed July 22, 2022. https://www.pmi.org/learning/library/change-readiness-11126
3. Antony J, Lizarelli FL, Fernandes MM, Dempsey M, Brennan A, McFarlane J. A study into the reasons for process improvement project failures: results from a pilot survey. *Int J Qual Reliab Manag*. 2019;36(10):1699-1720. https://doi.org/10.1108/ijqrm-03-2019-0093
4. Erlingsdottir G, Ersson A, Borell J, Rydenfält C. Driving for successful change processes in healthcare by putting staff at the wheel. *J Health Organ Manag.* 2018;32(1):69-84. doi:10.1108/JHOM-02-2017-0027
5. Niñerola A, Sánchez-Rebull MV, Hernández-Lara AB. Quality improvement in healthcare: Six Sigma systematic review. *Health Policy*. 2020;124(4):438-445. doi:10.1016/j.healthpol.2020.01.002
6. Topiwala P. Laboratory employee's reflections towards change in transitioning from a public to a private laboratory service. Victoria University of Wellington Research Archive. 2015. Accessed July 6, 2022. http://researcharchive.vuw.ac.nz/bitstream/handle/10063/4961/paper.pdf?sequence=1
7. Weiner BJ. A theory of organizational readiness for change. *Implementation Science.* 2009;4(67):1-9. https://doi.org/10.1186/1748-5908-4-67
8. Herscovitch L, Meyer JP. Commitment to organizational change: extension of a three-component model. *J Appl Psychol.* 2002;87(3):474-487. doi:10.1037/0021-9010.87.3.474
9. Bouckenooghe D, Schwarz GM, Minbashian A. Herscovitch and Meyer's three-component model of commitment to change: meta-analytic findings. *Euro J Work Organ Psychol*. 2014;24(4):578-595. https://doi.org/10.1080/1359432x.2014.963059
10. Genevičiūtė-Janonienė G, Endriulaitienė A. Employees' organizational commitment: its negative aspects for organizations. *Procedia - Soc Behav Sci*. 2014;140:558-564. doi:10.1016/j.sbspro.2014.04.470
11. Vandenberghe C, Mignonac K, Manville C. When normative commitment leads to lower well-being and reduced performance. *Human Relations*. 2014;68(5):843-870. https://doi.org/10.1177/0018726714547060
12. Bass BM, Riggio RE. *Transformational Leadership*. Taylor & Francis Group, Psychology Press; 2006.
13. Graban M. *Lean Hospitals, Improving Quality, Patient Safety, and Employee Engagement*. CRC Press; 2016
14. Lutz Allen S, Smith JE, da Silva N. Leadership style in relation to organizational change and organizational creativity: perceptions from nonprofit organizational members. *Nonprofit Manage Leadership.* 2013;24(1):23-42. doi:10.1002/nml.21078
15. Samarasekera DD, Yeo JHT, Shah H. *Leading Health Profession Educational Programs for Better Health Care Services: Challenges and Opportunities in Health Professions Education*. Springer; 2022. https://doi.org/10.1007/978-981-16-7232-3_9
16. Musinguzi C, Namale L, Rutebemberwa E, Dahal A, Nahirya-Ntege P, Kekitiinwa A. The relationship between leadership style and health worker motivation, job satisfaction and teamwork in Uganda. *J Healthc Leadersh.* 2018;10:21-32. https://doi.org/10.2147/JHL.S147885
17. Willis S, Clarke S, O'Connor E. Contextualizing leadership: transformational leadership and management-by-exception-active in safety-critical contexts. *J Occup Organ Psychol.* 2017;90(3):281-305. https://doi.org/10.1111/joop.12172
18. Xenikou A. Transformational leadership, transactional contingent reward, and organizational identification: the mediating effect of perceived innovation and goal culture orientations. *Front Psychol.* 2017;8:1754. https://doi.org/10.3389/fpsyg.2017.01754
19. Braathu N, Laukvik EH, Egeland KM, Skar AMS. Validation of the Norwegian versions of the Implementation Leadership Scale (ILS) and Multifactor Leadership Questionnaire (MLQ) in a mental health care setting. *BMC Psychol*. 2022;10(1):1-11. https://doi.org/10.1186/s40359-022-00725-8
20. Pahi MH, Umrani WA, Hamid KA, Ahmed U. Examining Multifactor Leadership Questionnaire construct: a validation study in the public hospitals of Sindh, Pakistan context. *Bus Manag Rev*. 2015;7(2):27-39. https://e-journal.uum.edu.my/index.php/gbmr/article/view/16794
21. Meyer JP, Allen NJ. TCM employee commitment survey academic users guide 2004. University of Western Ontario. 2004. Accessed June 23, 2022. https://employeecommitment.com/TCM-Employee-Commitment-Survey-Academic-Package-2004.pdf
22. Portney LG, Watkins MP. *Foundations of Clinical Research: Applications to Practice*. F.A. Davis; 2015.
23. Laerd Statistics. How to perform a linear regression in SPSS. Accessed August 22, 2022, https://statistics.laerd.com/premium/spss/lr/linear-regression-in-spss-10.php
24. Cohen J. *Statistical Power Analysis for the Behavioral Sciences*. Psychology Press; 1988.
25. Katz I. In the eye of the beholder: motivational effects of gender differences in perceptions of teachers. *J Exp Educ*. 2016;85(1):73-86. https://doi.org/10.1080/00220973.2015.1101533
26. Orsini C, Evans P, Jerez O. How to encourage intrinsic motivation in the clinical teaching environment? A systematic review from the self-determination theory. *J Educ Eval Health Prof*. 2015;12:8. https://doi.org/10.3352/jeehp.2015.12.8
27. Rodríguez-Fernández M, Herrera J, De Las Heras-Rosas C. Model of organizational commitment applied to health management systems. *Int J Environ Res Public Health.* 2021;18(9):4496. https://doi.org/10.3390/ijerph18094496
28. Shao H, Fu H, Ge Y, Jia W, Li Z, Wang J. Moderating effects of transformational leadership, affective commitment, job performance, and job insecurity. *Front Psychol.* 2022;13:847147. https://doi.org/10.3389/fpsyg.2022.847147
29. Tuan Luu T. Ambidextrous leadership, entrepreneurial orientation, and operational performance. *Leadership & Organization Development Journal*. 2017;38(2):229-253. https://doi.org/10.1108/lodj-09-2015-0191
30. Rafferty AE, Jimmieson NL, Armenakis AA. Change Readiness. *J Manage.* 2013;39(1):110-135. https://doi.org/10.1177/0149206312457417
31. Lam M, O'Donnell M, Robertson D. Achieving employee commitment for continuous improvement initiatives. *Int J Oper Prod Manag*. 2015;35(2):201-215. https://doi.org/10.1108/ijopm-03-2013-0134
32. von Treuer K, Karantzas G, McCabe M, et al. Organizational factors associated with readiness for change in residential aged care settings. *BMC Health Serv Res.* 2018;18(1):77. https://doi.org/10.1186/s12913-018-2832-4
33. Hawkins R. Managing the pre- and post-analytical phases of the total testing process. *Ann Lab Med*. 2012;32(1):5-16. https://doi.org/10.3343/alm.2012.32.1.5
34. Plebani M. Errors in clinical laboratories or errors in laboratory medicine? *Clin Chem Lab Med.* 2006;44(6):750-759. https://doi.org/10.1515/CCLM.2006.123
35. Costa F, Lispi L, Staudacher AP, Rossini M, Kundu K, Cifone FD. How to foster sustainable continuous improvement: a cause-effect relations map of lean soft practices. *Oper Res Perspect.* 2019;6:100091. https://doi.org/10.1016/j.orp.2018.100091
36. Sanchez-Ruiz L, Blanco B, Gomez-Lopez R. Continuous improvement enablers: defining a new construct. *J Ind Eng Manag.* 2019;12(1):51-69. https://doi.org/10.3926/jiem.2743
37. Erkutlu H, Chafra J. Value congruence and commitment to change in healthcare organizations. *J Adv Manag Res.* 2016;13(3):316-333. https://doi.org/10.1108/jamr-11-2015-0078

Diagnostic value of pleural effusion Krebs von den Lungen-6 in malignant pleural effusion of patients with non–small cell lung cancer

Junjun Wang, MS,[1] Liqun Ling, MS,[1,] Shuhui Chen, MS,[1] Lunan Chou, MS,[1] Yumin Wang, MD,[1] Lijuan Hu, MS[1,*]*

[1]Department of Clinical Laboratory, Key Laboratory of Clinical Laboratory Diagnosis and Translational Research of Zhejiang Province, the First Affiliated Hospital of Wenzhou Medical University, Wenzhou, China. Corresponding author: Lijuan Hu; hljsonya2012@163.com. *Contributed equally.

Key words: Krebs von den Lungen-6; benign pleural effusion; malignant pleural effusion; diagnostic value; non–small cell lung cancer; pleural effusion

Abbreviations: KL-6, Krebs von den Lungen-6; MPE, malignant pleural effusion; NSCLC, non–small cell lung cancer; pKL-6, pleural effusion KL-6; BPE, benign PE; pADA, pleural effusion adenosine deaminase; pCEA, pleural effusion carcinoembryonic antigen; sCRP, serum C-reactive protein; pFer, pleural effusion ferritin; pCA, pleural effusion carbohydrate antigen; pRBC, pleural effusion red blood cell; pWBC, pleural effusion white blood cell; ROC, receiver operating characteristic curve; AUC, area under the curve

Laboratory Medicine 2024;55:271-276; https://doi.org/10.1093/labmed/lmad076

ABSTRACT

Objective: The aim of this study was to investigate the diagnostic potential of Krebs von den Lungen-6 (KL-6) in differentiating between malignant pleural effusion (MPE) induced by non–small cell lung cancer (NSCLC) and benign pleural effusion (BPE).

Methods: We collected 143 pleural effusion samples from August 2018 to March 2021. The samples included 91 cases of MPE and 52 cases of BPE. The KL-6 and other indicators in pleural effusion were detected.

Results: The level of pleural effusion KL-6 (pKL-6) in the MPE group was significantly higher than in the BPE group (Mann-Whitney U = 442.500, P = .000). The area under the curve (AUC) of pKL-6/pleural effusion adenosine deaminase (pADA) + pleural effusion carcinoembryonic antigen (pCEA)/pADA (AUC = 0.992) in diagnosing MPE was higher than that of pKL-6 alone (AUC = 0.903), with a sensitivity of 93.26% and specificity of 100%.

Conclusion: The measurement of pKL-6 can differentiate NSCLC-induced MPE from BPE. Furthermore, the combined detection of pKL-6/pADA and pCEA/pADA can significantly improve the diagnostic efficiency for distinguishing NSCLC-induced MPE.

Lung cancer is the malignant tumor with the highest incidence rate and mortality in the world. Non–small cell lung cancer (NSCLC) accounts for about 80% of lung cancer, and 50% to 60% of NSCLC is advanced at the time of diagnosis.[1] Malignant pleural effusion (MPE) is one of the common complications in NSCLC.[2] The median survival period of MPE is only 4 to 12 months.[3] Epidemiological surveys show that there are about 200,000 MPE patients in the United States every year, with a mortality rate of about 12% and related medical costs of up to $5 billion.[4] The median survival time of lung cancer patients without MPE (12.65 months) was significantly longer than that of lung cancer patients with MPE (7.49 months).[5]

The diagnostic gold standard for MPE is the presence of cancer cells in pleural effusion cytology or pleural biopsy, but their sensitivity is low. When there are few tumor cells, the sensitivity of pleural effusion cytology is about 40% to 87%.[6] Additionally, cytological examination is invasive, and patient and family compliance is often low. Tumor marker detection is noninvasive, but the sensitivity and specificity of conventional tumor markers are not very high. Among the widely used tumor markers, carcinoembryonic antigen (CEA) has high diagnostic efficiency in diagnosing MPE, but it still requires joint diagnosis with other tumor markers to improve accuracy.[7] Therefore, finding tumor markers with high diagnostic efficiency is an urgent scientific research topic.

Krebs von den Lungen-6 (KL-6) was discovered by Kohno, a Japanese scholar, when preparing monoclonal antibodies using the human lung adenocarcinoma cell line VMRC-LCR.[8] Type II alveolar epithelial cells are the main source of KL-6 expression. When type II alveolar epithelial cells are injured, KL-6 leaks into the blood through the basement membrane of the injured pulmonary interstitium, which can lead to the increase of the serum KL-6 level.[9] KL-6 is also a clinically useful biomarker for interstitial lung disease, given its high sensitivity in serum detection.[10] Recent studies have found that the serum KL-6 level is significantly increased in patients with lung adenocarcinoma, which can be used as a potential tumor biomarker.[11] Tomita et al[12] found that

whether patients had interstitial lung diseases or not, the serum KL-6 level could be used as a prognostic marker for NSCLC patients. However, at present, the diagnostic value of pleural effusion KL-6 (pKL-6) for MPE in patients with NSCLC has not been studied.

The purpose of this study is to investigate the potential of pKL-6 as a tumor marker for MPE in NSCLC patients and to explore its ability to differentiate between MPE and BPE. The objective is to offer valuable insights for clinical diagnosis and treatment.

Material and Methods

Study Subjects

From August 2018 to March 2021, 143 patients with lung disease who received treatment at the First Affiliated Hospital of Wenzhou Medical College in China were enrolled and their PE samples were collected. Among them, 91 cases of MPE were from NSCLC patients, and 52 cases of BPE were from pneumonia and tuberculosis patients. The MPE group consisted of 56 male and 35 female patients, with an age range of 42 to 93 years (mean, 65.99 ± 9.69 years). The BPE group consisted of 41 male and 11 female patients, with an age range of 20 to 86 years (mean, 58.40 ± 19.00 years). Samples from patients with digestive tract–related diseases, hypoproteinemia, or kidney damage were excluded. There were no statistically significant differences in gender or age between the MPE and BPE groups ($P > .05$). The signed informed consent forms of all patients in this study were kept in written or electronic form by the Institutional Ethics Review Committee of the First Affiliated Hospital of Wenzhou Medical University. The samples of MPE caused by NSCLC and samples of BPE caused by pneumonia and tuberculosis underwent confirmation by the following departments: bacterial culture of the microbiome and cell morphology analysis by the pathology department, imaging by the radiology department, and gene analysis by the molecular biology laboratory.

Laboratory Methods

A total of 5 mL of each patient's whole blood was collected into a vacuum sampling tube containing coagulant and separating gel through a disposable venous sampler and centrifuged at 2588 *g* for 15 minutes using a high-speed centrifuge. The separated plasma was transferred to a storage tube and stored in a refrigerator at −80°C. A total of 8 mL of the patient's PE was collected into a sterile tube, centrifuged for 15 minutes at a speed of 475*g* using a centrifuge, and the supernatant of the centrifuged pleural effusion was sucked up with a disposable pipette and transferred to a storage tube at −80°C for storage. Using a Siemens automatic protein analyzer, the level of serum C-reactive protein (sCRP) was detected by turbidimetry. In a model DXI800 immunoluminescence analyzer (Beckman Coulter), the levels of PE ferritin (pFer), PE carcinoembryonic antigen (pCEA), PE carbohydrate antigen (pCA) 199, and pCA125 were detected by chemiluminescence immunoassay. On Niu Bao's counting board, the levels of PE red blood cells (pRBC) and PE white blood cells (pWBC) were detected by manual counting and conversion. An automatic biochemical analyzer (model AU5800, Beckman), was used to detect PE adenosine deaminase (pADA). Using a Sharay 4000 automatic chemiluminescence tester (C-Luminary Biotech), the level of pKL-6 was detected by magnetic microparticle chemiluminescence immunoassay. The KL-6 reagent manual shows that the blank limit (representing sensitivity) is not higher than 20.00 U/mL, and the coefficient of variation (representing imprecision) is within the range of ±10.0%. The linearity (representing the reportable range) is within the range of 50.00 U/mL to 5000.00 U/mL, and the correlation coefficient is not less than 0.9900. Healthy individual serum KL-6 is <500.00 U/mL.

Statistical Analysis

The data was assessed for normality using the Kolmogorov–Smirnov test and presented as median (P25, P75). The Mann-Whitney *U* test was used to compare the 2 groups, and the receiver operating characteristic (ROC) curve was used for diagnostic efficacy analysis. The statistical analysis was conducted using SPSS 20.0, where a *P* value less than .05 was deemed statistically significant.

Results

The levels of pKL-6, pCEA, pCA125, pCA199, pRBC, pKL-6/pADA, and pCEA/pADA were significantly higher in the MPE group than in the BPE group (Mann-Whitney $U = 442.500$, 77.500, 1097.500, 1019.000, 1682.500, 367.500, and 133.000, respectively; $P = .000$, .000, .000, .000, .005, .000, and .000, respectively). Conversely, the levels of pADA and sCRP were significantly lower in the MPE group than those in the BPE group (Mann-Whitney $U = 1258.000$ and 973.000, respectively; $P = .000$ and .000, respectively). No significant difference was observed in the levels of pFer and pWBC between the MPE group and the BPE group (Mann-Whitney $U = 1472.500$ and 2038.000, respectively; $P = .291$ and .201, respectively). In the MPE group, 78% (71/91) of KL-6 levels were higher than 500 U/mL (considered healthy in the reagent manual). Please refer to **FIGURE 1** and **TABLE 1** for more information.

The area under the curve (AUC) of pKL-6/pADA + pCEA/pADA (0.992) was higher than the AUCs of pKL-6 (0.903), pCEA (0.981), pADA (0.754), pFer (0.554), pCA125 (0.687), pCA199 (0.727), sCRP (0.749), pWBC (0.534), pRBC (0.664), pKL-6/pADA (0.943), and pCEA/pADA (0.991). The diagnostic sensitivity and specificity of pKL-6/pADA + pCEA/pADA for MPE were 93.26% and 100%, respectively. Please refer to **FIGURE 2** and **TABLE 2**.

The levels of pKL-6 showed no significant difference among different age, sex, smoking status, histopathological type, lymphatic metastasis, and distant metastasis groups (Mann-Whitney $U = 810.550$, 893.550, 993.000, 107.000, 622.000, and 550.000, respectively; $P = .761$, .480, .866, .060, .727, and .420, respectively). Please refer to **TABLE 3**.

Discussion

According to its nature, PE can be categorized as either BPE or MPE. The pathogenesis and treatment strategies of BPE and MPE are completely different. Clarifying the nature of PE is of great significance in assisting clinicians in diagnosing diseases and selecting treatment plans.[13] The differentiation of effusion properties mainly relies on laboratory examination, including cytology and tumor marker detection.[14,15] Using only cytological smear diagnosis often fails to provide effective screening. Due to the subjective influence of human factors on cytology, there are deficiencies, such as low positive rates and high missed diagnosis rates.[16] Combining the analysis of tumor markers in PE with cell morphology may improve the efficiency of distinguishing between MPE and BPE. Tumor markers are commonly used to determine the possibility of malignant diseases, with CEA, CA125, and CA199 being clinically common

FIGURE 1. **Comparison of the parameters in malignant pleural effusion (MPE) and benign pleural effusion (BPE). The levels of pleural effusion KL-6 (pKL-6), pleural effusion carcinoembryonic antigen (pCEA), pKL-6/pleural effusion adenosine deaminase (pADA), and pCEA/pADA were significantly higher in the MPE group compared to the BPE group (Mann-Whitney *U* = 442.500, 77.500, 367.500, and 133.000, respectively; *P* = .000, .000, .000, and .000, respectively). **P* < .001. pCA, pleural effusion carbohydrate antigen; pFer, pleural effusion ferritin; pRBC, pleural effusion red blood cell; pWBC, pleural effusion white blood cell; sCRP, serum C-reactive protein.**

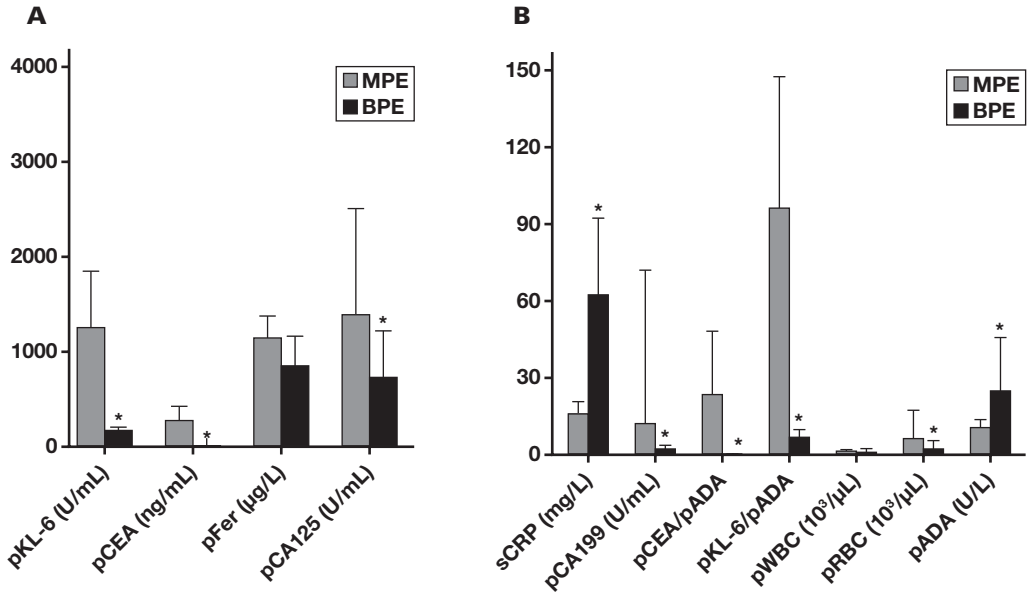

TABLE 1. **Comparison of the parameters in pleural effusion in the 2 groups[a]**

Parameter	MPE	BPE	Mann-Whitney *U*	*P*
pKL-6, U/mL	1261.00 (518.00, 3126.00)	181.50 (126.25, 215.00)	442.500	.000
pCEA, ng/mL	277.50 (62.24, 1190.22)	1.00 (0.65, 2.00)	77.500	.000
pADA, U/L	11.0 (8.2, 18.0)	25.3 (10.0, 58.0)	1258.000	.000
pFer, μg/L	1152.2 (606.6, 1956.8)	860.0 (520.6, 1393.0)	1472.500	.291
pCA125, U/mL	1398.8 (659.7, 5027.7)	743.0 (265.4, 1431.4)	1097.500	.000
pCA199, U/mL	12.6 (2.5, 278.2)	2.3 (1.9, 4.0)	1019.000	.000
sCRP, mg/L	16.0 (7.0, 32.9)	63.0 (24.3, 99.5)	973.000	.000
pWBC, 10^3/μL	1.60 (0.75, 2.88)	1.22 (0.28, 3.00)	2038.000	.201
pRBC, 10^3/μL	6.40 (1.44, 41.50)	2.86 (1.00, 7.96)	1682.500	.005
pKL-6/pADA	95.12 (46.27, 192.25)	6.5 8(2.43, 19.63)	367.500	.000
pCEA/pADA	21.69 (4.60, 99.56)	0.04 (0.01, 0.08)	133.000	.000

BPE, benign pleural effusion; MPE, malignant pleural effusion; pADA, pleural effusion adenosine deaminase; pCA, pleural effusion carbohydrate antigen; pCEA, pleural effusion carcinoembryonic antigen; pFer, pleural effusion ferritin; pKL-6, pleural effusion KL-6; pRBC, pleural effusion red blood cell; pWBC, pleural effusion white blood cell; sCRP, serum C-reactive protein.
[a]*The values in parentheses represent 25th quantiles (P25) and 75th quantiles (P75). The values not in parentheses represent medians.*

tumor markers. There is evidence from multiple studies that tumor markers can help distinguish between MPE and BPE.[17-19] However, we still need new and suitable tumor markers to improve the diagnostic efficiency of MPE. Therefore, finding appropriate tumor markers is of great significance for differentiating BPE and MPE.

KL-6 is a glycoprotein with a relative molecular weight of approximately 200 kDa, which is encoded by the *MUC1* gene.[20] The expression of KL-6 in the human body is closely related to the occurrence and development of various tumors, and it can serve as a potential biological marker for tumor diagnosis, treatment, and disease monitoring. In epithelial ovarian cancer, the high expression level of KL-6 is associated with tumor stage, grade, and histological type, and indicates a shorter progression-free survival for patients.[21,22] The expression or glycosylation changes of KL-6 in colorectal cancer, gastric cancer, and pancreatic cancer are believed to affect the invasive and adhesive abilities of cancer cells.[23,24] Studies have also found that KL-6 expression is closely related to the diagnosis and prognosis of breast cancer and cholangiocarcinoma.[25,26] KL-6 is expressed in both the serum and tumor tissue of lung cancer patients, and its expression level is closely related to the clinical characteristics and prognosis of lung cancer.[11,27,28]

Although KL-6 is associated with many types of tumors, its relationship with MPE has not been extensively studied. Moreover, most studies have focused on KL-6 levels in serum, with little attention paid to KL-6 in PE. When studying KL-6, the Japanese researcher Kohno[8] detected KL-6 levels in the PE of 17 patients with lung adenocarcinoma and found that 82% (14/17) of the pKL-6 levels were higher than 520 U/mL (258 + 2*131U/mL, mean + 2SD of KL-6 levels in serum of 160 normal individuals) but did not statistically compare or analyze the ROC curve of KL-6 in MPE and BPE. In this study, 78% (71/91) of malignant PE KL-6 levels were higher than 500 U/mL (considered in the reagent manual as healthy), similar to previous studies. Meanwhile, the MPE group exhibited a significantly higher pKL-6 level than the BPE group. The reason for this may be that elevated KL-6 levels in MPE are caused by KL-6 released from tumor cells entering the PE or by KL-6 entering the PE from the alveolar cavity due to damage to the alveolar-capillary membrane and damage to the alveolar epithelial cells. In addition, KL-6 may be associated with lung cancer infiltration and metastasis,[29] further leading to an increase in KL-6 in MPE.

FIGURE 2. Receiver operating characteristic of parameters for diagnosis of malignant pleural effusion (MPE). The area under the curve (AUC) of pleural effusion KL-6 (pKL-6)/ pleural effusion adenosine deaminase (pADA) + pleural effusion carcinoembryonic antigen (pCEA)/pADA (0.992) was higher than the AUCs of pKL-6 (0.903), pCEA (0.981), pADA (0.754), pKL-6/pADA (0.943), and pCEA/pADA (0.991).

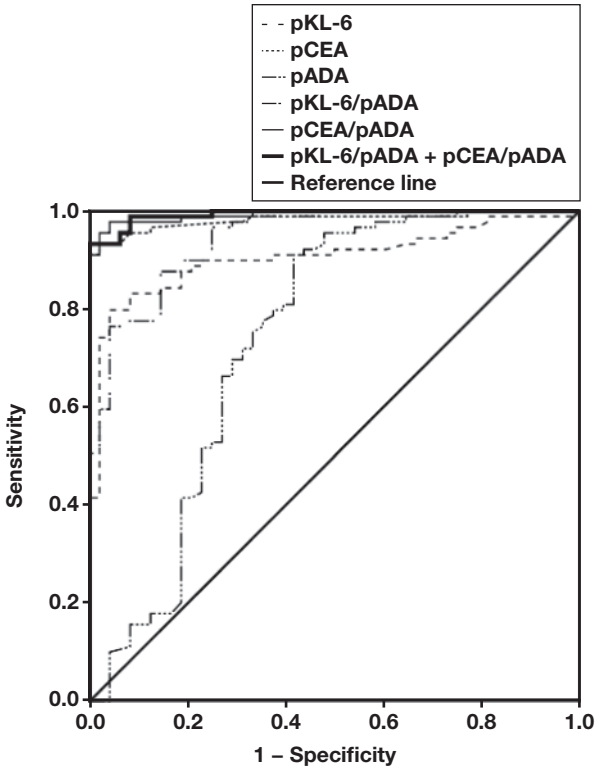

This study found through ROC curve analysis that when the cutoff of pKL-6 was 437.99 U/mL, the AUC for distinguishing NSCLC-induced MPE was 0.903, with specificity and sensitivity of 96.15% and 80.22%, respectively. The pCEA in this study is a routine clinical PE detection item,[30,31] and its diagnostic accuracy (AUC = 0.981) is also higher than pKL-6. After the ratios of pKL-6, pADA, and pCEA were combined for detection, it was found that although the sensitivity of pKL-6/pADA + pCEA/pADA (93.26%) was lower than that of pCEA (95.56%) and pCEA/pADA (97.75%), the specificity (100%) was higher than that of pCEA (95.83%) and pCEA/pADA (95.83%). The AUC (0.992) of pKL-6/pADA + pCEA/pADA is higher than that of pCEA (0.981), and slightly higher than that of pCEA/pADA (0.991). Overall, pKL-6/pADA + pCEA/pADA is more suitable for identifying NSCLC-induced MPE. This is the first report on using pKL-6/pADA and pCEA/pADA combined detection to identify NSCLC-induced MPE in BPE.

The limitation of this study is that the selected samples come from a part of the same hospital, and there will be selection bias. The biomarkers studied have false positives and false negatives, which cannot replace the "gold standard" effect of pathological examination. In the future, it is necessary to increase the sample size and expand the research area, combined with other tests, to reduce the impact of selection bias and biomarker limitations.

TABLE 2. The area under the curve (AUC), cut-off value, sensitivity, and specificity of parameters for the diagnosis of malignant pleural effusion

Parameter	AUC	95% CI	*P*	Cutoff	Sensitivity (%)	Specificity (%)
pKL-6, U/mL	0.903	0.843-0.962	.000	437.99	80.22	96.15
pCEA, ng/mL	0.981	0.958-1.000	.000	3.01	95.56	95.83
pADA, U/L	0.754	0.644-0.864	.000	23.2	91.11	54.90
pFer, μg/L	0.554	0.445-0.664	.340	1296.3	47.30	71.11
pCA125, U/mL	0.687	0.591-0.784	.001	2347.1	42.50	97.78
pCA199, U/mL	0.727	0.634-0.820	.000	8.5	53.57	93.18
sCRP, mg/L	0.749	0.652-0.845	.000	36.2	79.78	67.35
pWBC, 10^3/μL	0.534	0.416-0.652	.547	0.67	80.00	38.46
pRBC, 10^3/μL	0.664	0.565-0.763	.004	18.88	38.89	94.23
pKL-6/pADA	0.943	0.902-0.983	.000	46.05	76.67	94.12
pCEA/pADA	0.991	0.980-1.000	.000	0.18	97.75	95.83
pKL-6/pADA + pCEA/pADA	0.992	0.981-1.000	.000	0.870	93.26	100.00

pADA, pleural effusion adenosine deaminase; pCA, pleural effusion carbohydrate antigen; pCEA, pleural effusion carcinoembryonic antigen; pFer, pleural effusion ferritin; pKL-6, pleural effusion KL-6; pRBC, pleural effusion red blood cell; pWBC, pleural effusion white blood cell; sCRP, serum C-reactive protein.

TABLE 3. Relationship between the levels of pKL-6 and clinicopathologic factors in patients with non–small cell lung cancer

Clinical variable	Number	pKL-6 (U/mL)[a]	Mann-Whitney *U* test	*P*
Age, y			810.500	.761
>60	65	1261.00 (538.75, 3935.06)		
≤60	26	1224.50 (487.50, 2916.44)		
Gender			893.500	.480
Male	56	1217.40 (472.50, 3754.44)		
Female	35	1285.00 (691.00, 3126.00)		
Smoking status			993.000	.866
Smoker	39	1391.00 (507.60, 3966.92)		
Nonsmoker	52	1087.55 (551.99, 3080.65)		
Histological type			107.000	.060
Squamous cell carcinoma	5	507.60 (186.33, 1044.45)		
Adenocarcinoma	86	1338.00 (538.82, 3453.46)		
Lymph node metastasis			622.000	.727
Positive	73	1261.00 (518.00, 3121.50)		
Negative	18	1297.71 (558.38, 4591.03)		
Distant metastases			550.000	.420
Positive	74	1244.75 (538.82, 3919.13)		
Negative	17	1550.14 (204.00, 2759.06)		

[a]*The values in parentheses represent 25th quantiles (P25) and 75th quantiles (P75). The values not in parentheses represent medians.*

Conclusion

In summary, the measurement of pKL-6 can distinguish NSCLC-induced MPE from BPE. In addition, the determination of pKL-6 is useful, simple, and fast, and is expected to become a tumor marker for diagnosing NSCLC-induced MPE. On the other hand, the combined detection of pKL-6/pADA and pCEA/pADA can greatly improve the diagnostic efficiency for distinguishing NSCLC-induced MPE.

Funding

Key Laboratory of Clinical Laboratory Diagnosis and Translational Research of Zhejiang Province (2022E10022).

Conflict of Interest Disclosure

The authors have nothing to disclose.

REFERENCES

1. Siegel RL, Miller KD, Fuchs HE, Jemal A. Cancer statistics, 2021. *CA Cancer J Clin.* 2021;71(1):7-33. https://doi.org/10.3322/caac.21654
2. Bibby AC, Dorn P, Psallidas I, et al. ERS/EACTS statement on the management of malignant pleural effusions. *Eur Respir J.* 2018;52(1):1800349. https://doi.org/10.1183/13993003.00349-2018
3. Dorry M, Davidson K, Dash R, et al. Pleural effusions associated with squamous cell lung carcinoma have a low diagnostic yield and a poor prognosis. *Transl Lung Cancer Res*. 2021;10(6):2500-2508. https://doi.org/10.21037/tlcr-21-123
4. Taghizadeh N, Fortin M, Tremblay A. US hospitalizations for malignant pleural effusions: data from the 2012 national inpatient sample. *Chest.* 2017;151(4):845-854. https://doi.org/10.1016/j.chest.2016.11.010
5. Porcel JM, Gasol A, Bielsa S, Civit C, Light RW, Salud A. Clinical features and survival of lung cancer patients with pleural effusions. *Respirology.* 2015;20(4):654-659. https://doi.org/10.1111/resp.12496
6. Tang Y, Wang Z, Li Z, et al. High-throughput screening of rare metabolically active tumor cells in pleural effusion and peripheral blood of lung cancer patients. *Proc Natl Acad Sci U S A.* 2017;114(10):2544-2549. https://doi.org/10.1073/pnas.1612229114
7. Yang Y, Liu YL, Shi HZ. Diagnostic accuracy of combinations of tumor markers for malignant pleural effusion: an updated meta-analysis. *Respiration.* 2017;94(1):62-69. https://doi.org/10.1159/000468545
8. Kohno N, Akiyama M, Kyoizumi S, Hakoda M, Kobuke K, Yamakido M. Detection of soluble tumor-associated antigens in sera and effusions using novel monoclonal antibodies, KL-3 and KL-6, against lung adenocarcinoma. *Jpn J Clin Oncol.* 1988;18(3):203-216. https://doi.org/10.1093/oxfordjournals.jjco.a039239
9. Tomita M, Ayabe T, Chosa E, Nose N, Nakamura K. Prognostic significance of a tumor marker index based on preoperative serum carcinoembryonic antigen and Krebs von den Lungen-6 levels in non-small cell lung cancer. *Asian Pac J Cancer Prev.* 2017;18(1):287-291. https://doi.org/10.22034/APJCP.2017.18.1.287
10. Zheng M, Lou A, Zhang H, Zhu S, Yang M, Lai W. Serum KL-6, CA19-9, CA125 and CEA are diagnostic biomarkers for rheumatoid arthritis-associated interstitial lung disease in the Chinese population. *Rheumatol Ther*. 2021;8(1):517-527. https://doi.org/10.1007/s40744-021-00288-x
11. Yatsuyanagi E, Sato K, Sato K. Immunohistochemical analysis of Krebs von den Lungen-6 (KL-6) expression in lung tissue in primary lung cancer patients with high serum KL-6 levels. *Kyobu Geka*. 2015;68(10):815-819.
12. Tomita M, Ayabe T, Chosa E, Nose N, Nakamura K. Prognostic significance of preoperative serum Krebs von den Lungen-6 level in non-small cell lung cancer. *Gen Thorac Cardiovasc Surg.* 2016;64(11):657-661. https://doi.org/10.1007/s11748-016-0706-4
13. Chen X, Zhang N, Dong J, Sun G. Reactive oxygen species modulator 1, a novel protein, combined with carcinoembryonic antigen in differentiating malignant from benign pleural effusion. *Tumour Biol.* 2017;39(5):1010428317698378. https://doi.org/10.1177/1010428317698378
14. Elmas H, Biancosino C, Önal B, et al. Combination of biochemical and cytological findings for better diagnosis in pleural effusions. *Adv Exp Med Biol.* 2022;1374:51-62. https://doi.org/10.1007/5584_2021_703

15. Dixit R, Agarwal KC, Gokhroo A, et al. Diagnosis and management options in malignant pleural effusions. *Lung India*. 2017;34(2):160-166. https://doi.org/10.4103/0970-2113.201305
16. Zhou S, Xu B, Qi L, Zhu D, Liu B, Wei J. Next-generation sequencing reveals mutational accordance between cell-free DNA from plasma, malignant pleural effusion and ascites and directs targeted therapy in a gastric cancer patient. *Cancer Biol Ther.* 2019;20(1):15-20. https://doi.org/10.1080/15384047.2018.1504720
17. Porcel JM, Civit C, Esquerda A, Salud A, Bielsa S. Utility of CEA and CA 15-3 measurements in non-purulent pleural exudates in the diagnosis of malignancy: a single-center experience. *Arch Bronconeumol.* 2017;53(8):427-431. https://doi.org/10.1016/j.arbres.2016.12.013
18. Yang Q, Zhang P, Wu R, Lu K, Zhou H. Identifying the best marker combination in CEA, CA125, CY211, NSE, and SCC for lung cancer screening by combining ROC curve and logistic regression analyses: is it feasible? *Dis Markers.* 2018;2018:2082840. https://doi.org/10.1155/2018/2082840
19. Guo J, Yu J, Song X, Mi H. Serum CA125, CA199 and CEA combined detection for epithelial ovarian cancer diagnosis: a meta-analysis. *Open Med (Wars)*. 2017;12:131-137. https://doi.org/10.1515/med-2017-0020
20. Yu JF, Jin YB, He J, An Y, Li ZG. Changes of serum Krebs von den Lungen-6 levels in interstitial lung disease associated with dermatomyositis and secondary Sjögren's syndrome: a case report. *Beijing Da Xue Xue Bao.* 2017;49(5):910-914. https://doi.org/10.3969/j.issn.1671-167X.2017.05.030
21. Sato S, Kato T, Abe K, et al. Pre-operative evaluation of circulating KL-6 levels as a biomarker for epithelial ovarian carcinoma and its correlation with tumor MUC1 expression. *Oncol Lett*. 2017;14(1):776-786. https://doi.org/10.3892/ol.2017.6254
22. Nakao M, Oguri T, Miyazaki M, et al. Diagnosis of ovarian cancers using thoracoscopy: three case reports and review of the literature. *Exp Ther Med*. 2012;4(1):141-145. https://doi.org/10.3892/etm.2012.541
23. Inagaki Y, Xu H, Nakata M, et al. Clinicopathology of sialomucin: MUC1, particularly KL-6 mucin, in gastrointestinal, hepatic and pancreatic cancers. *Biosci Trends*. 2009;3(6):220-232.
24. Xu H, Inagaki Y, Seyama Y, et al. Expression of KL-6/MUC1 in pancreatic cancer tissues and its potential involvement in tumor metastasis. *Oncol Rep.* 2011;26(2):371-376. https://doi.org/10.3892/or.2011.1315
25. Tezuka K, Miura K, Nakano Y, et al. Interstitial lung disease associated with adjuvant and neoadjuvant chemotherapy in early breast cancer. *World J Surg Oncol.* 2021;19(1):169. https://doi.org/10.1186/s12957-021-02289-0
26. Onoyama T, Matsumoto K, Koda H, et al. Diagnostic usefulness of KL-6 concentration of bile in biliary tract cancer. *Mol Clin Oncol*. 2018;8(4):561-566. https://doi.org/10.3892/mco.2018.1571
27. Zhang K, Zhou C, Gao J, et al. Treatment response and safety of immunotherapy for advanced non-small cell lung cancer with comorbid chronic obstructive pulmonary disease: a retrospective cohort study. *Transl Lung Cancer Res*. 2022;11(11):2306-2317. https://doi.org/10.21037/tlcr-22-667
28. d'Alessandro M, Bergantini L, Cameli P, et al. Serum concentrations of KL-6 in patients with IPF and lung cancer and serial measurements of KL-6 in IPF patients treated with antifibrotic therapy. *Cancers*. 2021;13(4):689. https://doi.org/10.3390/cancers13040689
29. Shoji F, Yamazaki K, Kouso H, Mori R, Takeo S. Predictive impact for postoperative recurrence of preoperative serum Krebs von den Lungen-6 concentration in pathologic stage IA non-small cell lung cancer. *Ann Thorac Surg.* 2016;101(5):1903-1908. https://doi.org/10.1016/j.athoracsur.2015.11.066
30. Cheng C, Yang Y, Yang W, Wang D, Yao C. The diagnostic value of CEA for lung cancer-related malignant pleural effusion in China: a meta-analysis. *Expert Rev Respir Med*. 2022;16(1):99-108. https://doi.org/10.1080/17476348.2021.1941885
31. Wang S, Tian S, Li Y, et al. Development and validation of a novel scoring system developed from a nomogram to identify malignant pleural effusion. *EBioMedicine*. 2020;58:102924. https://doi.org/10.1016/j.ebiom.2020.102924

Genetic analysis of *TMPRSS6* catalytic domain variants in Mexican patients with iron treatment refractoriness

Rubiceli Hernández-Peña,[1,2] Eric Jonathan Maciel-Cruz,[1,2] Lourdes Del Carmen Rizo-De La Torre, PhD,[3] Francisco Javier Perea-Díaz, PhD,[2] Bertha Ibarra-Cortés, PhD[4]

[1]Doctorado en Genética Humana, Centro Universitario de Ciencias de la Salud, Universidad de Guadalajara, Guadalajara, México, [2]División de Genética, Centro de Investigación Biomédica de Occidente, Instituto Mexicano del Seguro Social, Guadalajara, México, [3]División de Medicina Molecular, Centro de Investigación Biomédica de Occidente, Instituto Mexicano del Seguro Social, Guadalajara, México, [4]Instituto de Genética Humana "Dr. Enrique Corona Rivera," Centro Universitario de Ciencias de la Salud, Universidad de Guadalajara, Guadalajara, México. Corresponding author: Bertha Ibarra Cortés; bibarrac2012@gmail.com

Key words: matriptase-2; anemia; iron deficiency; bioinformatic; thalassemia; IRIDA

Abbreviations: PCR, polymerase chain reaction; IDA, iron deficiency anemia; IRIDA, iron refractory IDA; RBC, red blood cells; Hb, hemoglobin; MCV, mean corpuscular volume; MCH, mean corpuscular hemoglobin; TSAT, transferrin saturation; NCBI, National Center for Biotechnology Information; PBI, with possible biological impact; WBI, without biological impact; MAF, minor allele frequency

Laboratory Medicine 2024;55:277-284; https://doi.org/10.1093/labmed/lmad077

ABSTRACT

Objective: To identify the *TMPRSS6* gene variants in Mexican patients with iron treatment refractoriness, to describe hematological and iron profile parameters, and to use bioinformatic prediction and protein modeling tools to assess a possible biological impact for the detected missense variants.

Methods: Nineteen patients referred with iron treatment refractoriness were studied. Peripheral blood was collected to determine hematic cytometry, iron profile, hemoglobin electrophoresis, and quantification. Molecular screening was carried out for exons 15 through 18 of the *TMPRSS6* gene by Sanger sequencing and for frequent thalassemia variants by amplification-refractory mutation system-polymerase chain reaction (PCR) and gap-PCR. The biological impact of the detected missense variants was assessed using bioinformatic prediction and protein modeling tools.

Results: We found 5 genetic variants in the matriptase-2 catalytic domain: 1 at intron-15/exon-16 junction (rs60484081) and 4 exonic, 3 missense (rs377054987, p.Gly626Asp; rs1384127820, p.Ser672Thr; rs855791, p.Val727Ala) and 1 synonymous (rs2235321, p.Tyr730=), with frequencies ranging from 0.18 to 0.53. No significant differences were observed in the hematological parameters or iron profile, considering type and number of variants. Bioinformatic predictions suggested a possible biological impact only for rs377054987.

Conclusions: The *TMPRSS6* variants observed in Mexican patients with oral iron treatment refractoriness have high frequencies; nevertheless, their relationship with hematological and iron profile parameters needs further research. The possible biological impact for rs377054987 is due to size and amino acid hydrophobicity changes and hydrogen bond modifications.

Introduction

Iron deficiency anemia (IDA) is the most common type of nutritional deficiency anemia worldwide, particularly in developing countries.[1] Additional causes of iron loss are iron malabsorption, chronic anemia, surgical procedures, gastrointestinal pathologies, occult blood loss, and others.[2,3] Although most patients are successfully treated with oral iron, some are refractory to iron treatment by this administration route, causing iron refractory IDA (IRIDA) and only partially respond to parenteral treatment. This characteristic has been associated with *TMPRSS6* gene variants.[4,5]

The *TMPRSS6* gene codes for matriptase-2, a transmembrane serine protease of the hepatocyte, which cleaves hemojuvelin to downregulate hepcidin synthesis. It is considered the key regulator of iron homeostasis.[6] Matriptase-2 consists of 5 different domains: transmembrane (TM); sperm protein, enterokinase, and agrin; complement C1r/C1s, Uegf, Bmp1; low-density lipoprotein receptor; and the catalytic domain named peptidase S1,[7,8] which is the domain with the highest reported variation in ClinVar. To date, 4 isoforms have been described: isoforms 1 (low expression) and 2 (major expression) are enzymatically active; isoforms 3 and 4 have altered proteolytic functions and present dominant-negative activity, and little is known about their biological role. Thus, isoform 2 presents the main biological activity.[7,9]

In the *TMPRSS6* gene, some variants have been associated with hepcidin upregulation[10] and observed in subjects with oral iron treatment refractoriness.[11] In addition, these variants can modify

hematological and iron profile parameters, such as red blood cells (RBC), hemoglobin (Hb), mean corpuscular volume (MCV), mean corpuscular hemoglobin (MCH), serum iron, transferrin saturation (TSAT), and serum ferritin.[12,13] Most *TMPRSS6* studies exclude patients with IDA, thalassemia, chronic pathologies, and cancer.[14,15] Nevertheless, to the best of our knowledge, a single study regarding the coexistence of refractoriness to iron treatment and thalassemia has been reported.[16]

According to ClinVar, 201 *TMPRSS6* gene variants have been described: 17 pathogenic, 7 likely pathogenic, 89 with uncertain significance, 24 likely benign, 56 benign, and 8 with contradictory interpretations. Thirty-seven variants are clustered at the peptidase S1 domain. In our population, the *TMPRSS6* gene variants have not yet been studied. The polymorphism rs855791 (T>C) has been studied in several populations, and despite having a benign clinical significance, studies in Chinese and Polish populations have reported lower Hb, MCV, and MCH in the presence of the wild-type allele[12,17] and vice versa in the Thai population.[16]

The aim of this study was to identify the *TMPRSS6* gene variants corresponding to the catalytic domain of the matriptase-2 in Mexican patients with iron treatment refractoriness, to describe hematological and iron profile parameters, and to use bioinformatic prediction and protein modeling tools to assess a possible biological impact for the detected missense variants.

Materials and Methods

Study Patients

The study included 19 patients with a mean age of 35.5 ± 14.7 years (18 females), who were referred by the hematology services of diverse Mexican health institutions (Instituto Mexicano del Seguro Social, Instituto de Seguridad y Servicios Sociales de los Trabajadores del Estado, and Hospital General de Occidente), from March 2019 to April 2022, with iron deficiency and refractoriness to iron treatment, defined as <1 g/dL increase in Hb after 4 to 6 weeks of oral iron treatment at a daily dose of 3 mg/kg. Additional clinical data were obtained from the electronic medical record. All patients or guardians of minors signed an informed consent letter. The project was approved by the Institutional Review Board.

Hematological and Biochemical Profile Parameters

Peripheral blood was collected in serum tubes with separating gel and with EDTA. Hematological parameters were obtained by cytometry: RBC, Hb, MCV, MCH, and mean corpuscular hemoglobin concentration. For the iron profile, serum iron and total iron-binding capacity were obtained by colorimetry, serum transferrin by immunoturbidimetry, and serum ferritin by chemiluminescence. Other tests included alkaline electrophoresis of Hb, fetal hemoglobin determination by Singer's alkaline denaturation test, and HbA2 quantification by diethylaminoethyl microchromatography.[18]

Molecular Screening

DNA was isolated by the salting-out procedure.[19] Exons 15 through18 (including adjacent intronic ends) of the *TMPRSS6* gene, which code for the matriptase-2 catalytic domain, were analyzed by Sanger sequencing, using previously described primers[20] (BigDye Terminator v3.1; Applied Biosystems). Chromosome 22q12.3 sequence (RefSeq: NG_012856.2) was used as a reference. All patients were screened for frequent thalassemia variants (NG_000006.1:g.34164_37967del3804, NG_000006.1:g.26264_45564del19301, NG_000006.1:g.11684_43534del31851, HBA2:c.-59C>T, HBA2:c.95 + 2_95 + 6delTGAGG, HBB:c.1A>G, HBB:c.118C>T, HBB:c.92 + 1G>A, HBB:c.92 + 5G>A, HBB:c.93-21G>A, and NG_000007.3:g.60375_153285del92911) by gap or amplification-refractory mutation system-PCR as previously reported by Rizo-de la Torre et al.[21] Descriptive and comparative analysis of hematological and iron parameters were performed using IBM SPSS Statistics v.29. Linkage disequilibrium analysis was carried out using SNPStats online software.[22]

Bioinformatic Analysis

Protein (NP_001361433.1) and nucleotide (NM_001374504.1) sequences were obtained from the National Center for Biotechnology Information (NCBI). The peptidase S1 domain model was predicted through the Phyre2 webserver using an intensive mode,[23] model refinement was made with ModRefiner,[24] and the ERRAT server was used to check the model quality.[25] Ten pathogenicity prediction tools were used: PROVEAN,[26] SIFT,[27] PredictSNP,[28] Mutation Taster,[29] PolyPhen2,[30] SNAP2,[31] Mut Pred,[32] AlignGVGD,[33] Project HOPE,[34] and Missense3D.[35] Each platform allows a prediction depending on a specific algorithm and considering each variant differently ("neutral," "benign," "deleterious," "damaging," "structural damage detected," etc). Thus, we categorized those with or without a possible pathogenic effect, as "with possible biological impact" (PBI) or "without biological impact" (WBI), respectively. Amino acid substitutions and structural modification analysis were generated through UCSF Chimera[36] using the highest probability position, final energy minimization, and hydrogen bonds analysis.

Results

Hematological and Iron Profile Parameters

Hematological and iron profiles in the studied patients showed decreased values of Hb (9.9 ± 1.7 g/dL), MCV (69.6 ± 6.2 fL), MCH (21.0 ± 2.8 pg), serum iron (23.1 ± 10.2 μg/dL), TSAT (5.3 ± 2.3%), and serum ferritin (median 8.0 [0.9-214.3] ng/mL) (**TABLE 1**). Additional clinical data related to other causes of iron deficiency and iron treatment refractoriness were intentionally investigated. Only 6 patients had a gastrointestinal disorder. Also, of the screened thalassemia alleles, 6 patients had alpha-thalassemia and 1 had beta-thalassemia (**TABLE 1**). The hematological parameters and iron profile data were analyzed considering the type and number of the observed variants, and no significant statistical differences ($P > .05$) were found, not even in the presence of thalassemic alleles or gastrointestinal disorders.

Molecular Screening

In the sequence analysis of exons 15 through18 (including adjacent intronic ends) of the *TMPRSS6* gene, 5 variants were found: 1 intronic and 4 exonic. In the intron-15/exon-16 junction, 7 patients were heterozygous for a pentanucleotide deletion (CCCCA) in a 6 short tandem repeat adjacent to the acceptor site (rs60484081, c.1842-31delCCCCA[1]; **TABLE 1**). This previously unreported allele has a minor allele frequency (MAF) of 0.18 in our study group.

In exon 16, 2 missense variants in the heterozygous state were observed in 15 patients: rs377054987 (c.1877G>A) and rs1384127820 (c.2014T>A) (**TABLE 1**). The latter was previously reported as T>C,

TABLE 1. Hematological and iron profiles and *TMPRSS6* variants of patients with iron treatment refractoriness

P	Age (y)	Hematological profile					Iron profile					*TMPRSS6* variants				Thalassemia variant	GI disorder
		RBC ($x10^6$/µL)	Hb (g/dL)	MCV (fL)	MCH (pg)	MCHC (%)	Iron (µg/dL)	TIBC (µg/dL)	TSAT (%)	Ferritin (ng/mL)	TF (mg/dL)	Intron 15 rs60484081	Exon 16 rs377054987 (G>A) rs1384127820 (T>A)	Exon 17 rs855791 (T>C)	Exon 17 rs2235321 (C>T)		
1	46	4.60	9.4	65.8	20.3	30.9	19	391	4.9	4.8	322	*	G/A T/A	T/C	*	HBB:c.1A>G	–
2	7	5.45	11.3	65.5	20.7	31.6	34	345	9.9	105.8	239	5/6	G/A T/A	T/C	C/T	g.34164_37967del3804 + HBA2:c.95 + 2_95 + 6delTGAGG	–
3	38	4.57	8.6	68.7	18.9	27.6	13	378	3.4	2.8	325	5/6	G/A T/A	C/C	C/T	HBA2:c.95 + 2_95 + 6delTGAGG	–
4	31	3.09	7.2	76.1	23.3	30.7	13	419	3.1	20.2	345	*	G/A T/A	T/C	*	HBA2:c.-59C>T	–
5	32	5.11	12.6	77.2	24.7	32.0	22	418	5.3	2.7	325	5/6	G/A T/A	T/C	C/T	*	+
6	43	4.68	10.2	65.4	21.9	33.5	20	451	4.4	0.9	360	5/6	G/A T/A	C/C	C/T	*	–
7	39	5.06	11.6	71.9	22.9	31.9	46	573	8.0	8.4	369	*	G/A T/A	C/C	*	*	–
8	44	4.61	11.3	78.0	24.6	31.5	25	463	5.4	3.7	342	5/6	G/A T/A	T/C	C/T	*	–
9	39	4.81	11.3	72.0	23.6	32.7	44	424	10.4	37.9	342	*	G/A T/A	T/C	C/T	*	–
10	10 mo	5.79	8.7	54.4	15.0	27.5	23	470	4.9	4.1	375	*	G/A T/A	T/C	*	*	–
11	34	4.30	9.0	73.5	21.0	28.6	22	432	5.1	9.5	320	*	G/A T/A	*	*	g.34164_37967del3804	+
12	38	4.25	8.9	71.7	20.9	29.2	16	280	5.7	214.3	187	5/6	G/A T/A	*	*	*	+
13	51	4.20	8.6	71.0	20.5	28.8	17	544	3.1	0.9	406	*	G/A T/A	*	*	*	+
14	36	4.89	7.3	59.5	15.0	25.2	16	550	2.9	8.1	455	*	G/A T/A	*	*	*	+
15	49	5.81	12.5	68.7	21.6	31.4	31	393	7.9	15.8	296	*	G/A T/A	*	*	*	–
16	31	4.42	10.9	78.7	24.6	31.3	33	513	6.4	2.6	407	5/6	*	C/C	C/T	g.34164_37967del3804	–
17[a]	13	4.19	8.4	67.7	20.0	29.6	10	414	2.4	3.2	324	*	*	C/C	*	*	–
18	46	5.62	11.1	66.9	19.7	29.4	19	498	3.8	8.0	408	*	*	T/C	*	*	+
19	57	4.65	9.2	70.3	19.9	28.3	15	421	3.6	12.6	369	*	*	*	*	HBA2:c.-59C>T	–
Total	35.5 ± 4.7	4.7 ± 0.7	9.9 ± 1.7	69.6 ± 6.2	21.0 ± 2.8	30.1 ± 2.1	23.1 ± 10.2	440.9 ± 73.1	5.3 ± 2.3	8.0 (0.9-214.3)	343.0 ± 60.1	5/6 = 7	G/A + T/A = 15	T/C = 8 C/C = 5	C/T = 7	α-thalassemia = 6 β-thalassemia = 1	+ = 6

GI, gastrointestinal; Hb, hemoglobin; MCV, mean corpuscular volume; MCH, mean corpuscular Hb; MCHC, MCH concentration; P, patient; RBC, red blood cells; TF, transferrin; TIBC, total iron binding capacity; TSAT, transferrin saturation.

[a]*Male.*

**Wild-type homozygous genotype positive for GI disorder (+). P5: gastroesophageal reflux disorder, gastritis; P11: rectal bleeding; P12: gastritis, gastric polyp; P13: upper gastrointestinal bleeding; P14: feces occult blood; P18: gastritis.*

both with MAF = 0.39 and in linkage disequilibrium (r = .999, P = .000). Two variants were detected at exon 17 (**TABLE 1**): (1) a missense variant, rs855791 (c.2180T>C), observed in 8 heterozygous and 5 homozygous patients; and (2) a synonymous variant, rs2235321 (c.2190C>T), observed in 7 heterozygous patients. Their MAFs were 0.53 and 0.21, respectively. Variants rs60484081 and rs2235321 were also observed in linkage disequilibrium (r = .933, P = .000). Exons 15 and 18 were normal in all patients.

Bioinformatic Analysis

For the 3 missense variants, in silico results showed that 8 of 9 platforms considered the p.Gly626Asp variant (rs377054987) as PBI; only Mutation Taster considered this variant WBI. For the p.Ser672Thr (rs1384127820) and p.Val727Ala (rs855791) variants, only PolyPhen2 and AlignGVGD considered them as PBI (**FIGURE 1**). These 3 variants presented amino acid size modification and were located in the peptidase S1 domain (**TABLE 2**); however, additional bioinformatic predictions were carried out solely for variant p.Gly626Asp.

For peptidase S1 domain modeling, Phyre2 scored >90% confidence for >92% of the residues, including the regions of interest where variants were found. The overall quality factor for this model was 92, which is considered by ERRAT to be highly favorable. For the p.Gly626Asp variant, HOPE's predictions are more specific in terms of the physicochemical amino acid properties (modification in charge, size, and hydrophobicity), in addition to the fact that the loss of glycine flexibility was considered to affect protein folding. Missense3D predicted a buried

FIGURE 1. In silico prediction for missense variants of peptidase S1domain isoform 2. PBI, with probable biological impact; WBI, without biological impact.

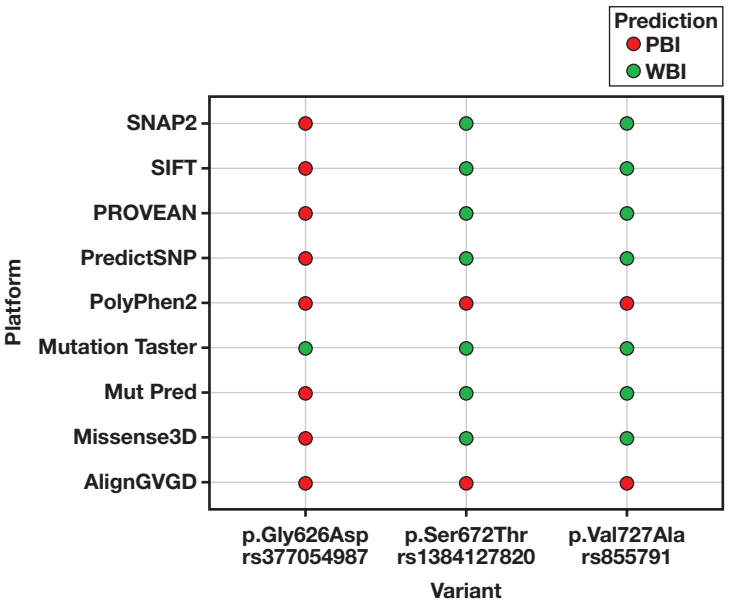

FIGURE 2. Structural snapshot of p.Gly626Asp hydrogen bond modifications in isoform 2. Residue 86 corresponds to residue 626 in the full protein. A, Green ribbons correspond to wild-type amino acids. B, Red ribbons correspond to variant type amino acids. Yellow lines correspond to hydrogen bonds; alpha-helices are in red and beta-sheets are in blue.

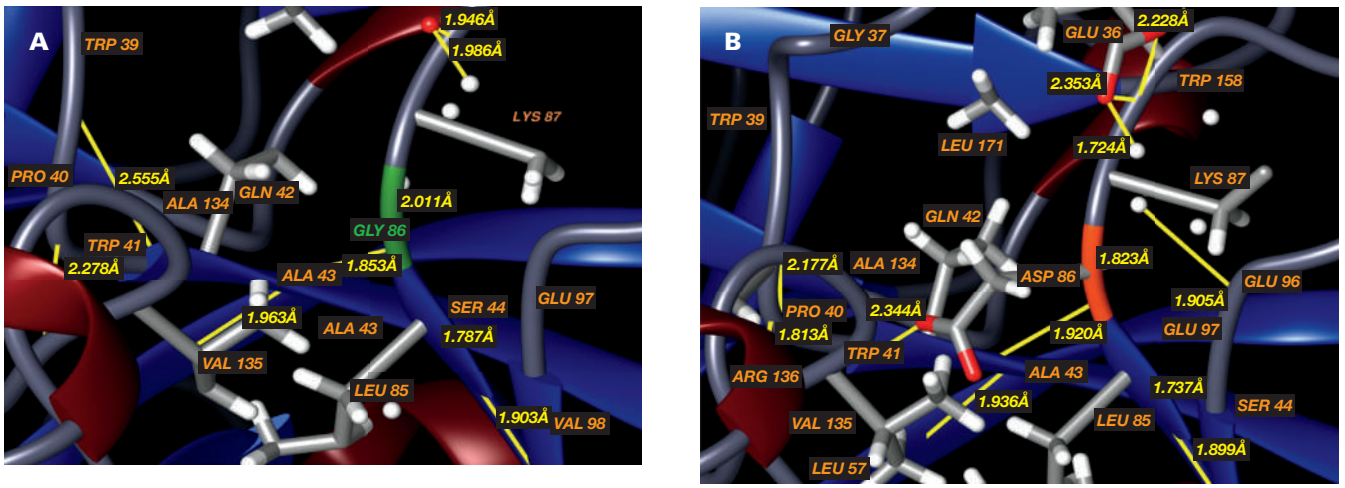

2024;55:277-284 | https://doi.org/10.1093/labmed/lmad077

TABLE 2. HOPE and Missense3D variant predictions for peptidase S1 domain isoform 2

	p.Gly626Asp	p.Ser672Thr	p.Val727Ala
HOPE			
Amino acid properties	VR is bigger than WR. WR charge is neutral, VR charge is negative. WR is more hydrophobic than VR. WR is buried in the core; VR charge and size might lead to protein misfolding.	VR is bigger than WR residue. WR is located in the surface of the protein; VR might disturb interaction with other molecules.	VR is smaller than WR. VR might cause a loss of external interactions.
Structure	Variation is in the peptidase S1 domain, which is the main domain for the protein activity; VR aa properties might disturb and abolish its function. WR is Gly, the most flexible of all residues. Lack of VR flexibility might disturb protein function.	Variant is located in the peptidase S1 domain, which is the main domain for the protein activity; VR aa properties might disturb and abolish its function.	Variant is located in the peptidase S1 domain, which is the main domain for the protein activity; VR aa properties might disturb and abolish its function.
Missense3D	Buried charge introduced; this substitution replaces a buried uncharged residue (Gly, RSA 5.9%) with a charged residue (Asp). Buried Gly replaced; this substitution replaces a buried Gly residue (RSA 5.9%) with a buried Asp residue (RSA 4.9%). Gly in a bend; this substitution replaces glycine originally located in a bend curvature.	No structural damage was observed.	No structural damage was observed.

RSA, relative solvent accessibility; VR, variant-type residue; WR, wild-type residue.

negative charge introduced as a replacement for the wild-type neutral charge, and a buried wild-type Gly replacement for the Asp variant; however, no structural damage was observed for the other 2 variants (**TABLE 2**). Additionally, Chimera's structural visualization revealed multiple modifications in hydrogen bonds (length, number, and involved atoms) between the wild type and the variant type (**FIGURE 2**).

Discussion

This is the first approach to screen the 15 to 18 exons (including adjacent intronic ends) of the *TMPRSS6* gene corresponding to the matriptase-2 catalytic domain in Mexican patients with iron treatment refractoriness. Five variants were observed in the intron-15/exon-16 junction, exon 16, and exon 17 with minor allele frequencies from 0.18 to 0.53 in this selected population. These variants were analyzed according to the hematological and iron profile findings in these patients, and missense variants were studied with bioinformatic prediction tools.

Hematological and Iron Profile Parameters

Hematological and iron profile analysis showed reduced MCV, MCH, serum iron, and TSAT in all 19 subjects, and Hb and ferritin were below normal levels in 17 and 13 patients, respectively (**TABLE 1**). Similar findings were observed in a study of Saudi women of reproductive age with IDA and IRIDA. Both groups had decreased RBC, Hb, MCV, and MCH as well as low serum iron and ferritin. Nevertheless, the IRIDA group presented more severe anemia (Hb 9.94 ± 1.64 vs 10.24 ± 1.94 g/dL) and lower serum iron (4.73 ± 2.75 vs 4.96 ± 3.78 μmol/L) and ferritin (6.21 ± 2.75 vs 6.56 ± 2.88 ng/mL) than the IDA group.[14] Also, a study in elderly Chinese women with anemia, abnormal iron profile, and *TMPRSS6* variants rs855791 and rs4820268 reported that wild-type allele carriers had decreased values for Hb, serum iron, ferritin, and transferrin.[12] In our study, hematological and iron profile data of rs855791 carriers (13/19) were no different than wild-type patients. Therefore, the effect of this *TMPRSS6* genetic variant on hematological and iron profile in patients with iron treatment refractoriness remains unknown.

We want to stress that our study group was mainly female (18/19) with a mean age of 35.5 ± 14.7 years, which could be a limitation because of iron loss by menstruation. It is known that iron deficiency in Mexican women in the general population of a similar age (20-49 years) is 25.7%.[37] However, our patients were selected because they do not respond to iron treatment, and no abnormal gynecological bleeding was reported in the electronic medical record.

In this study, 6 patients presented a gastrointestinal disorder that could explain the refractoriness to iron treatment, as previously suggested by Migone de Amicis et al[3] Moreover, it has been observed that *TMPRSS6* variants, such as rs855791, show a tendency to decrease Hb in children with celiac disease and anemia.[17] In our patients, despite some of them having variants in the catalytic domain of *TMPRSS6* and additional gastrointestinal disorders, no significant differences were observed regarding hematological or iron profile parameters. In the same way, in patients with α^{+}-thalassemia, the C allele of rs855791 was associated with high MCV (C/C: 81.5 ± 3.9 fL vs T/T: 77.8 ± 3.2 fL) and MCH (C/C: 26.5 ± 1.2 pg vs T/T: 25.6 ± 1.0 pg).[16] In our study, thalassemia alleles were observed in 7 patients; however, the statistical analysis of the studied parameters in patients with or without thalassemia was not significant (**TABLE 1**). Therefore, these patients were not excluded from our study. In the future, a larger number of patients should be analyzed for a better understanding of the biological effect of these variants in patients with iron treatment refractoriness or as a thalassemia modifier variant.

Molecular and Bioinformatic Analysis

Intron-15/Exon-16 Junction Variant

A 5-nucleotide deletion (CCCCA) was identified in the intron-15/exon-16 junction, corresponding to a short tandem repeat of 6 pentanucleotides. Deletion of 1 pentanucleotide has not been previously reported;

however, there are deletions of 2 to 5 repeats (rs60484081), and they are classified as of uncertain significance in IRIDA according to the Single Nucleotide Polymorphism Database of NCBI. In our patients, this variant was observed in co-inheritance with other variants; therefore, its role in hematological or iron profile parameters could not be established.

Exon 16 Variants

Two variants in exon 16 were found in linkage disequilibrium: rs377054987 and rs1384127820. These missense variants have low frequencies in other populations (<0.000)[38]; nevertheless, in this screened sample they were observed in high frequency, MAF = 0.39. To our knowledge, in previous *TMPRSS6* gene sequencing studies in patients with IDA or IRIDA, these variants have not been identified.[39,40]

According to NCBI, the pathogenicity of p.Gly626Asp (rs377054987) is unknown. Most of the bioinformatic platforms predict this variant with PBI. HOPE and Missense3D predicted deleterious effects given the amino acid modification and structural changes, such as size and hydrophobicity modifications. These properties possibly modify the structure or function of the protein.[41] As glycine is the most flexible amino acid, potentially any residue modification will affect the protein backbone.[42] According to Missense3D, the variant pathogenic effect, and possibly the biological activity, can be attributed to the substitution of glycine with aspartic acid. This modification introduces a negative charge in the core of the protein, a replacement in the bend curvature, and cavity modification. These effects are observed when the variant is located in a domain with cleavage of catalytic activity.[43,44]

Hydrogen bonds provide most of the protein structure, stability, and specificity for macromolecular interactions.[45] The domain activity is given by a charge relay system that involves hydrogen bonding of 3 amino acids (aspartic acid, histidine, and serine).[46] Aspartic acid physicochemical properties generate additional hydrogen bonds, which might affect the charge system and the protein function or contacts with other molecules, possibly decreasing the peptidase S1 domain activity and disturbing its interaction with hemojuvelin protein, and consequently affecting iron absorption and modifying hematological or iron profile parameters. This effect was not observed in our patients, probably due to the small sample size.

For the rs1384127820 (p.Ser672Pro), the only variant described is the c.2014T>C change, reported at ClinVar with uncertain significance, and no further studies were found. However, the observed p.Ser672Thr (c.2014T>A) was considered WBI according to the bioinformatic predictions performed, probably because both serine and threonine are substrates for kinases and no structural damage was observed by Missense3D (**TABLE 2**).

Exon 17 Variants

The rs855791 (T>C) has been studied in several populations. We found it in high frequency, MAF = 0.53. This single nucleotide variant was studied in IDA female Saudi students, and the T wild allele was associated with decreased serum iron and ferritin ($P < .05$).[13] However, this single nucleotide variant was not found to be related to serum iron levels in a Saudi study.[14] Nevertheless, in elderly Chinese women, the T allele was considered to be a risk factor for anemia, iron deficiency, and IDA (odds ration [OR] = 1.47, 95% CI = 1.07-2.00, $P = .02$; OR = 1.69, 95% CI = 1.40-1.98, $P \leq .001$; OR = 2.15, 95% CI = 1.68-2.61, $P = .001$; respectively).[12] In a recent study in α^{+}-thalassemia (-α/αα) and α^{0}-thalassemia (--/αα) patients, the C allele gradually expressed higher MCV and MCH values than those carriers of the T allele.[16] In patients with α-thalassemia alleles, no significant statistical differences were found in either allele, genotype, or inheritance models, likely due to the small sample size. Bioinformatic predictions considered this variant as WBI and no structural modification was observed, possibly because wild (valine) and variant (alanine) residues have similar physicochemical properties.

In addition, the synonymous rs2235321 has been associated with TSAT <10.0% in women with iron alterations ($P = .002$).[47] In this study, 6 of 7 carrier women had TSAT <10.0%, suggesting a similar effect.

We want to stress that bioinformatics tools are useful for predicting the pathogenic effect of a variant; however, they have their limitations, and it is necessary to continue investigating their biological impact in cell lines, large cohorts of patients, and family studies.

Conclusions

TMPRSS6 gene variants may modify hematological and iron profile parameters. The 5 genetic variants identified in this study have high frequencies (0.18-0.53); nevertheless, only rs855791 has been widely studied and considered as a risk factor for anemia, iron deficiency, and iron deficiency anemia. However, no statistical differences regarding the number or type of variants were found nor a clear trend in the parameters that constitute the hematological and iron profiles. Bioinformatics predictions suggested PBI only for rs377054987 (p.Gly626Asp) due to changes in amino acid size and hydrophobicity affecting protein function and hydrogen bond modifications disrupting macromolecular interactions. The sample size should be increased, and the remaining exons should also be included in further studies.

Acknowledgments

We thank CONACYT for R.H.P and E.J.M.C. scholarships for PhD degrees. This research was carried out in accordance with the ethical guidelines established in World Medical Association Declaration of Helsinki. The project was approved by the local Institutional Review Board. All patients or guardians of minors were fully informed and signed their voluntary informed consent. The protection of patient identity data was guaranteed.

Conflict of Interest Disclosure

The authors have nothing to disclose.

REFERENCES

1. World Health Organization. Nutritional anaemias: tools for effective prevention and control. World Health Organization; 2017. License: CC BY-NC-SA 3.0 IGO. https://apps.who.int/iris/handle/10665/259425
2. Camaschella C, Nai A, Silvestri L. Iron metabolism and iron disorders revisited in the hepcidin era. *Haematologica.* 2020;105(2):260-272. https://doi.org/10.3324/haematol.2019.232124
3. Migone De Amicis M, Rimondi A, Elli L, Motta I. Acquired refractory iron deficiency anemia. *Mediterr J Hematol Infect Dis*. 2021;13(1):e2021028. https://doi.org/10.4084/MJHID.2021.028
4. Xiong Y, Wu Z, Yang W, et al. A novel splicing mutation of TMPRSS6 in a Chinese child with iron-refractory iron deficiency anaemia. *Br J Haematol.* 2015;171(4):647-649. https://doi.org/10.1111/bjh.13416

5. Yaish HM, Farrell CP, Christensen RD, et al. Two novel mutations in TMPRSS6 associated with iron-refractory iron deficiency anemia in a mother and child. *Blood Cells Mol Dis.* 2017;65:38-40. https://doi.org/10.1016/j.bcmd.2017.04.002
6. Donker AE, Raymakers RA, Vlasveld LT, et al. Practice guidelines for the diagnosis and management of microcytic anemias due to genetic disorders of iron metabolism or heme synthesis. *Blood.* 2014;123(25):3873-3886; quiz 4005. https://doi.org/10.1182/blood-2014-01-548776
7. Dion SP, Désilets A, Lemieux G, Leduc R. Functionally impaired isoforms regulate TMPRSS6 proteolytic activity. *PLoS One.* 2022;17(8):e0273825. https://doi.org/10.1371/journal.pone.0273825
8. Paysan-Lafosse T, Blum M, Chuguransky S, et al. InterPro in 2022. *Nucleic Acids Res.* 2022;51(D1):D418-D427. https://doi.org/10.1093/nar/gkac993
9. Dion SP, Béliveau F, Désilets A, Ghinet MG, Leduc R. Transcriptome analysis reveals TMPRSS6 isoforms with distinct functionalities. *J Cell Mol Med.* 2018;22(4):2498-2509. https://doi.org/10.1111/jcmm.13562
10. Jallow MW, Campino S, Saidykhan A, Prentice AM, Cerami C. Common variants in the TMPRSS6 gene alter hepcidin but not plasma iron in response to oral iron in healthy Gambian adults: a recall-by-genotype study. *Curr Dev Nutr.* 2021;5(3):nzab014. https://doi.org/10.1093/cdn/nzab014
11. Malherbe JAJ, Cole CH. Double trouble: a case of fraternal twins with iron-refractory iron-deficiency anemia. *Clin Case Rep*. 2022;10(10):e6401. https://doi.org/10.1002/ccr3.6401
12. An P, Wu Q, Wang H, et al. TMPRSS6, but not TF, TFR2 or BMP2 variants are associated with increased risk of iron-deficiency anemia. *Hum Mol Genet.* 2012;21(9):2124-2131. https://doi.org/10.1093/hmg/dds028
13. Al-Amer O, Hawasawi Y, Oyouni AAA, et al. Study the association of transmembrane serine protease 6 gene polymorphisms with iron deficiency status in Saudi Arabia. *Gene.* 2020;751:144767. https://doi.org/10.1016/j.gene.2020.144767
14. Al-Jamea LH, Woodman A, Heiba NM, et al. Genetic analysis of TMPRSS6 gene in Saudi female patients with iron deficiency anemia. *Hematol Oncol Stem Cell Ther*. 2021;14(1):41-50. https://doi.org/10.1016/j.hemonc.2020.04.007
15. Batar B, Bavunoglu I, Hacioglu Y, et al. The role of TMPRSS6 gene variants in iron- related hematological parameters in Turkish patients with iron deficiency anemia. *Gene.* 2018;673:201-205. https://doi.org/10.1016/j.gene.2018.06.055
16. Suksangpleng T, Glomglao W, Viprakasit V. Common single nucleotide polymorphism of TMPRSS6, an iron regulation gene, associated with variable red blood cell indices in deletional α-globin genotypes. *Genes*. 2022;13(9):1502. https://doi.org/10.3390/genes13091502
17. Urbaszek K, Drabińska N, Szaflarska-Popławska A, Jarocka-Cyrta E. TMPRSS6 rs855791 polymorphism status in children with celiac disease and anemia. *Nutrients*. 2021;13(8):2782. https://doi.org/10.3390/nu13082782
18. Huisman THJ, Jonxis JHP. *The Hemoglobinopathies: Techniques of Identification*. Huisman THJ, Jonxis JHP, eds. M. Dekker; 1977.
19. Miller SA, Dykes DD, Polesky HF. A simple salting out procedure for extracting DNA from human nucleated cells. *Nucleic Acids Res.* 1988;16(3):1215. https://doi.org/10.1093/nar/16.3.1215
20. Bhatia P, Jain R, Singh A. A structured approach to iron refractory iron deficiency anemia (IRIDA) diagnosis (SAID): the more is "SAID" about iron, the less it is. *Pediatr Hematol Oncol J.* 2017a;2(2):48-53. https://doi.org/10.1016/j.phoj.2017.08.003
21. Rizo-de la Torre LDC, Rentería-López VM, Sánchez-López JY, Magaña-Torres MT, Ibarra-Cortés B, Perea-Díaz FJ. Molecular and hematological analysis of alpha- and beta-thalassemia in a cohort of Mexican patients. *Genet Test Mol Biomarkers.* 2021;25(3):247-252. https://doi.org/10.1089/gtmb.2020.0276
22. Solé X, Guinó E, Valls J, Iniesta R, Moreno V. SNPStats: a web tool for the analysis of association studies. *Bioinformatics.* 2006;22(15):1928-1929. https://doi.org/10.1093/bioinformatics/btl268
23. Kelley LA, Mezulis S, Yates CM, Wass MN, Sternberg MJE. The Phyre2 web portal for protein modeling, prediction and analysis. *Nat Protoc*. 2015;10(6):845-858. https://doi.org/10.1038/nprot.2015.053
24. Xu D, Zhang Y. Improving the physical realism and structural accuracy of protein models by a two-step atomic-level energy minimization. *Biophys J.* 2011;101(10):2525-2534. https://doi.org/10.1016/j.bpj.2011.10.024
25. Colovos C, Yeates TO. Verification of protein structures: patterns of nonbonded atomic interactions. *Protein Sci.* 1993;2(9):1511-1519. https://doi.org/10.1002/pro.5560020916
26. Choi Y, Chan AP. PROVEAN web server: a tool to predict the functional effect of amino acid substitutions and indels. *Bioinformatics.* 2015;31(16):2745-2747. https://doi.org/10.1093/bioinformatics/btv195
27. Ng PC, Henikoff S. SIFT: Predicting amino acid changes that affect protein function. *Nucleic Acids Res.* 2003;31(13):3812-3814.
28. Bendl J, Stourac J, Salanda O, et al. PredictSNP: robust and accurate consensus classifier for prediction of disease-related mutations. *PLoS Comput Biol.* 2014;10(1):e1003440. https://doi.org/10.1371/journal.pcbi.1003440
29. Steinhaus R, Proft S, Schuelke M, Cooper DN, Schwarz JM, Seelow D. MutationTaster2021. *Nucleic Acids Res.* 2021;49(W1):W446-W451. https://doi.org/10.1093/nar/gkab266
30. Adzhubei IA, Schmidt S, Peshkin L, et al. A method and server for predicting damaging missense mutations. *Nat Methods.* 2010;7(4):248-249. https://doi.org/10.1038/nmeth0410-248
31. Bromberg Y, Rost B. SNAP: Predict effect of non-synonymous polymorphisms on function. *Nucleic Acids Res.* 2007;35(11):3823-3835.
32. Pejaver V, Urresti J, Lugo-Martinez J, et al. Inferring the molecular and phenotypic impact of amino acid variants with MutPred2. *Nat Commun.* 2020;11(1):5918. https://doi.org/10.1038/s41467-020-19669-x
33. Tavtigian SV, Deffenbaugh AM, Yin L, et al. Comprehensive statistical study of 452 BRCA1 missense substitutions with classification of eight recurrent substitutions as neutral. *J Med Genet.* 2006;43(4):295-305. https://doi.org/10.1136/jmg.2005.033878
34. Venselaar H, Te Beek TA, Kuipers RK, Hekkelman ML, Vriend G. Protein structure analysis of mutations causing inheritable diseases. An e-Science approach with life scientist friendly interfaces. *BMC Bioinf.* 2010;11(1):548. https://doi.org/10.1186/1471-2105-11-548
35. Ittisoponpisan S, Islam SA, Khanna T, Alhuzimi E, David A, Sternberg MJE. Can predicted protein 3D structures provide reliable insights into whether missense variants are disease associated? *J Mol Biol.* 2019;431(11):2197-2212. https://doi.org/10.1016/j.jmb.2019.04.009
36. Pettersen EF, Goddard TD, Huang CC, et al. UCSF Chimera--a visualization system for exploratory research and analysis. *J Comput Chem.* 2004;25(13):1605-1612. https://doi.org/10.1002/jcc.20084
37. Mejía-Rodríguez F, Villalpando S, Shamah-Levy T, García-Guerra A, Méndez-Gómez Humarán I, De la Cruz-Góngora VV. Prevalence of iron deficiency was stable and anemia increased during 12 years (2006-2018) in Mexican women 20-49 years of age. *Salud Publica Mex.* 2021;63(3 May-Jun):401-411. https://doi.org/10.21149/12152
38. Karczewski KJ, Francioli LC, Tiao G, et al., Genome Aggregation Database Consortium. The mutational constraint spectrum quantified from variation in 141,456 humans. *Nature.* 2020;581(7809):434-443. https://doi.org/10.1038/s41586-020-2308-7
39. Bhatia P, Singh A, Hegde A, Jain R, Bansal D. Systematic evaluation of paediatric cohort with iron refractory iron deficiency anaemia (IRIDA) phenotype reveals multiple TMPRSS6 gene variations. *Br J Haematol.* 2017b;177(2):311-318. https://doi.org/10.1111/bjh.14554
40. Capra AP, Ferro E, Cannavò L, La Rosa MA, Zirilli G. A child with severe iron-deficiency anemia and a complex TMPRSS6 genotype. *Hematology*. 2017;22(9):559-564. https://doi.org/10.1080/10245332.2017.1317990

41. Ayariga JA, Villafane R. Single amino acid change mutation in the hydrophobic core of the N-terminal domain of P22 TSP affects the proteins stability. *bioRxiv*. 2021.
42. Melnikov S, Mailliot J, Rigger L, et al. Molecular insights into protein synthesis with proline residues. *EMBO Rep.* 2016;17(12):1776-1784. https://doi.org/10.15252/embr.201642943
43. Krieger F, Möglich A, Kiefhaber T. Effect of proline and glycine residues on dynamics and barriers of loop formation in polypeptide chains. *J Am Chem Soc.* 2005;127(10):3346-3352. https://doi.org/10.1021/ja042798i
44. Bauer F, Sticht H. A proline to glycine mutation in the Lck SH3-domain affects conformational sampling and increases ligand binding affinity. *FEBS Lett.* 2007;581(8):1555-1560. https://doi.org/10.1016/j.febslet.2007.03.012
45. Hubbard RE, Kamran Haider M. Hydrogen bonds in proteins: role and strength. In: *Encyclopedia of Life Sciences (ELS)*. John Wiley & Sons; 2010. doi: 10.1002/9780470015902.a0003011.pub2
46. Brenner S. The molecular evolution of genes and proteins: a tale of two serines. *Nature.* 1988;334(6182):528-530. https://doi.org/10.1038/334528a0
47. Lee PL, Barton JC, Khaw PL, Bhattacharjee SY, Barton James C. Common TMPRSS6 mutations and iron, erythrocyte, and pica phenotypes in 48 women with iron deficiency or depletion. *Blood Cells Mol Dis.* 2012;48(2):124-127. https://doi.org/10.1016/j.bcmd.2011.12.003

Single laboratory evaluation of umbilical cord blood units processing methodologies for banking

Francisco F. dos Santos, PhD,[1] Letícia Nunes, MSc,[1] Cátia Martins, MSc,[1] Margaret Ann Smith, PhD,[2] Carla Cardoso, PhD[1]

[1]Stemlab, FamiCord Group, Cantanhede, Portugal, [2]SmartCells, FamiCord Group, London, UK. Corresponding author: Francisco F. dos Santos; francisco.santos@crioestaminal.pt

Keywords: cord blood; processing; manual method; banking; HES; transplantation

Abbreviations: UCB, umbilical cord blood; HES, hydroxyethyl starch; TNC, total nucleated cells; CPDA-1, citrate-phosphate-dextrose adenine; CPD, citrate-phosphate-dextrose; DMSO, dimethyl sulfoxide; CFU, colony-forming units; IMDM, Iscove's Modified Dulbecco's Medium; APX, AutoXpress

Laboratory Medicine 2024;55:285-292; https://doi.org/10.1093/labmed/lmad073

ABSTRACT

Objective: To compare the efficiency of 3 different processing methods (Sepax, AutoXpress [AXP], and manual processing with hydroxyethyl starch [HES] sedimentation) used at Stemlab during a 10-year period.

Methods: Historical data were compiled and the analytical results obtained for the 3 different methods were compared.

Results: The manual processing (HES) method yielded the highest level of total nucleated cell recovery after processing, and the AXP system yielded the highest CD34+ cell number. The red blood cell reduction was also significantly higher with the HES method. Also, HES showed comparable results to Toticyte technology for umbilical cord blood (UCB) processing.

Conclusion: These results show that the HES method is as effective as automated technologies for UCB volume reduction; hence, it is a suitable methodology for private and public UCB banks. The HES method also proved to be superior to Toticyte technology for medical applications, with higher recovery yields of total nucleated cells after thawing and equivalent CD34+ cell recovery and functionality.

Umbilical cord blood (UCB) is a valuable source of hematopoietic cells for clinical applications, with several innovative therapies currently in clinical development. In the field of hematopoietic progenitor transplantation, the importance of UCB is well-established, with more than 45,000 registered transplants worldwide.[1] The clinical relevance of UCB for hematopoietic transplantation led to routine UCB banking, with the objective of making the cells available on clinical request. The most current estimate points to more than 7.5 million cryopreserved UCB units worldwide, in public and private banks.

To provide high-quality units for clinical applications, UCB banking requires rigorous standards and procedures for the collection, processing, and cryopreservation of UCB specimens. It is widely accepted that UCB processing should include the important step of volume and red blood cell (RBC) reduction. This step is crucial for the following reasons: in the case of ABO/Rh incompatibility, RBCs may cause an adverse reaction, and the cryopreservation process can cause lysis of RBCs and subsequent release of hemoglobin and ruptured cell membranes (RBC ghosts), which can seriously compromise kidney function.[2,3]

Although the vast majority of UCB banks use a processing method for volume and RBC reduction before cryopreservation, there are some banks that cryopreserve whole UCB. The arguments in favor of this technique mainly rely on the shorter processing time from collection to cryopreservation, which reduces the cell loss during this period. They also point to the fact that it allows storage of all the cell types and other substances present in the UCB unit, which might not be selected by the volume and RBC reduction methodologies.

Considering that the clinical potential of UCB is not yet fully explored, this technique allows the preservation of the complete content of the UCB units for potential future therapies. However, whole UCB banking requires larger volumes of cryoprotectant and larger cryogenic storage capacity. Also, it may require a technically challenging post-thawing washing procedure at the clinical site to remove RBCs and their lysis by-products, although it is not mandatory.[4-9]

UCB processing also minimizes the costs associated with cryogenic storage, including equipment and its monitoring and management, and the volume of liquid nitrogen needed to maintain thousands of UCB units for decades. Thus, the development and optimization of different methods for volume (and RBC) reduction has been a focal point of the industry in the past 30 years. The comparison of different methods has been published by different laboratories, and the conclusion is that it is not possible to refer to a single method as the most effective for UCB processing. The different processing protocols used by different laboratories present a major limitation for volume reduction method comparison and, thus, make it difficult to draw significant conclusions.[5-12]

Stemlab, FamiCord Group initiated its UCB banking activity in 2003 in Portugal. Throughout its 20 years of activity, the Stemlab processing laboratory has used 3 different volume reduction methods (the Sepax system between 2008 and 2013, the AutoXpress [AXP] system between 2013 and 2020, and the hydroxyethyl starch [HES] method since 2020), with several thousand units processed via each method. Stemlab is therefore in a privileged position to run a historical comparative analysis of these 3 processing methods. Such single-laboratory analysis presents some advantages compared to the multilaboratory analyses reported on in the literature,[13] because it rules out the impact of different training levels among technicians or different analytical methods.

The evaluation of the performance of each volume reduction method relies on the analyses of its output. These methods have been developed, focusing on obtaining UCB units for hematopoietic transplantation settings. The success of hematopoietic transplantation has been linked to several factors, including the cell dose of total nucleated cells (TNC) and viable CD34+ cells.[14,15] Thus, the number of TNC and viable CD34+ cells are considered critical properties of banked UCB units.[16]

In this study, we performed a retrospective comparative analysis among the 3 different UCB processing methods (Sepax, AXP, and the manual processing method [HES]) used at Stemlab. To our knowledge, this is the first study in the literature to compare these 3 processing methods using data from a single laboratory. The manual HES method shows equivalent efficacy to the automated systems Sepax and AXP regarding the critical attributes of UCB units for hematopoietic transplantation. Finally, as an adjunct to the comparison of processing technologies compared in this study, we compared the HES-based technique with published data from a report of a Toticyte methodology developed for UCB processing.[17]

Materials and Methods

UCB Specimens

UCB was collected in the delivery room by trained health care professionals immediately after birth and before delivery of the placenta. Before delivery, mothers gave their informed consent for collection of the UCB.

After clamping and disinfecting the umbilical cord, the umbilical vein was punctured as close as possible to the clamp. UCB specimens were collected by gravity into a sterile bag primed with anticoagulant (citrate-phosphate-dextrose adenine [CPDA-1], 21 mL) or citrate-phosphate-dextrose ([CPD], 25 mL). After collecting cord blood, the collection-bag clamps were closed, and 2 security knots were tied to prevent blood leakage during transport. The collected biological specimens were placed in a hermetic bag provided for transport. The collected UCB volume was not significantly impacted by the procedure of cord-delayed clamping (as long as 1 minute), when this information was available.

The specimens were transported to the processing bank in a time and temperature-controlled manner. They were stored at room temperature until processing within an average of 36 hours.

This study includes UCB specimens received by Stemlab from 2012 to 2022, processed using 3 different methods: Sepax, AXP (based on centrifugation) according to manufacturer methodologies, and sedimentation with HES followed by centrifugation. The time frame of data incorporated in this study was chosen because this was the period in which all 3 methods were used to process UCB. The processing method was altered throughout the years for strategic and technical reasons.

Sepax Method

The Sepax S-100 Cell Separation System CS-530.3 and CS-570 kits (Biosafe) was the first processing platform to allow the automated reduction of the initial volume of small-volume bone marrow and UCB collections in a closed and sterile system. This method allows the acquisition of the buffy coat fraction by reducing plasma and RBCs. The closed system utilizes centrifugation and optical sensor interrogation of cellular components and, with operator-determined protocols, can yield given volumes of product.

The single use processing kit consists of a chamber in which, in the first centrifugation, the sedimentation of UCB cellular fractions occurs. During the second centrifugation, each of the 3 fractions (RBCs, plasma, and nucleated cells) was separated into different bags, based on variations in light absorbance detected by an optical sensor.

AXP Method

The AXP system (ThermoGenesis) is very similar to Sepax. It consists of a rechargeable device and allows the separation of nucleated cells in an automatic, closed, and sterile manner, based on centrifugation cycles.

After transferring the specimen material to a single-use processing kit, it was placed in a proprietary device that separates the components through 2 centrifugation cycles. In the first cycle, the 3 blood fractions (plasma, RBCs, and buffy coat) were sedimented, and in a second cycle, the components were separated into different bags according to their relative optical densities.

Manual Processing Method (HES Sedimentation)

HES belongs to a group of synthetic polymers and is used by cell storage banks for the agglutination and sedimentation of RBCs. The use of HES in UCB volume reduction exploits gravity sedimentation by HES.

After the addition of HES to the specimen in the collection bag and sterile connection of transfer bags, this mixture was mixed thoroughly and placed in a plasma expresser. After this step, the entire process was performed in a closed and sterile system. At this stage of the process, gravitational sedimentation of RBCs and, consequently, the separation of blood fractions occur.

When the blood fractions were completely separated, the plasma and buffy coat were expressed together into one of the transfer bags. This combination was subjected to centrifugation and placed again in the plasma expresser. Plasma was subsequently removed and transferred into the second transfer bag, leaving the separated stem cell–rich mononuclear cell fraction in the first bag (approximately 20 mL).

Cryopreservation

After volume reduction using the methods described earlier herein, the final products were collected in cryopreservation bags. A cryoprotectant solution comprising 55% dimethyl sulfoxide (DMSO) and 5% DEX40 was added, yielding a final concentration of 10% DMSO.

The specimens were placed in a controlled-rate freezing device (ICE Cube 14 S, Sy-lab Geräte), which allows a gradual decrease in temperature of 1°C/minute until reaching −150°C. After stabilization at this temperature, the specimens were transferred and stored in gas-phase nitrogen at temperatures below −150°C.

Specimen Thawing

For the comparative study with Toticyte, donated cryopreserved UCB units for analysis were thawed using a 37°C water bath. The cell suspensions were washed using a medium constituted by a combination of Iscove's Modified Dulbecco's Medium (IMDM; Thermo Fisher Scientific) and penicillin/streptomycin.

Specimen Analysis

Cell Counting

Hematological cell counting after processing and after thawing was performed using an automated analyzer (ACT Diff [Beckman Coulter]), Sysmex XE-2100L [Sysmex], or ADVIA 2120i [Siemens]).

Flow Cytometry Analysis

Viable CD34+ cells were quantified by flow cytometry analysis using the Cytomics FC 500 flow cytometer (Beckman Coulter) according to manufacturer protocols. Briefly, 10 µL of CD45-FITC monoclonal antibody (Beckman Coulter-A07782), 10 µL of CD34-PE monoclonal antibody (Beckman Coulter-A07776), and 10 µL of 7-AAD (Beckman Coulter-A07704) were added to the specimens. Cells were then incubated in the dark for 15 minutes at room temperature. Then, 1 mL of cell lysis solution (VersaLyse Lysing Solution [Beckman Coulter]) was added, followed by a second incubation in the dark for 20 minutes. The cell suspension was then centrifuged (150*g* for 5 minutes) and resuspended in 300 µL of PBS. Finally, 50 µL of fluorescent counting beads were added (Flow-Count Fluorosphere Counting Beads [Beckman Coulter]).

Colony-Forming Units (CFU) Assay

For functional testing, thawed UCB specimens were added to MethoCult media (STEMCELL Technologies) in a 1:10 ratio, and the cell suspension was carefully plated in 35-mm plates. The cells were then incubated for 14 days at 37°C in 5% CO_2. After this period, the colonies were identified (CFU-GEMM, CFU-GM, CFU-M, and BFU-E) and quantified.

Statistical Analysis

Data were analyzed using JASP software, version 0.16.4. Results are presented as mean (SD). Mann-Whitney *U* testing was used to determine statistical significance.

Results and Discussion

Pre- and Postprocessing Analyses: Sepax vs AXP vs Manual Processing (HES)

The data obtained for each processing method are presented in **TABLE 1** and include UCB units processed by Stemlab between 2012 and 2022. These data are presented graphically in **FIGURES 1** and **2** before and after processing, respectively. The results of statistical analyses are presented in **TABLE 2**.

The results presented in **TABLE 1** show relatively small differences between the 3 processing methods for the different attributes analyzed. Regarding the preprocessing analyses, the mean input volume of the UCB is higher for the Sepax method (mean [SD], 84.7 [24.2] mL), whereas the HES method had a lower mean input volume (73.3 [23.2] mL). This parameter was related to the UCB unit collection step at the birth site. Considering that each method examined was in use during different time periods, we note that the volume of UCB units had been decreasing during the 10-year period of our analysis. This may be related to the standard operational procedures at each hospital where the UCB is collected, namely, delayed cord-clamping procedures.

The same trend is observed for the numbers of TNC in the UCB units at the time of collection, with a statistically significant decrease throughout the years ($P < .001$). Nevertheless, the concentration factor and yields obtained for TNC were similar for all the processing methods we studied. The reduction in number of TNC, therefore, correlates with the reduction of unit volumes during the study period. We noted the same correlation in input numbers of RBC and hematocrit for all the UCB units throughout the years.

TABLE 1. Data from UCB Units Processed by the Stemlab Laboratory Using the 3 Studied Processing Methods[a]

Variable	Before Processing		
	Sepax (n = 3729)	AXP (n = 6271)	HES (n = 11,464)
Volume, mL, mean (SD) (range)	84.7 (24.2) (34.4-195)	79.1 (24.0) (34.7-177)	73.3 (23.2) (34.4-256)
TNC × 10^8, mean (SD) (range)	7.03 (3.35) (0.76-30.8)	6.88 (3.70) (0.82-55.1)	6.51 (4.04) (0.29-35.5)
TNC concentration × 10^8/mL, mean (SD) (range)	0.08 (0.03) (0.02-0.29)	0.08 (0.03) (0.02-0.42)	0.08 (0.03) (0.01-0.29)
RBC × 10^9, mean (SD) (range)	3.25 (0.48) (1.12-5.14)	3.09 (0.50) (1.08-5.51)	2.97 (2.29) (0.12-231)
Hematocrit, %, mean (SD) (range)	35.7 (5.15) (14.1-57.7)	34.1 (5.49) (4.07-62.2)	34.4 (6.37) (1.60-60.6)
Variable	**After Processing**		
	Sepax (n = 3729)	**AXP (n = 6271)**	**HES (n = 11,464)**
TNC × 10^8, mean (SD) (range)	5.53 (2.62) (0.57-24.9)	5.78 (3.12) (0.68-46.9)	5.57 (3.36) (0.33-29.1)
TNC recovery, %, mean (SD) (range)	79.3 (7.69) (38.5-99.3)	84.4 (6.81) (47.8-104)	85.2 (8.89) (12.8-110)
TNC viability, %, mean (SD) (range)	92.1 (4.58) (63.7-99.4)	92.7 (4.57) (45.4-100)	89.6 (6.30) (18.9-100)
RBC × 10^9, mean (SD) (range)	3.86 (0.79) (1.15-6.49)	2.86 (0.50) (1.68-30.3)	0.89 (0.76) (0-4.8)
Hematocrit, %, mean (SD) (range)	43.9 (8.69) (13.8-80.0)	33.0 (3.91) (8.00-71.3)	10.4 (9.25) (0-49.3)
$CD34^+$ cells × 10^6, mean (SD) (range)	2.26 (2.17) (0.15-28.2)	2.43 (2.37) (0.12-28.6)	1.93 (2.05) (0.01-47.6)
$CD34^+$ cell viability (%), mean (SD) (range)	99.5 (0.69) (94.3-100)	99.4 (0.69) (85.3-100)	99.1 (1.24) (50.0-100)

APX, AutoXpress; HES, hydroxyethyl starch; RBC, red blood cells; TNC, total nucleated cells; UCB, umbilical cord blood.
[a]*The methods studied were Sepax, AXP, and manual processing with HES sedimentation.*

FIGURE 1. Graphical representation of the data from umbilical cord blood (UCB) units before processing with each technology under investigation. A, Volume. B, Number of total nucleated cells (TNC). C, TNC concentration. D, Number of red blood cells (RBC). E, Hematocrit (Htc). APX, AutoXpress; HES, hydroxyethyl starch.

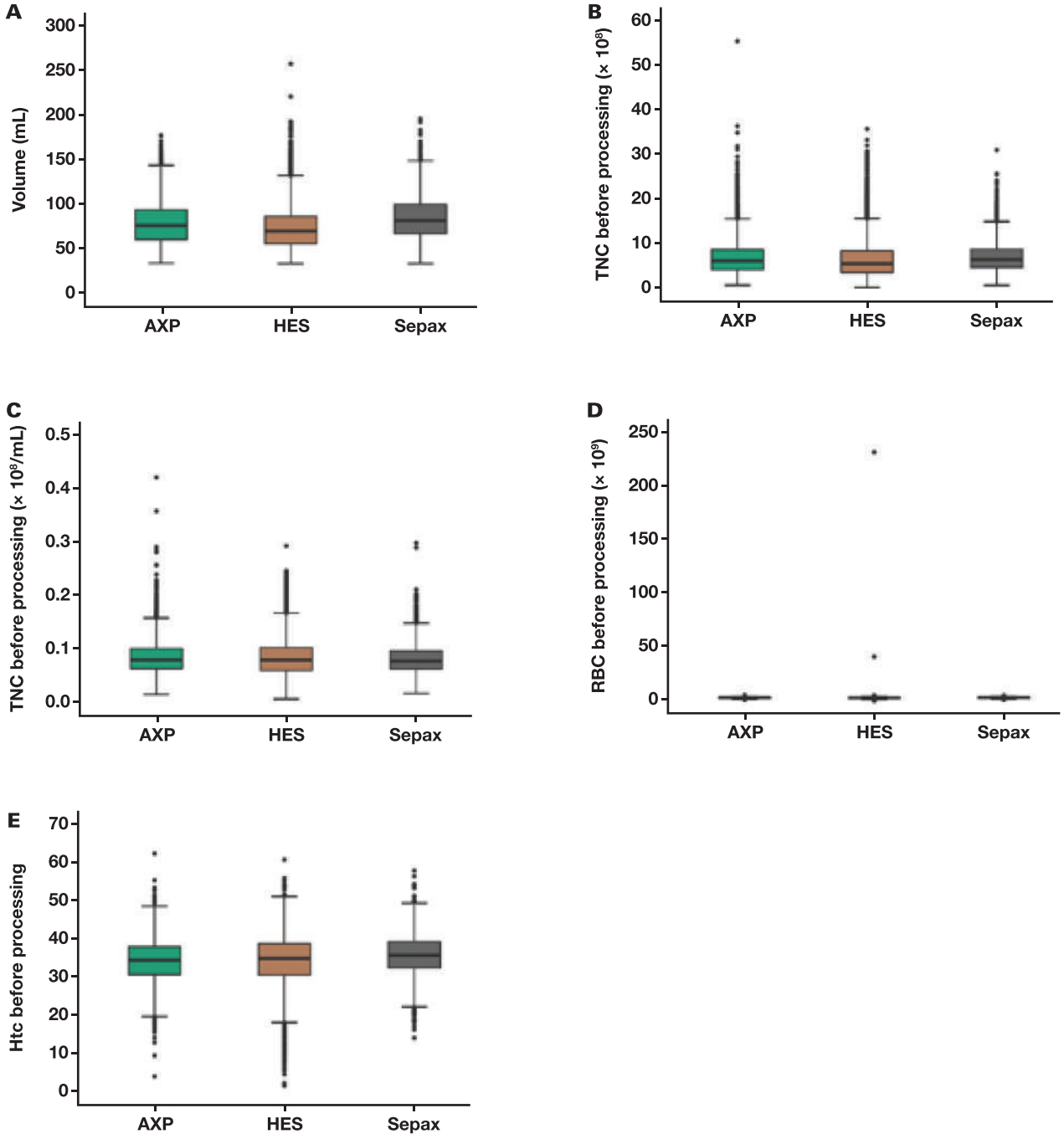

Data analysis after processing enables a direct comparison of the efficacy of the 3 processing methods. The HES method presented a statistically significant higher TNC recovery (mean [SD], 85.2% [8.89%]), when compared with Sepax (79.3% [7.69%]; $P < .001$) and AXP (84.4% [6.81%]; $P < .001$). However, TNC viability was significantly lower for HES (89.6% [6.30%]) than for Sepax (92.1% [4.58%]; $P < .001$) and AXP (92.7% [4.57%]; $P < .001$). Regarding the reduction of RBC and hematocrit, HES methodology presented significantly higher efficacy (reducing RBC to mean [SD] 0.89 [0.76 × 10^9 and the hematocrit to 10.4 [9.25], $P <$ .001 for both), compared with the Sepax and AXP methods.

Regarding the capacity to recover hematopoietic progenitors for the original UCB unit, the AXP method yielded a significantly higher number of viable CD34+ cells (mean [SD], 2.43 [2.37] × 10^6) than Sepax (2.26 [2.17] × 10^6; $P = .001$) and HES (1.93 [2.05] × 10^6; $P = .001$) methods. For all the 3 methods, the CD34+ cell viability was higher than 99%.

Overall, the 3 processing methods described herein can be considered effective for the volume reduction of banked UCB units, with similar levels of TNC viable and CD34+ cell recovery. We note that the manual method was able to achieve a significantly higher depletion of RBC, which is a critical parameter for clinical applications. The major

FIGURE 2. Graphical representation of the data from umbilical cord blood (UCB) units after processing with each technology under investigation. A, Number of total nucleated cells (TNC). B, TNC viability. C, TNC recovery. D, Number of red blood cells (RBC). E, Hematocrit (Htc). F, Viable CD34+ cell number. G, CD34+ cell viability. APX, AutoXpress; HES, hydroxyethyl starch.

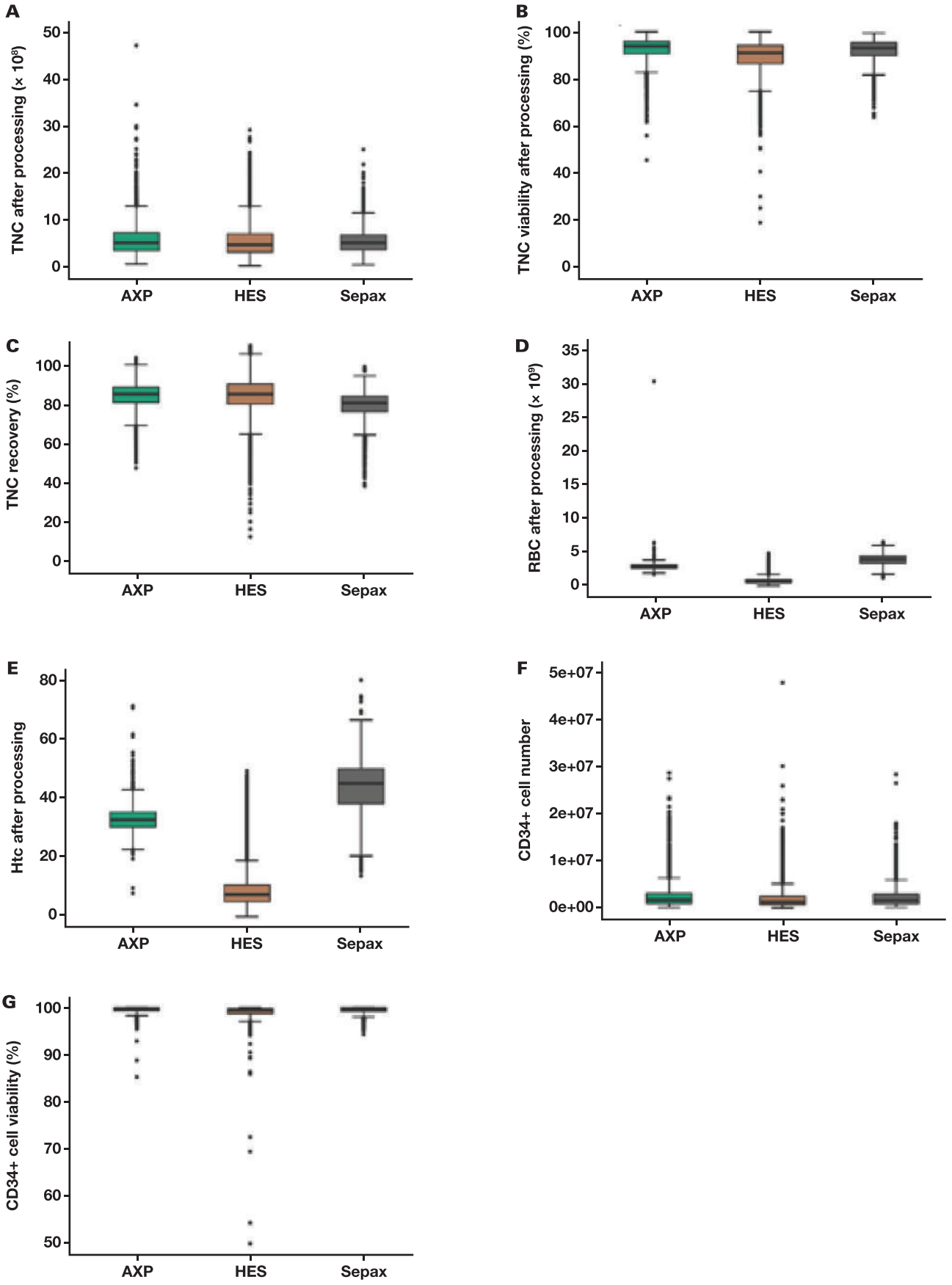

TABLE 2. Results of Statistical Analyses Comparing the Processing Methods for the Different Variables[a]

P Value	Parameters
Sepax vs AXP	
P <.001	Before processing: volume, TNC number, TNC concentration, RBC number, hematocrit After processing: TNC recovery, TNC viability, RBC number, hematocrit, and CD34+ cell viability
P = .001	After processing: CD34+ cell number
P = .097	After processing: TNC number
Sepax vs HES	
P <. 001	Before processing: volume, TNC number, RBC number, hematocrit After processing: TNC number, TNC recovery, TNC viability, RBC number, hematocrit, and CD34+ cell viability
P = .001	After processing: CD34+ cell number
P = .045	Before processing: TNC concentration
AXP vs HES	
P < .001	Before processing: volume, TNC number, RBC number, hematocrit After processing: TNC number, TNC recovery, TNC viability, RBC number, hematocrit, and CD34+ cell viability
P = .001	After processing: CD34+ cell number
P = .008	Before processing: TNC concentration

AXP, AutoXpress; HES, hydroxyethyl starch; RBC, red blood cells; TNC, total nucleated cells.
[a]For comparative purposes, P values shown are applicable to all individually listed parameters.

TABLE 3. Comparative Data Between UCB Units Processed With HES Methodology in the Stemlab Laboratory and Toticyte[17a]

Variable	After Processing, Mean (SD)	
	HES	Toticyte
TNC recovery, %	79.6 (9.3)	84.8 (12.6)
CD34+ cell recovery, %	84.0 (13.1)	89.8 (11.9)
Hematocrit (%)	6.8 (3.3)	0.9 (0.1)
RBC depletion (%)	81.2 (10.2)	99 (0)
Variable	**After Thawing, Mean (SD)**	
	HES	Toticyte
TNC recovery, %	74.2 (8.4)	36.3 (9.5)
CD34+ cell recovery, %	68.7 (12.9)	66.2 (9.9)
CFU/CD34+ cell	0.38 (0.18)	0.47 (0.1)

CFU, colony-forming units; HES, hydroxyethyl starch; TNC, total nucleated cells; UCB, umbilical cord blood.
[a]In the Stemlab laboratory, n = 30 for patient specimens.

difference between the 3 processing methodologies is that, although Sepax and AXP are automated methods using specific devices, the HES method requires continuous and rigorous personnel training and evaluation to guarantee reproducible results.

Also, the analysis of the Stemlab laboratory data demonstrates that the HES method efficacy is comparable to that of the 2 automated methods previously used. Similar results have been observed in a parallel analysis performed by another laboratory of the Famicord Group, the Polish Stem Cells Bank, which also opted to use the manual processing with HES for UCB units (data not published). Despite being more labor-intensive, the HES method also presents advantages economically (lower direct costs) and operationally (it is easy to customize and not dependent on a unique supplier). Finally, the manual method with HES could be better than automated platforms for processing very small or very large volume UCB units (because the protocol has more flexibility than the automated technologies) by allowing for adjustments according to specimen characteristics (for example, to deal with the decreasing volume of UCB observed in recent years).

Postthawing Analyses: HES Method vs Toticyte

Most published studies compare only the impact of the processing methods on the critical attributes of banked UCB units, as presented earlier herein. However, it is also important to evaluate the quality of UCB units after thawing and to determine whether quality attributes and therapeutic potential are maintained. Such data are still scarce in the literature.

In this research work, 30 UCB units donated for research and development purposes were processed using the HES method and later thawed, as described herein, for an analysis similar to that used for the Toticyte method, as described by Drew et al.[17] Toticyte is described as a method for UCB processing that relies on a proprietary reagent and that claims to have superior efficacy compared with the other methods in recovering CD34+ cells after thawing. **TABLE 3** presents the results obtained for postthaw viable TNC, CD34+ cells, and CFU recovery after our laboratory HES-based processing, compared with the published data from the Toticyte study (also depicted in **FIGURE 3**).

The Toticyte method is quoted by its inventors as apparently being capable of achieving considerably higher rates of RBC depletion (mean [SD], 99 vs 81.2 [10.2]) and, consequently, much lower hematocrit concentrations after processing (0.9 [0.1] vs 6.8 [3.3]), when compared with specimens processed via the HES method. We note that the level of RBC depletion using the HES method is highly dependent on the protocol used. In the Stemlab laboratory, the protocol is optimized to avoid complete RBC depletion, to mitigate against any loss of buffy coat fraction at the interface, thus resulting in a higher hematocrit level after processing. The levels of TNC and CD34+ cell recovery are similar in both methods, although they are slightly higher with Toticyte.

After thawing, the HES protocol in our experiments resulted in a considerably higher TNC number (mean [SD], 74.2% [8.4%]) than quoted for Toticyte (CD45+ cells, 36.3% [9.5%]). This higher level of TNC recovery after thawing is a substantial advantage of the HES method because the TNC dosage is a critical criterion for hematopoietic transplantation, and also a lower TNC number may result in a disqualification of these UCB units in a transplant setting.[15] This observation may be partly related to a protective effect on the cryopreservation of UCB cells exerted by HES, which also has been observed in similar studies.[18,19]

We were intrigued that, when comparing our laboratory data with the quoted Toticyte data, the viable CD34+ cell recovery is comparable for both processing methodologies (mean [SD], 68.7% [12.9%] and 66.2% [9.9%] for HES and Toticyte, respectively). The functional capacity of these hematopoietic progenitors to generate viable CFU is also similar (0.38 [0.18] and 0.47 [0.1] for HES and Toticyte, respectively).

FIGURE 3. **Comparative data from hydroxyethyl starch (HES) sedimentation and Toticyte methods after processing and after thawing. A, Full blood count and flow cytometric analysis. B, Clonogenic data. Colony-forming unit (CFU) formation is expressed as an extrapolation of the relative number of colonies from 1 viable CD34+ cell. Htc, hematocrit; TNC, total nucleated cells.**

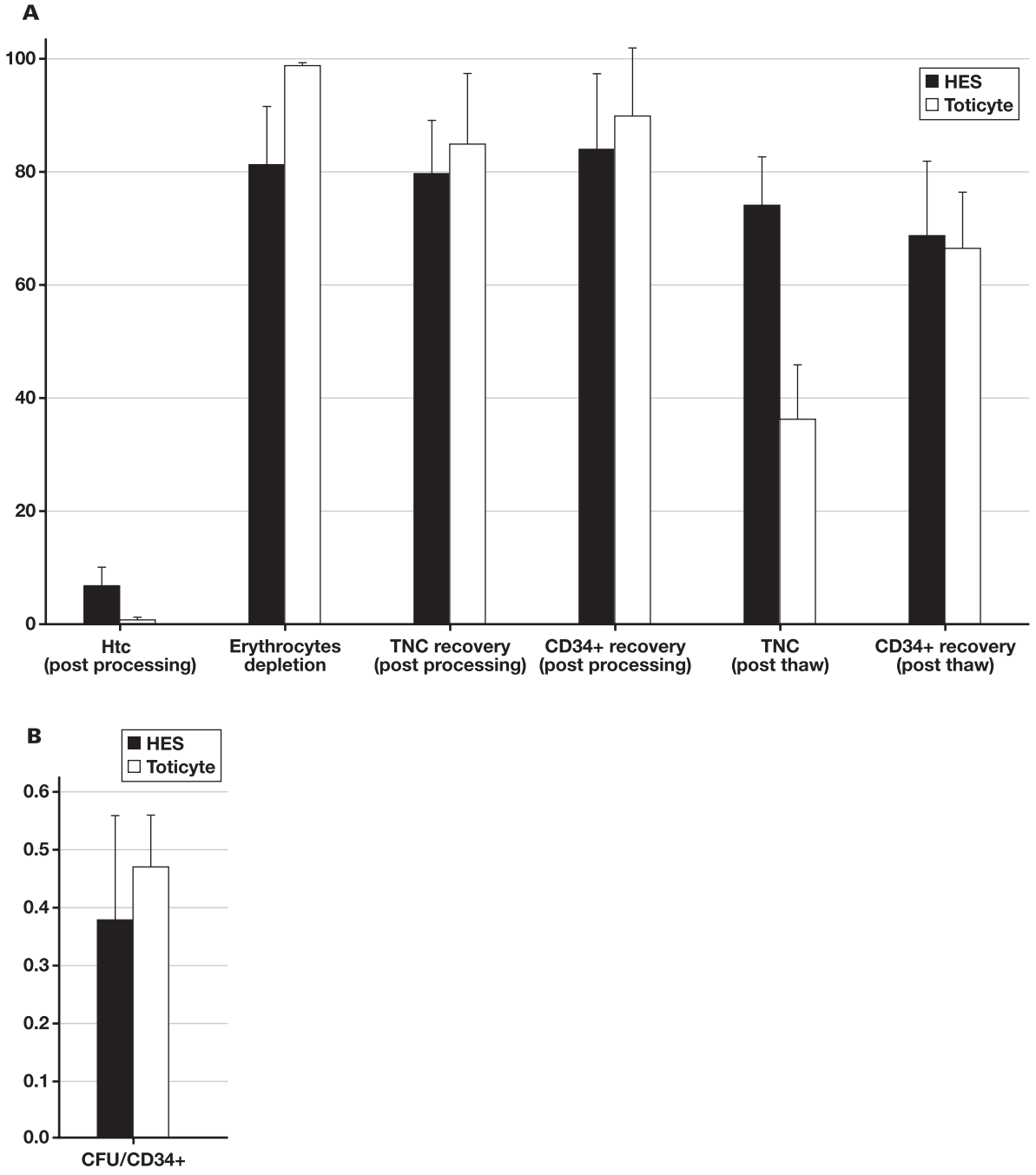

Discussion

Although it would have been ideal to do so, it was not possible to compare the 3 processing methods simultaneously using given UCB specimens because these were being processed for therapeutic and not experimental purposes. We acknowledge this limitation; however, this was a retrospective analysis of accumulated data across 3 different time frames, which was the only legitimate way to make the comparison. All 3 methods were validated before being applied to client specimens for potential clinical use.

Despite the different numbers of specimens for each UCB processing method, the large cohorts in the 3 groups support a valid statistical analysis of the results, even when determining statistical significances between very similar average data. The use of large data sets for all of the methods also minimizes the impact of some limitations of this retrospective analysis, namely, the operator and UCB unit variability throughout the years studied. Nevertheless, it would also be of interest to conduct a direct comparison study among the 3 processing methods for each UCB unit, although such a study could also

face technical and operational limitations (for example, the low volume of UCB units precludes splitting given units for use with 3 processing methodologies).

Our findings confirm that the manual HES method is superior to Toticyte technology from the medical application perspective, with higher postcryopreservation yields of TNC after thawing while maintaining equivalent levels of CD34+ cell recovery and functionality. Although more operator input and specialized labor are required with the HES method, and this may be perceived to have inherent risks, the HES method has proven to be as safe as commercially produced automated devices for UCB processing. The HES method should, therefore, be considered as a valid alternative for UCB banks that aim to reduce operational costs and to operate independently of a specific device supplier. The latter is a particularly pertinent consideration because of current supply-chain problems affecting medical and laboratory consumables and components.

Conflict of Interest Disclosure

Coauthors dos Santos, Nunes, Martins, and Cardoso are employees of Stemlab. Coauthor Smith is an employee of SmartCells, FamiCord Group.

REFERENCES

1. Wagner JE. Cord blood 2.0: State of the art and future directions in transplant medicine. *Blood Res*. 2019;54(1):7-9. doi:10.5045/br.2019.54.1.7
2. Barker JN, Scaradavou AR. Response: the controversy of red blood cell–replete cord blood units. *Blood.* 2011;118(2):480-480. doi:10.1182/BLOOD-2011-03-341438
3. Areman EM, Loper K, eds. *Cellular Therapy: Principles, Methods, and Regulations*. 2nd ed. AABB; 2016.
4. Hahn T, Bunworasate U, George MC, et al. Use of nonvolume-reduced (unmanipulated after thawing) umbilical cord blood stem cells for allogeneic transplantation results in safe engraftment. *Bone Marrow Transplant.* 2003;32(2):145-150. doi:10.1038/sj.bmt.1704091
5. Solves P, Planelles D, Mirabet V, Blanquer A, Carbonell-Uberos F. Qualitative and quantitative cell recovery in umbilical cord blood processed by two automated devices in routine cord blood banking: a comparative study. *Blood Transfus*. 2013;11(3):405-411. doi:10.2450/2012.0037-12
6. Solves P, Mirabet V, Planelles D, et al. Red blood cell depletion with a semiautomated system or hydroxyethyl starch sedimentation for routine cord blood banking: a comparative study. *Transfusion.* 2005;45(6):867-873. doi:10.1111/j.1537-2995.2005.04357.x
7. Solves P, Mirabet V, Blanquer A, et al. A new automatic device for routine cord blood banking: critical analysis of different volume reduction methodologies. *Cytotherapy.* 2009;11(8):1101-1107. doi:10.3109/14653240903253865
8. Basford C, Forraz N, Habibollah S, Hanger K, McGuckin CP. Umbilical cord blood processing using Prepacyte-CB increases haematopoietic progenitor cell availability over conventional Hetastarch separation. *Cell Prolif.* 2009;42(6):751-761. doi:10.1111/j.1365-2184.2009.00646.x
9. Lapierre V, Pellegrini N, Bardey I, et al. Cord blood volume reduction using an automated system (Sepax) vs. a semi-automated system (Optipress II) and a manual method (hydroxyethyl starch sedimentation) for routine cord blood banking: a comparative study. *Cytotherapy.* 2007;9(2):165-169. doi:10.1080/14653240701196811
10. Schwandt S, Korschgen L, Peters S, Kogler G. Cord blood collection and processing with hydroxyethyl starch or non-hydroxyethyl starch. *Cytotherapy.* 2016;18(5):642-652. doi:10.1016/j.jcyt.2016.02.003
11. Kaur I, Zulovich JM, Gonzalez M, et al. Comparison of two methodologies for the enrichment of mononuclear cells from thawed cord blood products: the automated Sepax system versus the manual Ficoll method. *Cytotherapy.* 2017;19(3):433-439. doi:10.1016/j.jcyt.2016.11.010
12. Kim C, Wilke-Douglas M, Sivilotti M. *Meta-Analysis of the AXP® and Sepax® Automated Cord Blood Processing Systems.* Cesca Therapeutics; 2015.
13. Takahashi TA, Rebulla P, Armitage S, et al. Multi-laboratory evaluation of procedures for reducing the volume of cord blood: influence on cell recoveries. *Cytotherapy.* 2006;8(3):254-264. doi:10.1080/14653240600735677
14. Laughlin MJ, Eapen M, Rubinstein P, et al. Outcomes after transplantation of cord blood or bone marrow from unrelated donors in adults with leukemia. *N Engl J Med.* 2004;351(22):2265-2275. doi:10.1056/NEJMoa041276
15. Kurtzberg J. Update on umbilical cord blood transplantation. *Curr Opin Pediatr.* 2009;21(1):22-29. doi:10.1097/mop.0b013e32832130bc
16. European Directorate for the Quality of Medicines & HealthCare (EDQM). *Guide to the Quality and Safety of Tissues and Cells for Human Application.* 5th ed. EDQM; 2022.
17. Drew J, Slaughter R, Klimentov A, et al. TotiCyte, a paradigm shift in stem cell isolation and storage from umbilical cord blood. *J Stem Cells Res Dev Ther.* 2021;7(3):1-7. doi:10.24966/srdt-2060/100073
18. Mantri S, Kanungo S, Mohapatra PC. Cryoprotective effect of disaccharides on cord blood stem cells with minimal use of DMSO. *Indian J Hematol Blood Transfus*. 2015;31(2):206. doi:10.1007/S12288-014-0352-X
19. Rowley SD, Feng Z, Chen L, et al. A randomized phase III clinical trial of autologous blood stem cell transplantation comparing cryopreservation using dimethylsulfoxide vs dimethylsulfoxide with hydroxyethylstarch. *Bone Marrow Transplant.* 2003;31(11):1043-1051. doi:10.1038/sj.bmt.1704030

Retrospective comparison of false-positive result frequencies of 3 syphilis serology screening tests in pregnant and nonpregnant patients at an academic medical center in Appalachia

Jianbo Yang, PhD[1], Danyel H. Tacker, PhD[1], Sijin Wen, PhD[2], P. Rocco LaSala, MD[1]

[1]Department of Pathology, Anatomy & Laboratory Medicine, and [2]Department of Epidemiology and Biostatistics, West Virginia University, Morgantown, WV, US.
Corresponding author: Jianbo Yang; jianbo.yang@hsc.wvu.edu

Key words: syphilis; serology test; immunoassay; false positive; pregnancy; positive predictive value

Abbreviations: RPR, rapid plasma reagin; TP-PA, *Treponema pallidum* particle agglutination

Laboratory Medicine 2024;55:293-298; https://doi.org/10.1093/labmed/lmad078

ABSTRACT

Objective: This study retrospectively compared false-positive result frequencies of 3 syphilis serology screening tests and assessed whether false positivity was associated with pregnancy and age.

Methods: Results for 3 screening tests were retrieved from the laboratory database, including rapid plasma reagin (RPR) assay between October 2016 and September 2019, BioPlex 2200 Syphilis Total immunoassay between May 2020 and January 2022, and Alinity i Syphilis TP assay between February 2022 and April 2023. The false-positive result frequencies were calculated based on testing algorithm criteria.

Results: False-positive result frequency for BioPlex was 0.61% (90/14,707), significantly higher than 0.29% (50/17,447) for RPR and 0.38% (55/14,631) for Alinity (both $P < .01$). Patients with false-positive results were significantly older than patients with nonreactive results for RPR (median age: 36 vs 28, $P < .001$), but not for BioPlex or Alinity. For all 3 tests, the positive predictive values in pregnant women were lower than those in nonpregnant women or men. However, pregnant women did not exhibit a higher false-positive result frequency.

Conclusion: Although false-positive result frequencies were low overall for all 3 syphilis serology tests, there is a significant difference between different tests. Pregnancy was not associated with more false-positive results for all 3 tests.

Introduction

Syphilis is a sexually transmitted infection caused by a subspecies of *Treponema pallidum*. It can also be transmitted vertically from mother to fetus, causing congenital syphilis. Recent surveillance data from the US Centers for Disease Control and Prevention showed an upsurge of all syphilis stages nationally.[1,2] In West Virginia specifically, between 2015 and 2021, the reported rates of primary and secondary syphilis increased from 2.8 to 11.9 cases per 100,000 population and those of congenital syphilis rose from 0 to 87 cases per 100,000 live births.[2] Current US guidelines for syphilis recommend screening any adolescent or adult with increased risk for infection[1] as well as screening all pregnant women.[3]

Treponemal and nontreponemal serological tests remain the standard for syphilis diagnosis, and traditional and reverse testing algorithms are both endorsed.[1,3,4] The traditional algorithm is a 2-tiered approach that incorporates a nontreponemal antibody test as the initial screen followed by a treponemal antibody test to confirm all reactive samples. By contrast, the reverse algorithm uses a treponemal antibody test, typically performed on an automated high-throughput platform, as the initial screen followed by a nontreponemal antibody test to confirm all reactive samples. For specimens with discordant results, a second treponemal antibody test is used as an adjudicating test to differentiate false-positive screening results from true positives accompanied by negative rapid plasma reagin (RPR) results, as seen in patients with previously treated or late latent syphilis. False-positive syphilis serology results are well described in the literature, with frequencies varying by test method and population evaluated.[4–7] Such results may complicate diagnostic interpretation because disagreement between screening and confirmatory tests may be due to nonspecificity of the first-tier assay or low antibody levels among patients with early primary or late latent disease (ie, analytical sensitivity limitations of the second-tier or third-tier assays).[8,9]

For patients with conflicting results in either testing algorithm, the Association of Public Health Laboratories recommends thorough clinical evaluation to rule out current active syphilis or past history of infection and to repeat testing in 2 to 4 weeks if recent exposure is suspected.[10] For universal screening among pregnant women, false-positive results may be particularly problematic due to the concern for potential congenital disease, leading not only to unnecessary anxiety

and further clinical assessment but also to unwarranted antimicrobial treatment.[3,11,12] Several reviews cite an association between pregnancy itself and false-positive nontreponemal or treponemal results,[4,5,13,14] although another describes the association as controversial.[15] A higher proportion of false-positive to true-positive results (ie, lower positive predictive value of testing) has been demonstrated among pregnant women.[7] This is not unexpected, as pregnant populations undergoing universal screening generally have lower prevalence of infection (ie, pretest probabilities) or lower true-positive result frequency than symptomatic or high-risk groups being tested for diagnostic purposes. However, a higher proportion of false positives to true positives does not imply that pregnant women also have a higher false-positive result frequency.

Given the lack of recent primary studies characterizing the occurrence of false-positive syphilis serology results among different testing methodologies, the primary aim of our project was to compare the false-positive result frequencies among different populations tested at a tertiary care academic medical center using both the traditional (October 2016 to September 2019) and reverse (May 2020 to Apr 2023) algorithms and to evaluate the purported association between pregnancy and false positivity. Association between age and false-positive result occurrences was evaluated as a secondary aim because older age has been considered a risk factor for false-positive results in both nontreponemal and treponemal tests.[14,16,17]

Materials and Methods

Study Design

This was a retrospective study performed at the West Virginia University J.W. Ruby Memorial Hospital, a tertiary academic center in Morgantown, WV, with a catchment area encompassing ~1.2 million people. The study was conducted as a quality assurance project in accordance with institutional review board protocol (IRB 1306049573). All test results from each syphilis serology testing algorithm verified between October 2016 and April 2023 were retrieved from the Laboratory Information System (Epic Beaker) along with patient medical record number, gender, diagnosis code, and diagnosis description attached to the test order. Results between October 2019 to April 2020 were excluded because patient samples were screened by a multiplex assay simultaneously detecting both treponemal and nontreponemal antibodies and the assay was eventually recalled by the manufacturer due to specificity problems. Results were further excluded in sequence using the following 4 criteria: (1) patient age was ≤10 years, (2) patient gender was undisclosed or transgender, (3) patient had a prior reactive result, and (4) patient had a previous nonreactive result unless testing represented a first reactive result. Criterion 3 was adopted to mitigate repeated counting of patients with persistent false-positive or true-positive results, whereas criterion 4 was used to avoid artificially increasing the total test count of patients who were repeatedly screened as nonreactive. The overall effect was that only initial test results were included in the analysis for the majority of patients, with the sole exception being patients whose screening results changed from nonreactive to reactive during the study period. All remaining patient results were classified into 4 population cohorts: (1) pregnant women, (2) nonpregnant women, (3) women without an accompanying diagnosis code or description, and (4) men.

Definition of False-Positive Syphilis Screening Test Results

From October 2016 to September 2019 (period 1), patient samples were tested by the traditional testing algorithm, with BD Macro-Vue RPR Card Test (Becton, Dickinson and Company) as the initial screening test followed by *Treponema pallidum* particle agglutination (TP-PA) at a national academic reference laboratory to confirm reactive samples. Reactive RPR results were considered true positives when confirmed by TP-PA or false positives when not confirmed.

In May 2020, the reverse syphilis serology testing algorithm was implemented to meet increasing testing demand within the institution. Patient samples were screened using a treponemal serology test, initially by BioPlex 2200 Syphilis Total immunoassay (Bio-Rad Laboratories) from May 2020 to January 2022 (period 2), and subsequently by Alinity i Syphilis TP assay (Abbott Laboratories) from February 2022 to April 2023 (period 3). The switch from BioPlex to Alinity in 2022 was made for purposes of standardization among different laboratories within our health system. Samples reactive for either treponemal screen were followed by BD Macro-Vue RPR Card Test for confirmation. For conflicting samples (ie, reactive treponemal test and nonreactive RPR), Serodia TP-PA (Fujirebio Diagnostics) was used as the third-tier final adjudicator. Reactive BioPlex or Alinity i syphilis screening results were considered true positives if samples were reactive for either RPR or TP-PA or false positives if samples were nonreactive for both RPR and TP-PA.

Primary Outcome and Statistical Analysis

The primary outcome variable of this study was false-positive result frequency (calculated for each syphilis screening assay as the percentage of false-positive samples in all samples with either nonreactive or false-positive results). Secondary outcome variables included: (1) the true-positive test frequency (calculated as the percentage of total samples tested that were true positive); (2) the positive predictive value of the syphilis screening test (calculated as the percentage of positive samples that were true positive). The χ^2 test (or Fisher's exact test when expected counts were less than 5) was used to compare false-positive result frequencies among different patient populations or among different test methods. Mann-Whitney *U* test was used to compare patient age between the testing result groups (eg, false positive vs nonreactive). For each testing algorithm, multivariable binary logistic regression analysis was used to assess the association between the binary outcomes (false-positive results or not) and patient populations, adjusting for age as a potential confounding variable. The odds ratios with *P* values were reported. Any 2-sided $P < .05$ implied statistical significance for this study.

Results

Patient Populations and Results of the 3 Syphilis Testing Algorithms

A total of 17,515 samples screened by RPR assay during period 1, 14,983 samples screened by BioPlex 2200 Syphilis Total Immunoassay during period 2, and 14,857 samples screened by Alinity i Syphilis TP assay during period 3 were included in the analysis (Supplementary Table 1). The distribution of samples by patient population during the 3 test periods ranged 36.9%-39.6% for pregnant women, 22.4%-25.4% for nonpregnant women, 11.9%-15.8% for women without a

diagnosis code or description, and 20.1%-25.8% for men (**TABLES 1** and **2**).

Overall true-positive result frequencies were 0.39% (68/17,515) for RPR, 1.84% (276/14,983) for BioPlex (comprising 0.83% RPR positive and 1.01% RPR negative results), and 1.52% (226/14,857) for Alinity (comprising 0.81% RPR positive and 0.71% RPR negative results) (**TABLES 1** and **2**). For the 3 testing periods combined, men accounted for the greatest absolute number (400/570, 70%), the highest true-positive result frequency (400/11,286, 3.54% collectively), and the highest testing positive predictive value (400/459, 87.1%) compared with all other populations. Pregnant women, on the other hand, demonstrated the lowest collective true-positive result frequency (18/18,098, 0.10%), and the lowest testing positive predictive value (18/69, 26.1%), among all patient populations for all 3 testing periods combined (**TABLES 1** and **2**).

The overall false-positive result frequency was 0.29% (50/17,447) for the RPR assay, which was significantly lower than 0.61% (90/14,707) observed for the BioPlex treponemal test ($P < .001$) but not statistically different from 0.38% (55/14,631) noted for the Alinity treponemal test ($P = .16$). Comparing the 2 treponemal screening tests, the BioPlex assay showed a significantly higher false-positive result frequency relative to the Alinity assay for all samples (0.61% vs 0.38%, $P = .0039$), with statistical significance in nonpregnant women (24/3326, 0.72% vs 11/3503, 0.31%, odds ratio = 2.31, $P = .018$), borderline significance in pregnant women (25/5731, 0.44% vs 14/5884, 0.24%, odds ratio = 1.84, $P = .065$), but no significant difference in men (22/3326, 0.66% vs 25/3091, 0.81%, odds ratio = 0.82, $P = .49$) (**TABLE 2**).

Association of False-Positive Results with Pregnancy and Age

During period 1, the false-positive result frequency for the RPR assay in pregnant women was lower than that in nonpregnant women with borderline statistical significance (12/6465, 0.19% vs 17/4442, 0.38%, odds ratio = 0.48, $P = .049$) (**TABLE 1**). Although similar trends were observed during periods 2 and 3, the differences did not reach statistical significance for Bioplex (25/5731, 0.44% vs 24/3326, 0.72%, odds ratio = 0.60, $P = .075$) or Alinity (14/5884, 0.24% vs 11/3503, 0.31%, odds ratio = 0.76, $P = .49$) screening tests (**TABLE 2**).

Patients with false-positive RPR results were significantly older than patients with nonreactive results (median age 36 vs 28, $P < .001$), with differences noted primarily among nonpregnant women (median age 37 vs 25, $P = .019$) and women without a diagnosis (median age 55 vs 32, $P = .040$) (**TABLE 3**). By contrast, nonpregnant women with false-positive screening results by the BioPlex assay were younger than those with nonreactive results (median age 25 vs 30, $P = .047$), although age was not associated with false positivity in any other patient populations during period 2 (**TABLE 3**). No significant association between false positive results and age was noted for any patient populations tested by the Alinity assay during period 3.

After adjusting for age in the logistic regression model, pregnant women showed significant association with fewer false-positive results when compared with nonpregnant women for the BioPlex treponemal test (odds ratio = 0.57, $P = .049$). However, this association did not reach statistical significance for the RPR assay (odds ratio = 0.57, $P = .15$) or the Alinity treponemal test (odds ratio = 0.77, $P = .53$). In summary, pregnant women did not demonstrate more false-positive results when compared with nonpregnant women during any testing periods, whether or not age adjustment was used.

Discussion

Based on true-positive samples reactive for both treponemal and nontreponemal serology tests, we observed an increase in syphilis infections within the tested population, from 0.39% (period 1) to 0.83% (period 2) and 0.81% (period 3). This is consistent with the surveillance data showing the upsurge of all syphilis stages in West Virginia.[2] In our study, pregnant women exhibited the lowest true-positive result frequencies compared with nonpregnant women and men when tested by any algorithm. This is not unexpected, as other populations are tested primarily due to risk factors for syphilis.[1] As a result, the positive predictive values of the RPR assay, BioPlex 2200 Syphilis Total Immunoassay, and Alinity i Syphilis TP assay were the lowest for pregnant women, ranging from 14% to 31%, which is consistent with previous studies.[7,11,12,18,19] This observation underscores the importance of following algorithms that incorporate confirmatory testing to distinguish true-positive from false-positive serology results. Overall false-positive result frequencies were 0.29%, 0.61%,

TABLE 1. Result patterns among different patient populations during period 1

	Patient results when screened by nontreponemal antibody test						
	Total	TP (RPR+, TP-PA+)	NR (RPR–)	FP (RPR+, TP-PA–) and its comparison			
	n (%)[a]	n (%)[b]	n (%)[b]	n (%)[c]	*P*[d]	*P*[e]	PPV
All samples screened by RPR assay (period 1)	17,515 (100.0)	68 (0.39)	17,397 (99.33)	50 (0.29)	NA	NA	58%
Nonpregnant women	4448 (25.4)	6 (0.13)	4425 (99.48)	17 (0.38)	Reference group	Reference group	26%
Pregnant women	6467 (36.9)	2 (0.03)	6453 (99.78)	12 (0.19)	.049	.15	14%
Women without diagnosis	2076 (11.9)	5 (0.24)	2062 (99.33)	9 (0.43)	.75	.80	36%
Men	4524 (25.8)	55 (1.22)	4457 (98.52)	12 (0.27)	.34	.15	82%

FP, false positive; NR, nonreactive; PPV, positive predictive value; TP, true positive.
[a]*Calculated as percentage (%) of all samples tested by the algorithm.*
[b]*Calculated as percentage (%) within each patient population.*
[c]*Calculated as percentage (%) within all samples with NR and FP results.*
[d]*P value from χ^2 test to compare false-positive result frequency with the reference group.*
[e]*P value from a logistic regression analysis adjusted for age.*

TABLE 2. Result patterns among different patient populations during period 2 and period 3

	Patient results when screened by treponemal antibody tests							
	Total	TP (TT+, RPR+)	TP (TT+, RPR−, TP−PA+)	NR (TT-)	FP (TT+, RPR−, TP-PA−) and its comparison			
	n (%)[a]	n (%)[b]	n (%)[b]	n (%)[b]	n (%)[c]	*P*[d]	*P*[e]	PPV
All samples screened by Bioplex assay (period 2)	14,983 (100.0)	124 (0.83)	152 (1.01)	14,617 (97.56)	90 (0.61)	NA	NA	75%
Nonpregnant women	3361 (22.4)	14 (0.42)	21 (0.62)	3302 (98.24)	24 (0.72)	Reference group	Reference group	59%
Pregnant women	5742 (38.3)	7 (0.12)	4 (0.07)	5706 (99.37)	25 (0.44)	.075	.049	31%
Women without diagnosis	2364 (15.8)	28 (1.18)	12 (0.51)	2305 (97.50)	19 (0.82)	.68	.72	68%
Men	3516 (20.1)	75 (2.13)	115 (3.27)	3304 (93.97)	22 (0.66)	.76	.96	90%
All samples screened by Alinity assay (period 3)	14,857 (100.0)	120 (0.81)	106 (0.71)	14,576 (98.11)	55 (0.38)	NA	NA	80%
Nonpregnant women	3542 (23.8)	24 (0.68)	15 (0.42)	3492 (98.59)	11 (0.31)	Reference group	Reference group	78%
Pregnant women	5889 (39.6)	5 (0.08)	0 (0.00)	5870 (99.68)	14 (0.24)	.49	.53	26%
Women without diagnosis	2180 (14.7)	17 (0.78)	10 (0.46)	2148 (98.53)	5 (0.23)	.57	.58	84%
Men	3246 (21.8)	74 (2.28)	81 (2.50)	3066 (94.45)	25 (0.81)	.0065	.031	86%

FP, false positive; NR, nonreactive; PPV, positive predictive value; TP, true positive; TT, BioPlex 2200 or Alinity i treponemal test.
[a]*Calculated as percentage (%) of all samples tested by the algorithm.*
[b]*Calculated as percentage (%) within each patient population.*
[c]*Calculated as percentage (%) within all samples with NR and FP results.*
[d]*P value from χ^2 test or Fisher's exact test to compare false-positive result frequency with the reference group.*
[e]*P value from a logistic regression analysis adjusted for age.*

and 0.38% for samples screened by the RPR, BioPlex, and Alinity assays, respectively. These figures are similar to the ranges of 0.05% to 0.60% reported in previous studies.[20–24] With the current resurgence of syphilis in the United States, positive predictive values for screening methods will likely increase, whereas false-positive result frequencies should remain relatively stable unless assay performance is improved.

Interestingly, between the 2 treponemal antibody tests, the BioPlex assay yielded more false-positive results than the Alinity assay, but only for women. Additional studies using a parallel rather than sequential testing approach could help confirm this apparent difference in specificity. Our results suggest that factors contributing to false-positive results are more likely to be assay specific, and that some factors more prevalent in females may interfere with the BioPlex assay and contribute to false-positive results. If such interfering factors could be identified, assay specificity may be improved accordingly.

Irrespective of the syphilis screening test used, pregnant women did not show higher false-positive result frequencies than nonpregnant women, suggesting that pregnancy is not a strong risk factor for false positivity. Identifying an association between pregnancy and false-positive results was complicated in this study because the nonpregnant women included as the reference comparator were not a selected group of healthy age-matched female subjects but rather were older than the pregnant women. Age is a potential confounding variable because aging has been associated with false-positive results in both nontreponemal and treponemal tests.[14,16,17] In our study, a significant association between older age and false-positive syphilis testing results was only observed for the RPR assay during period 1 and not for either treponemal screening test during periods 2 and 3. After adjusting for age, pregnant women still failed to show higher false-positive result frequencies than nonpregnant women for any of the 3 syphilis screening tests. These findings are consistent with 2 previous studies evaluating the CAPTIA syphilis G treponemal test, both of which reported higher specificity in pregnant women than in nonpregnant patients[25] or in patients with suspected sexually transmitted infections.[26]

Our study is not without limitations. First, 12% to 16% of samples were obtained from women with no accompanying diagnosis code. These likely represented a mixture of pregnant and nonpregnant women and were evaluated as a separate group for that reason. Second, due to the retrospective study design, comparisons between different screening assays were made using different samples tested over distinct periods. It is possible that factors contributing to false-positive results may change over time, temporally affecting assay performance. One example is the US Food and Drug Administration's warning about the potential for false-positive RPR results among patients who had received a COVID-19 vaccine.[27] For this reason, "split-sample" parallel testing approaches should be considered for direct comparisons between methods, algorithms, or assays. Third, false-positive screening results were defined based on testing algorithm criteria. Ideally, false-positive results should be defined by well-characterized gold-standard tests if available, although this is not feasible for a retrospective study. We also did not have access to all patient histories and medical records to distinguish true-positive from false-positive results based on clinical impression or patient history. We used the TP-PA test, which demonstrates near-perfect specificity,[8,9] for confirmation in the traditional testing algorithm as well as for the third-tier adjudication assay in both reverse testing algorithms. However, the TP-PA test may rarely produce false-negative results,[9,28] which introduces the possibility of slightly overestimated false-positivity frequencies for all 3 methods. Finally, repeatedly nonreactive and reactive results from the same patient were excluded based on criteria 3 and 4 described in the Materials and Methods section, so that the calculated false-positive and true-positive result frequencies more closely represented the prevalence of false positives and true positives in the tested population. However, when those results were not excluded, our findings and conclusions remain essentially unchanged (Supplementary Tables 2 and 3).

TABLE 3. Age comparison between patients with nonreactive and false-positive screening test results

	Period 1			Period 2			Period 3		
	Age of patients with NR results	Age of patients with FP results	Age comparison (FP vs NR)	Age of patients with NR results	Age of patients with FP results	Age comparison (FP vs NR)	Age of patients with NR results	Age of patients with FP results	Age comparison (FP vs NR)
	Median (IQR)	Median (IQR)	P^a	Median (IQR)	Median (IQR)	P^a	Median (IQR)	Median (IQR)	P^a
All samples	28 (22-36)	36 (27-55)	<.001	29 (23-37)	29 (22-40)	.35	29 (24-37)	32 (22-51)	.42
Nonpregnant women	25 (20-37)	37 (25-55)	.019	30 (22-43)	25 (19-35)	.047	31 (23-44)	26 (20-43)	.33
Pregnant women	27 (23-31)	29 (25-32)	.46	27 (23-31)	26 (22-31)	.29	27 (23-31)	28 (23-32)	.99
Women without diagnosis	32 (25-50)	55 (25-69)	.040	29 (24-36)	31 (22-50)	.49	30 (25-38)	26 (21-71)	.84
Men	31 (22-50)	43 (29-60)	.23	38 (26-57)	46 (23-54)	.74	39 (27-57)	47 (30-60)	.54

FP, false-positive; IQR, interquartile range; NR, nonreactive.
[a]*P value derived from Mann-Whitney* U *test.*

In summary, we conclude that pregnant women do not experience a higher false-positive syphilis test result frequency than nonpregnant women or other patient populations, irrespective of the testing algorithm used. In addition, although overall false-positive result frequencies for all 3 syphilis serology screening tests were low, there appears to be a significant difference between different syphilis serology tests, with the Alinity treponemal test showing higher specificity than the BioPlex treponemal test, particularly among women.

Supplementary Material

Supplementary material is available at *Laboratory Medicine* online.

Conflict of Interest Disclosure

The authors have nothing to disclose.

REFERENCES

1. US Preventive Services Task Force; Mangione CM, Barry MJ, Nicholson WK, et al. Screening for syphilis infection in nonpregnant adolescents and adults: US Preventive Services Task Force reaffirmation recommendation statement. *JAMA.* 2022;328(12):1243-1249. doi:10.1001/jama.2022.15322
2. Centers for Disease Control and Prevention. Sexually Transmitted Disease Surveillance 2021. Accessed May 27, 2023. https://www.cdc.gov/std/statistics/2021/default.htm
3. US Preventive Services Task Force; Curry SJ, Krist AH, Owens DK, et al. Screening for syphilis infection in pregnant women: US Preventive Services Task Force reaffirmation recommendation statement. *JAMA.* 2018;320(9):911-917. doi:10.1001/jama.2018.11785
4. Satyaputra F, Hendry S, Braddick M, Sivabalan P, Norton R. The laboratory diagnosis of syphilis. *J Clin Microbiol.* 2021;59(10):e0010021. doi:10.1128/JCM.00100-21
5. Larsen SA, Steiner BM, Rudolph AH. Laboratory diagnosis and interpretation of tests for syphilis. *Clin Microbiol Rev.* 1995;8(1):1-21. doi:10.1128/CMR.8.1.1
6. Ishihara Y, Okamoto K, Shimosaka H, et al. Prevalence and clinical characteristics of patients with biologically false-positive reactions with serological syphilis testing in contemporary practice: 10-year experience at a tertiary academic hospital. *Sex Transm Infect.* 2021;97(6):397-401. doi:10.1136/sextrans-2020-054628
7. Henrich TJ, Yawetz S. Impact of age, gender, and pregnancy on syphilis screening using the Captia Syphilis-G assay. *Sex Transm Dis.* 2011;38(12):1126-1130. doi:10.1097/OLQ.0b013e31822e60e1
8. Cole MJ, Perry KR, Parry JV. Comparative evaluation of 15 serological assays for the detection of syphilis infection. *Eur J Clin Microbiol Infect Dis.* 2007;26(10):705-713. doi:10.1007/s10096-007-0346-9
9. Park IU, Fakile YF, Chow JM, et al. Performance of treponemal tests for the diagnosis of syphilis. *Clin Infect Dis.* 2019;68(6):913-918. doi:10.1093/cid/ciy558
10. Association of Public Health Laboratories. Suggested Reporting Language for Syphilis Serology Testing. Accessed May 27, 2023. https://www.aphl.org/aboutAPHL/publications/Documents/ID-2020Aug-Syphilis-Reporting-Language.pdf
11. O'Connor NP, Burke PC, Worley S, Kadkhoda K, Goje O, Foster CB. Outcomes after positive syphilis screening. *Pediatrics.* 2022;150(3):e2022056457. doi:10.1542/peds.2022-056457
12. Mmeje O, Chow JM, Davidson L, Shieh J, Schapiro JM, Park IU. Discordant syphilis immunoassays in pregnancy: perinatal outcomes and implications for clinical management. *Clin Infect Dis.* 2015;61(7):1049-1053. doi:10.1093/cid/civ445

13. Hook EW 3rd, Marra CM. Acquired syphilis in adults. *N Engl J Med.* 1992;326(16):1060-1069. doi:10.1056/NEJM199204163261606
14. Ratnam S. The laboratory diagnosis of syphilis. *Can J Infect Dis Med Microbiol.* 2005;16(1):45-51. doi:10.1155/2005/597580
15. Ghanem KG, Ram S, Rice PA. The modern epidemic of syphilis. *N Engl J Med.* 2020;382(9):845-854. doi:10.1056/NEJMra1901593
16. Carr RD, Becker SW, Carpenter CM. The biological false-positive phenomenon in elderly men. *Arch Dermatol.* 1966;93(4):393-395.
17. Tuffanelli DL. Ageing and false positive reactions for syphilis. *Br J Vener Dis*. 1966;42(1):40-41. doi:10.1136/sti.42.1.40
18. Williams JEP, Bazan JA, Turner AN, et al. Reverse sequence syphilis screening and discordant results in pregnancy. *J Pediatr.* 2020;219:263-266.e1. doi:10.1016/j.jpeds.2019.11.035
19. Boonchaoy A, Wongchampa P, Hirankarn N, Chaithongwongwatthana S. Performance of chemiluminescent microparticle immunoassay in screening for syphilis in pregnant women from low-prevalence, resource-limited setting. *J Med Assoc Thai.* 2016;99(2):119-124.
20. Nah EH, Cho S, Kim S, Cho HI, Chai JY. Comparison of traditional and reverse syphilis screening algorithms in medical health checkups. *Ann Lab Med*. 2017;37(6):511-515. doi:10.3343/alm.2017.37.6.511
21. Zhuang YH, Liu H, Tang J, et al. Screening for syphilis with dual algorithms: analysis of discordant and concordant serology results in a population with a low prevalence of syphilis. *J Eur Acad Dermatol Venereol.* 2019;33(1):178-184. doi:10.1111/jdv.15251
22. Huh HJ, Chung JW, Park SY, Chae SL. Comparison of automated treponemal and nontreponemal test algorithms as first-line syphilis screening assays. *Ann Lab Med*. 2016;36(1):23-27. doi:10.3343/alm.2016.36.1.23
23. Binnicker MJ, Jespersen DJ, Rollins LO. Direct comparison of the traditional and reverse syphilis screening algorithms in a population with a low prevalence of syphilis. *J Clin Microbiol.* 2012;50(1):148-150. doi:10.1128/JCM.05636-11
24. Mishra S, Boily MC, Ng V, et al. The laboratory impact of changing syphilis screening from the rapid-plasma reagin to a treponemal enzyme immunoassay: a case-study from the Greater Toronto Area. *Sex Transm Dis.* 2011;38(3):190-196. doi:10.1097/OLQ.0b013e3181f07e91
25. Silletti RP. Comparison of CAPTIA syphilis G enzyme immunoassay with rapid plasma reagin test for detection of syphilis. *J Clin Microbiol.* 1995;33(7):1829-1831. doi:10.1128/jcm.33.7.1829-1831.1995
26. Ross J, Moyes A, Young H, McMillan A. An analysis of false positive reactions occurring with the Captia Syph G EIA. *Genitourin Med*. 1991;67(5):408-410. doi:10.1136/sti.67.5.408
27. The US Food and Drug Administration (FDA). Possible false RPR reactivity with BioPlex 2200 Syphilis Total & RPR Test Kit following a COVID-19 vaccine - letter to clinical laboratory staff and health care providers. Accessed May 27, 2023. https://www.fda.gov/medical-devices/letters-health-care-providers/possible-false-rpr-reactivity-BioPlex-2200-syphilis-total-rpr-test-kit-following-covid-19-vaccine
28. Zhiyan L, Meiling W, Ping L, Jinhua D, Zhenlin Y, Zhenru F. Consistency between *Treponema pallidum* particle agglutination assay and architect chemiluminescent microparticle immunoassay and characterization of inconsistent samples. *J Clin Lab Anal.* 2015;29(4):281-284. doi:10.1002/jcla.21765

Study of the diagnostic efficiency of anti-ZnT8 autoantibodies for type 1 diabetes in pediatric patients

Sandra Fuentes-Cantero,[1] Concepción González-Rodríguez,[1] Carmen Rodríguez-Chacón,[1] Raquel Galvan-Toribio,[1] Joaquín Hermosín-Escudero,[1] Antonio Pérez-Pérez,[1] Antonio León-Justel[1]

[1]Unit of Clinical Biochemistry, University Hospital Virgen Macarena, Seville, Spain. Corresponding author: Concepción González-Rodríguez; concepcion.gonzalez.r.sspa@juntadeandalucia.es

Key words: autoantibodies, type 1 diabetes, GAD65, islet antigen-2 autoantibodies, Zinc transporter 8, diagnosis

Abbreviations: ZnT8A, zinc transporter 8 autoantibodies; T1D, type 1 diabetes; GADA, glutamic acid decarboxylase autoantibodies; IA-2A, islet antigen autoantibodies; ELISA, enzyme-linked immunosorbent assay; CLIA, chemiluminescent immunoassay; TG2A-IgA, anti-transglutaminase IgA antibody; HbA1c, glycosylated hemoglobin

Laboratory Medicine 2024;55:299-303; https://doi.org/10.1093/labmed/lmad079

ABSTRACT

Objective: Zinc transporter 8 autoantibodies (ZNt8A) are 1 of the 4 main autoantibodies used for the diagnosis of type 1 diabetes (T1D), with glutamic acid decarboxylase autoantibodies (GADA), islet antigen-2 autoantibodies (IA-2A), and insulin autoantibodies (IAA). The objective of this study is to evaluate the diagnostic efficiency of these autoantibodies for the diagnosis of T1D in pediatric patients.

Methods: A retrospective analysis of patients under 16 years of age with suspected T1D was made between June 2020 and January 2021. A total of 80 patients were included in the study, with 1 sample per patient. Subjects were classified according to diagnosis.

Results: Of the subjects included in the study, 50 developed T1D. The diagnostic efficacy was IA-2A (cutoff ≥ 28 U/L) sensitivity 0.26 (95% CI: 0.14-0.38) and specificity 0.97 (95% CI: 0.79-1.0); GADA (cutoff ≥ 17 U/mL) sensitivity 0.40 (95% CI: 0.26-0.54) and specificity 0.87 (95% CI: 0.75-0.99); ZnT8A (cut off ≥ 15 U/L) sensitivity 0.62 (95% CI: 0.49-0.75) and specificity 0.97 (95% CI: 0.90-1.0). ZnT8A obtained the most significantly global diagnostic accuracy (0.75), and GADA with ZnT8A showed the highest correlation.

Conclusion: The results obtained indicate a higher efficiency of anti-ZnT8 autoantibodies for the diagnosis of T1D in pediatric patients. Clinical efficiency of diabetic autoantibodies is method and assay dependent and influences combined diagnostic strategies.

Introduction

Zinc transporter 8 autoantibodies (ZNt8A) are 1 of the 4 major islet autoantibodies, with glutamic acid decarboxylase autoantibodies (GADA), islet antigen-2 autoantibodies (IA-2A), and insulin autoantibodies (IAA).

ZnT8A are the most recently characterized islet autoantibodies, found in 66% to 80% of White patients at diagnosis and are detectable in approximately 26% of individuals with type 1 diabetes (T1D) previously categorized as autoantibody negative.[1]

Several international studies have shown that around two-thirds of children are ZnT8A-positive at diagnosis and, depending on the age group considered, the prevalence is similar to IA-2A.[2,3]

Humoral islet autoimmunity can develop in children as young as 6 months of age with a peak incidence of seroconversion at 2 to 3 years and a probable second peak in puberty.[4] Typically, IAA and GADA are the first autoantibodies to develop in young children, whereas IA-2A and ZnT8A arise later in prediabetes and are more common in adolescents at diagnosis.[5] However, it has been reported that ZnT8A autoimmune reactivity towards the extracellular domain are the earliest major islet autoantibodies to appear in young children, followed by IAA, GADA, IA-2A, and intracellular ZnT8A.[6] Almost all ZnT8A data in the literature and clinical laboratory, by default, indicate autoimmune reactivity towards the intracellular domain.[7]

Although the gold standard method to measure ZNt8A and islet autoantibodies is radioimmunoassay, alternative assays, such as enzyme-linked immunosorbent assay (ELISA) or chemiluminescent immunoassay (CLIA), are real alternatives, matching or including exceeding radioimmunoassay analytical performance while avoiding the use of radioactive isotopes.[7]

This study aims to analyze the diagnostic efficiency of ZNt8A with respect to GADA and IA-2A in pediatrics samples received in a routine care clinical laboratory.

Materials and Methods

Patients and Study Design

This is a retrospective analysis of patients with suspected T1D who were studied by the Endocrinology Department of the University Hospital Virgen Macarena in Seville, Spain, between June 2020 and January 2021. A total of 80 patients were evaluated, with only 1 sample per patient. These subjects were subsequently classified according to diagnosis.

Subjects included were patients under 16 years of age who were studied for having glycemia levels above 126 mg/dL, symptoms compatible with T1D, and/or a family history of T1D who had also requested a study of islet autoantibodies.

The study was approved by the Institutional Review Board of Virgen Macarena and Virgen del Rocío Hospitals, Znt8A code, according to the ethical principles included in the Declaration of Helsinki 1964 (2013 update). Written consent was not required.

Laboratory Analysis

Blood samples were collected after overnight fasting. ZnT8A analyzed using an ELISA commercial kit (Euroimmun Dcs enzyme-linked immunosorbent assay) automated in a Euroimmun I2P-analyzer. This test provides quantitative in vitro determination of human ZnT8A in serum or plasma with a manufacturer's recommended cutoff for positivity ≥15U/mL. Intra-assay coefficients of variation (CVs) at medium (24.5 U/mL) and high (159.5 U/mL) Znt8A concentrations are 3.5% and 6.6%, respectively, whereas inter-assay CVs at medium (26.6 U/mL) and high (101.9 U/mL) Znt8A are 6.2% and 9.3%, respectively.

GADA and IA-2A were routinely measured according to hospital protocol by the fully automated SnibeDcs sandwich CLIA, automated in the Maglumi 1000 analyzer. The antigens recognized by these antibodies include 65 kDa glutamic acid decarboxylase and islet cell antigen IA-2. The manufacturer's recommended cutoff for GADA and anti-IA2A positivity are ≥17 IU/mL and 28 IU/mL, respectively.

C-peptide and vitamin D concentration were determined in serum samples using chemiluminescence immunoassay methods (Roche Diagnostic; reference ranges: C-peptide 0.48-5.05 ng/mL and vitamin D 20-60 ng/mL). Triglycerides were determined by colorimetric enzymatic assay (Roche Diagnostics; reference range: <150 mg/dL).

Glycosylated hemoglobin (HbA1c) levels were determined by high performance liquid chromatography (HORIBA Laboratory) in the Tosoh G8 analyzer (reference range: <5.5%).

Anti-transglutaminase IgA antibody (TG2A-IgA) levels were also collected and analyzed by fluroenzyme-immunoassay on the Phadia 250 (Thermo Fisher Scientific) with a cutoff point ≥7 U/mL.

The time elapsed between the date of first appearance and the date of the analytical study and family history were recorded.

Statistics

Statistical analysis was performed using SPSS Statistics version 25.0 (IBM). Quantitative results are expressed as median and interquartile range. For the comparative analysis of qualitative variables, the χ^2 test was used. Nonparametric Mann-Whitney test was used to compare quantitative variables. Correlation analysis was performed using the Spearman rank correlation test. Statistical significance was assumed at $P < .05$.

Results

Study Cohort

A total of 80 patients were studied, 34 boys (42.5%) and 46 girls (57.5%), of whom 50 finally developed diabetes according to current diagnostic criteria. The ages of the children screened ranged from 4 to 16 years with a median age of 12.0 years, and the median time from first appearance to diagnosis was 17 months (0.0-52.0) (**TABLE 1**). Of the 50 patients, 34 had a family history of diabetes and 3 had positive TG2A-IgA but no celiac disease.

Descriptive variables and laboratory results are shown in **TABLE 1**. Positive ZnT8A were detected in 32 patients (40%), IA-2A in 14 patients (17.5%), and GADA in 24 patients (30%).

Study Positivity Patterns

The pattern of positivity of the antibodies studied is shown in **TABLE 2**, where 17 patients (21.3%) were positive for only 1 antibody, 16 patients (20%) for 2 antibodies, and 7 patients (8.8%) were positive for all 3

TABLE 1. Descriptive summary of study variables[a]

	Diabetic (n = 50)	Nondiabetic (n = 30)	*P*
Age, y, No.	12.0 (4.0)	11.0 (6.0)	.818
Sex, M/F, No.	20/30	14/16	.559
Family history of diabetes, yes/no, No.	34/16	10/20	.003
Glucose, mg/dL	160.0 (101.0)	85.5 (14.0)	.000
HbA1c, %	7.8 (1.7)	5.4 (0.3)	.000
Triglycerides, mg/dL	74.0 (40.0)	65.0 (23.0)	.029
LDL-cholesterol, mg/dL	84.0 (38.0)	80.5 (34.0)	.903
Vitamin D, ng/mL	22.8 (12.0)	30.0 (21.1)	.004
C-peptide, ng/mL	0.3 (0.8)	1.6 (0.89)	.000
GADA, U/mL	8.9 (35.6)	3.8 (4.1)	.000
IA-2A, U/mL	8.2 (51.2)	7.3 (2.4)	.226
TG2A-IgA, U/mL	0.4 (0.6)	0.1 (0.3)	.001
ZnT8A, U/mL	5.5 (19.0)	1.0 (0.0)	.000
Time since first appearance, mo	17.0 (52.0)	-	

GADA, glutamic acid decarboxylase autoantibodies; IA-2A, islet antigen autoantibodies; TG2A-IgA, anti-transglutaminase IgA antibody; ZnT8A, zinc transporter 8 autoantibodies.

[a]*Results are expressed as median (interquartile range) except where otherwise specified.*

TABLE 2. Age-related positive pattern of the islet cell autoantibodies in diabetes children and global relation with glucose, HbA1c, C peptide, and vitamin D

	Age group, No.				Parameter			
Positive pattern	<6 years	6-12 years	>12 years	Total	Glucose, mg/dL	HbA1c, %	C-peptide, ng/mL	Vitamin D, ng/mL
Single antibody	0	10	7	17	147	7.1	0.55	23.3
2 antibodies	4	8	4	16	151	8.7	0.22	25.9
3 antibodies	2	3	2	7	138	6.3	0.02	17.9
ZnT8A	6	17	9	32	151.0	7.7	0.26	19.7
GADA	5	13	6	24	130.5	7.3	0.065	24.5
IA-2A	3	5	6	14	161.0	6.5	0.59	19.1
ZnT8A+GADA	3	6	1	10	125	8.4	0.08	26.7
ZnT8A+I A-2A	1	1	2	4	164	10.3	1.29	23.9
GADA+ IA-2A	0	1	1	2	164	—	—	—

GADA, glutamic acid decarboxylase autoantibodies; HbA1c, glycosylated hemoglobin; IA-2A, islet antigen autoantibodies; ZnT8A, zinc transporter 8 autoantibodies.

TABLE 3. Summary of Znt8A correlation study

		Vitamin D	GADA	IA-2A	C-peptide	TG2A-IgA	Age	Time since first appearance
ZnT8A	Spearman correlation	–0.097	0.486	0.323	–0.281	0.255	–0.191	–0.311
	P[a]	.480	**.000**	**.004**	**.015**	**.032**	.090	**.030**

GADA, glutamic acid decarboxylase autoantibodies; IA-2A, islet antigen autoantibodies; TG2A-IgA, anti-transglutaminase IgA antibody; ZnT8A, zinc transporter 8 autoantibodies.
[a]*Bold values indicate significance at* P < *.05.*

antibodies studied. **TABLE 2** also shows the pattern of positivity according to age grouped into 3 groups (under 6 years, between 6 and 12 years, and over 12 years). As can be observed in this table, patients who were positive for 2 antibodies had significantly higher blood glucose (*P* = .022 by Kruskal-Wallis test) whereas HbA1c did not reach significance (*P* = .104). C-peptide declined as antibodies number increased (*P* = .004 by Kruskal-Wallis test).

A more specific analysis of the patients with positive ZnT8A with the other antibodies studied showed that 10 patients also had GADA and 4 also had AI-2A (**TABLE 2**).

Study Correlations

Analysis (**TABLE 3**) showed that level of ZnT8A had a significant positive correlation with GADA, IA-2A, and TG2A-IgA level, whereas correlation was significantly negative for C-peptide level and date from first appearance to diagnosis. Thus, C-peptide levels were lower in patients with higher levels of ZnT8A, and as the time since first appearance increased, ZnT8 A levels decreased.

Analysis of Diagnostic Efficiency

Diagnostic efficiency data for our cohort of pediatric patients are shown in **TABLE 4**. ZnT8A antibodies performed better than GADA and IA-2A, with a sensitivity of 62% and a specificity of 94% and better positive and negative likelihood ratios, whereas IA-2A showed low sensitivity (26%), with similar specificity to ZnT8A. These differences are consistent with the statistically significant differences found in the reliability analysis of the diagnostic efficacy of 3 antibodies (Cohen's kappa index; *P* =.001).

Discussion

This study showed that ZnT8A had better diagnostic efficiency for the diagnosis of T1D in pediatric patients than GADA or IA-2A. The sensitivity (62 %) and specificity (94 %) of the ZnT8A assay in the cohort of patients were in line with other studies[8,9] and other methods such as CLIA. Previously, 99.8% specificity (normal controls) and 62.3% sensitivity (new-onset T1D patients) have been found for ZnT8A by CLIA.[10] Although the gold standard assay for the determination of these antibodies is the radio-binding assay, it has also been reported that ELISA and CLIA assay are comparable or better than the radio-binding assay in independent clinical trial studies.[7]

The diagnostic performance was obtained without modifying the cutoff point suggested by the manufacturer (15 U/mL). An Italian multicenter study analyzed the efficiency of other commercial ZnT8A ELISAs using a slightly lower cutoff point (10 U/mL) and found 61% sensitivity and 97% specificity, very similar to our results.[11] This study also emphasizes that the sensitivity of immunofluorescence beta islet cell antibodies is much lower than that of individual islet antibodies determined by quantitative immunoassays and that there was a very significant percentage of false negatives that were later confirmed to be positive with the individual autoantibodies.[11] Another study performed in 2021 analyzed the ZnT8A age-dependent cutoff threshold and demonstrated that the cutoff was significantly higher in those tested who were under 30 years of age than in those tested at age 30 years or older. Therefore, with the cutoff recommended by the ELISA manufacturer (6 U/mL), specificity was 79% and 95% in patients aged <30 or ≥30 years, respectively, and they recommend increasing commercial cutoff for those tested under 30 years by 3 times.[12] The ZnT8A ELISA used in our study has a 15U/mL cutoff with a 94% specificity in patients up to 16 years old.

TABLE 4. Diagnostic efficiency of the 3 antibody assays according to the cutoff point established by the manufacturer

	IA-2A (cutoff ≥28 U/mL)		GADA (cutoff ≥17 U/mL)		ZnT8A (cutoff ≥ 15 U/mL)	
	Negative	Positive	Negative	Positive	Negative	Positive
Nondiabetic subjects	29	1	26	4	29	1
Diabetic subjects	37	13	30	20	19	31
Sensitivity (95% CI)	0.26 (0.14-0.38)		0.40 (0.26-0.54)		0.62 (0.49-0.75)	
Specificity (95% CI)	0.97(0.79-1.0)		0.87 (0.75-0.99)		0.94 (0.90-1.0)	
LR+ (95% CI)	7.80 (1.07-56.66)		3.00 (1.13-7.94)		18.60 (2.67-129.33)	
LR– (95% CI)	0.77 (0.63-0.93)		0.69 (0.53-0.91)		0.39 (0.27-0.56)	
Global diagnostic accuracy[a]	0.40		0.57		0.75	

GADA, glutamic acid decarboxylase autoantibodies; IA-2A, islet antigen autoantibodies; LR, likelihood ratio; ZnT8A, zinc transporter 8 autoantibodies.
[a]Global diagnostic accuracy is the ratio of true results (both true positives and true negatives) to the total number of cases tested (true positives, false positives, true negatives, and false negatives).

The most frequently detected antibody in the study cohort was ZnT8A (40%), being more prevalent in children aged 6 to 12 years. These results are consistent with those reported in the French study of Garnier et al.[13] On the other hand, it should be noted that CLIA IA-2A obtained the lowest sensitivity (26%) in this work and it only increased the number of diabetic children with positive antibodies by 1, therefore limiting its contribution to diagnosis.

Studying the pattern of positivity, we observed the highest frequency of positivity for a single antibody, followed by 2 positive antibodies, with least frequent being positivity for 3 antibodies. These results do not coincide with those previously reported, in which up to 70% of diabetics have 3 or 4 autoantibodies, whereas only 10% are positive for a single autoantibody.[14,15] Niechial et al[16] reported that the occurrence of a single autoantibody is rare in children, affecting only 7.8%; whereas 2 (37.8 %) or 3 (49.5 %) diabetes-associated autoantibodies were more frequently detected. A higher percentage has been described in smaller series; Basu et al[17] found at least 1 antibody in 97.8% and at least 2 antibodies in 67.3% diabetic children.

Usually, HbA1c levels increase more when diabetes first appears with 3 antibodies than when 1 antibody first appears. Despite the limitation of the sample size of the study, higher HbA1c levels were observed in 2 (8.7%) vs single (7.1%) islet autoantibodies. Also, we report similarly to others that lower HbA1c levels are associated with anti-IA2.[18]

The most frequent combination found in the children in our study was ZnT8A with GADA antibodies, in contrast to other publications, which indicated a higher frequency of ZnT8A and IA-2A.[16] This is probably affected by the low sensitivity of the IA-2A assay in our study.

ZnT8A antibodies correlated positively with the other antibodies and negatively with C-peptide levels. Furthermore, it was observed that mainly GADA and then ZnT8A were associated with lower C-peptide levels. ZnT8A have been associated with rapid onset of hyperglycemia and a more acute onset of disease.[16,19] There is evidence of beta-cell damage due to the presence of these autoantibodies, which get involved in the synthesis, storage, and secretion of insulin. ZnT8A have been shown to be trafficked to the surface of β-cells during insulin secretion.[15,20]

This study also showed a significant decrease in the level of ZnT8A antibodies as the time between first appearance and diagnosis increased. Wenzlau et al[21] also reported that ZnT8A positivity decreases significantly as the disease progresses, resulting in a lower positivity rate. Some studies have detected pancreatic autoantibodies in longstanding T1D, with anti-GADA being the most frequent in such cohorts,[22] but it remains unclear whether ZnT8A is a useful marker for longstanding T1D.[23] Some authors, such as Sosenko et al,[24] have indicated that in children, the GADA titer tends to decline at diagnosis. Recently, it has been shown that ZnT8A targeting extracellular epitopes of ZnT8 on the surface of β-cells in patients with T1D appear earlier than all other autoantibodies and are an early predictor of disease.[7]

In studying levels of vitamin D, significantly lower levels were found in the diabetic subjects. Also, an inverse correlation was found between vitamin D and ZnT8A levels that was not significant. Vitamin D deficiency has been associated with T1D in observational studies, but clinical trials have so far been unsuccessful, and larger randomized controlled studies are needed to investigate small effects.[25]

With regard to the diagnostic efficiency of ZnT8A as a function of age, the study seems to reveal better sensitivity and specificity in patients younger than 10 years. The prevalence of these antibodies has been shown to be related to age at diagnosis, being more frequent in some studies in cohorts of patients between 8 and 16 years and between 6 and 17 years.[2,13]

The main limitation of this study is the lack of patient follow-up data to assess the evolution of the antibodies studied and the sample size. There were also no ICA and IAA antibody measurements. However, the aim of investigating ZnT8A clinical efficiency took place in a clinical context, where the interest in ICA and IAA is limited. Also, only patients under 16 years of age were included. This age range captures most new diagnoses of pediatric T1D seen in a pediatric unit. However, it excludes patients in late adolescence or early adulthood, who could be diagnosed at a pediatric center and cared for initially by pediatric endocrinologists.

Conclusions

ZnT8A are an excellent marker for the diagnosis of autoimmune diabetes in the pediatric population. However, clinical efficiency of diabetic autoantibodies is method and assay dependent. In this work, the CLIA IA-2A assay was found to have the lowest global diagnostic accuracy with a poor contribution to diagnosis.

Conflict of Interest Disclosure

The authors have nothing to disclose.

REFERENCES

1. Wenzlau JM, Juhl K, Yu L, et al. The cation efflux transporter ZnT8 (Slc30A8) is a major autoantigen in human type 1 diabetes. *Proc Natl Acad Sci U S A.* 2007;104(43):17040-17045. doi:10.1073/pnas.0705894104
2. Wenzlau JM, Liu Y, Yu L, et al. A common nonsynonymous single nucleotide polymorphism in the SLC30A8 gene determines ZnT8 autoantibody specificity in type 1 diabetes. *Diabetes.* 2008;57(10):2693-2697. doi:10.2337/db08-0522
3. Long AE, Gillespie KM, Rokni S, Bingley PJ, Williams AJ. Rising incidence of type 1 diabetes is associated with altered immunophenotype at diagnosis. *Diabetes.* 2012;61(3):683-686. doi:10.2337/db11-0962
4. Ziegler AG, Rewers M, Simell O, et al. Seroconversion to multiple islet autoantibodies and risk of progression to diabetes in children. *JAMA.* 2013;309(23):2473-2479. doi:10.1001/jama.2013.6285
5. Williams CL, Long AE. What has zinc transporter 8 autoimmunity taught us about type 1 diabetes? *Diabetologia.* 2019;62(11):1969-1976. doi:10.1007/s00125-019-04975-x
6. Gu Y, Merriman C, Guo Z, et al. Novel autoantibodies to the β-cell surface epitopes of ZnT8 in patients progressing to type-1 diabetes. *J Autoimmun.* 2021;122:102677. doi:10.1016/j.jaut.2021.102677
7. Jia X, Gu Y, High H, Yu L. Islet autoantibodies in disease prediction and pathogenesis. *Diabetol Int*. 2019;11(1):6-10. doi:10.1007/s13340-019-00414-9
8. Petruzelkova L, Ananieva-Jordanova R, Vcelakova J, et al. The dynamic changes of zinc transporter 8 autoantibodies in Czech children from the onset of type 1 diabetes mellitus. *Diabet Med.* 2014;31(2):165-171. doi:10.1111/dme.12308
9. Shivaprasad C, Mittal R, Dharmalingam M, Kumar PK. Zinc transporter-8 autoantibodies can replace IA-2 autoantibodies as a serological marker for juvenile onset type 1 diabetes in India. *Indian J Endocrinol Metab*. 2014;18(3):345-349. doi:10.4103/2230-8210.131174
10. Jia X, He L, Miao D, et al. High-affinity ZnT8 autoantibodies by electrochemiluminescence assay improve risk prediction for type 1 diabetes. *J Clin Endocrinol Metab.* 2021;106(12):3455-3463. doi:10.1210/clinem/dgab575
11. Fabris M, Zago S, Liguori M, et al. Anti-zinc transporter protein 8 autoantibodies significantly improve the diagnostic approach to type 1 diabetes: an Italian multicentre study on paediatric patients. *Auto Immun Highlights*. 2015;6(1-2):17-22. doi:10.1007/s13317-015-0068-4
12. Grace SL, Cooper A, Jones AG, McDonald TJ. Zinc transporter 8 autoantibody testing requires age-related cutoffs. *BMJ Open Diabetes Res Care*. 2021;9(1):e002296. doi:10.1136/bmjdrc-2021-002296
13. Garnier L, Marchand L, Benoit M, et al. Screening of ZnT8 autoantibodies in the diagnosis of autoimmune diabetes in a large French cohort. *Clin Chim Acta.* 2018;478:162-165. doi:10.1016/j.cca.2017.12.043
14. Andersson C, Kolmodin M, Ivarsson SA, et al; Better Diabetes Diagnosis Study Group. Islet cell antibodies (ICA) identify autoimmunity in children with new onset diabetes mellitus negative for other islet cell antibodies. *Pediatr Diabetes.* 2014;15(5):336-344. doi:10.1111/pedi.12093
15. Regnell SE, Lernmark A. Early prediction of autoimmune (type 1) diabetes. *Diabetologia.* 2017;60(8):1370-1381. doi:10.1007/s00125-017-4308-1
16. Niechciał E, Rogowicz-Frontczak A, Piłaciński S, et al. Autoantibodies against zinc transporter 8 are related to age and metabolic state in patients with newly diagnosed autoimmune diabetes. *Acta Diabetol.* 2018;55(3):287-294. doi:10.1007/s00592-017-1091-x
17. Basu M, Pandit K, Banerjee M, Mondal SA, Mukhopadhyay P, Ghosh S. Profile of auto-antibodies (disease related and other) in children with type 1 diabetes. *Indian J Endocrinol Metab*. 2020;24(3):256-259. doi:10.4103/ijem.IJEM_63_20
18. Salami F, Tamura R, You L, et al; TEDDY Study Group. HbA1c as a time predictive biomarker for an additional islet autoantibody and type 1 diabetes in seroconverted TEDDY children. *Pediatr Diabetes.* 2022;23(8):1586-1593. doi:10.1111/pedi.13413
19. Burke GW 3rd, Chen LJ, Ciancio G, Pugliese A. Biomarkers in pancreas transplant. *Curr Opin Organ Transplant*. 2016;21(4):412-418. doi:10.1097/MOT.0000000000000333
20. Davidson HW, Wenzlau JM, O'Brien RM. Zinc transporter 8 (ZnT8) and β cell function. *Trends Endocrinol Metab.* 2014;25(8):415-424. doi:10.1016/j.tem.2014.03.008
21. Wenzlau JM, Frisch LM, Hutton JC, Fain PR, Davidson HW. Changes in zinc transporter 8 autoantibodies following type 1 diabetes onset: The Type 1 Diabetes Genetics Consortium Autoantibody Workshop. *Diabetes Care.* 2015;38(Suppl 2):S14-S20. doi:10.2337/dcs15-2004
22. Thewjitcharoen Y, Prasartkaew H, Tongsumrit P, et al. Prevalence, risk factors, and clinical characteristics of lipodystrophy in insulin-treated patients with diabetes: an old problem in a new era of modern insulin. *Diabetes Metab Syndr Obes*. 2020;13:4609-4620. doi:10.2147/DMSO.S282926
23. Trisorus C, Aroonparkmongkol S, Kongmanas HB, Sahakitrungruang T. Prevalence of islet autoantibodies in Thai juvenile-onset type 1 diabetes. *Pediatr Int.* 2018;60(11):1002-1007. doi:10.1111/ped.13687
24. Sosenko JM, Skyler JS, Palmer JP, et al; Diabetes Prevention Trial–Type 1 and Type 1 Diabetes TrialNet Study Groups. A longitudinal study of GAD65 and ICA512 autoantibodies during the progression to type 1 diabetes in Diabetes Prevention Trial-Type 1 (DPT-1) participants. *Diabetes Care.* 2011;34(11):2435-2437. doi:10.2337/dc11-0981
25. Manousaki D, Harroud A, Mitchell RE, et al. Vitamin D levels and risk of type 1 diabetes: a Mendelian randomization study. *PLoS Med.* 2021;18(2):e1003536. doi:10.1371/journal.pmed.1003536

Frequency of antithyroid antibodies in patients with primary biliary cholangitis

Mariam Ghozzi, MD[1,2,3], Amani Mankai, PhD[4,5], Zeineb Chedly, MS[2], Ikram Mlika, MS[2], Wiem Manoubi, MD[6], Sarra Melayah, MD[1,2,7], Ibtissem Ghedira, PhD[1,2]

[1]Laboratory of Immunology, Farhat Hached University Hospital, Sousse, Tunisia, [2]Faculty of Pharmacy, Department of Immunology, University of Monastir, Monastir, Tunisia, [3]Research Laboratory for "Epidemiology and Immunogenetics of Viral Infections" (LR14SP02), Sahloul University Hospital, University of Sousse, Sousse, Tunisia, [4]High School of Sciences and Techniques of Health, Tunis El Manar University, Tunis, Tunisia, [5]Research Unit "Obesity: Etiopathology and Treatment, UR18ES01," National Institute of Nutrition and Food Technology, Tunis, Tunisia, [6]Erasmus University Medical Centre, Department of Neuroscience, Rotterdam, Netherlands, [7]LR12SP11, Biochemistry Department, Sahloul University Hospital, Sousse, Tunisia. Corresponding author: Mariam Ghozzi; E-mail: mariam_80@hotmail.fr

Key words: primary biliary cholangitis; antithyroperoxidase antibodies; antithyroglobulin antibodies; anti–thyroid-stimulating hormone receptor antibodies; antithyroid antibodies; autoimmunity

Abbreviations: PBC, primary biliary cholangitis; TPO-Ab, anti–thyroid peroxidase antibodies; TG-Ab, antithyroglobulin antibodies; TSHR-Ab, anti–thyrotropin receptor antibodies; HBD, healthy blood donors; ELISA, enzyme-linked immunosorbent assay; ATA, antithyroid antibodies; AITD, autoimmune thyroid diseases; HT, Hashimoto's thyroiditis; GD, Graves' disease; AMA, antimitochondrial antibodies; AID, autoimmune diseases; PBS, phosphate-buffered saline; Ig, immunoglobulin; β2GPI, β2 glycoprotein I; aβ2GPI, anti-β2GPI

Laboratory Medicine 2024;55:304-309; https://doi.org/10.1093/labmed/lmad080

ABSTRACT

Objective: Primary biliary cholangitis (PBC) is an autoimmune disease of liver that may be associated with other conditions, including autoimmune thyroid diseases. We aimed to investigate the frequency of antithyroperoxidase antibodies (TPO-Ab), antithyroglobulin antibodies (TG-Ab), and anti–thyrotropin receptor antibodies (TSHR-Ab) in Tunisian patients with PBC.

Methods: Sera of 80 patients with PBC were collected over a 9-year period. A total of 189 healthy blood donors (HBD) were included in the control group. Measurements of TPO-Ab and TG-Ab were performed using indirect enzyme-linked immunosorbent assay (ELISA). Competitive ELISA was used to assess TSHR-Ab.

Results: Antithyroid antibodies (ATA) were significantly more frequent in PBC patients than in the control group (13.7% vs 1.6%; $P < 10^{-3}$). Out of 11 patients with ATA, 10 (90.9%) were female. Nine patients and 2 HBD had TPO-Ab (11.2% vs 1%; $P < 10^{-3}$). TG-Ab were more frequent in patients than in healthy subjects but the difference was not statistically significant (6.2% vs 1.6%; $P = .1$). TPO-Ab and TG-Ab were present together in 3 patients (3.7%). TSHR-Ab were absent in patients and controls.

Conclusion: This study shows that PBC is associated with a high frequency of ATA but not TG-Ab or TSHR-Ab.

Introduction

Autoimmune thyroid diseases (AITD) include, among others, Hashimoto's thyroiditis (HT) and Graves' disease (GD). HT is characterized by chronic inflammation, hypothyroidism, and the presence of anti–thyroid peroxidase antibodies (TPO-Ab) and antithyroglobulin antibodies (TG-Ab).[1] GD manifests as hyperthyroidism and is characterized by anti–thyrotropin receptor antibodies (TSHR-Ab) production.[2] HT affects more women than men.[3,4] HT is the most common thyroid disorder worldwide; its prevalence is around 10% to 12%. The prevalence of GD is 1% to 1.5%.[5]

Primary biliary cholangitis (PBC) is an autoimmune cholestatic liver disease characterized by progressive nonsuppurative inflammation involving small- and medium-sized intrahepatic bile ducts that are consequently destroyed. Untreated PBC may lead to liver cirrhosis.[6] PBC is characterized by the presence of antimitochondrial antibodies (AMA) or other PBC-specific autoantibodies, that is, anti-gp210 and anti-sp100.[7] PBC affects predominantly middle-aged women.[8,9]

PBC is associated with other autoimmune diseases (AID) in up to 73% of cases.[10] AITD are among the most frequent AID associated with PBC, their frequency reaching 24%.[11] Among AITD, HT is particularly associated with PBC.[12-15] A major similarity between PBC and HT is the T-cell infiltration of the liver and thyroid gland, respectively. This process is followed by inflammation and biliary epithelial cell (BEC) and thyroid destruction, whereas in GD there is neither cell infiltration nor thyroid destruction.[16] The frequency of AITD in PBC has generally been determined by data collection from medical records.[11-15,17-20] To the best of our knowledge, active screening by serological markers has been performed in only 1 study.[21]

The objectives of our study were to investigate the frequency of antithyroid antibodies (ATA) (TPO-Ab, TG-Ab, and TSHR-Ab) in a cohort of Tunisian patients with PBC and to try to explain why PBC could be associated with AITD.

Methods

Study Participants

Eighty PBC patients were included in the present study. The diagnosis of PBC was made according to diagnosis criteria of the American Association for the Study of Liver Diseases.[7] All patients had AMA. Patients with known AITD were excluded. Sera were collected from 4 hospitals in the center of Tunisia over a period of 9 years. The control group was made up of 189 healthy blood donors (HBD). All sera were conserved at −80°C until use. The ethical committee of Farhat Hached Hospital gave approval for the study.

Antimitochondrial Antibodies

The detection of AMA was conducted using indirect immunofluorescence. Rat liver, kidney, and stomach tissue sections were used as substrates for this assay. Sections of 4 μm diameter were prepared in our immunology laboratory using a cryostat and stored at −80°C until their use for this study. The substrates were first incubated with diluted sera (at a 1:100 ratio in phosphate-buffered saline [PBS]) for 30 minutes in a humid environment. After 3 washes with PBS, a second incubation in a dark, humid chamber with antibodies specific for human immunoglobulin (Ig)G was carried out. These anti–human IgG antibodies were conjugated to a fluorescent compound called fluorescein isothiocyanate (BioRad). After 30 minutes of incubation, the sections underwent 3 additional washes in PBS. They were then mounted between a microscope slide and a cover slip using a buffered glycerol. Finally, the slides were examined using a fluorescence microscope equipped with an ultraviolet lamp, allowing the visualization and the analysis of the immunofluorescent signals.

The characteristic granular pattern in the cytoplasm seen in the microscope is a hallmark of the presence AMA-Ab.

Serological Markers of Autoimmune Thyroid Diseases

Antithyroperoxidase Antibodies

TPO-Ab detection was performed using a commercial enzyme-linked immunosorbent assay (ELISA) kit (Euroimmun). The assay kit provided a quantitative assessment of human TPO-Ab of the IgG isotype. The TPO was bound to microwells and served as an antigen. For each sample, the serum was diluted at 1/201 in the sample buffer provided with the kit and 100 μL was incubated in the wells. If the sample contained TPO-Ab of the IgG isotype, these specific antibodies bound to the immobilized TPO antigen. After incubation, a washing step was performed and a second incubation of peroxidase-labeled anti-human IgG antibodies was carried out to detect the antibody-antigen complexes formed. After incubation, a second washing step was performed to eliminate the unbound enzyme conjugate. A color reaction was initiated by adding a substrate solution containing a chromogenic substrate catalyzed by the peroxidase enzyme. Finally, the addition of an acid stopped the reaction and generated a yellow end product. The intensity of the resulting yellow color is proportional to the concentration of TPO-Ab in the serum samples. The optical density of this color reaction was measured at a wavelength of 450 nm. The cutoff value for positivity was set at 50 IU/mL.

Antithyroglobulin Antibodies

The TG-Ab detection was performed using a commercial ELISA kit (Euroimmun). The kit provided a quantitative assay for human TG-Ab of the IgG isotype. The wells of the microplates were coated with TG antigen. Patient samples were diluted at 1/201 in the sample buffer provided with the kit and 100 μL was incubated in the wells. If samples contained TG-Ab, specific IgG antibodies bound to the immobilized TG antigen. After incubation, a washing step was performed and subsequently added peroxidase-labeled anti–human IgG bound to the antibody-antigen complexes formed. A second washing step removed unbound enzyme conjugate. The bound enzyme conjugate catalyzed a color reaction when the substrate solution, containing a chromogenic substrate, was added. The addition of an acid stopped the reaction, generating a yellow end product. The intensity of the resulting color is proportional to the concentration of TG-Ab in the serum. Finally, the optical density of the color intensity was measured photometrically at a wavelength of 450 nm. The cutoff value for positivity was set at 100 IU/mL.

Anti–Thyrotropin Receptor Antibodies

TSHR-Ab were assessed with competitive ELISA (Euroimmun). The ELISA test kit provided quantitative assay for human TSHR-Ab. Wells of microplates were coated with TSH receptor. Patients' sera were incubated in the wells. If samples contain TSHR-Ab, specific antibodies bound to the TSHR. After incubation, a washing step was carried out. Bound antibodies inhibited the binding of biotin-labeled TSH added in a second incubation step. A second washing step was made to evacuate the unbound biotin-labeled TSH. Finally, bound TSH biotin was detected by using enzyme-labeled avidin. This enzyme conjugate catalyzed a color reaction when the substrate solution was added and the intensity of the color is inversely proportional to the concentration of TSHR-Ab in the serum. The cutoff for positivity was 2 IU/L.

Statistical Analysis

Statistical analyses were performed using EpiInfo version 3 software. The comparison of frequencies of ATA was done using the Fisher exact test or χ^2 test. A P value ≤ .05 was considered statistically significant. For significant results, 95% confidence interval and odds ratio were determined using WinPepi software.

Results

Our study included 80 patients with PBC (mean age: 59 ± 13.6 years, age range: 22-85 years; sex ratio, female/male: 73/7) and 189 HBD (mean age: 39 ± 11.5 years, age range: 18-57 years; sex ratio, female/male: 104/85).

All PBC patients had positive AMA. AMA were absent for all HBD.

ATA were significantly more frequent in PBC patients than in control group (13.7% vs 1.6%; $P < 10^{-3}$). Out of 11 patients with ATA, 10 (90.9%) were female. Nine patients and 2 HBD had TPO-Ab (11.2% vs 1%; $P < 10^{-3}$). TG-Ab were more frequent in patients than in healthy subjects but the difference was not statistically significant (6.2% vs 1.6%; $P = .1$). TPO-Ab and TG-Ab were present together in 3 patients (3.7%). TSHR-Ab were absent in patients and controls. Results

TABLE 1. Frequency of antithyroid antibodies in patients with primary biliary cholangitis

	Patients (n = 80) n (%)	Control group (n = 189) n (%)	*P*	95% CI	Odds ratio
TPO-Ab or TG-Ab	11 (13.7%)	3 (1.6%)	$<10^{-3}$	[2.82-38.07]	10.36
TPO-Ab	9 (11.2%)	2 (1%)	$<10^{-3}$	[2.63-58.58]	12.42
TG-Ab	5 (6.2%)	3 (1.6%)	0.1	–	–
TPO-Ab and TG-Ab	3 (3.7%)	2 (1%)	0.3	–	–
TSHR-Ab	0 (0%)	0 (0%)	NS	–	–

NS, not significant; TG-Ab, antithyroglobulin antibodies; TPO-Ab, anti–thyroid peroxidase antibodies; TSHR-Ab, anti–thyrotropin receptor antibodies.

TABLE 2. Levels of antithyroid antibodies in patients with positive results

Patient	Sex	Age (y)	TPO-Ab (IU /mL)	TG-Ab (IU /mL)	TSHR-Ab (IU/L)
1	F	66	114	200	–
2	F	71	–	305	–
3	F	78	385	–	–
4	F	46	>500	>1000	–
5	F	43	>500	–	–
6	F	79	–	292	–
7	F	41	218	–	–
8	F	55	80	–	–
9	F	60	246	>1000	–
10	F	45	>500	–	–
11	m	60	228	–	–

TG-Ab, antithyroglobulin antibodies; TPO-Ab, anti–thyroid peroxidase antibodies; TSHR-Ab, anti–thyrotropin receptor antibodies.

are summarized in **TABLE 1**. The ATA levels of the 11 patients are presented in **TABLE 2**.

Discussion

In this study, we aimed to investigate an active screening of AITD in PBC patients. Eleven patients out of 80 (13.7%) had ATA (TPO-Ab or TG-Ab), a frequency significantly higher than in healthy controls (1.6%). TSHR-Ab were absent in the PBC patients. TSHR-Ab is a highly sensitive and specific serological marker of GD.[2] So, a negative test of TSHR-Ab could exclude GD. Our result was in accordance with those previously reported on the frequency of GD in PBC patients by Floreani et al,[14,15] Liu et al,[19] and Efe et al[20] (1.9%, 1.6%, 0.6%, and 1.5% respectively) (**TABLE 3**). GD was described in association with PBC, especially in case reports.[22,23] The frequency of TPO-Ab in our PBC patients (11.2%) was significantly higher than in the control group (1%). The frequency of ATA was lower in our study than in that of Crowe et al[21] who also did a screening of ATA in PBC patients through research of autoantibodies (13.7% vs 26% respectively) (**TABLE 4**). The discrepancy between the results could be due to the difference between the methods used for ATA detection. Indeed, we used ELISA, whereas Crowe et al[21] used hemagglutination, an old method for the detection of ATA, because when they conducted their study 40 years ago (1980), ELISA was not yet used for ATA research. In our study, the positivity of TPO-Ab and TG-Ab and the negativity of TSHR-Ab could reflect the frequency of HT in our PBC patients. The rate of positivity of ATA (TPO-Ab or TG-Ab) was similar to that of AITD in the study of Floreani et al[15] (13.7% and 12.7%, respectively). Our frequency of TPO-Ab (11.2%) was similar to that of HT in 2 studies by Floreani et al[15,16] (12.5% and 10.2%). Efe et al,[20] who conducted the largest study on the frequency of extrahepatic AID in PBC, found similar results; 10.6% of PBC patients had AITD and most of them were HT (9.1%). In summary, AITD are frequent in PBC patients and particularly in HT.

HT could precede, coincide with, or follow PBC. So, how could both diseases (HT and PBC) induce each other and why was GD rarely associated with PBC? Polymorphism of the *PTPN22* gene, which is known to be associated with GD[24] and HT,[25] has been demonstrated to be significantly associated with the risk of developing PBC and to have concomitant PBC-AITD.[26] Apart from genetic predisposition and environmental triggers, gut microbiota plays a key role in the pathogenesis of many AID. Gut dysbiosis and leaky gut[27] are additional elements in the puzzle of autoimmunity. Gut microbiota dysbiosis has been reported not only in PBC[28-30] but also HT[31-33] and GD.[31,34,35] Among the abnormalities of gut microbiota composition is the abundance of *Prevotella*. Both in PBC[28] and in HT[33,34] a significant decrease in *Prevotella* has been reported. However, in GD, a significant increase of *Prevotella* has been noted.[31] In HT, *Prevotella* level was found to be inversely correlated to levels of TPO-Ab and TG-Ab.[33] Also, in PBC a negative correlation has been noted between the microbiota richness in *Prevotella* and high-risk HLA genes. Thus, could we imagine that GD patients are protected against PBC thanks to the richness of their gut microbiota in *Prevotella*? The impairment of microbiota will drive to increased intestinal permeability leading to a leaky gut reported in PBC,[28,30] HT,[36] and GD.[37] A leaky gut results in bacterial translocation. The gut-liver axis and gut-thyroid axis have been reported to be implicated in the pathogenesis of PBC[28] and of AITD.[5,38,39] Proinflammatory cytokines are therefore induced and have been demonstrated in PBC[40-43] and AITD.[44,45] The cytokine profile of HT is different from that of GD but similar to that of PBC. In fact, IL-17A has been reported to be significantly higher in HT than controls and GD.[45] Moreover, IL-17 production was induced by TPO in HT but not in GD.[45] In PBC, IL-17A was significantly higher in PBC patients than healthy controls and correlated with disease severity.[40] The results of all these mechanisms are the break of tolerance and onset of chronic inflammatory disease in which tissue damage could happen.[26] In PBC, there is cholangiocyte and bile duct destruction. In HT but not in GD, there is thyrocyte destruction.[16] In HT, apoptosis is increased in situ whereas in GD, apoptosis is reduced.[46] When BEC and thyrocytes are destroyed by inflammation, many apotopes are generated and are thus exposed to the immune system, which produces autoantibodies against

TABLE 3. Frequency of autoimmune thyroid disease in primary biliary cholangitis according to medical records

First author/reference No.	Year	Country	Number of PBC patients	HT or GD n (%)	HT n (%)	GD n (%)
Inoue[12]	1995	Japan	874	nd	49 (5.6)	nd
Gershwin[17]	2005	USA	1032	93 (9)	nd	nd
Mantaka[13]	2012	Greece	111	nd	20 (18)	nd
Muratori[11]	2015	Italy	281	67 (24)	nd	nd
Floreani[14]	2015	Italy	361	52 (14.4)	45 (12.5)	7 (1.9)
Floreani[15]	2016	Spain Italy	545 376	109 (12.7)	94 (10.2)	15 (1.6)
Zeng[18]	2020	China	137	25 (18.2)	20 (14.6)	5 (3.6)
Liu[19]	2021	China	505	4 (0.8)	1 (0.2)	3 (0.6)
Efe[20]	2021	Europe USA Canada	1554	165 (10.6)	141 (9.1)	24 (1.5)

GD, Graves' disease; HT, Hashimoto's thyroiditis; nd, not determined; PBC, primary biliary cholangitis.

TABLE 4. Comparison between our study and that of Crowe et al[21]

First author/reference No.	Year	Country	Number of PBC patients	TPO-Ab or TG-Ab n (%)	TPO-Ab n (%)	TG-Ab n (%)	TSHR-Ab n (%)
Crowe[21]	1980	England	95	25 (26)	21 (22.1)	16 (16.8)	nd
Our study	2023	Tunisia	80	11(13.7)	9 (11.2)	5 (6.2)	0 (0)

nd, not determined; PBC, primary biliary cholangitis; TG-Ab, antithyroglobulin antibodies; TPO-Ab, anti–thyroid peroxidase antibodies; TSHR-Ab, anti–thyrotropin receptor antibodies.

TABLE 5. Frequency of antiphospholipid antibodies in primary biliary cholangitis patients with antithyroid antibodies[50]

Patient	Sex	aCL-IgG (U/mL)	aCL-IgA (U/mL)	aCL-IgM (U/mL)	aβ2GPI-IgG (U/mL)	aβ2GPI-IgA (U/mL)	aβ2GPI-IgM (U/mL)
1	F	–	–	–	–	15	–
2	F	–	–	–	–	–	–
3	F	–	–	–	–	–	–
4	F	–	21	12.5	19	>100	21
5	F	–	–	–	–	26	–
6	F	–	–	–	–	31	–
7	F	–	–	–	–	34	–
8	F	–	–	–	–	22	12.5
9	F	–	–	–	–	17.9	–
10	F	–	–	–	–	21	–
11	M	–	–	–	–	13.2	–

aCL, anticardiolipin antibodies; aβ2GPI, anti–β2 glycoprotein antibodies.

liver and thyroid autoantigens, respectively. Apoptotic blebs secondary to BEC and thyrocyte destruction are normally eliminated by β2 glycoprotein I (β2GPI), which is considered as a scavenger protein.[47] β2GPI is highly expressed in the liver, where it is synthesized.[48] β2GPI is also present in the thyroid gland, where it is considered as a megalin receptor.[49] In a previous study on PBC, a high frequency of anti-β2GPI (aβ2GPI; 70%) has been shown.[50] Also, a significantly higher frequency of aβ2GPI in HT (34.5%) but not in GD in comparison with healthy subjects has been demonstrated before.[51] As has been shown before in PBC and HT patients,[50,51] aβ2GPI was predominantly of IgA isotype (62.5% and 27.3% respectively). Measurement of anticardiolipin antibodies and aβ2GPI antibodies was previously performed in PBC patients in our study.[51] Frequencies of antiphospholipid antibodies in the 11 PBC patients with ATA are presented in **TABLE 5**. Fascinatingly, out of 11 PBC patients with ATA, 9 (81.8%) had aβ2GPI-IgA. So, both in PBC and in HT, when aβ2GPI bind to their target antigen β2GPI, they block the function of the latter, leading to an accumulation of apoptotic blebs and a production of more and more antibodies, and a vicious cycle ensues.

It is interesting to note that a close link exists between the liver and the thyroid gland.[52,53] Indeed, serum and liver thyroid hormones are positively related to mitochondrial population.[52] Thyroid hormones

regulate the metabolic rate of hepatocytes and the liver metabolizes thyroid hormones.[53] Furthermore, liver antigens are expressed in the thyroid gland and vice versa; that is, thyroid antigens are expressed in the liver.[54–58] Sato et al[56] reported that hepatocyte nuclear factor 3 plays a role in the transcriptional regulation of the thyroperoxidase promoter and was expressed in cultured thyroid cells and in the adult thyroid gland.

In conclusion, we report herein finding a higher frequency of TPO-Ab in PBC patients than in the control group, and we tried to explain why PBC seems to be frequently associated with HT. Large epidemiological and prospective studies must be performed to demonstrate the true prevalence of AITD in Tunisian patients with PBC.

Conflict of Interest Disclosure

The authors have nothing to disclose.

REFERENCES

1. Weetman AP. An update on the pathogenesis of Hashimoto's thyroiditis. *J Endocrinol Invest.* 2021;44(5):883-890. doi:10.1007/s40618-020-01477-1
2. Mankaï A, Toumi D, Chadli-Chaieb M, et al. Anti-thyroid-stimulating hormone receptor antibodies determined by second-generation assay. *Clin Chem Lab Med.* 2007;45(1):26-29. doi:10.1515/CCLM.2007.016
3. Ihnatowicz P, Drywień M, Wątor P, Wojsiat J. The importance of nutritional factors and dietary management of Hashimoto's thyroiditis. *Ann Agric Environ Med.* 2020;27(2):184-193. doi:10.26444/aaem/112331
4. Chabchoub G, Uz E, Maalej A, et al. Analysis of skewed X-chromosome inactivation in females with rheumatoid arthritis and autoimmune thyroid diseases. *Arthritis Res Ther.* 2009;11(4):R106. doi:10.1186/ar2759
5. Knezevic J, Starchl C, Tmava Berisha A, Amrein KT. How does the microbiota influence thyroid function? *Nutrients*. 2020;12(6):1769. doi:10.3390/nu12061769
6. Colapietro F, Gershwin ME, Lleo A. PPAR agonists for the treatment of primary biliary cholangitis: old and new tales. *J Transl Autoimmun*. 2023;6:100188. doi:10.1016/j.jtauto.2023.100188
7. Lindor KD, Bowlus CL, Boyer J, Levy C, Mayo M. Primary biliary cholangitis: 2018 practice guidance from the American Association for the Study of Liver Diseases. *Hepatology.* 2019;69(1):394-419. doi:10.1002/hep.30145
8. Janik MK, Wunsch E, Milkiewicz P. Variants of autoimmune liver diseases: how to diagnose and treat them? *Pol Arch Intern Med*. 2023;133(1):16408. doi:10.20452/pamw.16408
9. Asselta R, Paraboschi EM, Gerussi A, et al, Canadian-US PBC Consortium. X chromosome contribution to the genetic architecture of primary biliary cholangitis. *Gastroenterology.* 2021;160(7):2483-2495.e26. doi:10.1053/j.gastro.2021.02.061
10. Chalifoux SL, Konyn PG, Choi G, Saab S. Extrahepatic manifestations of primary biliary cholangitis. *Gut Liver*. 2017;11(6):771-780. doi:10.5009/gnl16365
11. Muratori P, Fabbri A, Lalanne C, Lenzi M, Muratori L. Autoimmune liver disease and concomitant extrahepatic autoimmune disease. *Eur J Gastroenterol Hepatol.* 2015;27(10):1175-1179. doi:10.1097/MEG.0000000000000424
12. Inoue K, Hirohara J, Nakano T, et al. Prediction of prognosis of primary biliary cirrhosis in Japan. *Liver.* 1995;15(2):70-77. doi:10.1111/j.1600-0676.1995.tb00110.x
13. Mantaka A, Koulentaki M, Chlouverakis G, et al. Primary biliary cirrhosis in a genetically homogeneous population: disease associations and familial occurrence rates. *BMC Gastroenterol.* 2012;12:110. doi:10.1186/1471-230X-12-110
14. Floreani A, Franceschet I, Cazzagon N, et al. Extrahepatic autoimmune conditions associated with primary biliary cirrhosis. *Clin Rev Allergy Immunol.* 2015;48(2-3):192-197. doi:10.1007/s12016-014-8427-x
15. Floreani A, Mangini C, Reig A, et al. Thyroid dysfunction in primary biliary cholangitis: a comparative study at two European centers. *Am J Gastroenterol.* 2017;112(1):114-119. doi:10.1038/ajg.2016.479
16. Zhang QY, Ye XP, Zhou Z, et al. Lymphocyte infiltration and thyrocyte destruction are driven by stromal and immune cell components in Hashimoto's thyroiditis. *Nat Commun.* 2022;13(1):775. doi:10.1038/s41467-022-28120-2
17. Gershwin ME, Selmi C, Worman HJ, et al, USA PBC Epidemiology Group. Risk factors and comorbidities in primary biliary cirrhosis: a controlled interview-based study of 1032 patients. *Hepatology.* 2005;42(5):1194-1202. doi:10.1002/hep.20907
18. Zeng Q, Zhao L, Wang C, et al. Relationship between autoimmune liver disease and autoimmune thyroid disease: a cross-sectional study. *Scand J Gastroenterol.* 2020;55(2):216-221. doi:10.1080/00365521.2019.1710766
19. Liu Y, Han K, Liu C, Duan F, Cheng J, Yang S. Clinical characteristics and prognosis of concomitant primary biliary cholangitis and autoimmune diseases: a retrospective study. *Can J Gastroenterol Hepatol*. 2021;2021:5557814. doi:10.1155/2021/5557814
20. Efe C, Torgutalp M, Henriksson I, et al. Extrahepatic autoimmune diseases in primary biliary cholangitis: prevalence and significance for clinical presentation and disease outcome. *J Gastroenterol Hepatol.* 2021;36(4):936-942. doi:10.1111/jgh.15214
21. Crowe JP, Christensen E, Butler J, et al. Primary biliary cirrhosis: the prevalence of hypothyroidism and its relationship to thyroid autoantibodies and sicca syndrome. *Gastroenterology.* 1980;78(6):1437-1441.
22. Shetty S, Rajasekaran S, Venkatakrishnan L. Grave's disease and primary biliary cirrhosis-an unusual and challenging association. *J Clin Exp Hepatol*. 2014;4(1):66-67. doi:10.1016/j.jceh.2013.08.001
23. Suzuki Y, Ishida K, Takahashi H, et al. Primary biliary cirrhosis associated with Graves' disease in a male patient. *Clin J Gastroenterol*. 2016;9(2):99-103. doi:10.1007/s12328-016-0635-x
24. Zheng J, Ibrahim S, Petersen F, Yu X. Meta-analysis reveals an association of PTPN22 C1858T with autoimmune diseases, which depends on the localization of the affected tissue. *Genes Immun.* 2012;13(8):641-652. doi:10.1038/gene.2012.46
25. Criswell LA, Pfeiffer KA, Lum RF, et al. Analysis of families in the multiple autoimmune disease genetics consortium (MADGC) collection: the PTPN22 620W allele associates with multiple autoimmune phenotypes. *Am J Hum Genet.* 2005;76(4):561-571. doi:10.1086/429096
26. Kuś A, Arłukowicz-Grabowska M, Szymański K, et al. Genetic risk factors for autoimmune thyroid disease might affect the susceptibility to and modulate the progression of primary biliary cholangitis. *J Gastrointestin Liver Dis.* 2017;26(3):245-252. doi:10.15403/jgld.2014.1121.263.kus
27. Fasano A. All disease begins in the (leaky) gut: role of zonulin-mediated gut permeability in the pathogenesis of some chronic inflammatory diseases. *F1000Res*. 2020;9:F1000 Faculty Rev-F1000 Faculty R69. doi:10.12688/f1000research.20510.1
28. Giordano DM, Pinto C, Maroni L, Benedetti A, Marzioni M. Inflammation and the gut-liver axis in the pathophysiology of cholangiopathies. *Int J Mol Sci.* 2018;19(10):3003. doi:10.3390/ijms19103003
29. Huang MJ, Liaw YF. Clinical associations between thyroid and liver diseases. *J Gastroenterol Hepatol.* 1995;10(3):344-350. doi:10.1111/j.1440-1746.1995.tb01106.x
30. Ma HD, Zhao ZB, Ma WT, et al. Gut microbiota translocation promotes autoimmune cholangitis. *J Autoimmun.* 2018;95:47-57. doi:10.1016/j.jaut.2018.09.010
31. Sawicka-Gutaj N, Gruszczyński D, Zawalna N, et al. Microbiota alterations in patients with autoimmune thyroid diseases: a

systematic review. *Int J Mol Sci* . 2022;23(21):13450. doi:10.3390/ijms232113450

32. Ishaq HM, Mohammad IS, Guo H, et al. Molecular estimation of alteration in intestinal microbial composition in Hashimoto's thyroiditis patients. *Biomed Pharmacother.* 2017;95:865-874. doi:10.1016/j.biopha.2017.08.101
33. Zhao F, Feng J, Li J, et al. Alterations of the gut microbiota in Hashimoto's thyroiditis patients. *Thyroid.* 2018;28(2):175-186. doi:10.1089/thy.2017.0395
34. Liu H, Liu H, Liu C, Shang M, Wei T, Yin P. Gut microbiome and the role of metabolites in the study of Graves' disease. *Front Mol Biosci*. 2022;9:841223. doi:10.3389/fmolb.2022.841223
35. Hou J, Tang Y, Chen Y, Chen D. The role of the microbiota in Graves' disease and Graves' orbitopathy. *Front Cell Infect Microbiol.* 2021;11:739707. doi:10.3389/fcimb.2021.739707
36. Cayres LCF, de Salis LVV, Rodrigues GSP, et al. Detection of alterations in the gut microbiota and intestinal permeability in patients with Hashimoto thyroiditis. *Front Immunol.* 2021;12:579140. doi:10.3389/fimmu.2021.579140
37. Zheng D, Liao H, Chen S, et al. Elevated levels of circulating biomarkers related to leaky gut syndrome and bacterial translocation are associated with Graves' disease. *Front Endocrinol (Lausanne)*. 2021;12:796212. doi:10.3389/fendo.2021.796212
38. Fröhlich E, Wahl R. Microbiota and thyroid interaction in health and disease. *Trends Endocrinol Metab.* 2019;30(8):479-490. doi:10.1016/j.tem.2019.05.008
39. Shirvani Rad S, Nikkhah A, Orvatinia M, et al. Gut microbiota: a perspective of precision medicine in endocrine disorders. *J Diabetes Metab Disord*. 2020;19(2):1827-1834. doi:10.1007/s40200-020-00593-2
40. Jia H, Chen J, Zhang X, et al. IL-17A produced by invariant natural killer T cells and $CD3^+$ $CD56^+$ αGalcer-CD1d $tetramer^-$ T cells promote liver fibrosis in patients with primary biliary cholangitis. *J Leukoc Biol.* 2022;112(5):1079-1087. doi:10.1002/JLB.2A0622-586RRRR
41. Chen S, Lv T, Sun G, et al. Reciprocal alterations in circulating and hepatic gamma-delta T cells in patients with primary biliary cholangitis. *Hepatol Int*. 2022;16(1):195-206. doi:10.1007/s12072-021-10267-7
42. Fujinaga Y, Namisaki T, Tsuji Y, et al. Macrophage activation markers predict liver-related complications in primary biliary cholangitis. *Int J Mol Sci* . 2022;23(17):9814. doi:10.3390/ijms23179814
43. Wang Q, Wang Y, Qiao W, et al. The effect of serum IL-2 levels on the prognosis of primary biliary cholangitis-related liver failure and the preliminary exploration of its mechanism. *Front Immunol.* 2022;13:995223. doi:10.3389/fimmu.2022.995223
44. Kristensen B, Hegedüs L, Madsen HO, Smith TJ, Nielsen CH. Altered balance between self-reactive T helper (Th)17 cells and Th10 cells and between full-length forkhead box protein 3 (FoxP3) and FoxP3 splice variants in Hashimoto's thyroiditis. *Clin Exp Immunol.* 2015;180(1):58-69. doi:10.1111/cei.12557
45. Lu Y, Xing C, Zhang C, et al. Promotion of IL-17/NF-κB signaling in autoimmune thyroid diseases. *Exp Ther Med*. 2022;25(1):51. doi:10.3892/etm.2022.11750
46. Kalarani IB, Veerabathiran R. Impact of iodine intake on the pathogenesis of autoimmune thyroid disease in children and adults. *Ann Pediatr Endocrinol Metab*. 2022;27(4):256-264. doi:10.6065/apem.2244186.093
47. Cabrera-Marante O, Rodríguez de Frías E, Serrano M, et al. The weight of IgA anti-β2glycoprotein I in the antiphospholipid syndrome pathogenesis: closing the gap of seronegative antiphospholipid syndrome. *Int J Mol Sci* . 2020;21(23):8972. doi:10.3390/ijms21238972
48. Averna M, Paravizzini G, Marino G, et al. Liver is not the unique site of synthesis of beta 2-glycoprotein I (apolipoprotein H): evidence for an intestinal localization. *Int J Clin Lab Res.* 1979;27(3):207-212. doi:10.1007/BF02912460
49. Moestrup SK, Schousboe I, Jacobsen C, Leheste JR, Christensen EI, Willnow TE. Beta2-glycoprotein-I (apolipoprotein H) and beta2-glycoprotein-I-phospholipid complex harbor a recognition site for the endocytic receptor megalin. *J Clin Invest.* 1998;102(5):902-909. doi:10.1172/JCI3772
50. Mankaï A, Manoubi W, Ghozzi M, Melayah S, Sakly W, Ghedira I. High frequency of antiphospholipid antibodies in primary biliary cirrhosis. *J Clin Lab Anal.* 2015;29(1):32-36. doi:10.1002/jcla.21723
51. Mankaï A, Melayah S, Bousetta S, Ghozzi M, Yacoub-Jemni S, Ghedira I. Antiphospholipid antibodies in autoimmune thyroid diseases. *J Clin Lab Anal.* 2022;36(12):e24788. doi:10.1002/jcla.24788
52. Barletta A, Liverini G, Goglia F, Di Meo S, De Leo T. Thyroid state and mitochondrial population during maturation and ageing. *J Endocrinol Invest.* 1980;3(3):293-296. doi:10.1007/BF03348278
53. Malik R, Hodgson H. The relationship between the thyroid gland and the liver. *QJM.* 2002;95(9):559-569. doi:10.1093/qjmed/95.9.559
54. Fava G, Ueno Y, Glaser S, et al. Thyroid hormone inhibits biliary growth in bile duct-ligated rats by PLC/IP(3)/Ca(2+)-dependent downregulation of SRC/ERK1/2. *Am J Physiol Cell Physiol.* 2007;292(4):C1467-C1475. doi:10.1152/ajpcell.00575.2006
55. Pang Y, von Turkovich M, Wu H, et al. The binding of thyroid transcription factor-1 and hepatocyte paraffin 1 to mitochondrial proteins in hepatocytes: a molecular and immunoelectron microscopic study. *Am J Clin Pathol.* 2006;125(5):722-726. doi:10.1309/EBCB-6H54-K1N2-P9QL
56. Sato K, Di Lauro R. Hepatocyte nuclear factor 3beta participates in the transcriptional regulation of the thyroperoxidase promoter. *Biochem Biophys Res Commun.* 1996;220(1):86-93. doi:10.1006/bbrc.1996.0361
57. Masini-Repiso AM, Bonaterra M, Spitale L, et al. Ultrastructural localization of thyroid peroxidase, hydrogen peroxide-generating sites, and monoamine oxidase in benign and malignant thyroid diseases. *Hum Pathol.* 2004;35(4):436-446. doi:10.1016/j.humpath.2003.03.001
58. Libert F, Ruel J, Ludgate M, et al. Thyroperoxidase, an autoantigen with a mosaic structure made of nuclear and mitochondrial gene modules. *EMBO J.* 1987;6(13):4193-4196. doi:10.1002/j.1460-2075.1987.tb02766.x

Utility of a microRNA panel in diagnosis and prognosis of hepatitis C–associated hepatocellular carcinoma

Abeer Ahmed ALrefai, MD,[1,2] *Sara Kamal Rizk, MD,*[1] *Ahmed Kamal Khamis, MD,*[3] *Zeinab A. Kasemy, MD,*[4] *Mona Salah Eldin Habieb, MD*[1,5]

[1]Medical Biochemistry and Molecular Biology Department, [3]Internal Medicine Department, National Liver Institute, and [4]Department of Public Health and Community Medicine, Faculty of Medicine, Menoufia University, Shibin El Kom, Egypt; [2]Biochemistry Department, Faculty of Medicine, UQU, Mecca, Kingdom of Saudi Arabia; [5]Medical Biochemistry Department, Najran University, Najran, Kingdom of Saudi Arabia. Corresponding author: Abeer Ahmed ALrefai; abeer.elrefai@med.menoufia.edu.eg

Key words: HCV; cirrhosis; HCC; miRNAs

Abbreviations: miRNA, microRNA; HCC, hepatocellular carcinoma; HCV, hepatitis C virus; AFP, alpha fetoprotein; AUC, area under the curve; HB, hepatitis B; HBs-Ag, HB surface antigen; HBc-Ab, HB core antibody; BCLC, Barcelona Clinic Liver Cancer Staging System; CBC, complete blood count; RT-PCR, reverse transcription–polymerase chain reaction; ALT, alanine aminotransferase; AST, aspartate aminotransferase; ROC, receiver operating characteristic; TNBC, triple-negative breast cancer; HPV16, human papillomavirus type 16

Laboratory Medicine 2024;55:310-319; https://doi.org/10.1093/labmed/lmad081

ABSTRACT

Background: Hepatocellular carcinoma (HCC) is the most common type of primary liver cancer and the leading cause of cancer mortality. Various studies have linked dysregulated microRNA expression to liver cancers, but those related to viral hepatitis–related HCC are limited.

Methods: We investigated the diagnostic and prognostic roles of circulating miR-331-3p, miR-23b-3p, and miR-3194-5p in EDTA-treated blood samples of 50 hepatitis C virus (HCV) HCC patients, 50 HCV cirrhotic patients, and 50 healthy controls using quantitative real-time polymerase chain reaction.

Results: We found that miR-23b-3p and miR-3194-5p were significantly downregulated, whereas miR-331-3p was upregulated in HCC patients compared with controls. Also, these miRNAs were significantly dysregulated in HCC compared with cirrhotic patients. For the diagnosis of HCC, miR-331-3p and the combined miRNAs panel had the highest area under the curve (AUC), followed by miR-3194-5p. The highest AUC for differentiating metastatic from nonmetastatic patients was shown by miR-331-3p and the combined miRNAs panel, followed by miR-23b-3p. Dysregulation of miRNAs was associated with poor clinicopathological manifestations. Finally, miR-331-3P was found to be an independent risk factor for metastatic lesions in HCC.

Conclusion: Overall, the assessed miR-331-3p, miR-23b-3p, and miR-3194-5p were significantly associated with poor clinicopathological features of HCC and could be used to discriminate HCV-related HCC patients from cirrhosis and differentiating metastatic from nonmetastatic patients, primarily miR-331-3p along with combined miRNAs. Moreover, miR-331-3p was found to be an independent factor for metastatic lesions.

Introduction

Hepatocellular carcinoma (HCC) is the second leading cause of cancer-related death in the world and the fifth most common solid tumor.[1] It is induced by alcohol intake, obesity, and chronic liver illnesses, particularly viral hepatitis B (HB) or hepatitis C virus (HCV).[2] The common biomarker that can be used to predict treatment response and track illness recurrence is alpha fetoprotein (AFP). However, its sensitivity and specificity are significantly restricted, especially when used independently of other biomarkers. As a result, additional or supplementary biomarkers are critically necessary for improving the standard of care for HCC patients.[3] MicroRNAs (miRNAs) are novel biomarkers with clinical potential that were discovered as tumor indicators in tissues and the blood by Lawrie et al[4] in 2008. They are single noncoding short RNAs (20 to 24 nt) that play a role in the regulation of gene expression posttranscriptionally by influencing the stability and translation of mRNAs.[5] In terms of patient safety, miRNAs detected in a liquid biopsy are of special importance. The appealing potential of these RNAs as less invasive biomarkers is mostly due to their stability and release into the bloodstream.[6,7] Cancer research has recently focused on miRNAs.[3] It is considered that miRNAs might be involved in the onset and progression of a variety of diseases, including HCC.[8] It has been proposed that the use of miRNAs as biomarkers for early detection and treatment of HCC could increase the possibility of a cure, reduce mortality, and lessen the burden of the disease.[9] It is possible that miRNAs have a dual role as either tumor suppressors or oncogenes depending on cellular requirements.[10,11] miR-331-3p, located on 12q22n,[12] has been implicated in prostate cancer, glioblastoma, colorectal cancer,

and breast cancer by regulating the expressions of epidermal growth factor receptor and HER-2 via lowering Akt activity.[13,14] Furthermore, it has been linked to HCC.[15] miR-23b-3p, on chromosome 9, is a component of the intronic miR-23b/27b/24-1 cluster and is located at q22.32.[16] miR-23b-3p, a tumor suppressor with low expression in a number of malignancies, has also been investigated.[17] On the other hand, the function of miR-3194, which is situated at 20q13.2, remains uncertain in HCC. Recent research has revealed that HCC tissues had abnormal expression of miR-331-3p and miR-23b-3p, although their serum levels have not yet been thoroughly examined.[18] Using miRNA combinations is a possible option for providing new HCC diagnostic tools and enhancing therapeutic observation.[3] Combined miRNAs were significantly more accurate in predicting the presence of liver disease or cirrhosis than conventional biomarkers.[19] Therefore, the aim of this study was to evaluate the potential diagnostic and prognostic roles of the miRNA panel composed of miR-331-3p, miR-23b-3p, and miR-3194-5p in patients with HCV-related HCC.

Methods

Study Design

There were 150 subjects enrolled in this study, which was conducted at the National Liver Institute in cooperation with the Medical Biochemistry and Molecular Biology Departments, Faculty of Medicine, Menoufia University, Shibin El Kom, Egypt. They were categorized into 3 groups. Patients in group I (50 patients) had HCC in relation to chronic HCV and those in group II (50 patients) had HCV-positive chronic liver disease. The controls (group III; 50 subjects) were healthy participants who were matched for age and gender, were negative for hepatitis virus indicators (HCV antibody, HB surface antigen [HBs-Ag], and HB core antibody [HBc-Ab]). Patients over the age of 18 who were infected with HCV were eligible. Patients with positive HBs-Ag or HBc-Ab, secondary liver cancer, other neoplasms, chronic hepatitis or cirrhosis induced by any cause other than HCV infection, HCC treatment, and antiviral medication were all excluded from the study. Detailed history, thorough physical examination, and laboratory and imaging procedures (ultrasonography and computed tomography [CT]) were performed to diagnose chronic liver disease.[20] Specific criteria in triphasic spiral CT and/or magnetic resonance imaging were used to diagnose HCC.[21] To evaluate HCC staging, the Barcelona Clinic Liver Cancer Staging System (BCLC) was used.[22] The Child-Pugh score was used to evaluate the severity of liver disease.

Ethical Approval

This research was conducted in compliance with the Declaration of Helsinki. All participants signed a written informed consent form, which was authorized by the Ethics Committee of Menoufia University's Faculty of Medicine.

Blood Sampling and Laboratory Tests

Six milliliters of venous blood were drawn by sterile venipuncture and separated into 2 portions. The first portion (4 mL) was put in a plain tube to assess liver function, hepatitis viral markers, and AFP. The second portion (2 mL) was placed in an EDTA tube for complete blood count (CBC), HCV reverse transcription–polymerase chain reaction (RT-PCR), and miRNA expression analysis.

Laboratory Procedures

CBC was assessed by a Sysmex XN-1000.[23] The kinetic UV optimized method according to the International Federation of Clinical Chemistry (LTEC kit) was used to assess alanine aminotransferase (ALT) and aspartate aminotransferase (AST).[24,25] The method with enhanced specificity of the bromocresol purple colorimetric test was used to measure albumin (DIAMOND diagnostic kit).[26] HCV antibody was assessed using an electrochemiluminescence immunoassay on a COBAS immunoassay analyzer,[27] and HBs-Ag was determined using a Sorin Biomedica kit.[28] AFP was tested using an enzyme-linked immunosorbent assay kit from Siemens Medical Solutions Diagnostics (IMMULITE 1000 system).[29] HCV-RNA was quantified by RT-PCR using the COBAS TaqMan HCV quantitative test, version 2.0 (Roche Molecular Systems).[30]

Molecular Analysis

miRNA Extraction and cDNA Generation

miRNA extraction from EDTA-treated blood samples was done by using the miRNeasy Mini kit (Qiagen). A Nano-Drop instrument was used to evaluate the quantity and purity of extracted miRNA (Thermo Scientific). The purified miRNA was kept at –80°C. Using an miScript II RT kit (Qiagen), the separated miRNA was analyzed by reverse transcription to yield single-stranded cDNA. Reverse transcription was conducted on an iced in overall volume of 20 µL for every reaction. Ten microliters of purified miRNA was dispensed just after a mixture of 4 µL 5x miScript HiSpec RT buffer, 2 µL 10x miScript Nucleics Mix, 2 µL miScript reverse transcriptase, and 2 µL nuclease free water had been pipetted into each well. The experiment was carried out in a 2720 Applied Biosystems thermal cycler (Bioline) for 1 cycle at 37°C for 60 minutes and 95°C for 5 minutes. The cDNA was kept at –20°C.

Amplification

A miScript SYBR Green PCR kit provided by Qiagen was used for amplification. The cDNA samples were diluted 1:5 with nuclease-free water prior to amplification. A total of 12.5 µL SYBR Green Master Mix, 3.5 µL nuclease free water, 4 µL diluted cDNA, 2.5 µL miScript universal primer, and 2.5 µL miScript primer assay was used in a whole volume of 25 µL. The miScript primer assay, which includes specific forward primers of miRNA was used to identify miR-331-3p, miR-23b-3p, and miR-3194-5p. As a reference, the miRNA RNU6 was used. The amplification was carried out in ABI 7500 real-time PCR (software version 2.0.1) as follows: initial activation at 95°C for 15 minutes followed by 40 cycles of 94°C for 15 seconds, 55°C for 30 seconds, and 70°C for 30 seconds. The relative quantifications of miR-331-3p, miR-23b-3p, and miR-3194-5p were determined using the comparative $2^{-\Delta\Delta Ct}$ method after normalizing the expression levels of miR-331, miR-23b-3p, and miR-3194-5p to that of RNU6. For each run, melting curve analysis was conducted for miR-331-3P, miR-23-3P, and miR-3194-5P to demonstrate amplification specificity and primer dimer absence.

Statistical Analysis

The data were input into the computer and evaluated using the IBM SPSS software package version 20.0. (IBM). The normality of the variable distribution was confirmed using the Kolmogorov-Smirnov test. The χ^2 test (Monte Carlo) was used to compare categorical data between groups. For abnormally distributed quantitative variables, the

Mann–Whitney test was used to compare 2 groups, the 3 study groups were compared using analysis of variance (ANOVA), the Tukey post hoc test was used for pairwise comparison, and the Kruskal-Wallis test was used to compare different groups for abnormally distributed quantitative data followed by the Dunn's post hoc test for multiple comparisons for pairwise comparison. The receiver operating characteristic (ROC) curve was used to evaluate diagnostic performance of the markers. Regression analysis was performed. Significance was determined to be at the 5% level.

Results

This study involved 150 subjects who were divided into 2 groups: group I, those with HCC on top of chronic HCV, and group II, those with HCV-positive chronic liver disease. The controls (group III; 50 subjects) were age- and gender-matched apparently healthy volunteers. All the participant demographic and clinicopathological characteristics are summarized in **TABLE 1**. They were matched for age, gender, body mass index, and smoking status (P = .129, P = .373, P = .137, and P = .7, respectively). Of subjects with HCC, 72% revealed significant associations with bilharziasis (P < .001). However, in terms of associated comorbidities (diabetes mellitus, P = .523; hypertension, P = .129; hepatic encephalopathy, P = .338; splenomegaly, P =.091; ascites, P = .141; and Child-Pugh class, P = .154), the HCC group did not differ significantly from patients with cirrhosis.

As shown in **TABLE 2** and **FIGURE 1**, 40% and 24% of patients with HCC had vascular invasion and lymph node metastasis, respectively. The sites of distant metastasis were bone (12%), lung (6%), and kidney (6%). The right lobe of the liver was the most affected (52%), with 60% of patients having numerous tumor nodules and 46% having large tumors (>5 cm). In 66% of cases, TNM staging (III + IV) was advanced. By BCLC classification, 46% of HCC cases were classified as stage C.

Platelet count and serum albumin were significantly lower whereas ALT, AST, bilirubin, and AFP were significantly elevated in patients (mainly those with HCC) compared with the control group (**TABLE 3**).

The expression of miR-3194-5p (P_1 = .002, P_2 < .001, P_3 < .001) and miR-23b-3p (P_1 < .001, P_2 < .001, P_3 < .04) were significantly

TABLE 1. Comparison between the 3 studied groups according to demographic and clinical parameters[a]

	HCC (n = 50)	Cirrhosis (n = 50)	Control (n = 50)	Test of significance	*P*
Gender					
Male	41 (82)	38 (76)	35 (70)	χ^2 = 1.974	.373
Female	9 (18)	12 (2)	15 (30)		
Age (y)					
Minimum-maximum	47-74	39-64	46-65	F = 2.073	.129
Mean ± SD	59.74 ± 6.16	57.68 ± 4.77	58.78 ± 4.03		
BMI (kg/m^2)					
Minimum-maximum	20-33.1	18.5-35	18-30	F = 2.017	.137
Mean ± SD	26.23 ± 3.15	26.76 ± 4.17	25.22 ± 4.27		
Smoking					
No	27 (54)	23 (46)	25 (50)	χ^2 = 0.64	^{MC}P = .7
Smoker	23 (46)	27 (54)	25 (50)		
Comorbidities					
Diabetes	15 (30)	18 (36)	—	χ^2 = 0.407	.523
Hypertension	10 (20.4)	17 (34)	—	χ^2 = 2.305	.129
History of bilharziasis					
No	14 (28)	30 (60)	50 (100)	χ^2 = 55.623	<.001[b]
Yes	36 (72)	20 (40)	0 (0)		
Hepatic encephalopathy	4 (8()	7 (14)	—	χ^2 = 0.919	.338
Splenomegaly	37 (74)	29 (58)	—	χ^2 = 2.852	.091
Ascites					
No	38 (76)	43 (86)	—	χ^2 = 4.109	^{MC}P = .141
Mild	8 (16)	7 (14)	—		
Moderate	4 (8)	0 (0)	—		
Child-Pugh class					
A	31 (62)	35 (70)	—	χ^2 = 3.965	^{MC}P = .154
B	15 (30)	15 (30)	—		
C	4 ()	0 (0)	—		

F, analysis of variance test (pairwise comparison between each 2 groups was done using the Tukey post hoc test); MC, Monte Carlo.
[a]*Data are given as No. (%) unless otherwise indicated.*
[b]*Statistically significant at* P ≤ *.05.*

TABLE 2. Clinicopathological distribution of the hepatocellular carcinoma cases

	No. (%)
Vascular invasion	20 (40)
Lymph node metastasis	12 (24)
Metastatic site if present	
Bone	6 (12)
Lung	3 (6)
Renal	3 (6)
Tumor number	
Single	20 (40)
Multiple	30 (60)
Tumor size (cm)	
Small <3	9 (18)
Medium 3-5	18 (36)
Large >5	23 (46)
Tumor site	
Right lobe	26 (52)
Left lobe	8 (16)
Caudate lobe	3 (6)
Both	13 (26)
TNM staging	
I	14 (28)
II	3 (6)
III	15 (30)
IV	18 (36)
Barcelona Clinic Liver Cancer Staging System	
A	9 (18)
B	14 (28)
C	23 (46)
D	4 (8)

downregulated whereas miR-331-3p (P_1 = .001, P_2 < .001, P_3 < .001) was upregulated in HCC patients compared with cirrhotic patients and the control group, as it was in cirrhotic patients compared with the control group (**TABLE 3**). The analytical performance of the miRNAs to distinguish groups is shown in **TABLE 4** (**FIGURE 2**). miR-331-3p exhibited a sensitivity of 90%, AUC of 0.958, and P < .001 in distinguishing HCC cases from healthy controls, followed by miR-3194-5p (86%, AUC: 0.849, P < .001), AFP (80%, AUC: 0.811, P < .001), and the expression of miR-23b-3p reported sensitivity of 76% at <0.7 (AUC: 0.737, P < .001). The combination of the 3 investigated miRNAs revealed the highest sensitivity of 94% and specificity of 92% with AUC of 0.975 (P < .001) in differentiating HCC from control, as we expected. Additionally, this combined miRNA panel was 90% effective at differentiating HCC from patients with cirrhosis (AUC: 0.77, P < .001). miR-331-3p was efficient at differentiating HCC patients from cirrhotic patients at a cutoff value of >1.9 (sensitivity: 86%, AUC: 0.757, P < .001), followed by miR-3194-5p and AFP with sensitivity of 82% and 72% at a cutoff value of ≤0.99 and >31.3 (AUC: 0.73, P < .001; and AUC: 0.702, P = .001), respectively. In distinguishing patients with metastatic forms of the disease from nonmetastatic forms, miR-331-3p had a higher AUC of 0.982 and sensitivity of 91.67% at a cutoff value of >11.5 (P < .001) than miR-23b-3p, with sensitivity of 83.33% at a cutoff value of ≤0.25 (AUC: 0.813, P = .001), and miR-3194-5p (75%, AUC: 0.786, P = .003). Moreover, the combination of the 3 studied miRNAs showed sensitivity of 91.67% and specificity of 92.11 with AUC of 0.991 and P < .001. AFP failed to distinguish between metastatic and nonmetastatic HCC patients (P = .540).

The relation between the 3 studied miRNAs and the clinical features of the HCC subjects is shown in **TABLE 5**. A high level of miR-331-3p expression was significantly related to vascular invasion (P = .017), lymph node and distant metastasis (P < .001), advanced TNM stages (III + IV) (P = .003), and BCLC C and D staging (P = .004). However, low levels of miR-23b-3p were associated with vascular invasion (P = .007), metastasis (P = .001), multiple nodular tumors (P = .024), advanced TNM stages (III + IV) (P < .001), and advanced BCLC staging (P < .001). In addition, miR-3194-5p was significantly lower in HCC patients with Child-Pugh class C (P = .009), metastasis (P = .003), advanced TNM stages (III + IV) (P = .014), and advanced BCLC staging (P < .001).

Finally, the contributing role of miRNAs in metastasis was investigated using univariate and multivariate analysis (**TABLE 6**, **FIGURE 2**). The univariate analysis revealed significant association of miR-331-3p, miR-23b-3p, and 3194-5p with metastasis. Moreover, miR-331-3p was found to be an independent predictor of metastasis (P = .036; odds ratio [95% CI]: 1.970 [1.046-3.71])

Discussion

Our study evaluated the diagnostic and prognostic roles of miR-331-3p, miR-23b-3p, and miR-3194-5p expressions in HCV-related HCC vs HCV cirrhotic patients as well as apparently healthy subjects. Despite ongoing advancements in diagnostic tools and treatment efficacy, many patients with HCC are still evaluated at the end stage with acute liver failure. As a result, identifying new diagnostic and prognostic biomarkers for HCC treatment is critical.[31] Most chronic HCV cases follow a clinical path that begins with fibrosis, progresses to cirrhosis, and then ends with HCC. Liver fibrosis is associated with alteration in hepatic miRNA expression, and hence, the advancement of fibrosis affects circulating miRNAs.[32] Our results revealed significant upregulations of miR-331-3p and downregulations of both miR-23b-3p and miR-3194-5p in HCC patients compared with controls. Also, patients with HCC demonstrated significant dysregulations of miRNAs compared with those with cirrhosis. Moreover, miR-331-3p better differentiated HCC from controls. It reported the highest sensitivity compared with serum AFP. Similarly, Li et al[33] found that miR-331-3p was differentially expressed in serum of HCV-related HCC patients compared with liver cirrhosis patients, implying that miRNA might be used as an alternative HCC biomarker. It was postulated that miR-331-3p regulates BCL2 antagonist/killer 1 (BAK1) expression, which is substantially suppressed in HCC.[34] BAK1 belongs to the BCL2 protein family and is the principal regulator of the cell death process, and through its collaborates with other pro-apoptotic molecules, promotes mitochondrial apoptosis.[34] Chi et al[35] discovered that increased miR-331-3p had diagnostic and prognostic relevance in liver cancer. Research studies have shown the potential relevance of miR-331-3p in pancreatic cancer, glioblastoma, colorectal cancer, and breast cancer by regulating the expressions of epidermal growth factor receptor and HER-2 via reducing Akt activity.[12-14] Conversely, Zhao et al[36] discovered that miR-331-3p expression is downregulated in triple-negative breast

FIGURE 1. **A, Distribution of the studied cases according to vascular invasion and lymph node (LN) metastasis in the hepatocellular carcinoma (HCC) group. B, Distribution of the studied cases according to metastatic site if present in the HCC group. C, Distribution of the studied cases according to TNM staging in the HCC group. D, Distribution of the studied cases according to the Barcelona Clinic Liver Cancer Staging System (BCLC) in the HCC group.**

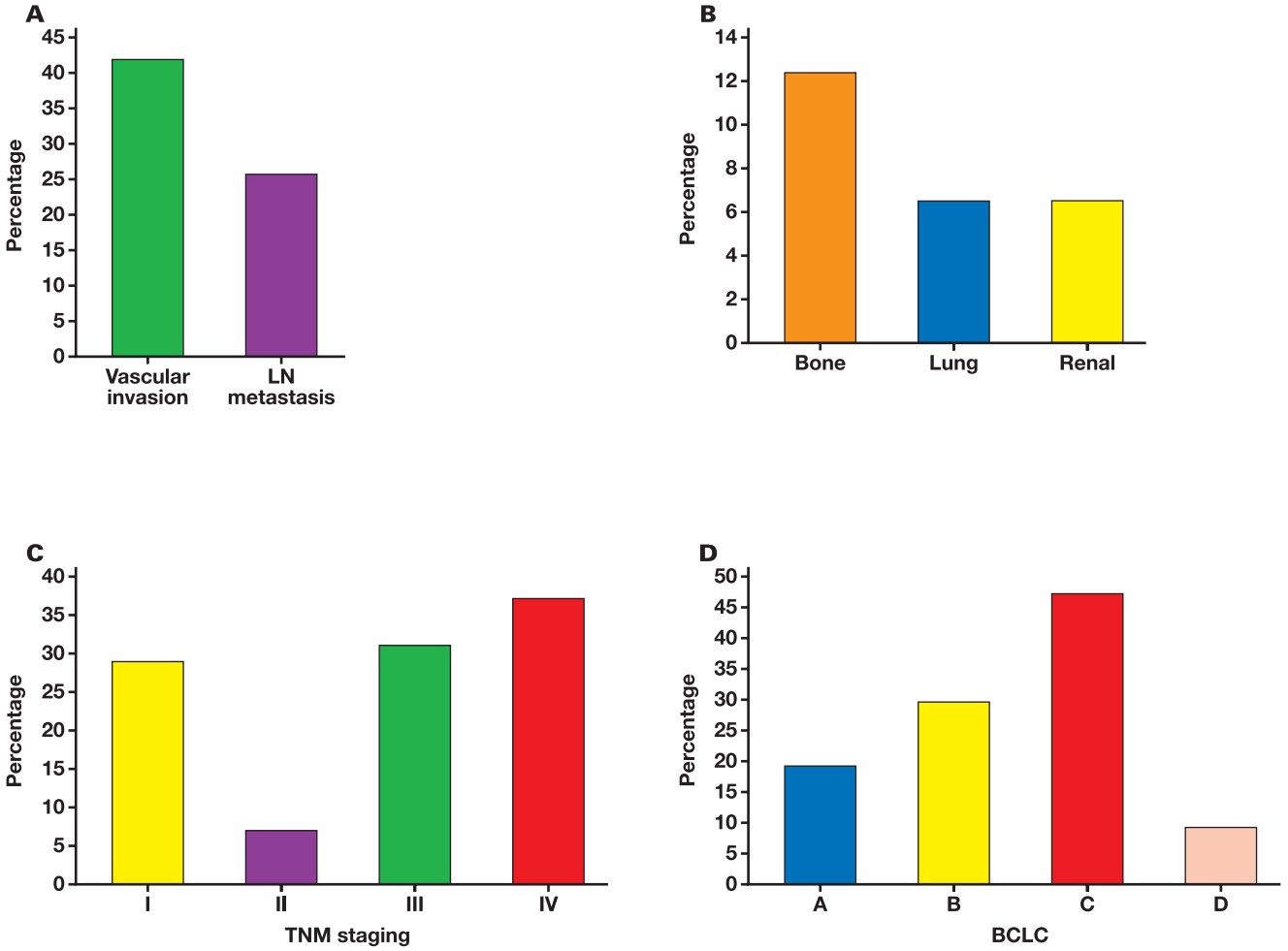

cancer (TNBC) tissues, and it was significantly associated with the advanced stage of TNBC. miR-331-3p at least partially inhibited the malignancy of TNBC by targeting neuropilin 2. miR-331-3p may therefore be a promising therapeutic target for TNBC. Hence, more research is still needed to fully understand the mechanism by which this miRNA functions.

Li et al[33] and He et al[37] reported that miR-23b-3p expression was clearly diminished in HCC tissues when compared with liver tissues. However, high miR-23b-3p expression did not significantly coincide with long-lived HCC patients.[38] miR-23b-3p is a tumor suppressor that may control HCC migration and invasion by aiming at Pyk2 via epithelial-mesenchymal transition regulation and could be a therapeutic target for the treatment of HCC.[39] On the other hand, overexpressed miR-23b-3p suppressed mitochondrial metabolism and was linked to advanced hepatocarcinogenesis and poor prognosis, indicating that it acts as oncogenic miRNA in HCC carcinogenesis.[40]

Consistent with our results, Namkung et al[41] showed that miR-3194-5p was downregulated in a high-risk pancreatic cancer group. Furthermore, Young et al[42] discovered that estrogen enhanced ring finger protein 4, which lowers Sp1 levels and increases CD44 expression by downregulating miR-3194-5p in young women with lung cancer. However, it is unknown whether estrogen can directly control the expression of miR-3194-5p. Dan et al[43] documented that miR-3194-5p was expressed in high levels among psoriatic patients. Also, the significant relation between miR-3194-5p and human papillomavirus type 16 (HPV16) infection suggests that this miRNA may play a role in HPV16-mediated neoplasia and metastasis as well as being relevant for oropharyngeal squamous cell carcinoma prognosis.[44]

The ROC curve of the combined miRNAs (miR-3194-5p, miR-23b-3p, and miR-331-3p) showed the combination had the highest sensitivity and effectively distinguished HCC from cirrhotic lesions. Also, Sun et al[18] reported that combining miR-331-3p, miR-23b-3p, and AFP may improve diagnostic performance and offer a new approach to identifying early-stage HCC in patients at high risk. The ROC curve of combined miRNAs also revealed improved sensitivity and specificity in discriminating metastatic from nonmetastatic forms; miR-331-3p had higher sensitivity, followed by miR-23b-3p, and finally miR-3194-5p. In line with these findings, it was demonstrated that patients with metastatic disease have higher expression of miR-331 and thus, miR-331 could be a promoter of breast cancer metastasis.[45] Therefore, adopting

TABLE 3. Laboratory analysis of the 3 studied groups

	HCC (n = 72)	Cirrhosis (n = 48)	Control (n = 47)	Test of significance	*P*
ALT (U/L)					
Minimum-maximum	28-162	6-168	20-29	H = 74.266	<.001[a]
Median (IQR)	43 (35-55)	33.50 (28-50)	22 (21-26)		
Significance between groups	P_1 = .005,[a] P_2 < .001,[a] P_3 < .001[a]				
AST (U/L)					
Minimum-maximum	25-135	8-104	18-29	H = 77.180	<.001[a]
Median (IQR)	50 (39-72)	39.50 (30-57)	24 (22-28)		
Significance between groups	P_1 = .018,[a] P_2 < .001,[a] P_3 < .001[a]				
Platelets (×10³/μL)					
Minimum-maximum	66-790	48-337	200-300	H = 49.959	<.001[a]
Median (IQR)	140 (93-189)	178 (138-219)	265 (210-290)		
Significance between groups	P_1 = .059, P_2 < .001,[a] P_3 < .001[a]				
Serum albumin (g/dL)					
Minimum-maximum	2.30-4.67	2-4.60	3.90-4.80	F = 30.586	<.001[a]
Mean ± SD	3.43 ± 0.76	3.74 ± 0.59	4.33 ± 0.32		
Total bilirubin (mg/dL)	P_1 = .023,[a] P_2 < .001,[a] P_3 < .001[a]				
Minimum-maximum	0.60-2.40	0.17-5	0.20-0.90	H = 54.482	<.001[a]
Median (IQR)	1.31 (0.84-1.8)	0.87 (0.70-1.6)	0.60 (0.40-0.70)		
Significance between groups	P_1 = .028,[a] P_2 < .001,[a] P_3 < .001[a]				
AFP (ng/mL)					
Minimum-maximum	3-6324	2.14-614	10-18	H = 29.062	<.001[a]
Median (IQR)	63.70 (23.5-698)	17 (8.9-73)	13 (12-15)		
Significance between groups	P_1 < .001,[a] P_2 < .001,[a] P_3 = .087				
miR-331-3p					
Minimum-maximum	0.76-20.8	0.14-15.0	0.1-1.55	H = 72.784	<.001[a]
Median (IQR)	5.2 (3.8-13.8)	1.75 (1.2-4.5)	0.78 (0.42-1.19)		
Significance between groups	P_1 = .001,[a] P_2 < .001,[a] P_3 < .001[a]				
miR-23b-3p					
Minimum-maximum	0.06-1.10	0.06-1.38	0.09-1.77	H = 16.706	<.001[a]
Median (IQR)	0.36 (0.10-0.7)	0.75 (0.09-0.9)	0.76 (0.46-1.56)		
Significance between groups	P_1 < .001[a], P_2 < .001,[a] P_3 < .04[a]				
miR-3194-5p					
Minimum-maximum	0.06-1.15	0.08-1.39	0.08-1.72	H = 47.723	<.001[a]
Median (IQR)	0.6 (0.32-0.90)	1.08 (0.57-1.27)	1.45 (1.15-1.56)		
Significance between groups	P_1 = .002,[a] P_2 < .001,[a] P_3 < .001[a]				

AFP, alpha fetoprotein; ALT, alanine aminotransferase; AST, aspartate aminotransferase; F, analysis of variance test (pairwise comparison between each 2 groups was done using the Tukey post hoc test); H, Kruskal-Wallis test (pairwise comparison between each 2 groups was done using Dunn's post hoc test for multiple comparisons); HCC, hepatocellular carcinoma; IQR, interquartile range; P_1, *P value for comparing HCC and cirrhosis;* P_2, *P value for comparing HCC and control;* P_3, *P value for comparing cirrhosis and control.*
[a]*Statistically significant at* P ≤ *.05.*

a comprehensive panel of miRNAs should improve HCC prognosis more than a single-biomarker procedure.

Our study also found a correlation between poor clinicopathological characteristics in HCC and high miR-331-3p as well as low miR-3194-5p and miR-23b-3p expression. Similarly, studies of other variables have shown associations between low miR-23b-3p expression and smoking history, vascular invasion, and lymphatic metastasis, implying that miR-23b-3p may play a significant role in the growth and development of HCC tumors via various mechanisms and may be one of the poor prognostic indicators for cases of HCC that have undergone resection.[37,46-48]

Multivariate analysis revealed that miR-331-3p was an independent predictor of HCC metastatic lesions. In accordance with our results, previous research revealed that the overexpression of miR-331-3p promotes liver cancer cell proliferation and metastasis via dephosphorylation of protein kinase B, which is accomplished through inhibiting leucine-rich repeat protein phosphatase.[49,50]

All of these miRNAs, alone or in combination, have sensitivity or specificity issues in diagnosis and in picking up metastatic forms of the disease. To successfully use these biomarkers in illness diagnosis and monitoring or for identifying people at risk for a significant adverse

TABLE 4. Analytical performance of miRNAs and AFP to distinguish different groups

	AUC	*P*	95% CI	Cutoff	Sensitivity	Specificity	PPV	NPV
HCC cases (n = 50) from controls (n = 50)								
miR-331-3p	0.958	<.001[a]	0.920-0.955	>1.41	90.0	88.0	88.2	89.8
miR-23b-3p	0.737	<.001[a]	0.642-0.833	≤0.7	76.0	54.0	62.3	69.2
miR-3194-5p	0.849	<.001[a]	0.969-1.0	≤1	86.0	82.0	82.7	85.4
Combination	0.976	<.001[a]	0.949-1.0		94.0	92.0	92.2	93.9
AFP	0.811	<.001[a]	0.705-0.917	>14	80.0	70.0	72.7	77.8
HCC patients (n = 50) from cirrhosis (n = 50)								
miR-331-3p	0.757	<.001[a]	0.662-0.852	>1.9	86.0	56.0	66.2	80.0
miR-23b-3p	0.617	<.043[a]	0.502-0.732	≤0.69	74.0	66.0	68.5	71.7
miR-3194-5p	0.730	<.001[a]	0.502-0.732	≤0.99	82.0	74.0	76.8	84.1
Combination	0.770	<.001[a]	0.679-0.862		90.0	60.0	69.2	85.7
AFP	0.702	.001[a]	0.600-0.803	>31.3	72.0	64.0	66.7	69.6
Metastatic cases (n = 12) from nonmetastatic (n = 38) in HCC group								
miR-331-3p	0.982	<.001[a]	0.949-1.015	>11.5	91.67	89.47	73.3	97.1
miR-23b-3p	0.813	.001[a]	0.688-0.937	≤0.25	83.33	73.68	50.0	93.3
miR-3194-5p	0.786	.003[a]	0.6538-0.934	≤0.5	75.0	71.05	45.0	90.0
Combination	0.991	<.001[a]	0.973-1.0		91.67	92.11	78.6	97.2
AFP	0.559	.540	0.348-0.771	>78	58.33	57.89	30.4	81.5

AFP, alpha fetoprotein; AUC, area under the curve; HCC, hepatocellular carcinoma; miRNA, microRNA; NPV, negative predictive value; PPV, positive predictive value.
[a]*Statistically significant at* P ≤ *.05.*

FIGURE 2. A, Receiver operating characteristic (ROC) curve for microRNA (miRNA) and alpha fetoprotein (AFP) to diagnose hepatocellular carcinoma (HCC) patients from control. B, ROC curve for miRNA and AFP to diagnose HCC from cirrhosis. C, ROC curve for miRNA and AFP to diagnose metastasis from nonmetastasis in the HCC group. D, Univariate logistic regression analysis for the parameters affecting metastasis. BCLC, Barcelona Clinic Liver Cancer Staging System.

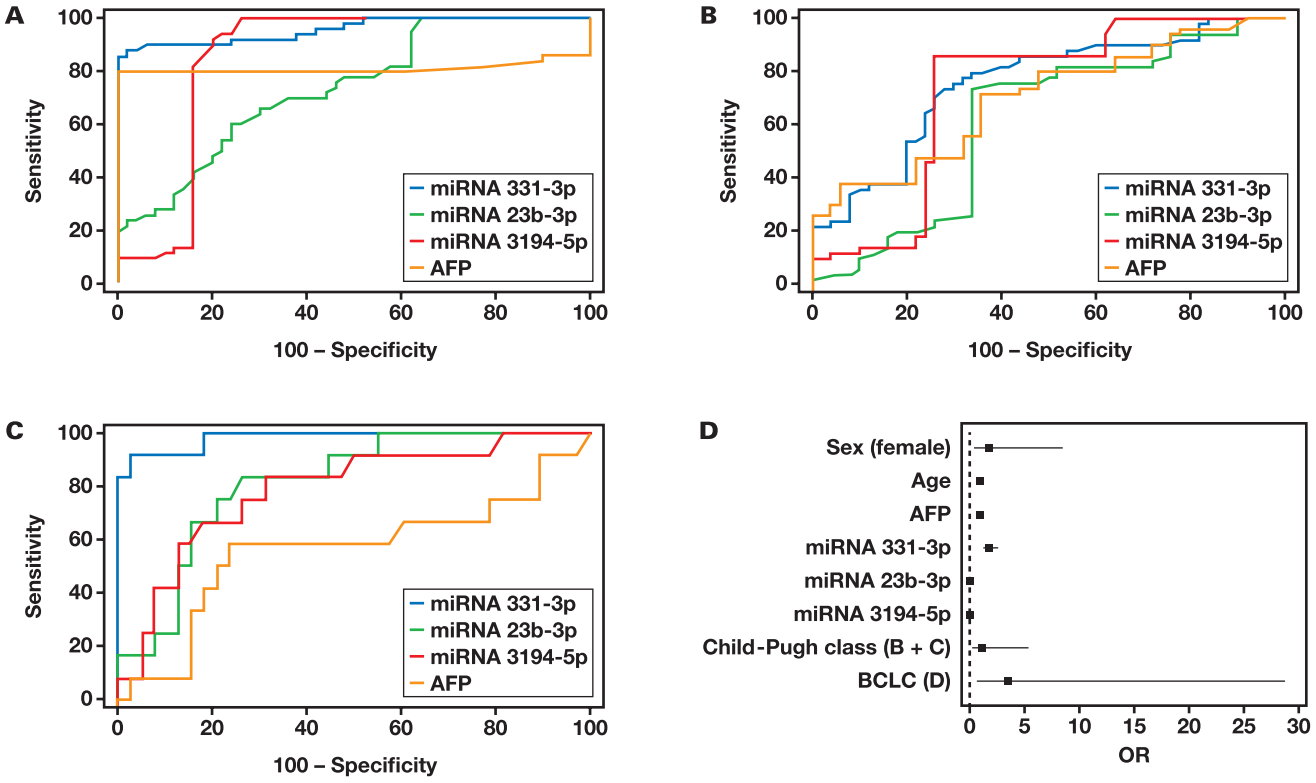

TABLE 5. Relation between miRNA and clinical parameters in HCC patients

	n	miR-331-3p		miR-23b-3p		miR-3194-5p	
		Mean ± SD	Median (IQR)	Mean ± SD	Median (IQR)	Mean ± SD	Median (IQR)
Child-Pugh class							
A	31	7.24 ± 6.07	4.80 (3.65-10.50)	0.48 ± 0.32	0.42 (0.24-0.72)	0.67 ± 0.33	0.69 (0.39-0.94)
B	15	9.78 ± 7.11	8.10 (4.45-16.55)	0.43 ± 0.39	0.25 (0.08-0.80)	0.61 ± 0.36	0.60 (0.32-0.86)
C	4	13.05 ± 7.97	14.80 (7.40-18.70)	0.17 ± 0.08	0.19 (0.13-0.22)	0.07 ± 0.01	0.07 (0.07-0.08)
H (*P*)		2.790 (.248)		3.942 (.139)		9.399 (.009[a])	
Vascular invasion							
No	30	6.39 ± 5.16	4.75 (2.90-9.50)	0.54 ± 0.34	0.48 (0.25-0.89)	0.66 ± 0.38	0.70 (0.33-1.0)
Yes	20	11.59 ± 7.47	13.0 (4.60-18.80)	0.28 ± 0.27	0.21 (0.07-0.38)	0.52 ± 0.33	0.51 (0.31-0.83)
U (*P*)		180.0(.017[a])		163.50 (.007[a])		228.50 (.157)	
LN metastasis							
No	38	5.43 ± 3.99	4.65 (2.60-6.20)	0.52 ± 0.34	0.46 (0.25-0.79)	0.69 ± 0.34	0.72 (0.42-0.98)
Yes	12	18.08 ± 3.21	19.10 (17.6-19.95)	0.17 ± 0.15	0.10 (0.07-0.23)	0.33 ± 0.30	0.27 (0.08-0.51)
U (*P*)		8.0 (<.001[a])		85.50 (.001[a])		97.50 (.003[a])	
Metastatic site if present							
Absent	38	5.43 ± 3.99	4.65 (2.60-6.20)	0.52 ± 0.34	0.46 (0.25-0.79)	0.69 ± 0.34	0.72 (0.42-0.98)
Present	12	18.08 ± 3.21	19.10 (17.6-19.95)	0.17 ± 0.15	0.10 (0.07-0.23)	0.33 ± 0.30	0.27 (0.08-0.51)
U (*P*)		8.0 (<.001[a])		85.50 (.001[a])		97.50 (.003[a])	
Tumor number							
Single	20	7.87 ± 7.34	4.60 (1.52-14.50)	0.60 ± 0.41	0.72 (0.18-0.99)	0.71 ± 0.40	0.83 (0.31-1.1)
Multiple	30	8.86 ± 6.22	5.25 (4.30-13.80)	0.33 ± 0.24	0.32 (0.08-0.47)	0.53 ± 0.32	0.53 (0.33-0.8)
U (*P*)		238.0 (.219)		186.0 (.024[a])		208.50 (.070)	
Tumor size (cm)							
Small <3	9	8.53 ± 7.71	4.80 (4.50-16.80)	0.38 ± 0.28	0.31 (0.16-0.57)	0.69 ± 0.44	0.84 (0.32-1.1)
Medium 3-5	18	7.43 ± 6.48	4.50 (3.50-10.30)	0.41 ± 0.35	0.35 (0.08-0.54)	0.65 ± 0.30	0.65 (0.42-0.9)
Large >5	23	9.25 ± 6.52	6.80 (4.45-13.25)	0.48 ± 0.36	0.42 (0.19-0.75)	0.53 ± 0.37	0.6 (0.15-0.85)
H (*P*)		1.526 (.466)		0.473 (.789)		1.992 (.369)	
TNM staging							
I + II	17	4.82 ± 4.12	3.80 (1.20-6.80)	0.76 ± 0.30	0.79 (0.64-0.99)	0.77 ± 0.40	0.90 (0.66-1.1)
III + IV	33	10.34 ± 6.95	6.10 (4.70-18.30)	0.27 ± 0.22	0.25 (0.08-0.40)	0.52 ± 0.31	0.51 (0.32-0.73)
U (*P*)		136.0 (.003[a])		64.0 (<.001[a])		161.0 (.014[a])	
BCLC							
A	9	3.99 ± 3.90	2.40 (0.88- 6.8)	0.95 ± 0.12	0.98 (0.89-0.99)	0.84 ± 0.42	1.10 (0.69-1.15)
B	14	4.80 ± 2.03	4.65 (4.10-5.3)	0.52 ± 0.20	0.48 (0.36-0.69)	0.75 ± 0.21	0.77 (0.53-0.90)
C	23	11.65 ± 7.09	12.20 (4.7-18.8)	0.24 ± 0.25	0.10 (0.07-0.33)	0.51 ± 0.32	0.49 (0.31-0.76)
D	4	13.05 ± 7.97	14.80 (7.40-18.7)	0.17 ± 0.08	0.19 (0.13-0.22)	0.07 ± 0.01	0.07 (0.07-0.08)
H (*P*)		13.446 (.004[a])		29.242 (<.001[a])		16.628 (.001[a])	

BCLC, BCLC, Barcelona Clinic Liver Cancer Staging System; H, Kruskal-Wallis test; IQR, interquartile range; LN, lymph node; U, Mann-Whitney U *test.*
[a]*Statistically significant at* P ≤ *.05.*

TABLE 6. Univariate and multivariate logistic regression analysis for the miRNAs related to metastasis

	Univariate		Multivariate[a]	
	P	OR (LL-UL 95% CI)	*P*	OR (LL-UL 95% CI)
miR-331-3p	.002[b]	1.767 (1.231-2.535)	.036[b]	1.970 (1.046-3.71)
miR-23b-3p	.01[b]	0.003 (0.0-0.24)	.162	0.0 (0.0-236.49)
miR-3194-5p	.006[b]	0.036 (0.003-0.389)	.525	0.192 (0.001-31.14)

LL, lower limit; miRNA, microRNA; OR, odds ratio; UL, upper limit.
[a]*All variables with* P < *.05 were included in the multivariate.*
[b]*Statistically significant at* P ≤ *.05.*

event or those who may benefit more from a pharmacological treatment, further multicenter clinical trials are required to show efficacy, evaluate cost effectiveness, and receive approval by an appropriate organization.

We investigated the role of miR-3194-5p expression in HCC and cirrhotic lesions as part of a panel of miRNAs for the first time.

However, our study had some limitations, such as the fact that the results are less inclusive because it is not a multicenter study. Second, the sample size was insufficient. More research is needed to determine the underlying potential functions of these miRNAs in the development and progression of HCC.

Conclusion

This work adds to the body of knowledge by evaluating, for the first time, the function of miR-3194-5p expression in HCC and cirrhotic lesions, and we reported a significant association of miRNAs (miR-331-3p, miR-23b-3p, and miR-3194-5p) with poor clinicopathological features of HCC that could be used to distinguish HCV-related HCC from cirrhosis, mainly miR-331-3p alongside combined miRNAs, followed by miR-3194-5p. miR-331-3p with combined miRNAs could distinguish metastatic from nonmetastatic forms of disease. Moreover, miR-331-3p was found to be an independent factor for metastatic lesions. The potential noninvasive diagnostic significance of the miRNAs panel in HCC and metastasis is clarified in this work, which advances biomedical science. Additionally, the miRNAs panel may contribute to our understanding of the pathophysiology of HCC. The miRNAs panel may also represent a therapeutic target for HCC.

Acknowledgments

We extend our gratitude to all medical personnel and technicians of the Hepatology Center and Faculty of Medicine who agreed to participate in this study.

Conflict of Interest Disclosure

The authors have nothing to disclose.

Data Availability

The corresponding author will provide the datasets used and/or analyzed during the study upon reasonable request.

REFERENCES

1. Altekruse F, McGlynn A, Reichman E. Hepatocellular carcinoma incidence, mortality, and survival trends in the United States from 1975 to 2005. *J Clin Oncol.* 2009;27:1485-1491. https://doi.org/10.1200/JCO.2008.20.7753. PMID: 19224838
2. Bartosch B, Thimme R, Blum E, Zoulim F. Hepatitis C virus- induced hepatocarcinogenesis. *J Hepatol.* 2009;51:810-820. https://doi.org/10.1016/j.jhep.2009.05.008. PMID: 19545926
3. Schlosser S, Tümen D, Volz B, et al. HCC biomarkers - state of the old and outlook to future promising biomarkers and their potential in everyday clinical practice. *Front Oncol.* 2022;12:1016952. https://doi.org/10.3389/fonc.2022.1016952
4. Lawrie C, Gal S, Dunlop H, et al. Detection of elevated levels of tumour-associated microRNAs in serum of patients with diffuse large b-cell lymphoma. *Br J Haematol.* 2008;14:672-675. https://doi.org/10.1111/j.1365-2141.2008.07077.x
5. Amirkhah R, Schmitz U, Linnebacher M, Wolkenhauer O, Farazmand A. MicroRNA-mRNA interactions in colorectal cancer and their role in tumor progression. *Genes Chromosomes Cancer.* 2015;54(3):129-141. https://doi.org/10.1002/gcc.22231
6. Han L, Lv Y, Guo H, Ruan P, Nan J. Implications of biomarkers in human hepatocellular carcinoma pathogenesis and therapy. *World J Gastroenterol.* 2014;20:10249-10261.
7. Wang J, Zhang Y, Liu M, Sen S. Tumor-associated circulating microRNAs as biomarkers of cancer. *Molecules.* 2014;19:1912-1938.
8. Bai X, Liu Z, Shao X, et al. The heterogeneity of plasma miRNA profiles in hepatocellular carcinoma patients and the exploration of diagnostic circulating miRNAs for hepatocellular carcinoma. *PLoS One.* 2019;14(2):e0211581. https://doi.org/10.1371/journal.pone.0211581
9. Chen J, Zhu M, Wu H, et al. Circulating microRNAs as a fingerprint for liver cirrhosis. *PLoS One.* 2013;8:e66577. https://doi.org/10.1371/journal.pone.0066577
10. Chen P, Jin X, Xiang Z, Chen H, Li M. Circulating MicroRNAs as potential biomarkers for alcoholic steatohepatitis. *Liver Int.* 2013;33:1257-1265. https://doi.org/10.1111/liv.12196
11. Wang W, Heegaard H, Orum H. MicroRNAs in liver disease. *Gastroenterology.* 2012;142:1431-1443.
12. Zhao D, Sui Y, Zheng X. MiR-331-3p inhibits proliferation and promotes apoptosis by targeting HER2 through the PI3K/Akt and ERK1/2 pathways in colorectal cancer. *Oncol Rep.* 2016;35(2):1075-1082. https://doi.org/10.3892/or.2015.4450
13. Shee M, Koh Y, Voon G, Chye M, Othman I, Ng Y. The roles of microRNA-331 family in cancers. *J Cancer Res Pract.* 2019;6:1-6.
14. Fujii T, Shimada K, Asano A, et al. MicroRNA-331-3p suppresses cervical cancer cell proliferation and E6/E7 expression by targeting NRP2. *Int J Mol Sci.* 2016;17(8):1351. https://doi.org/10.3390/ijms17081351
15. Chen L, Chu F, Cao Y, Shao J, Wang F. Serum miR-182 and miR-331-3p as diagnostic and prognostic markers in patients with hepatocellular carcinoma. *Tumor Biol.* 2015;36(10):7439-7447. https://doi.org/10.1007/s13277-015-3430-2
16. Liu W, Zabirnyk O, Wang H, et al. miR-23b targets proline oxidase, a novel tumor suppressor protein in renal cancer. *Oncogene.* 2010;29:4914-4924. https://doi.org/10.1038/onc.2010.237
17. Zheng H, Liu Y, Song J, Chen X. Advances in circulating microRNAs as diagnostic and prognostic markers for ovarian cancer. *Cancer Biol Med.* 2013;10:123-130.
18. Sun Q, Li J, Jin B, Wang T, Gu J. Evaluation of miR-331-3p and miR-23b-3p as serum biomarkers for hepatitis C virus-related hepatocellular carcinoma at early stage. *Clin Res Hepatol Gastroenterol.* 2020;44(1):21-28. https://doi.org/10.1016/j.clinre.2019.03.011
19. Ji J, Wang W. New kids on the block: diagnostic and prognostic microRNAs in hepatocellular carcinoma. *Cancer Biol Ther.* 2009;8:1686-1693.
20. Lin H, Xin N, Dong J, et al. Performance of the aspartate aminotransferase-to-platelet ratio index for the staging of hepatitis C-related fibrosis: an updated meta-analysis. *Hepatology.* 2011;53:726-736. https://doi.org/10.1002/hep.24105
21. Bruix J, Sherman M; American Association for the Study of Liver Diseases. Management of hepatocellular carcinoma: an update. *Hepatology.* 2011;53(3):1020-1022. https://doi.org/10.1002/hep.24199
22. Llovet M, Brú C, Bruix J. Prognosis of hepatocellular carcinoma: the BCLC staging classification. *Semin Liver Dis.* 1999;19:329-338. https://doi.org/10.1055/s-2007-1007122. PMID: 10518312
23. Pugh N, Murray-Lyon M, Dawson L, Pietroni C, Williams R. Transection of the oesophagus for bleeding oesophageal varices. *Br J Surg.* 1973;60:646-649. https://doi.org/10.1002/bjs.1800600817

24. Bergmeyer U, Scheibe P, Wahlefeld W. Optimization of method for aspartate aminotransferase and alanine aminotransferase. *Clin Chem.* 1978;24:58.
25. Saris E. Revised IFCC method for aspartate aminotransferase. *Clin Chem.* 1978;24:720-721.
26. Pinnell E, Northam E. New automated dye-binding method for serum albumin determination with bromocresol purple. *Clin Chem.* 1978;24:80-86.
27. Wu B, Ouyan Q, Tang Y, Zhou X. Double-antigen sandwich time-resolved immunofluorometric assay for the detection of anti-hepatitis C virus total antibodies with improved specificity and sensitivity. *J Microbiol.* 2008;57:163-168.
28. Adachi H, Fukuda T, Funahashi S, Kurahori T, Ishikawa E. Sandwich enzymoimmunoassay of hepatitis B surface antigen (HBsAg). *Vox Sang.* 1978;35(4):219-223. https://doi.org/10.1111/j.1423-0410.1978.tb02925.x
29. Engall E, Van Vunakis H, Langone J. *Methods in Enzymology*. Academic Press; 1980;70:419-492.
30. Ghany G, Strader B, Thomas L, Seeff B; American Association for the Study of Liver Diseases. Diagnosis, management, and treatment of hepatitis C: an update. *Hepatology.* 2009;49:1335-1374. https://doi.org/10.1002/hep.22759
31. Sun X, Ge X, Xu Z, Chen D. Identification of circular RNA–microRNA–messenger RNA regulatory network in hepatocellular carcinoma by integrated analysis. *J Gastroenterol Hepatol.* 2020;35(1):157-164. https://doi.org/10.1111/jgh.14762
32. Cermelli S, Ruggieri A, Marrero A, Ioannou N, Beretta L. Circulating microRNAs in patients with chronic hepatitis C and non-alcoholic fatty liver disease. *PLoS One.* 2011;6:e23937. https://doi.org/10.1371/journal.pone.0023937
33. Li J, Jin B, Wang T, et al. Serum microRNA expression profiling identifies serum biomarkers for HCV-related hepatocellular carcinoma. *Cancer Biomark.* 2019;26(4):501-512. https://doi.org/10.3233/cbm-181970
34. Wei C, Quan Y, Fan S, et al. Exosome-transmitted circular Rna Hsa_Circ_0051443 suppresses hepatocellular carcinoma progression. *Cancer Lett.* 2020;475(115):119-128.
35. Chi Q, Geng X, Xu K, Wang C, Zhao H. Potential targets and molecular mechanism of miR-331-3p in hepatocellular carcinoma identified by weighted gene coexpression network analysis. *Biosci Rep.* 2020;40(6):40. https://doi.org/10.1042/BSR20200124
36. Zhao M, Zhang M, Tao Z, Cao J, Wang L, Hu X. miR-331-3p suppresses cell proliferation in TNBC cells by downregulating NRP2. *Technol Cancer Res Treat.* 2020;19:153303382090582-153303382090589. https://doi.org/10.1177/1533033820905824
37. He Q, Wu R, Xiang L, et al. Downregulated miR-23b-3p expression acts as a predictor of hepatocellular carcinoma progression: a study based on public data and RT-qPCR verification. *Int J Mol Med.* 2018;41:2813-2831.
38. Yang Y, Gu X, Zhou M, Xiang J, Chen Z. Serum microRNAs: a new diagnostic method for colorectal cancer. *Biomed Rep.* 2013;1(4):495-498. https://doi.org/10.3892/br.2013.109
39. Cao J, Liu J, Long J, et al. MicroRNA-23b suppresses epithelial-mesenchymal transition (EMT) and metastasis in hepatocellular carcinoma via targeting Pyk2. *Biomed Pharmacother.* 2017;89:642-650. https://doi.org/10.1016/j.biopha.2017.02.030
40. Hayashi M, Yamada S, Kurimoto K, et al. miR-23b-3p plays an oncogenic role in hepatocellular carcinoma. *Ann Surg Oncol.* 2021;28(6):3416-3426. https://doi.org/10.1245/s10434-020-09283-y
41. Namkung J, Kwon W, Choi Y, et al. Molecular subtypes of pancreatic cancer based on miRNA expression profiles have independent prognostic value. *J Gastroenterol Hepatol.* 2016;31:1160-1167. https://doi.org/10.1111/jgh.13253
42. Young J, Chen C, Wang A, et al. Estradiol-mediated inhibition of Sp1 decreases miR-3194-5p expression to enhance CD44 expression during lung cancer progression. *J Biomed Sci.* 2022;29:3. https://doi.org/10.1186/s12929-022-00787-1
43. Dan W, Shiping C, Guoming Z, Xiongfei D. Paeoniflorin inhibits proliferation and migration of psoriatic keratinocytes via the lncRNA NEAT1/miR-3194-5p/Galectin-7 axis. *Anticancer Drugs.* 2022;33:e423-e433. https://doi.org/10.1097/CAD.0000000000001225
44. Hufbauer M, Maltseva M, Meinrath J, et al. HPV16 increases the number of migratory cancer stem cells and modulates their miRNA expression profile in oropharyngeal cancer. *Int J Cancer.* 2018;143:1426-1439.
45. McAnena P, Tanriverdi K, Curran C, et al. Circulating microRNAs miR-331 and miR-195 differentiate local luminal a from metastatic breast cancer. *BMC Cancer.* 2019;19(1):436. https://doi.org/10.1186/s12885-019-5636-y
46. Salvi A, Sabelli C, Moncini S, et al. MicroRNA-23b mediates urokinase and c-met downmodulation and a decreased migration of human hepatocellular carcinoma cells. *FEBS J.* 2009;276:2966-2982.
47. Chen L, Han L, Zhang K, et al. VHL regulates the effects of miR-23b on glioma survival and invasion via suppression of HIF-1α/VEGF and β-catenin/Tcf-4 signaling. *Neuro Oncol.* 2012;14(8):1026-1036. https://doi.org/10.1093/neuonc/nos122
48. Majid S, Dar A, Saini S, et al. MicroRNA-23b functions as a tumor suppressor by regulating Zeb1 in bladder cancer. *PLoS One.* 2013;8:e67686.
49. Cao Y, Chen J, Wang D, et al. Upregulated in hepatitis B virus-associated hepatocellular carcinoma cells, miR-331-3p promotes proliferation of hepatocellular carcinoma cells by targeting ING5. *Oncotarget.* 2015;6(35):38093-38106. https://doi.org/10.18632/oncotarget.5642
50. Chang M, Yang H, Fang F, Xu F, Yang Y. MicroRNA-331-3p promotes proliferation and metastasis of hepatocellular carcinoma by targeting PH domain and leucine-rich repeat protein phosphatase. *Hepatology.* 2014;60:1251-1263. https://doi.org/10.1002/hep.27221

A comparative study on outcomes of fasting vs postprandial thyroid function tests among pregnant mothers in a tertiary care setting in Sri Lanka

Shifaniya Banu Mohideen, MD[1], *Thamara Herath, MD*[1], *Supun Manathunga, MBBS*[2]

[1]Department of Biochemistry, Medical Research Institute, Colombo, Sri Lanka; [2]Department of Pharmacology, Faculty of Medicine, University of Peradeniya, Peradeniya, Sri Lanka. Corresponding author: Shifaniya Banu Mohideen; shifaniyabanu@gmail.com

Key words: thyroid function tests; fasting; postprandial; subclinical hypothyroidism in pregnancy

Abbreviations: TSH, thyrotropin; SCH, subclinical hypothyroidism; TFT, thyroid function test; MCMC, Markov chain Monte Carlo

Laboratory Medicine 2024;55:320-324; https://doi.org/10.1093/labmed/lmad084

ABSTRACT

Objective: Accurate estimation of serum thyrotropin (TSH) is crucial in the diagnosis of subclinical hypothyroidism (SCH) in pregnancy. We aimed to investigate whether there are significant differences between fasting and nonfasting thyroid function tests (TFTs) among pregnant mothers.

Methods: We studied 100 pregnant mothers with previously unknown thyroid dysfunction. An equal number of participants were included in each trimester. All pregnant mothers underwent fasting and 2-hour postprandial TFTs (TSH, free T4).

Results: Postprandial TSH (mean 1.01 mIU/L, SD 0.80) was significantly lower than the fasting TSH (mean 1.47 mIU/L, SD 1.18) in pregnancy ($P < .01$). Postprandial free T4 (mean 10.30 pmol/L, SD 2.01) was also lowered compared with fasting free T4 (mean 10.70 pmol/L, SD 1.99) in pregnancy ($P < .01$). The prevalence of SCH in pregnancy estimated using fasting TSH was 9.4% (SD 3%). In contrast, the prevalence was only 3.5% (SD 2%) when postprandial TSH was used.

Conclusion: Compared with the fasting state, postprandial TSH demonstrates a statistically significant reduction that greatly influences the diagnosis of SCH in pregnant mothers. Therefore, we conclude that the timing of sampling for TFTs should be standardized, especially in the pregnant population.

Introduction

Primary hypothyroidism is a commonly encountered endocrine disorder with an estimated prevalence of 0.3% globally.[1] Subclinical hypothyroidism (SCH) is a milder form of hypothyroidism but has a higher prevalence, ranging from 4% to 15%, and it is also higher in females.[2] SCH in pregnancy has a significant health impact on both mother and fetus,[3] so primary hypothyroidism and SCH should be diagnosed promptly and treated appropriately without delay.[4] As the earliest change with primary thyroid disorder is an alteration of serum thyrotropin (TSH) level, estimation of TSH is recommended by the guidelines of the American and European thyroid associations as a first-line test for thyroid disorders.[5,6] Subclinical hypothyroidism is diagnosed biochemically, as it can present with or without symptoms. In these circumstances, measuring TSH is more sensitive than T4 because TSH rises above the reference range before T4 falls. The available literature clearly demonstrates that there is a significant reduction of TSH following food intake; however, this is less studied in the pregnant population. Therefore, we aimed to investigate any variability of TSH and T4 between fasting and postprandial samples in pregnancy.

Methods

This study was conducted at a tertiary care hospital in Sri Lanka, and it was approved by the ethical review committees of Castle Street Hospital for Women and Medical Research Institute, Colombo, Sri Lanka. For our study, 100 pregnant mothers with previously unknown thyroid dysfunction aged between 18 and 50 years were recruited from the antenatal clinic. Participants from all 3 trimesters were covered in equal numbers (n = 33, 33, and 34). Patients with acute infection or illnesses, liver and renal disease, history of hypothalamic-pituitary disorders, or diabetes, or who were on steroid or other hormone replacement were not included in this study. Participants were advised to fast overnight for 8 to 10 hours. The first fasting venous sample was collected between 7 AM and 7:30 AM and the 2-hour postprandial venous sample was collected between 9 AM and 9:30 AM . All serum samples were analyzed for TSH and free T4 by Abbott Architect 2000i using the chemiluminescence technique. Abbott Architect reagents, quality control samples, and calibrators were used for the analysis. The analytical run was carried out after the validation of the quality control results.

Statistical Analysis

The empirical cumulative distribution functions of fasting TSH, postprandial TSH, fasting free T4, and postprandial free T4 were compared with the empirical cumulative distribution functions of mean and standard deviation-matched normally distributed random variables, and the Kolmogorov-Smirnov D statistics were calculated to assess normality.

Fasting and postprandial values of TSH and free T4 were compared with paired *t*-tests. Differences in mean fasting and mean postprandial TSH and free T4 in each trimester were analyzed using 1-way analysis of variance tests. A P value < .05 was taken as statistically significant.

Assuming a binomial distribution for the count of hypothyroid mothers (h), intercept-only Bayesian inference models informed by fasting and postprandial TSH values were fitted for logit-transformed prevalence (p) using weakly informative normally distributed priors.

$$h \sim binomial(1, \mathrm{p})$$

$$\mathrm{logit}(\mathrm{p}) = \mathrm{a}; \mathrm{a} \sim \mathcal{N}(0, 10)$$

The posterior distribution of prevalence was estimated using Markov chain Monte Carlo (MCMC) sampling.[7]

A Bayesian logistic regression model was used to estimate the false-negative rate for diagnosing SCH when using postprandial TSH instead of fasting TSH. The model assumed that the probability of a missed SCH diagnosis was a function of the intercept a and a binomial random variable with a probability p with weakly informative priors.

$$pN \sim binomial(1, \mathrm{p})$$

$$\mathrm{logit}(\mathrm{p}) = \mathrm{a}; \mathrm{a} \sim \mathcal{N}(0, 10)$$

Here, pN is the outcome variable representing whether a SCH diagnosis was missed. The posterior distribution of the model parameter a was estimated using the MCMC method, and the posterior predictive distribution was used to estimate the false-negative rate for diagnosing SCH.

Results

We analyzed TSH and free T4 results from 100 blood samples of pregnant mothers (mean age 29.3 years, SD 6.3). The P values of the calculated D statistics were 0.53 for fasting TSH, 0.39 for postprandial TSH, 0.59 for fasting free T4, and 0.66 for postprandial free T4, indicating that there is not sufficient evidence to reject the null hypothesis that the samples were derived from a normal distribution.

According to the data analysis, postprandial TSH (mean 1.01 mIU/L, SD 0.80) was significantly lower than fasting TSH (mean 1.47 mIU/L, SD 1.18) in pregnancy (P < .01) (**FIGURE 1**). This pattern was observed in both trimester-specific and non-trimester-specified cohorts (**FIGURE 2**). Postprandial free T4 (mean 10.30 pmol/L, SD 2.01) was also lower compared with fasting free T4 (mean 10.70 pmol/L, SD 1.99) in pregnancy (P < .01) (**FIGURE 3**). This pattern was seen in each trimester but the difference is too small to be statistically significant during the second trimester (**FIGURE 4**).

The prevalence of SCH in pregnancy estimated using fasting TSH was 9.4% (SD 3%). In contrast, the prevalence was only 3.5% (SD 2%) (**FIGURE 5**) when postprandial TSH was used. The posterior predictive density plots are depicted below (**FIGURE 6**).

The mean false-negative rate in screening SCH in pregnancy when postprandial TSH was used was 6.7% (SD 3.1%). The probability distribution is shown below for 10,000 samples from the posterior (**FIGURE 7**).

Discussion

SCH should be diagnosed promptly especially in the pregnant population, as it is associated with maternal and fetal complications. Estimation of TSH is critical in diagnosing SCH in pregnancy. Only a few studies have focused on the timing of TSH sampling, especially in the pregnant population. Our study demonstrates that postprandial TSH is significantly lower (30.8% reduction) compared with fasting levels in pregnant mothers. This decline is seen in each trimester as well (**FIGURES 1** and **2**). In a prospective randomized controlled study, Dong et al[8] found about 30% reduction in serum TSH following 75 g of glucose compared with the fasting sample, which is a similar finding but in nonpregnant participants.

Postprandial TSH decline has been reported in previous studies.[8-17] TSH and free T4 typically assume an inverse relationship, but postprandial reduction of free T4 is a new observation in our study. It is difficult to compare these results with the previous studies, as only 1 study included the pregnant population as participants (n = 65).[17] The complex catabolic status in pregnancy following food intake might have contributed to postprandial reduction of free T4 and it is difficult to explain the exact intrinsic mechanism. We hypothesize that increased metabolic rate following the fed state causing higher deiodinase activity[18] contributed to this finding. Future studies with a large sample size of pregnant persons should be carried out to confirm this.

There are significant variations in TSH and thyroid hormones in the blood, which can be attributed to preanalytical, analytical, and biological factors. The circadian rhythm of TSH levels in healthy individuals is well documented, with high levels peaking between 11 PM and 5 AM and reaching a nadir between 5 PM and 8 PM. In a large data study by Wang et al,[19] the authors concluded that there was no significant variation in serum TSH, free T4, and free T3 levels in samples collected in the morning. To minimize the compounding effect of diurnal variability,

FIGURE 1. Comparison of fasting and postprandial thyrotropin (TSH) in pregnancy. The distribution of fasting and postprandial TSH values are shown with box plots with individual data points overlaid. Corresponding observation pairs are connected by gray lines. $P = 1.9e^{-10}$ by paired *t*-test.

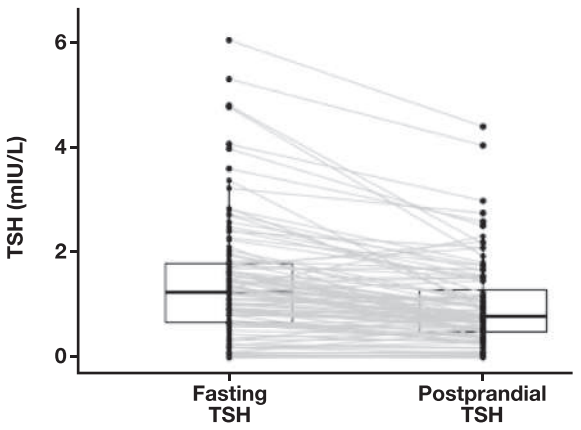

FIGURE 2. **Comparison of fasting and postprandial thyrotropin (TSH) in each trimester (A, trimester 1; B, trimester 2; C, trimester 3). The distribution of fasting and postprandial TSH values is shown with box plots with individual data points overlaid. Corresponding observation pairs are connected by gray lines. The *P* values for the paired *t*-test were *P* = .0035 (A), *P* = .00043 (B), and *P* = 1e^{-05} (C).**

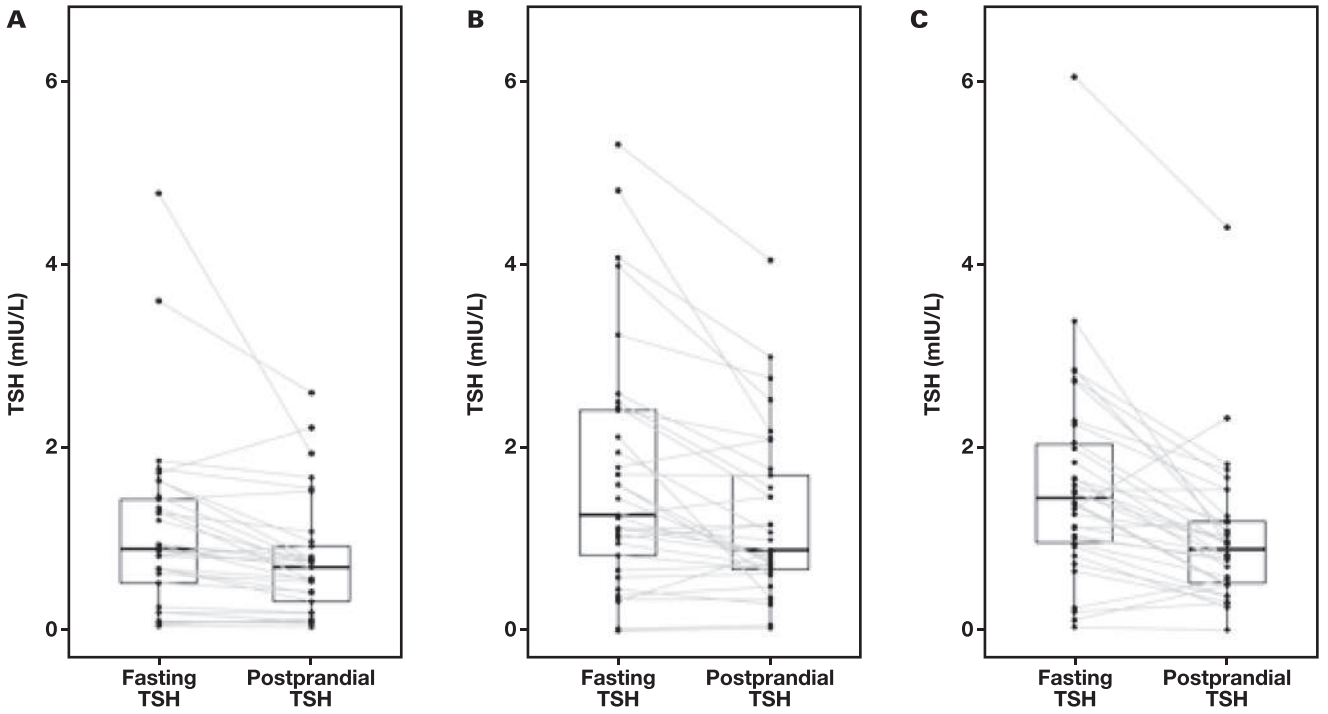

FIGURE 3. **Comparison of fasting free T4 (fT4) and postprandial fT4 in pregnancy. The distribution of fasting and postprandial fT4 values are shown with box plots with individual data points overlaid. Corresponding observation pairs are connected by gray lines. *P* = .0015 by paired *t*-test.**

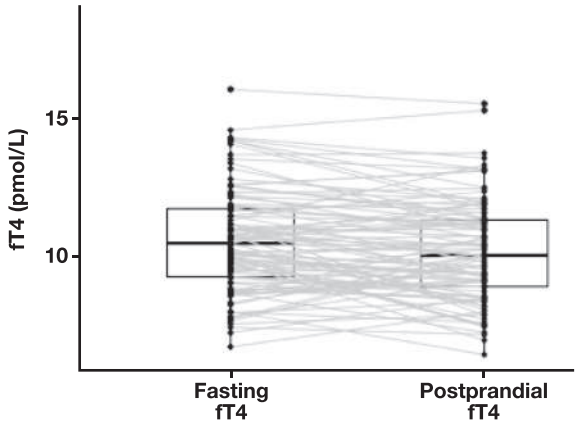

we collected postprandial thyroid function test (TFT) samples before 10 AM in our study.

TSH secretion is regulated primarily by thyroid-releasing hormone and somatostatin. It is considered that the somatostatin inhibits TSH secretion and thyroid-releasing hormone stimulates TSH secretion. A possible explanation of postprandial decline of TSH is the food-induced increase of somatostatin and cytokines.[20,21] The subclinical hypothyroidism in pregnancy is diagnosed based on elevated TSH with normal free T4. We have used trimester-specific reference ranges from the Endocrine Society and American Thyroid Association to diagnose SCH (first trimester >2.5 mIU/L, second and third trimester >3.0 mIU/L). Postprandial decline led to reclassification of 6 out of 100 subjects (6%) as euthyroid whose SCH may actually have been based on fasting TSH. The prevalence of hypothyroidism is also underestimated by using a postprandial TSH value (**FIGURES 5** and **6**). The overall result will be a high false-negative rate in screening SCH in pregnancy (**FIGURE 7**).

In routine clinical practice there are no clear guidelines that emphasize the time and fasting status for TFTs. Accurate estimation of TSH is critical to diagnosing borderline hypothyroidism, such as SCH, and monitoring thyroxine replacement. SCH is primarily diagnosed by TSH. Although it is a milder form of overt hypothyroidism, it can be associated with long-term complications and is considered an indirect risk factor for cardiovascular morbidity and mortality. SCH should be diagnosed promptly, especially in the pregnant population, as it is associated with maternal complications, such as pregnancy-induced hypertension, placental abruption, and postpartum hemorrhage, and fetal complications, such as miscarriage, intrauterine growth restriction, premature deliveries, stillbirth, and low intelligence quotient.[17] Therefore, it is crucial to standardize guidelines related to the timing of sampling for TFTs, especially during pregnancy, to minimize adverse outcomes.

In our study, the main limitation was the small number of participants. However, it is worth noting that this is the only study conducted in Sri Lanka that demonstrates the variation of TFT results postprandially in pregnant women. Based on our findings, we recommend that a future study with a larger sample of pregnant women should be conducted to formulate guidelines related to the timing of TFT sampling.

FIGURE 4. Comparison of fasting free T4 (fT4) and postprandial fT4 in each trimester (A, trimester 1; B, trimester 2; C, trimester 3). The distribution of fasting and postprandial fT4 values are shown with box plots with individual data points overlaid. Corresponding observation pairs are connected by gray lines. The *P* values for the paired *t*-test were *P* = .014 (A), *P* = .7 (B), and *P* = .0074 (C).

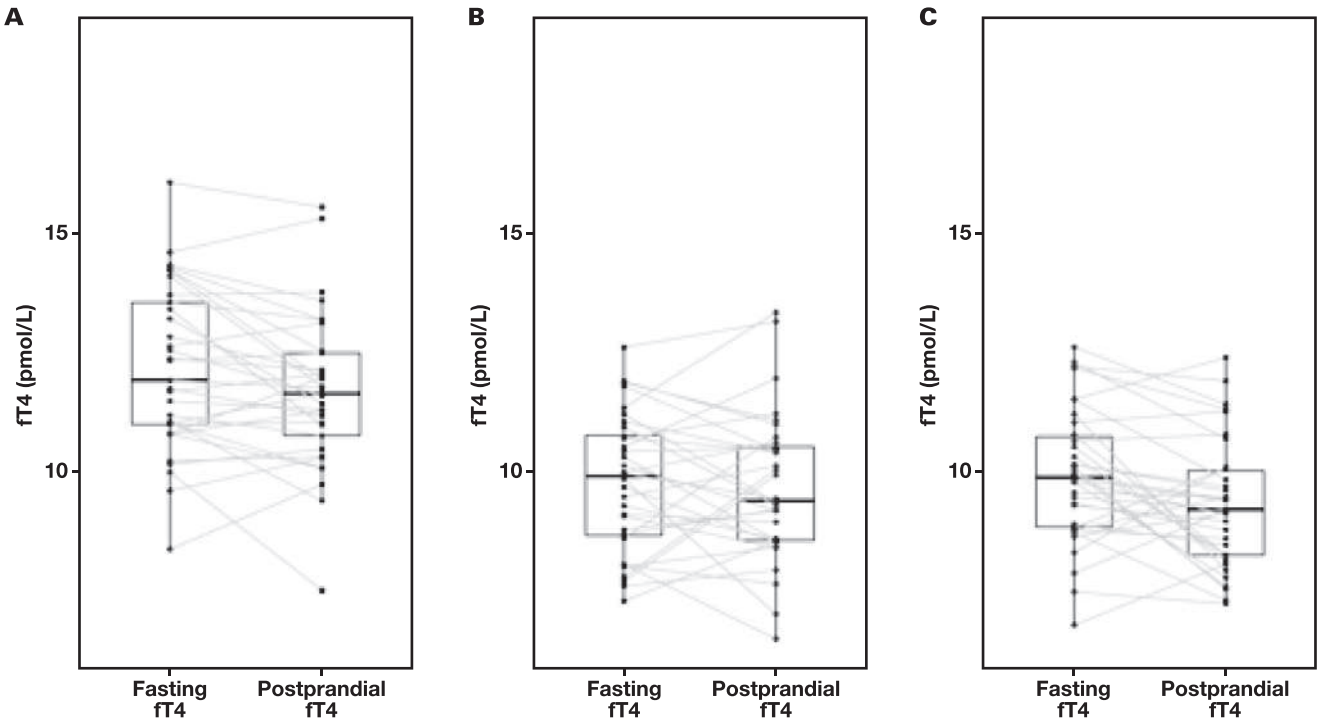

FIGURE 5. Posterior distribution of subclinical hypothyroidism prevalence based on fasting thyrotropin values (n = 10,000; bandwidth = 0.002077).

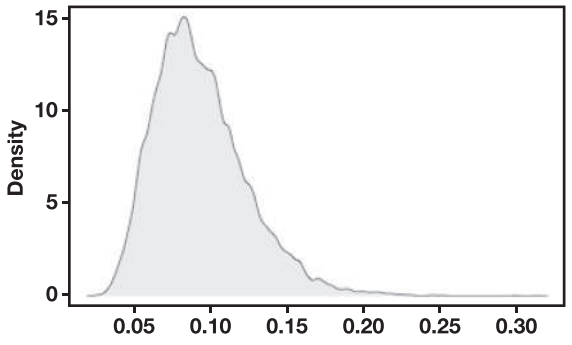

FIGURE 6. Posterior distribution of subclinical hypothyroidism prevalence based on postprandial thyrotropin values (n = 10,000; bandwidth = 0.00126).

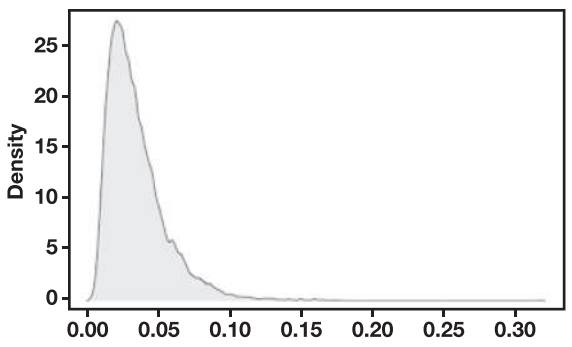

FIGURE 7. Posterior distribution of false-negative rate for subclinical hypothyroidism, when postprandial thyrotropin (TSH) values were used instead of fasting TSH values (n = 10,000; bandwidth = 0.004243).

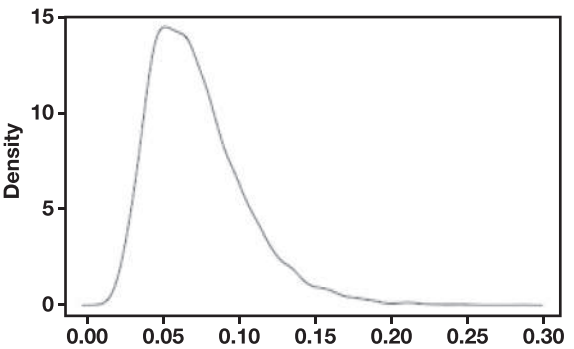

Conclusion

Compared with the fasting state, postprandial TSH levels demonstrate a statistically significant reduction, which can greatly influence the diagnosis of subclinical hypothyroidism in pregnant women. Based on our findings, we conclude that the timing of sampling for TFT should be standardized, particularly in the pregnant population.

Acknowledgments

The authors thank the participants for providing consent for publication.

Funding

This study was supported by the Research Committee, Medical Research Institute, Colombo, Sri Lanka.

Conflict of Interest Disclosure

The authors have nothing to disclose.

REFERENCES

1. Taylor P, Albrecht D, Scholz A, et al. Global epidemiology of hyperthyroidism and hypothyroidism. *Nat Rev Endocrinol.* 2018;14(5):301-316. https://doi.org/10.1038/nrendo.2018.18
2. Biondi B, Cappola AR, Cooper DS. Subclinical hypothyroidism: a review. *JAMA.* 2019;322(2):153-160. https://doi.org/10.1001/jama.2019.9052
3. Tunbridge WM, Evered DC, Hall R, et al. The spectrum of thyroid disease in a community: the Whickham survey. *Clin Endocrinol.* 1977;7(6):481-493. https://doi.org/10.1111/j.1365-2265.1977.tb01340.x
4. Deshauer S, Wyne A. Subclinical hypothyroidism in pregnancy. *Can Med Assoc J.* 2017;189(28):E941. https://doi.org/10.1503/cmaj.161388
5. Alexander EK, Pearce EN, Brent GA, et al. 2017 Guidelines of the American Thyroid Association for the diagnosis and management of thyroid disease during pregnancy and the postpartum. *Thyroid*. 2017;27(3):315-389. https://doi.org/10.1089/thy.2016.0457
6. Kahaly GJ, Bartalena L, Hegedüs L, Leenhardt L, Poppe K, Pearce SH. 2018 European Thyroid Association guideline for the management of Graves' hyperthyroidism. *Eur Thyroid J.* 2018;7(4):167-186. https://doi.org/10.1159/000490384
7. Gabry J, Simpson D, Vehtari A, Betancourt M, Gelman A. Visualization in Bayesian workflow. *J R Stat Soc Ser A Stat Soc*. 2019;182(2):389-402. https://doi.org/10.1111/rssa.12378
8. Dong A, Huang Y, Huang Y, Jia B. Effects of calorie intake and sampling time on thyroid stimulating hormone concentration. *BMC Endocr Disord*. 2022;22(1):85. https://doi.org/10.1186/s12902-022-01005-7
9. Almuhaidib SA. Effect of fasting and postprandial blood samples in results of thyroid function tests among euthyroid people and patients with thyroid problems: a systematic review and meta-analysis. *Am J Clin Pathol.* 2021;156(supplement_1):S53-S53. https://doi.org/10.1093/ajcp/aqab191.108
10. Bajaña W, Aranda E, Arredondo ME, et al. Impact of an Andean breakfast on biochemistry and immunochemistry laboratory tests: an evaluation on behalf of COLABIOCLI WG-PRE-LATAM. *Biochem Med*. 2019;29(2):020702. https://doi.org/10.11613/BM.2019.020702
11. Scobbo RR, VonDohlen TW, Hassan M, Islam S. Serum TSH variability in normal individuals: the influence of time of sample collection. *W V Med J.* 2004;100(4):138-142.
12. Kamat V, Hecht WL, Rubin RT. Influence of meal composition on the postprandial response of the pituitary–thyroid axis. *Eur J Endocrinol.* 1995;133(1):75-79. https://doi.org/10.1530/eje.0.1330075
13. Nair R, Mahadevan S, Muralidharan RS, Madhavan S. Does fasting or postprandial state affect thyroid function testing? *Indian J Endocrinol Metab*. 2014;18(5):705-707. https://doi.org/10.4103/2230-8210.139237
14. Mahadevan S, Sadacharan D, Kannan S, Suryanarayanan A. Does time of sampling or food intake alter thyroid function test? *Indian J Endocrinol Metab*. 2017;21(3):369-372. https://doi.org/10.4103/ijem.IJEM_15_17
15. Mirjanic-Azaric B, Stojakovic-Jelisavac T, Vukovic B, Stojanovic D, Vujnic M, Uletilovic S. The impact of time of sample collection on the measurement of thyroid stimulating hormone values in the serum. *Clin Biochem.* 2015;48(18):1347-1349. https://doi.org/10.1016/j.clinbiochem.2015.08.020
16. Futela D, Maheswari K, Khanna T. Fasting versus postprandial state: impact on thyroid function testing. *Thyroid Res Pract*. 2021;18(2):61-66. https://doi.org/10.4103/trp.trp_11_21
17. Pradeep TVS, Varma SH, Tirupati S, Sarathi V, Kumar KD. Postprandial decline in thyroid-stimulating hormone is significant but not its correlation with postprandial change in plasma glucose. *Thyroid Res Pract*. 2018;15(3):113.
18. Haddow JE, Metzger BE, Lambert-Messerlian G, et al, others. Maternal BMI, peripheral deiodinase activity, and plasma glucose: relationships between White women in the HAPO study. *J Clin Endocrinol Metab.* 2019;104(7):2593-2600. https://doi.org/10.1210/jc.2018-02328
19. Wang D, Yin Y, Yu S, Li H, Cheng X, Qiu L. Effect of sampling time on estimates of thyroid-stimulating hormone, free thyroxine, and free triiodothyronine levels. *Scand J Clin Lab Invest.* 2019;79(7):459-462. https://doi.org/10.1080/00365513.2019.1626904
20. Arosio M, Porretti S, Epaminonda P, et al. Elevated circulating somatostatin levels in acromegaly. *J Endocrinol Invest.* 2003;26(6):499-502. https://doi.org/10.1007/BF03345210
21. Hildebrand P, Ensinck JW, Buettiker J, et al. Circulating somatostatin-28 is not a physiologic regulator of gastric acid production in man. *Eur J Clin Invest.* 1994;24(1):50-56. https://doi.org/10.1111/j.1365-2362.1994.tb02059.x

Proteomic biomarker evaluation using antibody microarrays: association between analytical methods such as microarray and ELISA

Nadezhda G. Gumanova, PhD, Natalya L. Bogdanova, MS, Victoria A. Metelskaya, PhD

National Research Center for Preventive Medicine (NRCPM), Moscow, Russia.
Corresponding author: Nadezhda G. Gumanova, PhD, gumanova@mail.ru.

Key words: antibody microarray, proteomic biomarkers, proteome, microarray confirmation, analytical biochemistry, analytical methods

Abbreviations: AF, atrial fibrillation; OD, optical density; nNOS, neuronal nitric oxide synthase; qRT-PCR, quantitative real-time polymerase chain reaction; MS, mass spectrometry; MRM, multiple reaction monitoring

Laboratory Medicine 2024;55:325-333; https://doi.org/10.1093/labmed/lmad083

ABSTRACT

Objective: To evaluate the associations between analytical methods, such as microarray and enzyme-linked immunosorbent assay (ELISA); expedient cutoffs; and the lowest possible number of microarrays in analysis for target biomarker estimation in case-control studies.

Methods: This study included 321 serum specimens, gathered in different case-control studies to test for atherosclerosis and atrial fibrillation. Among them, 48 serum specimens were analyzed using microarray technology. We used ELISA and commercial kits for confirmation of the results.

Results: Three proteins—cadherin-P, neuronal nitric oxide synthase, and adenovirus fiber—were shown to have distinctly different values in the case group vs the control group. As a result, we used those proteins as the target for confirmation using our alternative analytical method. Also, these protein values represented the limiting range between the highest and lowest differences in case-control groups. The results of microarray assay were confirmed using ELISA and commercial kits in the same specimens, in which microarray profiling was performed, and also in separate large case-control groups.

Conclusions: A 1.5-fold difference in the protein content, as measured using microarray technology, was shown to be sufficient for further investigation of the candidate proteins. As few as 3 microarrays were considered sufficient for perspective evaluation of the target proteins. Microarray serum profiling, therefore, provides semiquantitative determination of protein in serum.

The human serum proteome is composed of thousands of various proteins. Antibody-based microarrays are rapid miniaturized assay systems for the detection of low protein concentrations in complex biological systems. Protein microarrays have several distinct advantages compared with traditional immunological methods, such as minimal consumption of reagents, screening of multiple parameters of proteins, and rapid readout of responses. Thus, microarray methods of analysis have evolved into an essential tool for biomedical research because antibody microarrays can identify novel target biomarkers of various diseases and multiple altered signaling pathways, as revealed in the results of case-control studies.[1,2]

We believe that it is necessary to confirm, via alternative methods, the biomarkers identified as being associated with disease in full-sized case-control and cohort studies. Taking into account the high cost of analysis using microarray technology, our study aim was to evaluate, in several case-control studies, the most pressing current issues, as follows. First, how many microarrays are sufficient for identification of the target proteins in case-control focus groups, for further confirmation using an alternative method? Second, what is the cutoff point below which one should not select target markers?

Methods

We analyzed a total of 321 serum specimens from subject individuals who had been recruited for various previous cohort studies. The specimens included those from 111 patients who had undergone coronary angiography in 2011-2012[3] and in 2018,[4] 98 patients with atrial fibrillation (AF),[5] and 112 healthy volunteers.[6] All specimens were stored at −27°C for as long as 12 years.

In total, 48 specimens were used for serum profiling using antibody microarrays (ASB600, Full Moon Biosystems). Among those were 18 specimens from patients who had undergone coronary angiography (with severe coronary lesions [n = 9] and without coronary lesions [n = 9]), as selected from the cohort from 2011-2012[3]; 7 specimens from patients

with diagnosed AF[5]; and 30 specimens from healthy volunteers.[6] Microarray profiles of 30 specimens from healthy volunteers were combined with the specimens from the control groups, to evaluate the associations between content of the target proteins evaluated using microarray analysis and enzyme-linked immunosorbent assay (ELISA) as alternative analytical methods. We compared protein profiles between the groups with coronary lesions (n = 9) and without coronary lesions (n = 9), and between the groups with AF (n = 7) and the apparently healthy controls (n = 3).

We identified target proteins by comparison of the corresponding signals and confirmed them via ELISA in a separate group of patients, which was sufficiently large to enable the evaluation of statistical significance at a suitable level of power. Separate groups of patients with specific diseases and the corresponding controls were selected from the corresponding cohorts[4–6] and were comprised of the specimens that had not been used for microarray profiling. The protocol of the study was approved by the Independent Ethics Committee of the National Research Center for Preventive Medicine, according to the guidelines of the Declaration of Helsinki and the World Health Organization (approval No. 07-05/12).

Blood Specimen Drawing

Blood was withdrawn from the cubital vein, and the serum was obtained by centrifugation at 1000*g* for 15 minutes at 4°C. The specimens were aliquoted and stored at −27°C. Before proteomic analysis, the serum was thawed and centrifuged at 10,000*g* for 15 minutes at 4°C. Protein concentrations were determined based on optical density (OD) at 260-280 nm using a NanoDrop One spectrophotometer (Thermo Fisher Scientific) using human serum albumin as the reference.

Labeling of Proteins and Microarray Assay Protocol

Serum was diluted in PBS (Sigma Aldrich) to a concentration of 1 mg protein/mL and mixed with 20 μL of protein-labeling buffer. The proteins were labeled using 1 μL of Green 540 reagent (Arrayit Corporation) for 60 minutes on ice to couple the Green 540 dye to the proteins. Stop solution (10 μL; Arrayit Corporation) was used to terminate the coupling reaction. After incubation on ice for 30 minutes, inactivated unbound dye was removed by gel filtration trough spin columns that were centrifuged at 750*g* for 2 minutes. Explorer antibody microarrays (ASB600; Full Moon Biosystems) contained 656 antibodies per slide in 2 replicates for each antibody. Labeled proteins (500 ng per slide) were loaded on the array slides and incubated in the presence of blocking buffer containing 3% dry milk (Full Moon Biosystems) for 1 hour, according to manufacturer instructions. After washing, the slides were incubated with coupling buffer containing 3% dry milk (Full Moon Biosystems) for 2 hours. The microarray slides were washed and dried by centrifugation.[7]

Slide Scanning and Image Processing

The slides were scanned using a laser scanner (InnoScan microarray scanner 900, Innopsys) using the following settings: scan mode: normal, velocity: 20 l/s, laser power: 5.0, photomultiplier gain: 100, pixel size: 10, and wavelength: 532 nm.[7] Gal files and grid settings were matched using the corresponding positive controls. We analyzed the images using Mapix software, version 7.0.0 (Innopsys). Identification of labeled proteins was based on specific gal files provided by Full Moon Biosystems. Also, we used protein identifiers from the UniProtKB/Swiss-Prot database.

Confirmation of the Microarray Data on Cadherin-P by ELISA

We measured the protein concentration in the serum specimens using NanoDrop One (Thermo Fisher Scientific) and used bovine serum albumin (BSA) as the reference. The wells of a microtiter plate were coated with serum proteins (100 μL per well, at a protein concentration of 20 μg/mL) in 14 mmol/L carbonate buffer (pH 9.6). The coating was performed overnight at 4°C, and the plate was washed 3 times with washing buffer (PBS containing 0.05% v/v Tween 20). Then, the wells were blocked by adding 150 μL of blocking solution (PBS containing 1% BSA) for 60 minutes at 37°C, and the plates were washed 4 times with washing buffer. Rabbit polyclonal anti-cadherin-P antibodies (100 μL/well, diluted to a concentration of 0.5 μg/mL; Invitrogen, Thermo Fisher Scientific) were added to the test wells, and the mixture was incubated for 1 hour at 37°C. Then, the wells were washed 3 times with washing buffer. Peroxidase-conjugated secondary anti-rabbit antibodies (Invitrogen, Thermo Fisher Scientific) were added to the wells (100 μL/well at a dilution of 1:300,000). The plate was incubated for 1 hour at 37°C and washed 3 times with washing buffer. We used 3,3′,5,5′-tetramethylbenzidine solution as a substrate (100 μL/well; Bio-Rad Laboratories).

The color was developed at room temperature in the dark for approximately 30 minutes, depending on the actual OD. Stop solution (50 μL/well; Bio-Rad Laboratories) was added, and absorbance was measured at 450 nm using a Tecan Infinite 200 PRO plate reader (Tecan Trading). The data were recalculated as the percentage of the corresponding control specimens assayed on each microplate using Magellan software.[8]

Confirmation of the Microarray Data on nNOS by ELISA

The plate was coated and blocked, as described earlier herein, at the protein concentration of 10 μg/mL. Mouse polyclonal anti–neuronal nitric oxide synthase (nNOS) antibodies (100 μL/well at a concentration of 0.5 μg/mL; Invitrogen, Thermo Fisher Scientific) were added to the test wells and incubated for 1 hour at 37°C. Then, the wells were washed and incubated with peroxidase-conjugated secondary anti-mouse antibodies (Invitrogen, Thermo Fisher Scientific) (100 μL/well, at a dilution of 1:10,000). The plate was incubated for 1 hour at 37°C and washed 3 times with washing buffer. Subsequent washing and color development were performed, as described earlier herein.

ELISA of IgG-Adenovirus

Serum adenovirus-IgG concentrations were measured using the Fine Test (Wuhan Fine Biotech), a qualitative ELISA kit for human adenovirus and IgG. The assay was based on indirect ELISA using adenovirus antigen–precoated 96-well plates. The specimens were diluted 10-fold in the specimen dilution buffer, added to the wells, and incubated according to manufacturer instructions. The unbound material was washed, and HRP-conjugate was added in combination with serum specimens to form the adenovirus-Ag-adenovirus-IgG-HRP-conjugate complex. TMB substrate was used to detect the formation of the conjugate, as described earlier herein. The positive reactivity cutoff value was calculated as the mean absorbance of OD of the negative control specimens plus 0.1. If the negative mean value was less than 0.05, it was assumed to be 0.05. The specimens with OD less than the cutoff value were considered to have tested negative for IgG-adenovirus. The specimens with OD results higher

than or equal to the cutoff value were considered to have tested positive for IgG-adenovirus.

Statistical Analysis

Statistica software, version 7.0, and SPSS software, version 23 (IBM), were used for evaluation. Normality of the distributions was tested using the Kolmogorov-Smirnov criterion. The data are shown as mean (SD) for normally distributed values and as the median and 25th and 75th percentiles for non–normally distributed data. The groups were compared using 2-tailed nonparametric analysis of variance (Kruskal-Wallis and Mann-Whitney tests).

The spots on the images were quantified as median pixel values minus background and normalized (%) to the positive controls for each slide. Spots with high variability in the parallel specimens, with a coefficient of variance (CV) higher than 25%, were not used in subsequent analysis. The groups were compared based on the mean values of normalized spots for each protein that had CV less than 25% for parallel specimens. Normalized spots with an area having CV that was different from the background area by less than 10% were considered similar to the background. *P* values less than .05 were considered statistically significant.

Results

All of the 48 proteome-profiled specimens were used to evaluate the associations between the analytical methods such as microarray and ELISA. Specific proteins were identified in the serum using Explorer antibody microarrays in specimens from the patients with severe coronary stenosis (n = 9), by comparison with those values in the patients with no coronary lesions (n = 9), the patients with AF (n = 7), and the healthy subjects (n = 3) (**TABLE 1**). Detailed description for atherosclerosis array profiling is presented elsewhere in the literature.[8]

The data were presented in pixels and also recalculated as the percentage of the reference control spots on each microarray slide (**TABLE 1**). The mean levels of these 2 serum proteins—cadherin-P (CADH3; UniProtKB P22223) and neuronal nitric oxide synthase (nNOS or NOS1; UniProtKB P29475) —were increased from 4- to 23-fold in the group with coronary lesions (n = 9), compared with those in the group with no coronary lesions (n = 9) (**TABLE 1**, **FIGURES 1** and **2**) selected from the cohort conducted in 2011-2012.[3] Microarrays of the other specimens (n = 48) were also used for calculation of selected proteins. We confirmed the microarray results in the same serum specimens using direct ELISA for serum CADH3 and nNOS.

Cadherin-P Confirmation

We measured cadherin-P levels in 48 serum specimens using indirect ELISA. The ELISA results indicated that the content of cadherin-P was increased in the group with coronary lesions (OD at 450 nm; mean [SD], 0.55 [0.07] vs 0.51 [0.07]; *P* = .01) or in normalized units (% of blank specimens), 110.6 [15.4] vs 100.0 [13.8]; *P* = .01); all specimens were run in triplicate. Also, the group with coronary lesions demonstrated an increase in the level of cadherin-P, as measured using microarrays (**TABLE 2**, **FIGURE 1**). These data were similar to our results published in a previous study report.[8]

We obtained additional confirmation of the differences in the levels of serum cadherin-P using direct ELISA in large separate group of 61 serum specimens selected from the cohort of a study conducted in 2018[4] (as described in the Methods section of this article). In that study cohort, 31 patients had severe coronary lesions and 30 patients had no coronary lesions, according to the results of coronary angiography diagnostic testing. The cadherin-P level was increased in the serum of patients with coronary lesions, compared with those levels in patients with no coronary lesions. Also, the mean (SD) relative cadherin-P levels (% of blank specimens) were 100.0 (40.4) vs 82.8 (43.9), respectively, *P* = .007; and the OD at 450 nm (mean [SD], 0.8 (0.3) and 0.6 [0.3], *P* = .007), as determined via ELISA (**TABLE 2**).

nNOS Confirmation

The mean nNOS level in serum was increased 4.5-fold in the group with coronary lesions, compared with that value in the group with no coronary lesions, according to the data generated by the microarray assays (**TABLE 1**, **FIGURE 2**). The levels of nNOS were expressed in pixels normalized to the levels of the reference spots on each microarray and in raw pixels minus background (**TABLE 1**).

In total, the levels of nNOS were measured in 48 serum specimens using microarray and direct ELISA. The values were compared with the values measured via ELISA, expressed in OD at 450 nm, and normalized to the blank-specimen values. The levels of nNOS in normalized pixels (%) were correlated with the levels of nNOS in OD at 450 nm (%), with the Spearman rank order correlation coefficient of $r = 0.53$ ($P < .05$). These data are illustrated in **FIGURE 3** and **FIGURE 4**.

The ELISA results indicated that the nNOS value in serum was increased in the group with coronary lesions (OD at 450 nm (mean [SD], 0.46 [0.02] vs 0.43 [0.04]; *P* < .001); the mean (SD) % of OD at 450 of control specimens was 108.2 (5.8) vs 100.0 (9.3), with *P* < .001 (**TABLE 2**). Also, the group with coronary lesions demonstrated increased levels of

TABLE 1. Serum Protein Levels, Determined via Microarray Analysis, in the Case and Control Groups[a]

		Case Group		Control Group		
		Coronary Lesions (n = 9)		No Coronary Lesions (n = 9)		
ID-ASB600	Name of Protein	Normalized Pixels (% of Positive Control)	Pixel Intensity With the Background Subtracted	Normalized Pixels (% of Positive Control)	Pixel Intensity With the Background Subtracted	Case:Control Ratio
567	Cadherin-P	82.1 (83.1)	6011.6 (6720.0)	3.55 (2.4)	280.5 (169.8)	23:23.4
555	nNOS	12.5 (10.2)	831.1 (785.1)	2.30 (2.1)	267.4 (164.1)	3:5.4
		Atrial Fibrillation (n = 7)		Healthy Subjects (n = 3)		
352	Adenovirus fiber	8.8 (2.9)	183 (43)	5.93 (4.3)	155 (71)	1.1:1.5

nNOS, neuronal nitric oxide synthase.
[a]Cadherin-P or CADH3 (UniProtKB—P22223); nitric oxide synthase, brain (NOS1, UniProtKB—P29475); adenovirus fiber (no UniProt number according to ASB600 microarray list). Data are given as mean (SD) serum protein content.

FIGURE 1. **Two microarrays from a representative slide of Explorer antibody microarray (ASB600; Full Moon Biosystems) results, with 656 antibodies per slide in 2 replicates for each antibody. The load of labeled serum protein was 500 ng per slide, scan settings: normal, velocity: 20 l/s, laser power: 5.0, detector gain: 100, pixel size: 10, and wavelength: 532 nm. Enlarged panels of individual specimens illustrate the differences in serum levels of cadherin-P from the case group (A) vs the control group (B).**

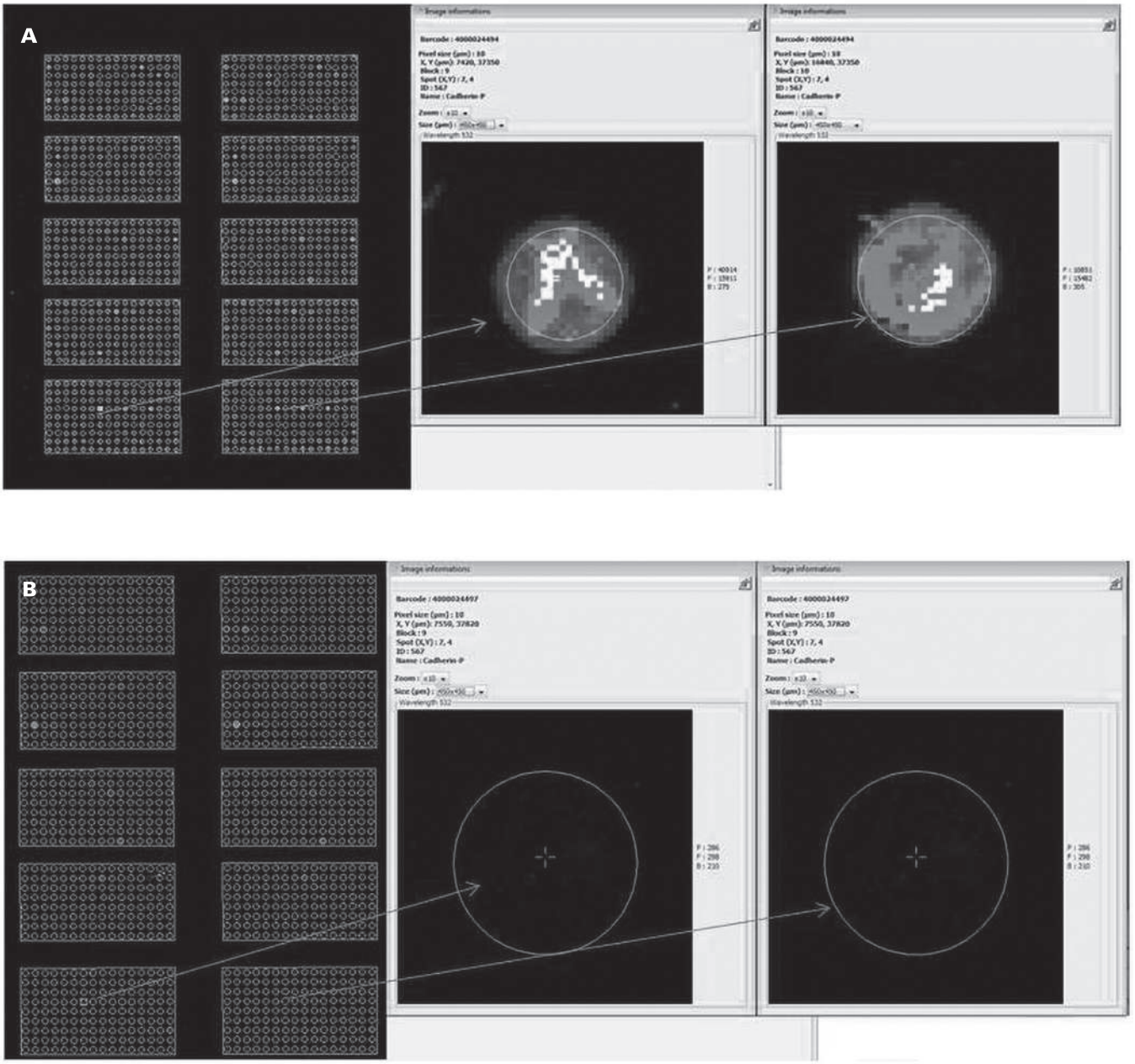

nNOS, per the microarray assay results (**TABLE 2**). Then, 48 specimens assayed using microarray testing were split into 3 groups with different levels of nNOS: group 1, with nNOS ranging from 17.9 to 29.7 pixels (%); group 2, with nNOS ranging from 2.0 to 6.6 pixels (%); and group 3, with nNOS ranging from 0 to 1.4 pixels (%). The levels of nNOS expressed in OD at 450 nm (%) were significantly different in all 3 groups (**FIGURE 4**). This result corresponded with a relatively high correlation ($r = 0.53$; $P < .05$) between the levels of nNOS measured in pixels (%) by microarray and as OD at 450 nm (%), as determined via ELISA.

We obtained additional confirmation of the differences in the levels of serum nNOS using indirect ELISA in a large separate group of 93 serum specimens from patients with coronary stenosis (n = 45) and no coronary lesions (n = 48) selected from the cohort of a study conducted in 2018, according to coronary angiography diagnostic results.[4] The nNOS level was increased in the serum of patients with coronary lesions, compared with that in patients with no coronary lesions, and the relative nNOS levels (mean [SD] % of control specimens) were 114.3 (4.5) vs 107.6 (5.3), respectively ($P < .001$), as determined by ELISA (**TABLE 2**).

FIGURE 2. Two microarrays from a representative slide of Explorer antibody microarray (ABS600; Full Moon Biosystems) results, illustrating the differences in serum neuronal nitric oxide synthase (nNOS) levels in the case group (A) vs the control group (B). For details, see the legend to FIGURE 1.

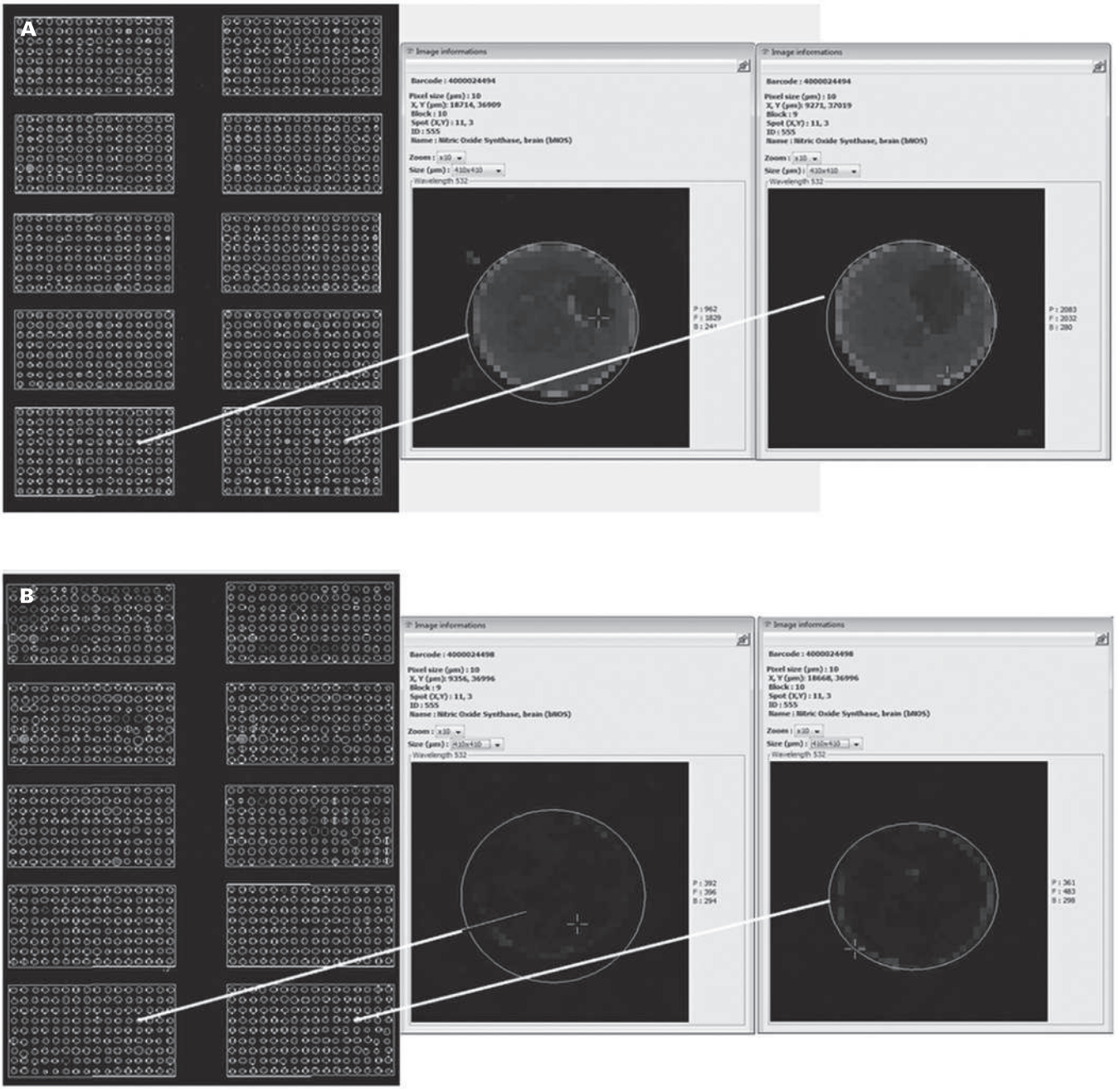

All assays were performed 3 to 10 times; all ELISA assays were repeated 3 times.

Adenovirus Confirmation

Serum proteome profiling was performed in a group of specimens from the patients with AF (n = 7) and from healthy subjects (n = 3) using Explorer antibody microarrays. The levels of adenovirus fiber were moderately different (1.1- to 1.5-fold) between the group with AF and healthy subjects (**TABLE 1**, **FIGURE 5**). (There is no UniProt number for Explorer antibody microarrays of adenovirus fiber; the target of this particular antibody does not have an assigned UniProt number according to the list provided by the manufacturer of the microarray. Presumably, the antibody could have been generated against the whole viral protein fraction.) The mean (SD) pixel intensity with the background subtracted was 183 (43) vs 155 (71), respectively (P = .07) (**TABLE 1**).

Adenovirus fiber testing results clearly indicated the presence or absence of adenovirus infection, so IgG against adenovirus was chosen

TABLE 2. Results of ELISA for Confirmation of Microarray Analysis in the Case and Control Groups and in the Large Separate Group, With and Without Coronary Lesions

Variable	With Coronary Lesions		Without Coronary Lesions		
Name of Protein	No.	Normalized OD 450 (% of Blank Specimens), Mean (SD)	No.	Normalized OD 450 (% of Blank Specimens), Mean (SD)	*P* Value
Cadherin-P in case and control groups	9	110.6 (15.4)	39	100.0 (13.8)	.01
Cadherin-P (in the large separate group)	31	100.0 (40.4)	30	82.8 (43.9)	.007
nNOS in case and control groups	9	108.2 (5.8)	39	100.0 (9.3)	<.001
nNOS (in the large separate group)	45	114.3 (4.5)	48	107.6 (5.3)	<.001

ELISA, enzyme-linked immunosorbent assay; OD, optical density; nNOS, neuronal nitric oxide synthase.

FIGURE 3. Serum neuronal nitric oxide synthase (nNOS) levels measured via direct enzyme-linked immunosorbent assay (ELISA) and microarray technology. The nNOS levels were expressed in pixels normalized to the reference spots on each slide (microarray) and were compared with the nNOS levels estimated based on optical density (OD) at 450 nm normalized to the blank specimens (ELISA). The levels of nNOS in pixels (%) correlated with the levels of nNOS determined as OD at 450 nm (%), with the Spearman rank order correlation coefficient $r = 0.53$ ($P < .05$).

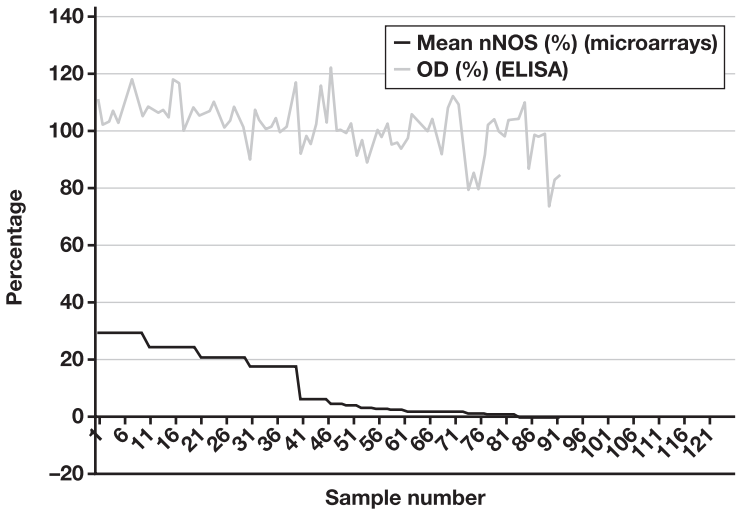

FIGURE 4. Levels of serum neuronal nitric oxide synthase (nNOS) measured via microarray technology. Group 1 had nNOS content ranging from 17.9 to 29.7 pixels (%); group 2, nNOS content ranging from 2.0 to 6.6 pixels (%); and group 3, nNOS content ranging from 0 to 1.4 pixels (%). The levels of nNOS expressed as optical density (OD) at 450 nm (%) were measured by enzyme-linked immunosorbent assay and were significantly different in all 3 groups ($P < .05$).

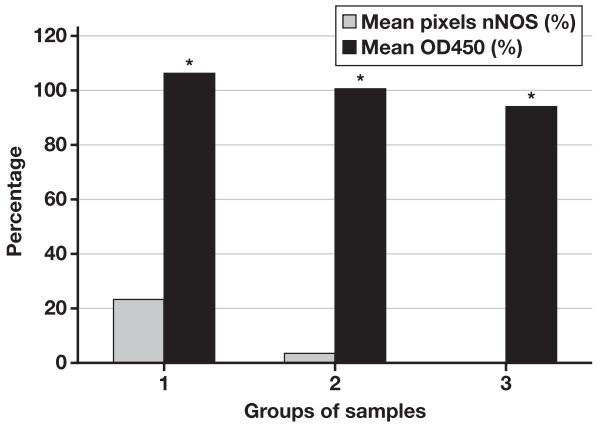

as the hypothesis confirmation using ELISA kits. IgG-adenovirus levels were determined in a large separate group (n = 180) selected from a cohort with AF,[5] in which 91 serum specimens were collected from patients with AF and 89 from healthy subjects. ELISA kits were handled according to manufacturer instructions. The prevalence of patients testing IgG-adenovirus positive was increased by 2-fold in group A (AF; n = 91) compared with group B (asymptomatic subjects; n = 89) (odds ratio, 2.06 [95% CI, 1.11-3.84]; $P = .02$) (**TABLE 3**).

Thus, proteomic biomarkers can be evaluated using antibody microarrays and confirmed using ELISA. The 1.5-fold differences in protein contents measured using the microarray assays could be sufficient to consider target proteins for further confirmation. Analysis of 3 microarrays could be sufficient for prospective evaluation of the target proteins.

Discussion

Confirmation of the data acquired by microarrays may improve the reliability of this technology. In most instances, validation has been presented in the case of gene expression analysis using microarrays. Thus, quantitative real-time polymerase chain reaction (qRT-PCR) is a commonly used validation tool for confirmation of gene-expression results of microarrays. We observed significant correlation between

FIGURE 5. **Two microarrays from a representative slide of Explorer antibody microarray (ABS600; Full Moon Biosystems) results, illustrating the differences in serum adenovirus fiber protein levels in the case group (A) vs the control group (B). For details, see the legend to FIGURE 1.**

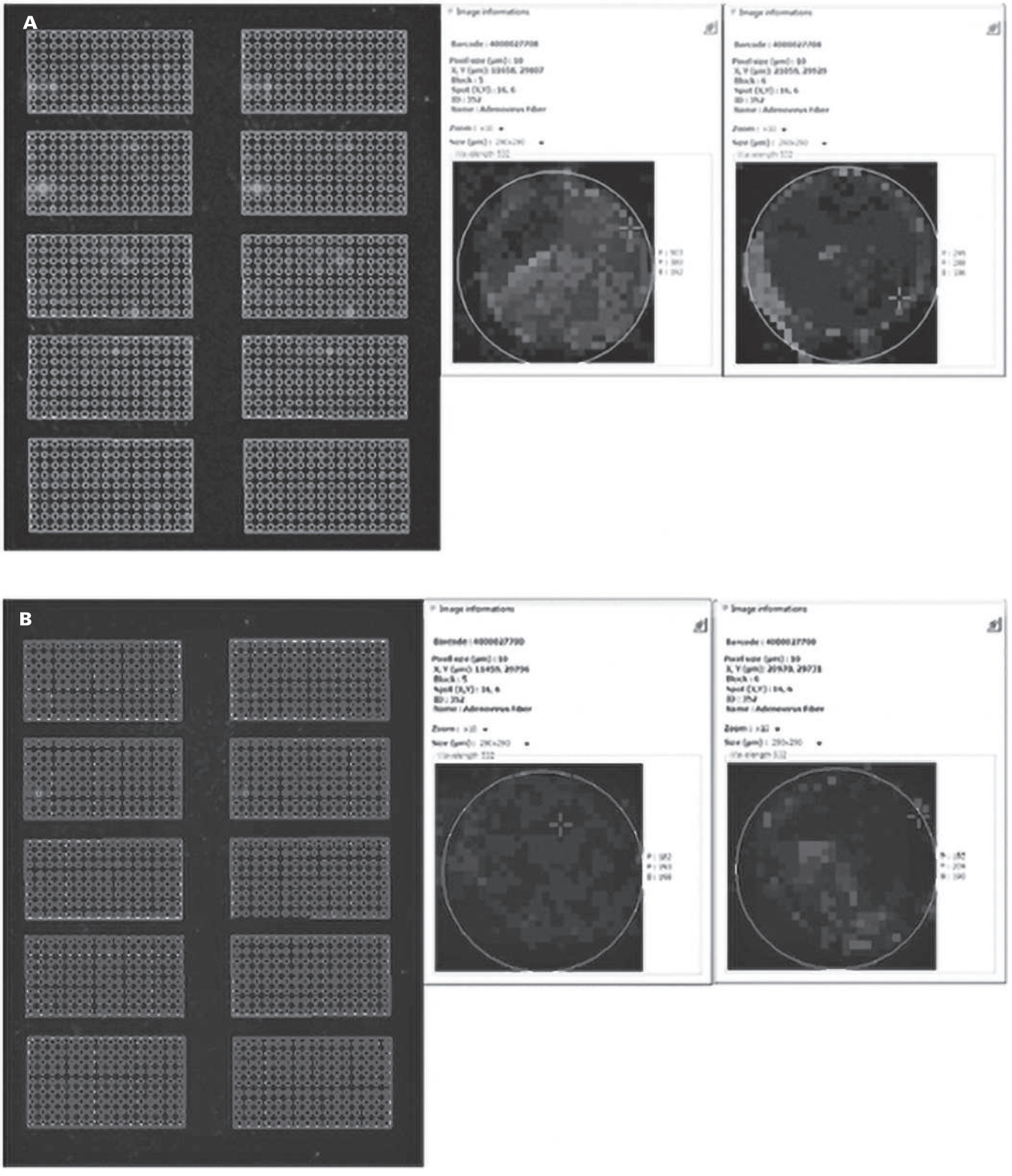

the results of microarrays and qRT-PCR ($r = 0.708$; $P < .001$) in a study report that assessed various factors contributing to correlations between these 2 methods.[9] In contrast to DNA microarray, standardized procedures for validation of the performance of antibody microarrays are not available, to our knowledge, including quantification and normalization of data and bioinformatics assessment.[10] Validation of the results obtained using protein and antibody microarrays has not been extensively reported previously.

TABLE 3. IgG-Adenovirus Status (Positive or Negative) in the Large Separate Group with Atrial Fibrillation and in Healthy Subjects

Group	Positive No. (%)	Negative No. (%)	Odds Ratio (95% CI); *P* Value
Atrial fibrillation (n = 91)	66 (72.5)	25 (27.5)	2.06 (1.11-3.84); .02
Healthy subjects (n = 89)	50 (56.2)	39 (43.8)	

In this study, we confirmed the results of antibody microarrays, which we believe are the most promising tools for serum protein profiling and evaluation of candidate proteins associated with various diseases. The 3 proteins we investigated in this study—cadherin-P, nNOS, and adenovirus—are ones we selected for validation of the results obtained using microarray technology. Additional data on cadherin-P validation have been recently published by us in another study.[8] Therefore, we dedicated particular attention to validation of the data for nNOS and adenovirus because these proteins defined the middle and lowest limit used for discrimination between the case/control groups of specimens in the present study.

Selected proteins, including cadherin-P and nNOS, represented the highest (23-fold), middle (4.5-fold), and lowest (1.1-1.5) range of levels, respectively, which were used to discriminate the case/control groups of the serum specimens (**TABLE 1**). We also used only 3 microarrays in our analysis and achieved the results after confirmation with an alternative method. So, we can conclude that as few as 3 microarrays for analysis could be sufficient for estimation of candidate-protein levels.

Selection and appropriate evaluation of normalization criteria play a role in the identification of relevant specific proteins via comparative protein profiling. The results obtained by microarray technology were confirmed using ELISA, which is widely considered a reliable standard, as an alternative method. Our findings will help researchers to apply microarray technology for biomarker research and to reduce usage of expensive materials in experimentation.

In summary, miniaturized antibody-based microarrays have already been multiplexed to provide the signals from 1358 proteins in a single run (Full Moon Biosystems), with minimal specimen preparation. The main application of antibody microarray analysis, in its current design, is rapid biomarker-candidate evaluation, which requires further confirmation by alternative methods that may include mass spectrometry (MS)–based approaches.

In our opinion, microarray antibody-based methods are not expected to provide a better result than the data generated by large-scale conventional MS proteomic methods. However, these methods have their own advantages and limitations in terms of accurate quantification of proteins and peptides in serum/plasma specimens. Recent studies of serum/plasma proteomes, such as the one from Anderson et al,[11] extensively use high-resolution gas and LC combined with MS, capillary electrophoresis combined with MS, or direct MS for individual-specimen analysis.

The main issues, with regard to MS in general, are of evaluation of the number of the plasma proteins that can be quantified in plasma digestion and the specific precision of these measurements, both of which are difficult to assess. To address these issues, Anderson et al[11] generated and tested multiple reaction monitoring (MRM) assays based on peptides from a variety of high- and medium-abundance plasma proteins. Their goal was to estimate how many proteins are effectively evaluated by LC-MS/MS with and without subtraction of the signals of the most abundant proteins (albumin, major globulins, and others). The results of their analysis indicate that only 30-40 specific protein signals can be quantified reliably in a single run using the MS-based technique. Moreover, the number of analytes depends on the number of internal standards. Apparently, a more comprehensive discovery-based approach is currently provided by the Seer Proteograph assay, which can profile as many as 2000 or even 4000 proteins in serum/plasma specimens. In either case, quantification of the proteins is limited by the number of internal standards.

In contrast to antibody microarrays, MS is useful for analysis of many small molecules (eg, drug metabolites and pesticides) that are routinely measured, using an approach based on discriminating power of mass analyzers at high throughput and precision. This MS-based approach can provide quantification of analytes according to the corresponding stable isotope-labeled internal standards. These measurements have been multiplexed to provide as many as 30 specific assays in a single run.[12] In the clinical laboratory, MS methods may be used for such purposes as routine measurements in newborns in screening for inborn metabolic defects[13] and to evaluate concentrations of some drugs, including immunosuppressants.[14]

The antibody-based microarray approach using this particular type of microarray has certain limitations. For instance, we have restricted our analysis to only 656 candidate proteins, and we encountered the significant issue of cross-reactivity with antibodies.

Conclusion

Despite the limitations, we have shown that measurements of the protein contents of serum using antibody microarray technology can be correlated with ELISA data obtained using antibodies from an alternative source. The Spearman rank correlation coefficient we observed was relatively high ($r = 0.53$; $P < .05$). Moreover, even a 1.5-fold difference in the protein content demonstrated using microarray technology was sufficient for consideration of the target proteins for further investigation. Analysis of as few as 3 microarrays could be sufficient for perspective evaluation of the target proteins. Finally, microarray serum profiling provides semiquantitative determination of protein in serum.

Conflict of Interest Disclosure

The authors have nothing to disclose.

REFERENCES

1. Wilson JJ, Burgess R, Mao Y-Q, et al. Antibody arrays in biomarker discovery. *Adv Clin Chem.* 2015;69:255-324. https://doi.org/10.1016/bs.acc.2015.01.002
2. Gahoi N, Ray S, Srivastava S. Array-based proteomic approaches to study signal transduction pathways: prospects, merits and challenges. *Proteomics.* 2015;15(2-3):218-231. https://doi.org/10.1002/pmic.201400261
3. Gumanova NG, Gavrilova NE, Chernushevich OI, Kots AY, Metelskaya VA. Ratios of leptin to insulin and adiponectin to endothelin are

sex-dependently associated with extent of coronary atherosclerosis. *Biomarkers*. 2017;22(3-4):239-245. https://doi.org/10.1080/1354750X.2016.1201539

4. Zhatkina MV, Gavrilova N, Makarova YK, Metelskaya V, Rudenko BA, Drapkina OM. Diagnosis of multifocal atherosclerosis using the Celermajer test. *Cardiovasc Ther Prev*. 2020;19(5):2638. https://doi.org/10.15829/1728-8800-2020-2638
5. Davtyan KV, Topchyan AH, Brutyan HA, et al. The predictive role of early recurrences of atrial arrhythmias after pulmonary vein cryoballoon ablation: is blanking period an outdated concept? Insights from 12-month continuous cardiac monitoring. *BMC Cardiovasc Disord.* 2021;21(1):483. https://doi.org/10.1186/s12872-021-02300-2
6. Gorshkov AY, Klimushina MV, Boytsov SA, Kots AY, Gumanova NG. Increase in perfused boundary region of endothelial glycocalyx is associated with higher prevalence of ischemic heart disease and lesions of microcirculation and vascular wall. *Microcirculation.* 2018;25(4):e12454. https://doi.org/10.1111/micc.12454
7. Klimushina MV, Gumanova NG, Metelskaya VA. Direct labeling of serum proteins by fluorescent dye for antibody microarray. *Biochem Biophys Res Commun.* 2017;486(3):824-826. https://doi.org/10.1016/j.bbrc.2017.03.136
8. Gumanova NG, Vasilyev DK, Bogdanova NL, Havrichenko YI, Kots AY, Metelskaya VA. Application of an antibody microarray for serum protein profiling of coronary artery stenosis. *Biochem Biophys Res Commun.* 2022;631:55-63. https://doi.org/10.1016/j.bbrc.2022.09.053
9. Morey JS, Ryan JC, Van Dolah FM. Microarray validation: factors influencing correlation between oligonucleotide microarrays and real-time PCR. *Biol Proced Online.* 2006;8:175-193. https://doi.org/10.1251/bpo126
10. Borrebaeck CA, Wingren C. High-throughput proteomics using antibody microarrays: an update. *Expert Rev Mol Diagn.* 2007;7(5):673-686. https://doi.org/10.1586/14737159.7.5.673
11. Anderson L, Hunter CL. Quantitative mass spectrometric multiple reaction monitoring assays for major plasma proteins. *Mol Cell Proteomics.* 2006;5(4):573-588. https://doi.org/10.1074/mcp.M500331-MCP200
12. Barr DB, Barr JR, Maggio VL, et al. A multi-analyte method for the quantification of contemporary pesticides in human serum and plasma using high-resolution mass spectrometry. *J Chromatogr B Analyt Technol Biomed Life Sci.* 2002;778(1-2):99-111. https://doi.org/10.1016/s0378-4347(01)00444-3
13. Röschinger W, Olgemöller B, Fingerhut R, Liebl B, Roscher AA. Advances in analytical mass spectrometry to improve screening for inherited metabolic diseases. *Eur J Pediatr.* 2003;162(suppl 1):S67-S76. https://doi.org/10.1007/s00431-003-1356-y
14. Streit F, Armstrong VW, Oellerich M. Rapid liquid chromatography-tandem mass spectrometry routine method for simultaneous determination of sirolimus, everolimus, tacrolimus, and cyclosporin A in whole blood. *Clin Chem.* 2002;48(6 pt 1):955-958.

Sixty years of conjecture over a urinary biomarker: a step closer to understanding the proposed link between anxiety and urinary pyrroles

Angela Sherwin, BSc[1,2], *Ian C. Shaw, DSc, PhD*[1]

[1]School of Physical & Chemical Sciences, and [2]School of Psychology, Speech & Hearing, University of Canterbury, Christchurch, New Zealand. Corresponding author: Angela Sherwin; Angela.Sherwin@pg.Canterbury.ac.nz

Key words: Mauve Factor; kryptopyrrole; hydroxypyrrole; biomarker for anxiety; urinary biomarker; generalized anxiety disorder

Abbreviations: GAD-7, Generalized Anxiety Disorder - 7 item scale; HPL, hydroxypyrrole; DMAB, 4-dimethylaminobenzaldehyde; GABA, γ-aminobutyric acid

Laboratory Medicine 2024;55:334-340; https://doi.org/10.1093/labmed/lmad086

ABSTRACT

Objective: For over 60 years there has been conjecture about the identity of an Ehrlich's test positive pyrrole (Mauve Factor) reputed to be a biomarker for psychological disorders, including anxiety. We reviewed studies that attempt to identify Mauve Factor and subjected authentic standards of the 2 main candidates, kryptopyrrole and hydroxypyrrole, to the Ehrlich's reaction.

Methods: Modified Ehrlich's test for kryptopyrrole and hydroxypyrrole were applied to urine samples from 10 volunteers, anxious and nonanxious.

Results: Based on the mechanistic chemistry of Ehrlich's reaction and reactions of the 2 compounds, Mauve Factor cannot be hydroxypyrrole. Analyses of urine samples from volunteers, identified by the Generalized Anxiety Disorder - 7 item scale (GAD-7 ≥10; n = 5) and control urine samples (GAD-7 <10; n = 5) using a kryptopyrrole calibration graph, show that concentrations are similar in both groups.

Conclusion: Kryptopyrrole may be the elusive Mauve Factor. Its possible origin from stercobilin via gut microbiome–mediated metabolism, its link to gut-mediated neurological effects via γ-aminobutyric acid (GABA) receptors, and its predicted interaction with Zn^{2+} and consequent impact on zinc homeostasis are discussed. The GAD-7 scale does not differentiate between state and trait anxiety and as such, the minimal difference in pyrrole levels between volunteer groups requires further study.

Introduction

Laboratory tests for biomarkers may be required more often in the future as personalized medicine becomes more widely used. Psychological disorders (eg, anxiety) are common, and therefore an easily applied laboratory test to aid in determining treatment options would be a useful adjunct to the available diagnostic tools.

Anxiety disorders are common worldwide, with a prevalence of 2.4% to 29.8% depending on age, gender, culture, and personal and national issues such as conflict and economic status.[1] Since there are likely to be biochemical aberrations underpinning this spectrum of psychological disorders, it is feasible that biochemical markers might be useful for screening and diagnosis of anxiety.

Approximately 60 years ago, D.J. Irvine showed that urine from patients with psychological disorders gave a characteristic mauve reaction with Ehrlich's reagent[2]; this was termed Mauve Factor. Irvine's group later identified the urinary compound as 2,4-dimethyl-3-ethylpyrrole (kryptopyrrole; **FIGURE 1**), following its chromatographic isolation from urine and mass spectrometry.[3] Sohler et al[4] confirmed Irvine's identification of Mauve Factor and showed that it has a sedative effect on the central nervous system of rabbits.

Further studies by Irvine[5] reidentified Mauve Factor as 2,4-dimethyl-3-ethyl-2,4-dihydropyrrol-4-one (hydroxypyrrole [HPL]; **FIGURE 1**).

The change in identity of the elusive Mauve Factor perhaps reflects the analytical methodology available at the time, and very importantly, the instability of the group of pyrroles to which Mauve Factor appeared to belong.

Hydroxypyrrole has been reported (although variously named due to changes in chemical nomenclature) in blood and urine[6-9] and in cerebrospinal fluid[6] but has not been reliably associated with a specific clinical disorder. However, its association with anxiety has been proposed[10]; such an association is attractive because it might be a useful biomarker in determining treatment options for anxiety.

This article was designed to review the historical literature in the area, highlight the uncertainties of the chemical structure of Mauve

FIGURE 1. Proposed molecular structures of Mauve Factor. Left: 2,4-dimethyl-3-ethylpyrrole (kryptopyrrole; Irvine et al[3]). Right: 2,4-dimethyl-3-ethyl-2-hydroxy-2,5-dihydropyrrol-2-one (hydroxypyrrole [HPL]; Irvine[5]). The pyrrole ring numbering system and α- and β-carbons are also shown.

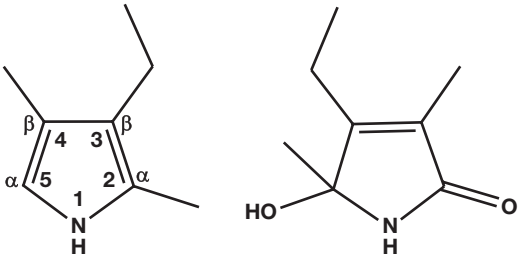

Factor, and apply the methodology as a proof of concept for the value of studying urinary pyrroles in relation to anxiety.

Urinary Pyrrole Nomenclature

The chemistry of pyrroles in the urine of patients with anxiety has spanned some 60 years. During this time, there have been significant changes in chemical nomenclature and advances in experimental methodologies. Initially, scientists referred to the compounds as "Mauve Factor," or similar because of their color reactions with Ehrlich's reagent, later naming them specifically according to knowledge about their molecular identities at the time. Not only have the names of the compounds changed as a better understanding of their structures has developed, but also the standard chemical nomenclature has changed during this time. This can lead to significant confusion; therefore, in this study, we have used the generic term "urinary pyrroles" throughout unless we are referring to a specific compound, in which case we use the pyrrole ring numbering system shown in **FIGURE 1**.

Biochemical Origins of HPL

There is significant conjecture about the biochemical origins of HPL. However, it is tempting to associate it with the biodegradation of heme because of the similarities in molecular structure between HPL and heme biodegradation products (**FIGURE 2**). At about the same time that Irvine postulated the existence of HPL,[5] Brown and King[11] proposed the mechanism of heme catabolism via biliverdin to bilirubin followed by bilirubin's further breakdown to a series of dipyrrolic fragments (**FIGURE 2**), which might conceivably be metabolic precursors of HPL.

Pyrroles in Psychological Disorders

An interest in concentrations of Mauve Factor in psychological disorders led O'Reilly et al[12] to report that of 200 patients admitted to a psychiatric ward, 89 (44.5%) were urinary Mauve Factor–positive. In addition, O'Reilly et al[13] showed that approximately 11% of the general population and 41.8% of the psychiatric population were Mauve Factor–positive. Furthermore, "neurotic" schizophrenia patients who were Mauve Factor–positive following treatment with nicotinamide (vitamin B3) became Mauve Factor–negative, which suggests that Mauve Factor can be used as an indicator of treatment success.[14] Pfeiffer and Iliev[15] used similar methodology to monitor treatment and found that pyridoxal-5'-phosphate (vitamin B6) was also an effective treatment. Other studies have shown a correlation between psychological disorders and urinary pyrroles, including

FIGURE 2. A dipyrrolic fragment of bilirubin from the catabolism of heme proposed by Brown and King.[11]

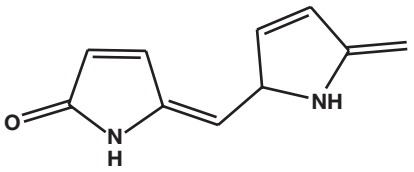

anxiety,[10] depression,[10,16] attention deficit hyperactivity disorder/attention deficit disorder,[17] autism,[17] and bipolar disorder.[16] Although Gorchein[8] found no difference between schizophrenia and general medical patients, this might reflect the anxiety levels of the hospitalized patients tested.

As a result of these and other studies that show links between an Ehrlich's positive compound in urine (termed Mauve Factor or identified as 1 of 2 pyrrole derivatives, namely HPL or kryptopyrrole [**FIGURE 1**]) and various psychological disorders (including anxiety), a plethora of commercial services (eg, Riordan Clinic,[18] Nutripath,[19] DHA Laboratory,[20] Amanda Nutrition,[21] Perpetual Wellbeing,[22] SAFE Analytical Laboratories,[23] and Applied Analytical Laboratories[24]) have been established to carry out the Ehrlich's test (or other unspecified analyses) on urine samples of individuals suspected of suffering from a psychological disorder, including anxiety, as a means of indicating treatment (often dietary supplements or herbal remedies). These services variously claim to be analyzing for HPL, kryptopyrrole, pyrroles generally, or give no clear indication of what they are testing for. Similarly, of the multitude of scientific publications purporting to study various pyrroles in urine of patients with psychological disorders, most have ill-defined descriptions of the analytical methodology, in particular, its validation,[25-30] and do not appear to use authentic standards (eg, HPL) for their analytical validation; as a result, their findings are unreliable. At the time of writing, the web-based companies that offer analyses to determine therapy rarely, if ever, describe their analytical methodology.

Chemistry of Ehrlich's Test

Based on Ehrlich's earlier work, Morton[31] noted that all pyrroles with unsubstituted α-carbons react with 4-dimethylaminobenzaldehyde (DMAB) to produce a characteristically colored compound. They also noted that the "reaction is partially successful with compounds that have a free beta position" and that α-carboxy or α-ester-substituted pyrroles gave a reaction when heated[31] (p 68). Recently Lamb et al[32] unraveled the mechanism of the reaction between DMAB and indole (**FIGURE 3**) and showed that reaction position is dependent on the chemical environment but that the conventional Ehrlich's reagent (ie, DMAB in acid solution) results in a reaction at the β-carbon of the pyrrole ring (**FIGURE 1**). This means that in Morton's terms,[31] either a free α- or β-carbon is required, and in the terms of Lamb et al,[32] a free β-carbon is required for the Ehrlich's reagent to react with a pyrrole. Hydroxypyrrole has both α- and β-carbons fully substituted, and its carbon-carbon double bond is in the wrong position (ie, it is a 2,4-dihydropyrrole), whereas kryptopyrrole has an unsubstituted α-carbon. Therefore, HPL is unlikely to give a positive Ehrlich's reaction, whereas kryptopyrrole is likely to react.

FIGURE 3. Ehrlich's reaction: the β-carbon of indole (A) reacts with 4-dimethylaminobenzaldehyde (DMAB) (B) to form purple β-bis(indolyl)dimethylaminobenzyl methane (C).[32]

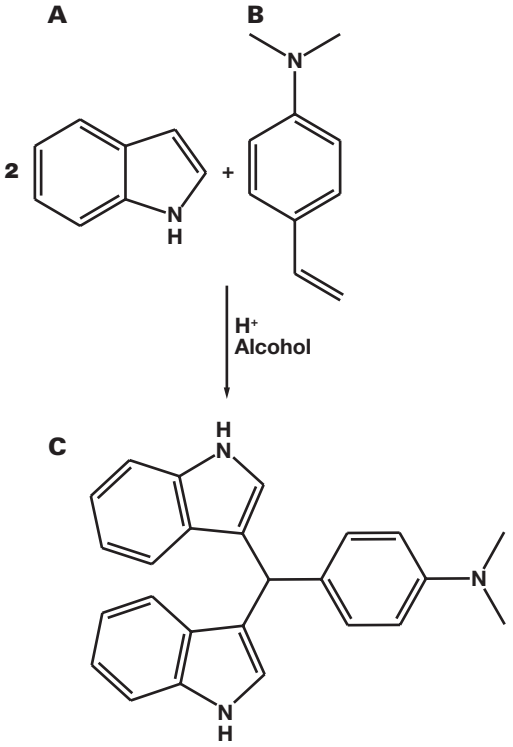

To determine pyrroles in urine, a modified Ehrlich's test is used.[33] In short, Ehrlich's reagent is prepared by dissolving DMAB in methanol and acidifying the methanolic solution with sulfuric acid. Pyrroles are extracted from urine samples with trichloromethane, thus leaving other Ehrlich's positive compounds (eg, urobilinogen) in the aqueous phase. The trichloromethane extract is mixed with Ehrlich's reagent and after a brief incubation period, the absorbance is read at 540 nm (see Materials and Methods).

As outlined above, there is significant conjecture about the presence and identity of pyrroles in urine and their link to psychological disorders (including anxiety). Two key questions remain unanswered: what does the modified (including trichloromethane extraction) Ehrlich's test measure in urine? And does the test reliably predict an intervention of therapeutic value?

In this study, we investigated the reaction of HPL and kryptopyrrole with Ehrlich's reagent and applied the modified Ehrlich's test to urine samples obtained from volunteers who were not suspected of suffering from a psychological disorder (including anxiety) using an authentic kryptopyrrole calibration graph to determine urinary kryptopyrrole concentrations. We discuss our findings in the context of psychological disorder (including anxiety) management.

Materials and Methods

Chemicals

All chemicals were general laboratory reagent grade and purchased from Merck except HPL (95% purity; Chem-Space.com), kryptopyrrole (97% minimum purity; LabSupply.co.nz), and trichloromethane (≥99.85% purity; ThermoFisher Scientific). Both HPL and kryptopyrrole were supplied with proton nuclear magnetic resonance or mass spectroscopic data, which confirmed their molecular structures.

Modified Ehrlich's Reagent

Modified Ehrlich's regent was prepared as described by Sohler et al.[33] In brief, DMAB (1 g) was dissolved in ice cold methanol (80 mL), concentrated sulfuric acid (10 mL) was added drop-wise, and the solution made up to 100 mL with methanol. The reagent was stored at 4°C and used within 24 hours.

HPL and Kryptopyrrole Calibration Graphs

Hydroxypyrrole (5 mL, 1-70 μg/mL [aq]) was extracted with trichloromethane (5 mL) in glass stoppered test tubes (25 mL). The trichloromethane layer was pipetted into a test tube, dried with anhydrous sodium sulfate (0.5 g), and modified Ehrlich's reagent (1 mL) was added (to 4 ml extract). The mixture incubated at room temperature for 30 minutes, then its absorbance at 540 nm was determined (Model T75+ UV/visible spectrophotometer, Bio-Strategy).

Kryptopyrrole (0.5 mg/mL in ethanol) was pipetted into a series of tubes and made up to 210 μL with ethanol and distilled water (4.79 mL) was added to give a range of final kryptopyrrole concentrations (1-5 μg/mL). Trichloromethane (5 mL) was added and the procedure described above for HPL was followed.

All HPL and kryptopyrrole concentrations were prepared and analyzed in triplicate. Results are expressed as mean ± SD.

Ehrlich's Spot Test for HPL

Hydroxypyrrole (1 mg) was dissolved in trichloromethane (1 mL), Ehrlich's reagent (250 μL) was added, the mixture was incubated at room temperature for 30 minutes, and its absorbance at 540 nm determined.

Volunteer Inclusion Criteria

Volunteers were screened using the Generalized Anxiety Disorder - 7 item scale (GAD-7),[34] a 7-point Likert scale with a maximum score of 21 (10 or above was the cut off point for anxiety for this study), and a general health questionnaire. All volunteers reported that they had no general health issues and were not taking any medications. Only females were chosen to help avoid confounding variables, as there is some suggestion that current psychometrics do not adequately pick up anxiety in men.[35,36]

Urine Samples

Midstream urine samples (~50 mL) were collected from female volunteers (n = 5, age 34 ± 11.3 years [mean ± SD]) with no known psychiatric disorders and GAD-7 <10 and females with symptoms of anxiety (n = 5, age 42.8 ± 8.2 years) and GAD-7 ≥10 (University of Canterbury Human Ethics Committee approval 17/STH/241). The urine samples were preserved with ascorbic acid (final concentration in urine ~0.1 g/mL) to inhibit pyrrole oxidation. Samples were stored at −18°C prior to analysis.

Urine Analysis

Urine samples (5 mL) were extracted with trichloromethane (5 mL). The trichloromethane extracts were analyzed with modified Ehrlich's

2024;55:334-340 | https://doi.org/10.1093/labmed/lmad086

reagent as described for HPL and kryptopyrrole calibration graphs above. All samples were analyzed in triplicate.

Results and Discussion

Reaction of HPL and Kryptopyrrole with Modified Ehrlich's Reagent

Kryptopyrrole reacted with modified Ehrlich's reagent in a concentration-dependent manner that obeys Beer's Law between 1 and 5 μg/mL (**FIGURE 4**). On the other hand, HPL did not react with modified Ehrlich's reagent (**FIGURE 4**) at any of the concentrations (1 to 70 μg/mL) tested. This lack of reaction with modified Ehrlich's reagent was confirmed with a higher concentration (1 mg/mL) of HPL, which also gave no color reaction ($A_{540\ nm}$ = 0.035). This is not surprising, as HPL does not have a free α- (or β-) carbon that is required for reaction with DMAB.[31,32] Kryptopyrrole does have a free α-carbon and therefore would be expected to react with DMAB.

This finding contradicts previous studies[5,25,27,28,37–42] that identify the urine component responsible for the Ehrlich's mauve reaction as HPL. Interestingly, none of the previous studies used a pure, authentic HPL standard and so based their conclusions on a possible misinterpretation of the chemistry of the Ehrlich's reaction. It is now clear that urinary Mauve Factor is not HPL but could be kryptopyrrole.

Rainforest et al[29] confirmed the importance of kryptopyrroles [sic] as a biomarker for psychological disorders in Australian clinical practice. However, they did not specify what was measured in the urine samples they reported on. Therefore, even the most current publication on urinary pyrroles in psychological disorders at this time purports to be measuring kryptopyrroles but might not be. The confusion continues.

FIGURE 4. Reaction of hydroxypyrrole (HPL) and kryptopyrrole with modified Ehrlich's reagent. This clearly shows that HPL does not react with 4-dimethylaminobenzaldehyde (DMAB) and that kryptopyrrole reacts in a concentration-related manner. Results are shown as mean ± SD (n = 3).

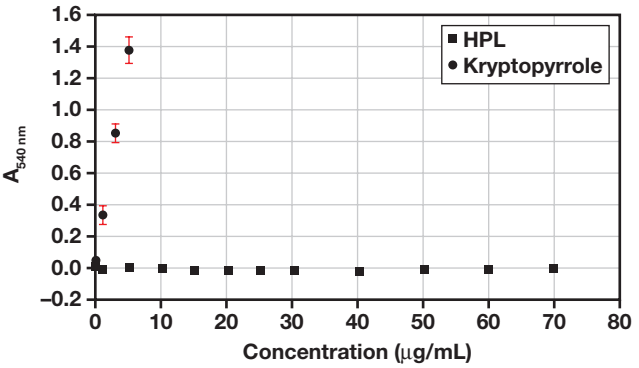

Importance of the Identity of the Urinary Pyrrole(s) in Anxiety

The use of a positive urine reaction with Ehrlich's reagent as an indicator of anxiety would be a useful tool for diagnosis. Additionally, identification of the specific urinary pyrrole(s) might help our understanding of the biochemistry of anxiety. For example, reduced serum Zn^{2+} concentrations have been shown in cases of anxiety, and zinc therapy has resulted in reduction in the symptoms of anxiety.[43] The importance of zinc (likely as Zn^{2+}) in anxiety might be related to its role in γ-aminobutyric acid (GABA)ergic neurotransmission[44,45] via glutamate regulation.[43] If a specific pyrrole has a role in Zn^{2+} homeostasis, it would be a key biochemical marker and might indicate a biochemical mechanism underpinning anxiety.

It has been suggested that zinc (likely as Zn^{2+}) is excreted as a pyridoxal phosphate kryptopyrrole chelate[46] (**FIGURE 5**). This might be a mechanism of Zn^{2+} depletion, resulting in reduced serum Zn^{2+} concentration, with its concomitant implications for GABA-mediated neurotransmission and perhaps its role in anxiety. The fact that a co-chelate between Zn^{2+} and pyridoxal phosphate/kryptopyrrole is the Zn^{2+} excretory vector would mean that

FIGURE 5. Postulated structure of the pyridoxal phosphate/kryptopyrrole-zinc chelate[46] (left) and possible, but unlikely, zinc-kryptopyrrole complex (right).

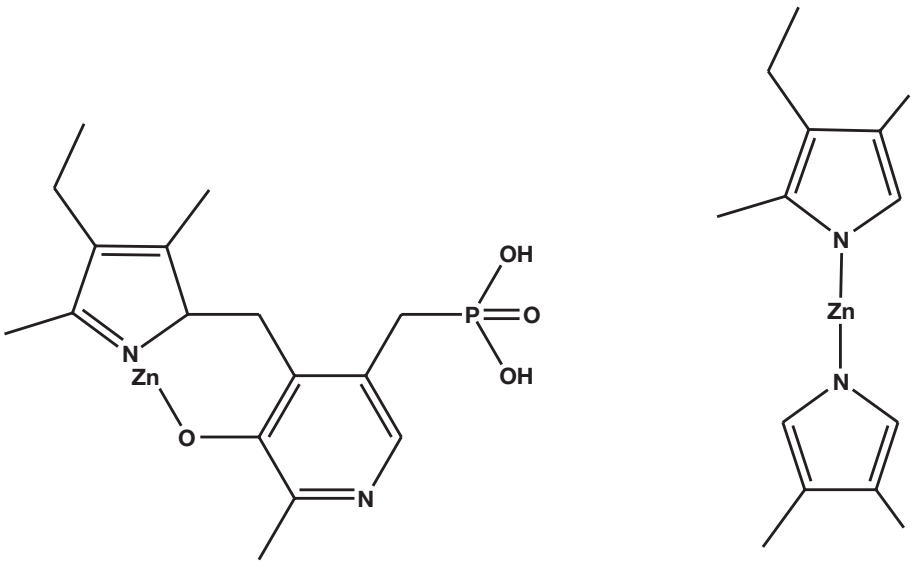

kryptopyrrole is a biomarker for anxiety. The question is, would the postulated zinc pyridoxal phosphate/kryptopyrrole complex react with Ehrlich's reagent to give the characteristic mauve color? This is unlikely because the pyrrole ring does not have a free α- (or β-) carbon. On the other hand, would excess urinary kryptopyrrole (ie, that remaining after reaction with pyridoxal phosphate) indicate loss of Zn^{2+} via the chelate pathway? If this were the case, the presence of kryptopyrrole in urine would likely indicate loss of zinc via the urinary route.

It is possible but unlikely that a zinc-kryptopyrrole complex (**FIGURE 5**) might be formed and that this underpins the mechanism of Zn^{2+} loss via urine. This is considered unlikely because the pyrrole nitrogen in kryptopyrrole is a very weak base (pyrrole pK_b = 13.6) and so does not support its interaction with Zn^{2+}.

TABLE 1. Modified Ehrlich's analysis of urine samples from female volunteers with GAD-7[a]

Volunteer	$A_{540\ nm}$ Mean ± SD	Kryptopyrrole equivalents μg/mL
GAD-7 <10		
1	0.075 ± 0.009	0.36
2	0.066 ± 0.006	0.31
3	0.098 ± 0.008	0.47
4	0.092 ± 0.010	0.44
5	0.094 ± 0.011	0.45
Mean ± SD		0.41 ± 0.065
GAD-7 ≥10		
1	0.092 ± 0.014	0.44
2	0.104[b]	0.49
3	0.081 ± 0.004	0.39
4	0.062 ± 0.011	0.30
5	0.103 ± 0.013	0.49
Mean ± SD		0.42 ± 0.083

GAD-7, Generalized Anxiety Disorder - 7 item scale.
[a]GAD-7 <10 (n = 5; mean ± SD age = 32.5 ± 10.8 years) and GAD-7 ≥10 (n = 5; mean ± SD age = 42.8 ± 8.2 years) showing kryptopyrrole equivalents.
[b]Single sample.

Analysis of Urine Samples

Modified Ehrlich's analysis of urine samples from volunteers showed the presence of an Ehrlich's-positive compound (or compounds) that absorbs at 540 nm (**TABLE 1**). If our hypothesis that this compound is kryptopyrrole is correct, using the kryptopyrrole calibration graph (**FIGURE 4**), it corresponds to a urine kryptopyrrole concentration of 0.40 ± 0.065 μg/mL (mean ± SD) for the nonanxious volunteers and 0.42 ± 0.083 for the anxious volunteers. Both are considered high.[17,20,42,47] On the face of it, the difference between the 2 groups in this study is interesting and surprising. Using an independent samples *t*-test with all assumptions met to determine whether there were differences in pyrrole absorbance between the 2 groups we see that there is no statistically significant difference, M = 0.16, 95% CI [0.09, 0.12], t(8) = 0.341, *P* = .7. It is important to note that our study was designed to investigate the application of the methodology to urine samples to inform future study rather than differentiate between the 2 groups. In addition, the GAD-7 scale does not differentiate between state and trait anxiety. It is possible that the nonanxious volunteers were in a state of anxiety not picked up by the GAD-7.

A cross-sectional analysis of pyrroles in psychiatric disorders[28] suggested that there is a correlation between histamine levels and pyrrole levels. Histamine itself is unlikely to react with Ehrlich's reagent as it does not have a free β-carbon.[31] Clearly, more research is needed to confirm the identity of the Ehrlich's-positive compound and understand its potential value as a clinical biomarker. This is made difficult by the likely instability (stability data not presented) of kryptopyrrole when extracted from urine.

It has been suggested that stress-related gut permeability changes might account for stress-associated HPL in blood.[9] This too is feasible, as bilirubin is excreted as a glucuronide conjugate in bile and gut microbiome β-glucuronidase releases the aglycone, which is normally further metabolized by the gut microbiome to stercobilin and eliminated in feces.[48] Stercobilin (**FIGURE 6**) is likely to be in part further degraded by the gut microbiome. Interestingly, stercobilin has parts of its molecular makeup that have remarkable structural analogy to HPL and kryptopyrrole (compare **FIGURES 1** and **6**).

Furthermore, recent research has shown that stercobilin is absorbed from the gut in mice and that its presence in blood is linked to

FIGURE 6. Stercobilin: the two 3-ethyl-4-methyl-3,5-dihydropyrrol-2-one moieties at each end of the molecule have significant structural similarities to hydroxypyrrole (HPL) and kryptopyrrole (see FIGURE 1).

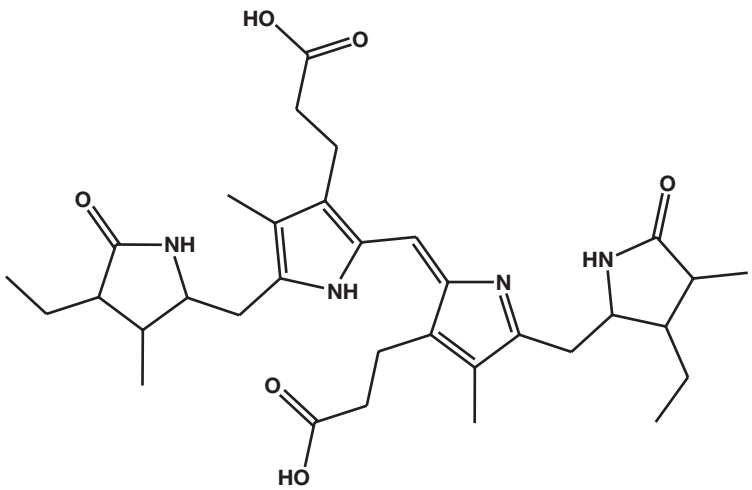

proinflammatory activity.[49] Interestingly, peripheral proinflammatory cytokines (eg, interleukins) have been linked to generalized anxiety disorder in Chinese patients[50]; this might furnish a link between leaky gut, stercobilin absorption, inflammatory response, and generalized anxiety disorder, which in turn presents a possible molecular association with alkylated pyrroles (perhaps derived from stercobilin).

If the Ehrlich's-positive compound in urine is kryptopyrrole, this might link its association with anxiety to a gut-mediated mechanism involving the biodegradation of stercobilin by the gut microbiome leading to a stercobilin-mediated inflammatory response.

Conclusion

Our study is the first to use authentic standards of HPL and kryptopyrrole and shows that urinary Mauve Factor is not HPL. Its identity remains unproved, but the molecular requirements for reaction with DMAB are met by kryptopyrrole (ie, α, β-unsubstituted pyrrole) and so kryptopyrrole is a likely candidate for the elusive Mauve Factor.

It is interesting to speculate that kryptopyrrole has its biochemical origins in stercobilin and might indicate a link with leaky gut syndrome, which has been reported to be associated with anxiety.[50] If kryptopyrrole is excreted in urine in clinical anxiety, the postulated co-chelate with pyridoxal phosphate and zinc[46] would suggest a biochemical mechanism of anxiety, point to a dietary supplement-based treatment, and present a biomarker for diagnosis; however, because there is no pyrrole concentration difference between control and anxious urine samples in this small sample set, more work is needed to assess the usefulness of kryptopyrrole as an anxiety biomarker.

Acknowledgments

We gratefully acknowledge Ben Warren's preliminary postgraduate work, which initiated this project. We thank Professor Richard Hartshorne for a very helpful discussion on the chemistry of pyrroles, Professor Julia Rucklidge for her supervision of A.S.'s PhD research and for many helpful discussions, and Dr Amie Steel for graciously answering our persistent questions about her recent article.

Funding

This research was supported by the School of Physical & Chemical Sciences and School of Psychology, Speech & Hearing, University of Canterbury, Christchurch, New Zealand. This research did not receive any specific grant from funding agencies in the public, commercial, or not-for-profit sectors.

Conflict of Interest Disclosure

The authors have nothing to disclose.

REFERENCES

1. Baxter AJ, Scott KM, Vos T, Whiteford HA. Global prevalence of anxiety disorders: a systematic review and meta-regression. *Psychol Med.* 2013;43(5):897-910. doi:10.1017/S003329171200147X
2. Irvine DG. Apparently non-indolic Ehrlich-positive substances related to mental illnesses. *J Neuropsychiatry Clin Neurosci*. 1961;2:292-305.
3. Irvine DG, Bayne W, Miyashita H, Majer JR. Identification of kryptopyrrole in human urine and its relation to psychosis. *Nature.* 1969;224(5221):811-813. doi:10.1038/224811a0
4. Sohler A, Beck R, Noval JJ. Mauve Factor re-identified as 2, 4-dimethyl-3-ethylpyrrole and its sedative effect on the CNS. *Nature.* 1970;228(5278):1318-1320. doi:10.1038/2281318a0
5. Irvine DG. Hydroxy-hemopyrrolenone, not kryptopyrrole, in the urine of schizophrenics and porphyrics. *Clin Chem.* 1978;24(11):2069-2070. https://doi.org/10.1093/clinchem/24.11.2069
6. Irvine DG. Kryptopyrrole and other monopyrroles in molecular neurobiology. *Int Rev Neurobiol.* 1974;16(0):145-182. doi:10.1016/s0074-7742(08)60196-8
7. Graham DJM. Quantitative determination of 3-ethyl-5-hydroxy-4, 5-dimethyl-Δ3-pyrrolin-2-one in urine using gas-liquid chromatography. *Clin Chim Acta.* 1978;85(2):205-210. doi:10.1016/0009-8981(78)90241-3
8. Gorchein A. Urine concentration of 3-ethyl-5-hydroxy-4, 5-dimethyl-Δ3-pyrrolin-2-one ("Mauve Factor") is not causally related to schizophrenia or to acute intermittent porphyria. *Clin Sci (Colch).* 1980;58(6):469-476. doi:10.1042/cs0580469
9. Durko I, Engelhardt J, Szilard J. The effect of haemodialysis on the excretion of the Mauve Factor in schizophrenia. *J. Orthomol. Psychiatry*. 1984;13(4):222-232.
10. Hoffer A. The discovery of kryptopyrrole and its importance in diagnosis of biochemical imbalances in schizophrenia and in criminal behavior. *J Orthomol Med*. 1995;10(1):3-6.
11. Brown SB, King RFGJ. The mechanism of haem catabolism: bilirubin formation in living rats by [18O]oxygen labelling. *Biochem J.* 1978;170(2):297-311. doi:10.1042/bj1700297
12. O'Reilly PO, Hughes G, Russell RT, Ernest M. The Mauve Factor: an evaluation. *Nervous System*. 1965;26(9):562-568.
13. O'Reilly PO, Ernest M, Hughes G. The incidence of malvaria. *Br J Psychiatry.* 1965;111(477):741-744. doi:10.1192/bjp.111.477.741
14. Hoffer A. Malvaria, schizophrenia and the HOD test. *Int J Neuropsychopharmacol*. 1966;2(2):175-178.
15. Pfeiffer CC, Iliev V. Pyroluria, urinary Mauve Factor, causes double deficiency of B-6 and zinc in schizophrenics. Federation Proceedings, 1973. Federation of American Societies for Experimental Biology, Rockville, MD: 276.
16. Mikirova N. Clinical test of pyrroles: usefulness and association with other biochemical markers. *CMRCR*. 2015;2(4):2378-3656. doi:10.23937/2378-3656/1410027
17. Jackson JA, Braud M, Neathery S. Urine pyrroles and other orthomolecular tests in patients with ADD/ADHD. *J Orthomol Med*. 2010;25(1):39-42.
18. Riordan Clinic. Accessed June 15, 2022 https://riordanclinic.org/lab_tests/pyrroles-urine-pyrroluria-kryptopyrrole-mauve-factor/
19. Nutripath. Accessed June 15, 2022. http://nutripath.com.au/product/mauve-factor-formerly-kryptopyrroles-spot-urine-test-code-4011/
20. DHA Laboratory. Accessed June 15, 2022. https://www.dhalab.com/shop/kryptopyrrole-quantitative/
21. Amanda Nutrition. Accessed June 15, 2022. https://amandanutrition.co.nz/kryptopyrroles-test/
22. Perpetual Wellbeing. Accessed June 15, 2022. https://www.perpetualwellbeing.com.au/pyrrole-testing/
23. SAFE Analytical Laboratories. Accessed June 15, 2022. http://www.safelabs.com.au/urinary_kryptopyrrole_testing.php
24. Applied Analytical Laboratories. Accessed June 15, 2022. https://www.apanlabs.com/pyrrole-test/
25. Fryar-Williams S, Strobel JE. Biomarkers of a five-domain translational substrate for schizophrenia and schizoaffective psychosis. *Biomarker Res.* 2015;3(1):1. https://doi.org/10.1186/s40364-015-0028-1
26. Fryar-Williams S, Strobel JE. Biomarker case-detection and prediction with potential for functional psychosis screening: development

and validation of a model related to biochemistry, sensory neural timing and end organ performance. *Front Psychiatry.* 2016;7:48. doi:10.3389/fpsyt.2016.00048

27. Hambly J, Francis K, Khan S, et al. Micronutrient therapy for violent and aggressive male youth: an open-label trial. *J Child Adolesc Psychopharmacol.* 2017;27(9):1-10. https://doi.org/10.1089/cap.2016.0199
28. Mikirova N. Cross-sectional analysis of pyrroles in psychiatric disorders: association with nutritional and immunological markers. *J Orthomol Med*. 2015;30(1):25-32.
29. Rainforest J, Schloss J, Foley H, Steel A. Clinical significance and importance of elevated urinary kryptopyrroles (UKP): self-reported observations and experience of Australian clinicians using UKP testing. *Adv Integr Med*. 2021;8(3):159-166. doi:10.1016/j.aimed.2021.04.002
30. Steel A, Rainforest J, Schloss J. Verifying the validity of urinary kryptopyrrole (UKP) testing in an adult population: protocol for a multi-stage research project. *Adv Integr. Med*. 2019;6(3):120-125. doi:10.1016/j.aimed.2019.02.001
31. Morton AA. *The Chemistry of Heterocyclic Compounds*. McGraw-Hill Book Company; 1946.
32. Lamb AC, Federico-Perez RA, Xue Z-L. Product in indole detection by Ehrlich's reagent. *Anal Biochem.* 2015;484:21-23. doi:10.1016/j.ab.2015.04.033
33. Sohler A, Holsztynska E, Pfeiffer CC. A rapid screening test for pyroluria: useful in distinguishing a schizophrenic subpopulation. *J Orthomol Psychiatr*. 1974;3(4):273-279.
34. Spitzer RL, Kroenke K, Williams JBW, et al. *Generalized Anxiety Disorder 7 (GAD-7) [Database record]*. APA PsycTests; 2006.
35. Petersen A. Anxiety looks different in men. *The Wall Street Journal*. July 30, 2019.
36. Fisher K, Seidler ZE, King K, Oliffe JL, Robertson S, Rice SM. Men's anxiety, why it matters, and what is needed to limit its risk for male suicide. *Discover Psychology*. 2022;2(1).
37. Aljamali NM, Jwad SM. Survey in pyrrole compounds and biological activity. *Int J Innov.* 2015;1(1):1-8.
38. Heitzman J, Gosek P, Wojciech L, et al. Elevated hydroxylactam of hemopyrrole level in urine in perpetrators of extremely violent acts diagnosed with psychosis. *Psychiatr Pol*. 2017;51(3):413-423.
39. Irvine DG. Pyrroles in neuropsychiatric and porphyric disorders: confirmation of a metabolite structure by synthesis. *Life Sci.* 1978;23(9):983-990. doi:10.1016/0024-3205(78)90226-6
40. Mikirova N, Casciari J, Hunninghake R. The assessment of the energy metabolism in patients with chronic fatigue syndrome by serum fluorescence emission. *Altern Ther Health Med.* 2012;18(1):36-40.
41. Mikirova N, Rogers AM, Taylor PR, et al. Metabolic correction for attention deficit/hyperactivity disorder: a biochemical-physiological therapeutic approach. *Functional Foods in Health and Disease*. 2013;3(1):1-20.
42. Stuckey R, Walsh W, Lambert B. The effectiveness of targeted nutrient therapy in treatment of mental illness. *Occup Environ Med*. 2010;29(3):3-8.
43. Russo A. Decreased zinc and increased copper in individuals with anxiety. *Nutr Metab Insights*. 2011;4:NMI.S6349. doi:10.4137/nmi.s6349
44. Takeda A, Hirate M, Tamano H, Oku N. Release of glutamate and GABA in the hippocampus under zinc deficiency. *J Neurosci Res.* 2003;72(4):537-542. doi:10.1002/jnr.10600
45. Takeda A, Itoh H, Imano S, Oku N. Impairment of GABAergic neurotransmitter system in the amygdala of young rats after 4-week zinc deprivation. *Neurochem Int.* 2006;49(8):746-750. doi:10.1016/j.neuint.2006.06.005
46. Pfeiffer C, Sohler A, Jenney E, et al. Treatment of pyroluric schizophrenia (malvaria) with large doses of pyridoxine and a dietary supplement of zinc. *J Appl Nutr.* 1974;26:21-28.
47. McGinnis WR, Audhya T, Walsh WJ, et al. Discerning the Mauve Factor, part 1. *Altern Ther Health Med.* 2008;14(2):40-50.
48. Seyfried H, Klicpera M, Leithner C, Penner E. Bilirubin metabolism (author's translation). *Wien Klin Wochenschr.* 1976;88(15):477-482.
49. Sanada S, Suzuki T, Nagata A, Hashidume T, Yoshikawa Y, Miyoshi N. Intestinal microbial metabolite stercobilin involvement in the chronic inflammation of ob/ob mice. *Sci Rep.* 2020;10(1):6479. doi:10.1038/s41598-020-63627-y
50. Tang Z, Ye G, Chen X, et al. Peripheral proinflammatory cytokines in Chinese patients with generalised anxiety disorder. *J Affect Disord.* 2018;225:593-598. doi:10.1016/j.jad.2017.08.082

Impact of anti–squamous cell carcinoma antigen antibodies on serum squamous cell carcinoma antigen levels measured by chemiluminescent immunoassay and chemiluminescent enzyme immunoassay

Chinami Oyabu, MT[1], Itsuko Sato, MT[1], Mari Yamamoto, MT[1], Takamitsu Imanishi, MT[1], Sho Sendo, MD[1], Yoshihiko Yano, MD[1]

[1]Department of Clinical Laboratory, Kobe University Hospital, Kobe, Japan.
Corresponding author: Yoshihiko Yano; yanoyo@med.kobe-u.ac.jp

Key words: squamous cell carcinoma antigen; chemiluminescent enzyme immunoassay; chemiluminescent immunoassay; absorption test; anti-SCCA antibody; autoantibody

Abbreviations: SCCA, squamous cell carcinoma antigen; Ig, immunoglobulin; CLIA, chemiluminescent immunoassay; CLEIA, chemiluminescent enzyme immunoassay; ELISA, enzyme-linked immunosorbent assay; ALP, alkaline phosphatase; PBS, phosphate-buffered saline; PRL, prolactin; T-TBS, Tween 20 tris-buffered saline; BSA, bovine serum albumin

Laboratory Medicine 2024;55:341-346; https://doi.org/10.1093/labmed/lmad088

ABSTRACT

Objective: The serum squamous cell carcinoma antigen (SCCA) level is a well-known tumor marker for squamous cell carcinoma. In this study, we examined the impact of immunoglobulin (Ig)-bound macromolecular SCCA on serum SCCA levels measured by 2 different methods.

Methods: Seventy-five serum samples with an SCCA level >5.0 ng/mL as determined by a chemiluminescent immunoassay (CLIA) were also analyzed using a chemiluminescent enzyme immunoassay (CLEIA). The levels of IgG- and IgA-type anti-SCCA antibodies, which form immunoglobulins and macromolecules, respectively, were determined using an enzyme-linked immunosorbent assay. An absorption test was performed to confirm the presence of anti-SCCA antibodies.

Results: The correlation coefficient between the values measured by CLEIA and CLIA was 0.768. The ratio of SCCA levels measured by CLEIA to those measured by CLIA in 14 samples with IgG-type anti-SCCA antibodies was significantly lower than that in samples without these antibodies ($P < .031$). Absorption tests showed that SCCA levels measured by CLIA might be falsely high in samples with IgG-type anti-SCCA antibodies, probably due to reactions with SCCA1.

Conclusion: The level of SCCA as measured by CLIA and CLEIA methods correlate well, but the presence of SCCA antibodies can affect the results of the CLIA method.

Squamous cell carcinoma antigen (SCCA) is a glycoprotein with a molecular mass of 45 kDa that is isolated from cervical squamous cell carcinoma cells.[1] Serum SCCA level is used for diagnosis, assessing the efficacy of treatment and predicting recurrence of various squamous cell carcinomas, including those of the cervix and lungs.

Although SCCA is generally measured by a chemiluminescent immunoassay (CLIA) or a chemiluminescent enzyme immunoassay (CLEIA), studies comparing different reagents have reported several cases with different values.[2-4] Differences in reactivity to SCCA1 and SCCA2 or binding of SCCA to an immunoglobulin (Ig) complex may contribute to markedly different values between these assay methods.

In this study, serum samples with SCCA levels above the CLIA cutoff level were measured by CLEIA. Furthermore, the levels of IgA- and IgG-type anti-SCCA antibodies (IgA- and IgG-SCCA antibodies) were detected by an enzyme-linked immunosorbent assay (ELISA), and their presence was confirmed by absorption testing. Differences in the SCCA levels between the CLIA and CLEIA were examined in terms of the presence of autoantibodies.

Materials and Methods

Study Participants

In this study of patient samples analyzed between January 2018 and March 2019, we used 75 residual samples from daily routine laboratory tests with SCCA levels of >5.0 ng/mL determined by CLIA. A further 5 healthy volunteers were enrolled as comparison subjects. Sera were collected by centrifugation and stored at −20°C until use. This study was conducted as joint research with Tosoh Corporation (Japan) with approval from the Ethics Committee of Kobe University Hospital (reference number: 180294). All participants were provided information disclosure and opportunities to opt out.

SCCA Assay Methods

The serum SCCA levels were measured by CLIA using the ARCHITECT SCC on an ARCHITECT i2000 (Abbott Japan) and by CLEIA using the CL AIA-PACK SCC on an AIA-CL2400 (Tosoh). Whereas ARCHITECT SCC is a 2-step sandwich immunoassay using an acridinium-labelled antibody, AIA-PACK SCC is based on delayed 1-step measurements and uses alkaline phosphatase (ALP) as a labelled substance. The measuring range is 0.1 to 100 ng/mL by AIA-CL2400 and 0.1 to 70.0 ng/mL by ARCHITECT. After SCCA routine measurement by the CLIA method using ARCHITECT SCC, measurement by the CLEIA method using AIA-PACK SCC was performed after thawing samples stored at −20°C.

ELISA Methods

The serum levels of IgG-, IgA-, and IgM-SCCA antibodies were measured using 2 ELISAs. In brief, 96-well ELISA plates were coated with 100 µL of recombinant SCCA (3 µg/mL) at room temperature for 2 hours, blocked with 1% bovine serum albumin (BSA) in phosphate-buffered saline (PBS) for 1 hour at pH 7.2, and washed 3 times with 0.05% Tween 20 tris-buffered saline (T-TBS). Then, 100 µL of serially diluted samples in 0.1% BSA in PBS was added to each well and the plate was incubated for 1 hour at room temperature. After washing with 0.05% T-TBS 3 times, 100 µL of serially diluted goat anti-human IgG against ALP (IgG-ALP) (Southern Biotech; 2040-04), goat anti-human IgM-ALP (Southern Biotech; 2023-04), or goat anti-human IgA-ALP (Southern Biotech; 2050-04) in 0.1% BSA in PBS was added to the well, and the plate was incubated for 1 hour at room temperature. After washing 3 times, 100 µL of serially diluted coloring reaction solution was added, comprising 26 mg of 4-methylumbelliferyl phosphate in 100 mL of 1 M diethanolamine and 0.5 mM $MgCl_2$, and the plate was incubated for 30 minutes at room temperature. The optical fluorescence was measured at 465 nm using a microplate reader (Infinite200; TECAN).

In the comparative method in which recombinant SCCA was not immobilized on a plate, immobilization on a plate was not performed, and the rest of the procedure was the same.

IgG and IgA Absorption Tests

Absorption tests were performed to confirm the presence of anti-SCCA antibodies. For this, 10 µL serum was mixed with 100 µL anti-IgA or anti-IgG polyclonal antibodies (Medical & Biological Laboratories; 105G, 103G) and incubated overnight at 4°C. After centrifugation (1710*g*, 10 min), the SCCA levels were measured by the CLIA and CLEIA.

Statistical Analysis

Correlation analysis was performed using linear regression and Spearman's correlation coefficient. Differences were analyzed using the Student *t*-test for comparison of 2 groups. One-way analysis of variance and multiple comparisons were performed for comparisons of 3 or more groups. All analyses were performed using GraphPad Prism version 7.0 software (GraphPad Software).

Results

Comparison of Serum SCCA Levels Determined by CLIA and CLEIA

We examined the correlation in serum SCCA levels between CLEIA and CLIA using serum samples from 75 patients with SCCA levels above the CLIA cutoff level. Nine of the samples had SCCA levels below the CLEIA cutoff level of 1.5 ng/mL (**FIGURES 1** and **2B**). Compared to measurements by the CLIA method, the correlation coefficient with the levels measured by CLEIA was 0.768 and the regression equation was y = 0.708x + 1.164 (**FIGURE 2A**). The SCCA levels of the 9 samples below the CLEIA cutoff were between 5 and 20 ng/mL according to CLIA. Samples with low SCCA levels according to the CLIA tended to show large variability relative to the CLEIA. **FIGURE 2B** compares the serum SCCA levels between the 2 methods for samples with levels of 5 to 20 ng/mL according to the CLIA. The SCCA value by Bland-Altman plot or CLEIA showed an average value 6.4 lower than CLIA, and there were samples whose average value was lower than −1.96 in the high concentration region (**FIGURE 2C**).

Detection of Anti-SCCA Antibodies

The fluorescent intensity ratios, with or without coated SCCA (anti-human IgG, IgA, IgM-ALP), are depicted by boxplots in **FIGURE 3**. Specificity was confirmed for samples with a fluorescence ratio of >2 times the average of 5 negative controls (IgG >2.176; IgM >2.280; IgA >3.998). We determined whether there was specific reactivity by adding 10 µg/mL of free SCCA to the ELISA reaction system and confirmed the signal specificity for SCCA. A multiple comparison test showed significant differences between without antigen and with antigen, and between with antigen, and with antigen plus free SCCA. Binding loss is defined as fluorescence intensity of with antigen/with antigen plus free SCCA of 0.65 or less. For IgG, samples except 50 showed a loss of binding (**FIGURE 4A**). For IgA, samples 12, 49, and 75 showed a loss of binding (**FIGURE 4B**). For IgM, all but 40 appeared to have loss of binding, but the signal was too small to be determined (**FIGURE 4C**). In the reproducibility tests, IgA and IgM results were reproducible (data not shown).

SCCA antibodies were detected in 15 samples: IgA in 1 sample, IgG in 12 samples, and both IgA and IgG in 2 samples (**FIGURE 1**, **TABLE 1**). In samples positive for IgG-SCCA antibodies, the SCCA levels measured by CLEIA were lower than those measured by CLIA except

FIGURE 1. Flow diagram. CLEIA, chemiluminescent enzyme immunoassay; CLIA, chemiluminescent immunoassay; ELISA, enzyme-linked immunosorbent assay; Ig, immunoglobulin; SCCA, squamous cell carcinoma antigen.

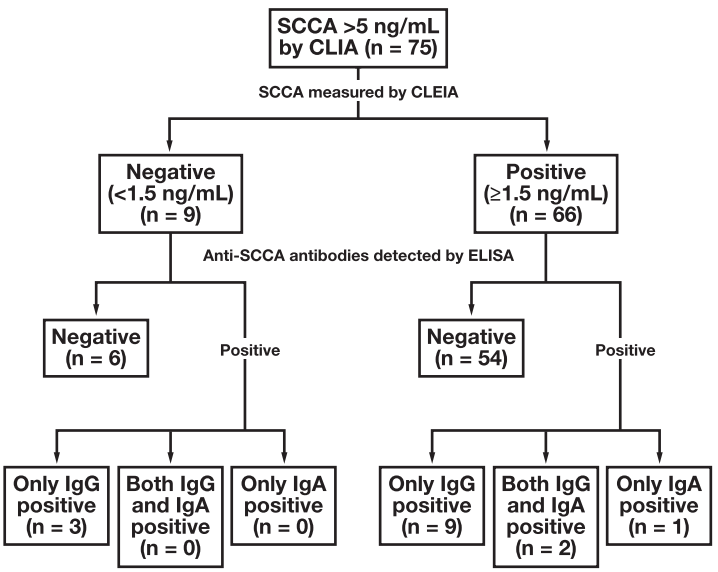

FIGURE 2. **Correlation between serum SCCA levels measured by CLEIA and CLIA. A, All samples (y = 0.708x + 1.164; *r* = 0.768). B, Samples with SCCA levels between 1.5 (cut-off) and 20 ng/mL measured by the CLIA. C, Bland-Altman plot analysis. CLEIA, chemiluminescent enzyme immunoassay; CLIA, chemiluminescent immunoassay; SCCA, squamous cell carcinoma antigen.**

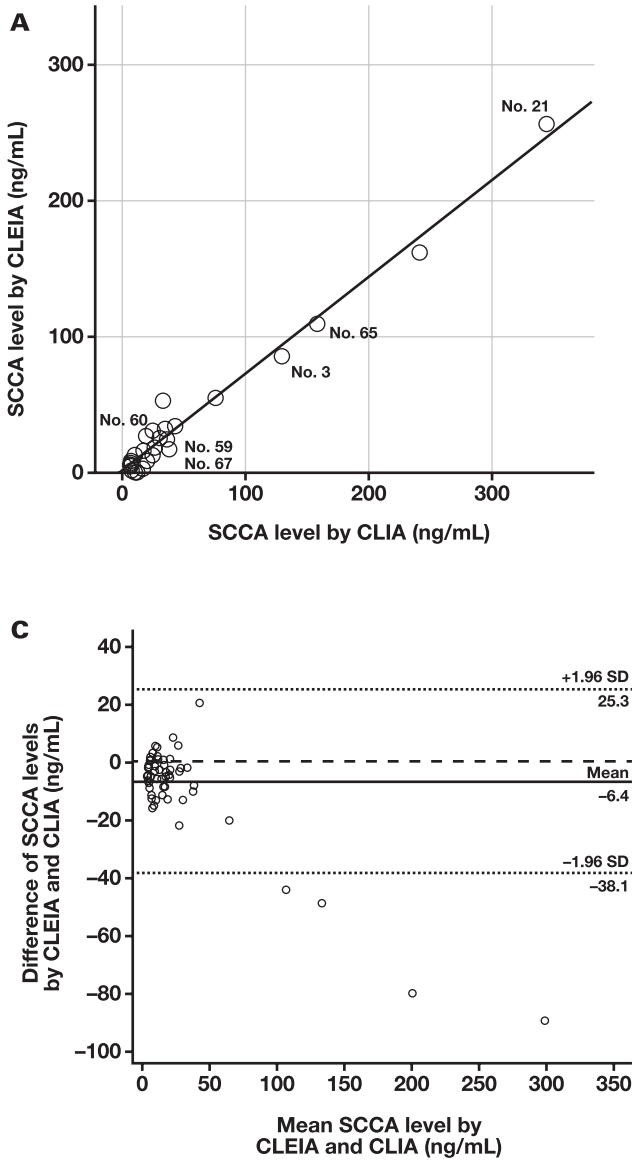

for sample 49. In samples positive for IgA-SCCA antibodies with or without IgG-SCCA antibodies, the SCCA levels measured by CLEIA were higher than those measured by CLIA, except for sample 75.

In 14 available samples out of 15 samples with SCCA antibodies, we performed absorption tests using anti-IgG or anti-IgA antibodies (**TABLE 2**). Statistical analysis between IgA, IgG, and IgA/G within CLEIA and CLIA samples showed no significant differences overall. The SCCA level of samples 74 and 75 decreased when incubated with anti-human IgG antibodies and measured by CLIA. Although some samples were suppressed by the absorption test, including 29 samples by the CLEIA method and 49 samples by the CLIA method, no consistent trend was observed. Therefore, we speculate that this fluctuation is caused by measurement variability.

Ratio of SCCA Levels by CLEIA to CLIA

The ratio of SCCA levels measured by CLEIA to those measured by CLIA was 0.83 overall, indicating a good correlation. However, SCCA levels

FIGURE 3. **ELISA fluorescent intensity ratio with/without coated SCCA (anti-human IgG, IgA, IgM-ALP). Boxes represent interquartile ranges and whiskers represent the range between the 2.5th and 97.5th percentiles. ALP, alkaline phosphatase; ELISA, enzyme-linked immunosorbent assay; Ig, immunoglobulin; SCCA, squamous cell carcinoma antigen.**

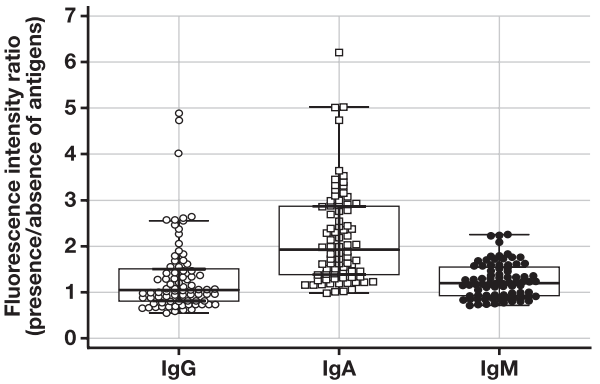

FIGURE 4. **ELISA signal comparison with/without coated SCCA in the presence of 10 μg/mL of free SCCA for anti-human IgG-ALP (A), anti-human IgA-ALP (B), and anti-human IgM-ALP (C). ALP, alkaline phosphatase; ELISA, enzyme-linked immunosorbent assay; Ig, immunoglobulin; SCCA, squamous cell carcinoma antigen.**

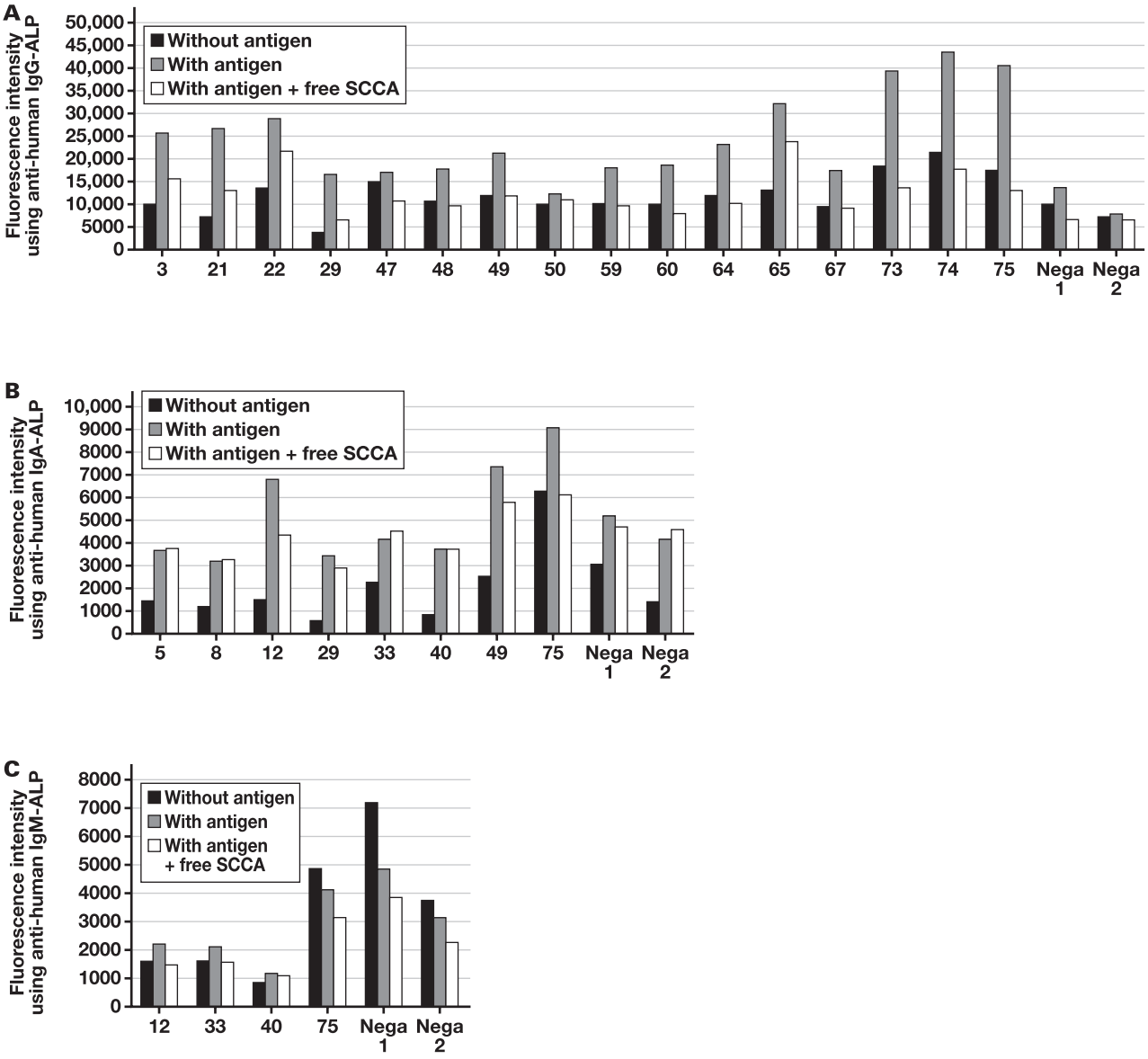

measured by CLEIA were mostly lower than those measured by CLIA. Of note, the ratio was 0.610 for samples positive for IgG-SCCA antibodies and was significantly lower than the ratio for samples without antibodies (0.876; P = .031). This may indicate that in samples with IgG-SCCA antibodies, the levels measured by CLIA are likely to be higher than those measured by CLEIA.

Analysis of False Positives Measured by CLIA

All 9 samples with SCCA levels below the CLEIA cutoff level of 1.5 ng/mL had SCCA levels of <20 ng/mL measured by CLIA. Therefore, we examined 52 samples with SCCA levels of <20 ng/mL measured by CLIA. No significant difference was observed between the presence and absence of IgG-SCCA antibodies, but IgG-SCCA antibodies were detected in 3 out of 9 samples (33%) in samples with <1.5 ng/mL and in samples >1.5 ng/mL, IgG-SCCA antibodies were detected with high probability compared with 5 out of 43 samples (12%).

Discussion

In prior studies that have examined the correlations between SCCA levels measured using different methods, the existence of an immune complex between SCCA and IgG or IgM autoantibodies was determined by analyzing SCCA samples by gel filtration for deviated samples.[2-4]

In this study, we examined 75 samples with high SCCA levels for the presence of an immune complex by performing ELISAs on samples with or without deviations between the SCCA assay methods. The ELISAs revealed anti-SCCA antibodies in 20% of the samples.

TABLE 1. Comparison of the SCCA levels measured by CLEIA and CLIA in samples with anti-SCCA antibodies

Sample No.	CLIA	CLEIA	Ratio[a]	Antibody type
3	129	85	0.66	IgG
12	7.4	12.7	**1.72**	IgA
21	344	254.8	0.74	IgG
22	5.1	3.7	0.73	IgG
29	9.7	6.6	0.68	IgG
48	16.8	15.8	0.94	IgG
49	18.8	27.1	**1.44**	IgG/IgA
59	22.4	18.3	0.82	IgG
60	36.9	23.7	0.64	IgG
64	7.9	0.9	0.11	IgG
65	158	109.2	0.69	IgG
67	22.2	16.8	0.76	IgG
73	9.8	0.7	0.07	IgG
74	12.4	1	0.08	IgG
75	16.5	3.3	0.20	IgG/IgA

CLEIA, chemiluminescent enzyme immunoassay; CLIA, chemiluminescent immunoassay; Ig, immunoglobulin; SCCA, squamous cell carcinoma antigen
[a]*Ratio of SCCA levels measured by CLEIA/CLIA.*

Autoantibodies against other tumor markers including carcinoembryonic antigen and prostate specific antigen[5,6] and hormones, such as prolactin (PRL) and thyrotropin,[7,8] have been reported. These autoantibodies cause abnormal values, and it is important to investigate the mechanism involved in the generation of autoantibodies.

In patients with hyperprolactinemia, anti-PRL autoantibodies were found in 10% to 25% of samples.[8] Hattori et al[9] suggested that PRL acidic isoform induces antigen stimulation in patients with anti-PRL autoantibodies. For SCCA, like PRL, a phosphorylated subfraction was detected by 2-dimensional electrophoresis combined with immunoblotting.[10]

The possibility that SCCA binds to IgA and IgG may be examined by performing absorption tests on samples in which the SCCA levels differed considerably.[11] In this study, we confirmed the presence of IgG- and IgA-SCCA antibodies by performing ELISAs. Abe et al[4] reported that CLIA uses antibodies with high reactivity to SCCA1, whereas CLEIA uses antibodies with high reactivity to SCCA2. Comparing the SCCA levels of the samples positive for anti-SCCA antibodies between the 2 assay methods, the SCCA levels measured by CLIA were higher than those measured by CLEIA in samples with IgG-SCCA antibodies, suggesting a predominance of SCCA1 in many samples. By comparison, in samples positive for only IgA-SCCA antibodies, the SCCA levels measured by

TABLE 2. Absorption tests using anti-human Ig (IgG, IgA or both) antibodies[a]

Sample No.	Antibody type	CLEIA			CLIA		
		IgA	IgG	IgA + IgG	IgA	IgG	IgA + IgG
3	IgG	7.74 (7.46) 104%	7.55 (7.55) 100%	7.07 (7.53) 94%	12.0 (11.6) 103%	12.9 (11.6) 111%	10.3 (11.6) 89%
12	IgA	1.06 (1.00) 106%	1.07 (1.07) 100%	1.04 (1.01) 103%	0.7 (0.7) 100%	0.7 (0.9) 78%	0.8 (0.7) 114%
21	IgG	21.77 (21.41) 102%	22.33 (21.00) 106%	21.80 (20.97) 104%	36.2 (34.4) 105%	39.6 (34.4) 115%	35.7 (34.4) 104%
22	IgG	0.36 (0.40) 89%	0.35 (0.40) 87%	0.36 (0.40) 91%	0.5 (0.5) 100%	0.4 (0.5) 80%	0.7 (0.5) 140%
29	IgG	0.62 (0.53) 117%	0.70 (0.55) 128%	0.66 (0.54) 122%	1.0 (0.9) 111%	0.8 (0.9) 89%	0.9 (0.9) 100%
48	IgG	1.66 (1.61) 103%	1.38 (1.56) 88%	1.55 (1.61) 96%	2.2 (2.0) 110%	1.5 (2.0) 75%	1.9 (2.0) 95%
49	IgA/IgG	2.18 (2.04) 107%	2.17 (2.06) 106%	2.35 (2.00) 117%	1.9 (1.6) 119%	1.8 (1.4) 129%	1.7 (1.7) 100%
59	IgG	1.27 (1.34) 95%	1.28 (1.33) 96%	1.56 (1.33) 117%	1.7 (1.6) 106%	1.5 (1.6) 94%	1.9 (1.6) 119%
60	IgG	2.14 (2.18) 98%	2.37 (2.21) 107%	2.09 (2.24) 93%	3.5 (3.7) 95%	4.4 (3.7) 119%	3.8 (3.7) 103%
64	IgG	0.26 (0.42) 62%	0.38 (0.42) 91%	0.27 (0.42) 65%	0.8 (1.1) 73%	0.9 (1.1) 82%	0.8 (1.1) 73%
65	IgG	9.12 (8.62) 106%	8.52 (8.72) 98%	8.88 (8.69) 102%	15.3 (13.2) 116%	13.7 (13.2) 104%	13.6 (13.2) 103%
73	IgG	0.18 (0.22) 83%	0.16 (0.21) 75%	0.22 (0.21) 103%	1.0 (1.1) 91%	0.9 (1.1) 82%	1.6 (1.1) 145%
74	IgG	0.18 (0.26) 68%	0.17 (0.26) 66%	0.19 (0.26) 72%	0.8 (1.6) 50%	0.8 (1.6) 50%	0.9 (1.6) 56%
75	IgA/IgG	0.29 (0.36) 80%	0.20 (0.38) 52%	0.24 (0.37) 65%	1.6 (1.8) 89%	0.6 (1.6) 38%	1.2 (1.6) 75%
Control		4.36 (4.26) 102%	4.38 (4.58) (96%)	4.39 (4.23) 104%	3.9 (4.0) 98%	3.6 (4.3) 84%	3.7 (3.6) 103%

CLEIA, chemiluminescent enzyme immunoassay; CLIA, chemiluminescent immunoassay; Ig, immunoglobulin; SCCA, squamous cell carcinoma antigen.
[a]*Incubated value (reference value) and absorption ratio are shown in each column.*

CLEIA were higher than those measured by CLIA, suggesting a predominance of SCCA2.

Of the 3 samples positive for IgA-SCCA antibodies for which the absorption test was performed, the SCCA level measured by CLIA was higher than that measured by CLEIA for sample 75, suggesting a predominance of SCCA1. By comparison, for samples 12 and 49, the SCCA levels tended to be higher with CLEIA than with CLIA, suggesting a predominance of SCCA2. For sample 75, although the SCCA level could not be determined by CLEIA because of the low level, the absorption test with anti-IgG antibodies showed a low value of 38% by CLIA These results indicate that the reactivity between SCCA1 and IgG-SCCA antibodies can affect the CLIA measurement system and may lead to falsely high SCCA levels. Because the absorption test showed a low value, it was considered that the immune complex reacted nonspecifically with the reagent and directly affected the reaction system. However, a limitation of this study is that we did not quantify SCCA1 or SCCA2 levels in the samples. In addition, due to the small number of samples and the characteristics of the assay, for example, in the case of IgM, the amount of antibody was small, so it is possible that the presence could not be accurately determined. Therefore, more detailed investigation would be useful in the future.

Conclusion

We detected IgG- and IgA-SCCA antibodies and clarified their effects on measuring SCCA levels using CLIA. The CLIA method may yield falsely high or false-positive results in samples with IgG-SCCA antibodies.

Acknowledgments

We thank Dr. Kazuhiro Shimazu of Tosoh for his contribution to ELISA development and other experiments.

Conflict of Interest Disclosure

The authors have nothing to disclose.

REFERENCES

1. Kato H, Torigoe T. Radioimmunoassay for tumor antigen of human cervical squamous cell carcinoma. *Cancer.* 1977;40(4):1621-1628. doi:10.1002/1097-0142(197710)40:4<1621::aid-cncr2820400435>3.0.co;2-i
2. Chen H, Tian L, Chen J, et al. Evaluation of 2 commercially systems for detection of serum squamous cell carcinoma antigen in pan squamous cell carcinoma. *Cancer Control*. 2020;27:1-9. doi: 10.1177/1073274820983025
3. Beneduce L, Castaldi F, Marino M, et al. Squamous cell carcinoma antigen-immunoglobulin M complexes as novel biomarkers for hepatocellular carcinoma. *Cancer.* 2005;103(12):2558-2565. doi:10.1002/cncr.21106
4. Abe M, Yagi M, Suzuki H. Comparison of measurement values of two different SCC measurement reagents-focusing on the relevance to SCCA-1 and SCCA-2 antigen levels in squamous cell carcinoma. *JCCLA.* 2019;44:224-230 (in Japanese).
5. Ura Y, Ochi Y, Hamazu M, Ishida M, Nakajima K, Watanabe T. Studies on circulating antibody against carcinoembryonic antigen (CEA) and CEA-like antigen in cancer patients. *Cancer Lett.* 1985;25(3):283-295. doi:10.1016/s0304-3835(15)30008-2
6. Zisman A, Zisman E, Lindner A, Velikanov S, Siegel YI, Mozes E. Autoantibodies to prostate specific antigen in patients with benign prostatic hyperplasia. *J Urol.* 1995;154(3):1052-1055.
7. Sakai H, Fukuda G, Suzuki N, Watanabe C, Odawara M. Falsely elevated thyroid-stimulating hormone (TSH) level due to macro-TSH. *Endocr J.* 2009;56(3):435-440. doi:10.1507/endocrj.k08e-361
8. Shimatsu A, Hattori N. Macroprolactinemia: diagnostic, clinical, and pathogenic significance. *Clin Dev Immunol.* 2012;2012:1-7. doi:10.1155/2012/167132
9. Hattori N, Ikekubo K, Nakaya Y, Kitagawa K, Inagaki C. Immunoglobulin G subclasses and prolactin (PRL) isoforms in macroprolactinemia due to anti-PRL autoantibodies. *J Clin Endocrinol Metab.* 2005;90(5):3036-3044. doi:10.1210/jc.2004-1600
10. Abe H, Okuno N, Takeda O, Suminami Y, Kato H, Nakamura K. Analysis on heterogeneity of squamous cell carcinoma antigen by two-dimensional electrophoresis. *Electrophoresis.* 1994;15(7):988-991. doi:10.1002/elps.11501501145
11. Mori E, Kurano M, Tobita A, Shimosaka H, Yatomi Y. Existence of a squamous cell carcinoma antigen-immunoglobulin complex causes a deviation between squamous cell carcinoma antigen concentrations determined using two different immunoassays: first report of squamous cell carcinoma antigen coupling with immunoglobulin A. *Ann Clin Biochem.* 2017;54(6):655-663. doi:10.1177/0004563216677584

Predictors of mortality and transfusion requirements in venoarterial extracorporeal membrane oxygenation patients

Jongmin Kim, MD[1], Hye Ju Yeo, MD, PhD[2,3], Woo Hyun Cho, MD, PhD[2,3], Hyun-Ji Lee, MD, PhD[3,4,5]

[1]Department of Laboratory Medicine, Pusan National University Hospital, Busan, Korea; [2]Division of Allergy, Pulmonary and Critical Care Medicine, Department of Internal Medicine, Pusan National University School of Medicine, Yangsan, Korea, [3]Research Institute for Convergence of Biomedical Science and Technology, Pusan National University Yangsan Hospital, Yangsan, Republic of Korea, and [4]Department of Laboratory Medicine, Pusan National University Yangsan Hospital, Yangsan, Korea; [5]Department of Laboratory Medicine, Pusan National University School of Medicine, Yangsan, Korea. Corresponding author: Hyun-Ji Lee; hilhj1120@gmail.com

Key words: extracorporeal membrane oxygenation; in-hospital mortality; thrombocytopenia; platelet count; blood transfusion

Abbreviations: ECMO, extracorporeal membrane oxygenation; VA, venoarterial; RBC, red blood cell; Hb, hemoglobin; APACHE, Acute Physiology and Chronic Health Evaluation; SOFA, Sequential Organ Failure Assessment; ICU, intensive care unit; ECPR, extracorporeal cardiopulmonary resuscitation; FFP, fresh frozen plasma; CNS, central nervous system; UFH, unfractionated heparin; aPTT, activated partial thromboplastin time

Laboratory Medicine 2024;55:347-354; https://doi.org/10.1093/labmed/lmad089

ABSTRACT

Objective: The aim of this study was to evaluate the prognostic impact of variables, including thrombocytopenia and the amount of platelet transfusion, for predicting survival in venoarterial extracorporeal membrane oxygenation (ECMO) recipients. Additionally, we aimed to identify the predictors of increased transfusion requirement during venoarterial ECMO support.

Methods: All patients who received venoarterial ECMO between December 2008 and March 2020 were retrospectively analyzed. Univariate and multivariate Cox regressions were used to evaluate in-hospital mortality according to variables including thrombocytopenia and daily average of platelet concentrate transfusion. Stepwise multiple linear regression analysis was used to identify independent predictors for transfusion requirements.

Results: Analysis of 218 patients demonstrated severe thrombocytopenia as an independent predictor of in-hospital mortality (hazard ratio = 2.840, 95% CI: 1.593-5.063, $P < .001$), along with age, pre-ECMO cardiac arrest, and pH. In contrast, the amount of platelet transfusion was not associated with in-hospital mortality. Multiple variables, including the type of indication for ECMO were associated with transfusion requirements.

Conclusion: Our findings identified severe thrombocytopenia as an independent prognostic factor of in-hospital mortality. However, daily average platelet transfusion was not associated with survival outcomes. Additionally, our study identified predictive variables of increased transfusion requirements.

Introduction

The use of extracorporeal membrane oxygenation (ECMO) has dramatically increased in recent years owing to several factors, such as availability of durable membranes and portable circuits, increased familiarity with the therapy, and the progress in durable mechanical circulatory support devices.[1] Despite these advancements, platelet dysfunction and thrombocytopenia remain significant challenges for ECMO patients,[1–10] particularly in venoarterial (VA) ECMO settings. Although bleeding and thrombotic events are the major complications of ECMO contributing to increased morbidity and mortality,[11–14] thrombocytopenia is not included in the scoring systems of some well-established prediction models.[15,16] Recent studies have evaluated the role of thrombocytopenia as a predictor of survival in ECMO patients and found that relative early decrease of platelets, persistent thrombocytopenia, and pre-ECMO thrombocytopenia defined as $<100 \times 10^3/\mu L$ were risk factors for mortality.[17-19] However, the relationship between thrombocytopenia and survival outcomes according to severity of thrombocytopenia has not been fully explored.

More than 20% of patients receiving VA ECMO suffer from thrombocytopenia,[7] leading to a higher demand for platelet transfusion. Currently, the Extracorporeal Life Support Organization recommends maintaining a platelet count $>80 \times 10^3/\mu L$ in patients without bleeding.[20] However, in the absence of evidence-based guidelines for transfusion in ECMO patients, exploration for adequate blood utilization is ongoing. Although multiple studies have reported that increased red blood cell (RBC) transfusion is associated with survival outcomes in patients receiving ECMO,[14,21]

studies evaluating the effect of platelet transfusion on mortality are scarce.[22] Therefore, we felt compelled to evaluate the effect of the amount of platelet transfusion on survival outcomes of ECMO patients.

The primary objective of this study was to evaluate the prognostic impact of variables, including pre-ECMO thrombocytopenia and the amount of platelet transfusion, for predicting survival in VA ECMO patients. The secondary objective was to identify the predictors of increased transfusion requirement during VA ECMO support. This study aimed to provide valuable information regarding the role of pre-ECMO thrombocytopenia and platelet transfusion in prognosis and prediction of transfusion requirements for patients receiving VA ECMO.

Materials and Methods

Data Collection

We retrospectively investigated all patients who received VA ECMO between December 2008 and March 2020 at the Pusan National University Yangsan Hospital, Yangsan, South Korea. All data were obtained from the electromedical records. The pre-ECMO variables included hemoglobin (Hb) level, platelet count, Acute Physiology and Chronic Health Evaluation (APACHE) II score and Sequential Organ Failure Assessment (SOFA) score at intensive care unit (ICU) admission, history of pre-ECMO cardiac arrest, immunocompromised status, steroid treatment, and infection. "Immunocompromised" was defined as hematologic malignancies, a solid organ tumor, HIV infection, or under immunosuppressant treatment. The pre-ECMO platelet count was classified into the following categories of thrombocytopenia severity: (1) normal, platelet count ≥140 × 10^3/μL; (2) mild, platelet count <140 × 10^3/μL and ≥100 × 10^3/μL; (3) moderate, platelet count <100 × 10^3/μL and ≥50 × 10^3/μL; and (4) severe, platelet count <50 × 10^3/μL. Additionally, arterial blood gas analyses for pH, partial pressure of carbon dioxide ($PaCO_2$), partial pressure of oxygen (PaO_2), and oxygen saturation (SaO_2) at ECMO initiation, duration of ECMO, and indications for ECMO were performed. The indications for ECMO were classified into 6 categories: bridge-to-transplant, extracorporeal cardiopulmonary resuscitation (ECPR), postcardiac surgery, cardiogenic shock due to acute coronary syndrome, cardiogenic shock due to acute myocarditis, and cardiogenic shock due to other causes (including refractory ventricular tachycardia, pulmonary thromboembolism, and septic shock). Average transfusion units per day (total units of transfused blood components during ECMO divided by the ECMO duration in days) of RBCs, platelet concentrates, and fresh frozen plasma (FFP) during ECMO were also investigated. Transfusion of platelet concentrate was classified into 2 groups, >8 units/day and ≤8 units/day, because a routine 8 units of platelet concentrate transfusion was adopted for ECMO patients who needed platelet transfusion. We assessed in-hospital survival status and length of hospital stay of patients on VA ECMO to analyze patient outcomes. In-hospital mortality was defined as in-hospital death from any cause among patients receiving VA ECMO. Furthermore, we assessed thrombotic or hemorrhagic complications, including pulmonary hemorrhage, central nervous system (CNS) infarction, CNS hemorrhage, surgical site bleeding, hemolysis, gastrointestinal bleeding, disseminated intravascular coagulation, cannula site bleeding, retroperitoneal bleeding, and pulmonary thromboembolism. Patients with missing data other than APACHE II or SOFA scores were excluded.

ECMO Implantation and Management

Management of the ECMO protocol is based on the ELSO guidelines,[20] and bedside care for patients undergoing ECMO was provided by a multidisciplinary intensive care team.[23] All catheters were managed using a standardized protocol and were inserted peripherally by an experienced cardiothoracic surgeon using the Seldinger approach under ultrasound guidance. The ECMO system consisted of a polymethylpentene fiber oxygenator system (Quadrox PLS; Maquet) with simplified bioline-coated circuits (Maquet). All patients were supported by centrifugal pumps (Maquet). The patients received an initial unfractionated heparin (UFH) bolus at 50 units/kg body weight when the cannula was placed, and UFH was infused continuously during the ECMO. The heparin infusion was regulated to maintain activated partial thromboplastin time (aPTT) at 80 to 90 seconds, which was obtained every 6 hours. In case of bleeding, the aPTT target was set at 60 to 70 seconds. If heparin-induced thrombocytopenia was suspected, a heparin-PF4 antibody test was conducted, UFH was discontinued, and argatroban was infused to maintain aPTT at 80 to 90 seconds. Transfusion was performed based on a platelet count of ≤80,000 × 10^3/μL and hemoglobin level of ≤80 g/L.

Statistical Analysis

Continuous variables are described as means with standard deviations, and categorical variables are described as percentages and counts. Normality tests were performed using the Kolmogorov-Smirnov and Shapiro-Wilk tests. Student *t*-test and Mann-Whitney *U* test were used for normally distributed and nonnormally distributed continuous variables, respectively. Categorical variables were analyzed using the χ^2 test when <25% of cells had expected frequencies less than 5 or Fisher's exact test when ≥25% of cells had expected frequencies less than 5. Univariate Cox regression analysis was performed for variables that were statistically significant ($P < .05$) using the Student *t*-test, Mann-Whitney test, χ^2 test, and Fisher's exact test. Multivariate Cox regression analysis was used to identify independent predictors of outcome among the variables that were shown to achieve statistical significance at $P < .05$ in the univariate Cox regression analysis. The log-rank test was used to compare cumulative survival according to the severity of thrombocytopenia or the amount of daily platelet transfusion. Stepwise multiple linear regression analysis was used to identify independent predictors for transfusion requirements. In the multiple linear regression analysis, platelet count (×10^3/μL) was used as a continuous variable instead of the severity classification of thrombocytopenia. All statistical analyses were performed using IBM SPSS Statistics for Windows, version 22 (IBM). Line art and graphs were generated using SPSS, Microsoft PowerPoint (Microsoft), and R Statistical Software (v4.1.3; R Core Team 2021) with the R package survminer version 0.4.9.

Ethical Statement

This study was approved by the Institutional Review Board of Pusan National University Yangsan Hospital, Yangsan, Korea (approval No.05-2022-004). The requirement for informed consent was waived because of the retrospective nature of the study and because the analysis used anonymous clinical data.

Results

A total of 265 patients received VA ECMO support, of which 47 were excluded from the study because of missing data. Two hundred and

eighteen patients, 111 in-hospital survivors and 107 nonsurvivors, with a median follow-up of 130.5 days (range: 0-4152 days) were analyzed. Characteristics of the patients are listed in **TABLE 1**, according to in-hospital survival outcomes. The nonsurvivors were older (60.7 ± 13.2 vs 55.0 ± 16.4 years, P = .002), had lower pre-ECMO Hb (112.4 ± 2.9.1 vs 122.0 ± 24.6 g/L, P = .035) and pH (6.9 ± 2.1 vs 7.4 ± 0.1, P = .007), and showed a higher percentage that experienced pre-ECMO cardiac arrest (51.4% vs 24.3%, P < .001). The severity of thrombocytopenia differed between the nonsurvivors and survivors, nonsurvivors demonstrating a higher ratio of severe thrombocytopenia compared with the survivors (20.6% vs 0.0%). Additionally, the indications for ECMO differed between the 2 groups (P < .001).

TABLE 1. Patient demographics and ECMO-related variables according to in-hospital outcomes[a]

	All patients (n = 218)	Survivors (n = 111)	Nonsurvivors (n = 107)	*P*
Demographics				
Age, y	57.8 ± 15.1	55.0 ± 16.4	60.7 ± 13.2	.002
Male	61.0% (133)	59.5% (66)	62.6% (67)	.633
Pre-ECMO characteristics				
Pre-ECMO Hb, g/L	117.3 ± 27.3	122.0 ± 24.6	112.4 ± 29.1	.035
Pre-ECMO thrombocytopenia				<.001
Normal	67.0% (146)	75.7% (84)	57.9% (62)	
Mild	10.6% (23)	11.7% (13)	9.3% (10)	
Moderate	12.4% (27)	12.6% (14)	12.1% (13)	
Severe	10.1% (22)	0.0% (0)	20.6% (22)	
Pre-ECMO cardiac arrest	37.6% (82)	24.3% (27)	51.4% (55)	<.001
Immunocompromised	3.2% (7)	4.5% (5)	1.9% (2)	.446
Steroid	5.5% (12)	8.1% (9)	2.8% (3)	.136
Infection	33.5% (73)	31.5% (35)	35.5% (38)	.568
APACHE II score[b]	12.1 ± 7.0	11.0 ± 6.6	13.2 ± 7.2	.053
SOFA score[c]	10.4 ± 4.8	8.6 ± 4.7	12.1 ± 4.2	<.001
Blood gas at ECMO initiation				
pH	7.1 ± 1.5	7.4 ± 0.1	6.9 ± 2.1	.007
$PaCO_2$, mmHg	32.7 ± 10.4	33.4 ± 7.7	31.9 ± 12.6	.760
PaO_2, mmHg	149.3 ± 108.8	147.8 ± 96.4	150.8 ± 120.8	.302
SaO_2, %	94.2 ± 18.6	97.7 ± 4.1	90.6 ± 25.8	.189
ECMO characteristics				
Days on ECMO	5.7 ± 7.4	5.7 ± 6.5	5.7 ± 8.3	.151
ECMO indication				<.001
Bridge to transplant	10.6% (23)	15.3% (17)	5.6% (6)	
ECPR	50.0% (109)	34.2% (38)	66.4% (71)	
Post cardiac surgery	7.3% (16)	4.5% (5)	10.3% (11)	
Cardiogenic shock, ACS	15.6% (34)	24.3% (27)	6.5% (7)	
Cardiogenic shock, acute myocarditis	6.4% (14)	10.8% (12)	1.9% (2)	
Cardiogenic shock, other	10.1% (22)	10.8% (12)	9.3% (10)	
Transfusion events on ECMO, unit/day				
RBC transfusions	4.8 ± 8.3	2.8 ± 3.5	6.8 ± 10.9	.002
FFP transfusions	2.8 ± 5.5	1.5 ± 2.5	4.4 ± 7.2	.033
PLT transfusions	5.3 ± 6.2	4.8 ± 6.2	5.6 ± 6.3	.202
PLT transfusions, categorical				.035
≤8	78.0% (170)	83.8% (93)	72.0% (77)	
>8	22.0% (48)	16.2% (18)	28.0% (30)	

ACS, acute coronary syndrome; APACHE, Acute Physiology and Chronic Health Evaluation; ECMO, extracorporeal membrane oxygenation; ECPR, extracorporeal cardiopulmonary resuscitation; FFP, fresh frozen plasma; Hb, hemoglobin; ICU, intensive care unit; $PaCO_2$, partial pressure of carbon dioxide; PaO_2, partial pressure of oxygen; PLT, platelet; RBC, red blood cell; SaO_2, oxygen saturation; SOFA, Sequential Organ Failure Assessment.
[a]Data are given as % (n) or mean ± SD.
[b]At ICU admission, 12 patients were missing data.
[c]At ICU admission, 10 patients were missing data.

Nonsurvivors demonstrated more cases of ECPR and postcardiac surgery and fewer cases of bridge-to-transplant, acute coronary syndrome, and acute myocarditis compared with survivors. Further, the nonsurvivors received more RBC (6.8 ± 10.9 vs 2.8 ± 3.5 unit/day, P = .002) and FFP (4.4 ± 7.2 vs 1.5 ± 2.5 unit/day, P = .033) transfusions compared with survivors. Additionally, nonsurvivors demonstrated a higher ratio of PLT concentrate transfusion >8 (28.0% vs 16.2%, P = .035). However, no significant difference in platelet transfusion was found between survivors and nonsurvivors when daily average of transfusion was analyzed in a continuous variable form (nonsurvivors: 5.6 ± 6.3 vs survivors: 4.8 ± 6.2 unit/day, P = .202).

The univariate Cox regression analysis revealed that age, pre-ECMO Hb, severe thrombocytopenia, pre-ECMO cardiac arrest, pH, SOFA score at ICU admission, and RBC and FFP transfusion were associated with in-hospital mortality (**TABLE 2**). However, PLT transfusion >8 unit/day was not associated with survival outcomes (hazard ratio = 1.377, 95% CI 0.902-2.101, P = .138). The multivariate Cox regression analysis identified severe thrombocytopenia as an independent predictor of in-hospital mortality (hazard ratio = 2.840, 95% CI, 1.593-5.063; P < .001), along with age, pre-ECMO cardiac arrest, and pH (**TABLE 2**). In contrast, the amount of RBC and FFP transfusion was not associated with in-hospital mortality in the multivariate analysis.

The Kaplan-Meier curves for in-hospital survival in VA ECMO patients according to thrombocytopenia and PLT transfusion are illustrated in **FIGURE 1**. During a mean of 35.07 days of hospital stay (range: 0-324 days), patients with pre-ECMO severe thrombocytopenia showed poor in-hospital survival compared with those with all other severities of thrombocytopenia (**FIGURE 1A**; P < .001).

The thrombotic or hemorrhagic complications according to the severity of thrombocytopenia are presented in **TABLE 3**. Our findings showed that among these complications, only CNS infarction was significantly associated with the severity of thrombocytopenia. However, none of the patients with pre-ECMO severe thrombocytopenia had a CNS infarction.

The stepwise multiple linear regression analysis for transfusion requirements is shown in **TABLE 4**. Lower pre-ECMO Hb and platelet count were associated with increased RBC and PLT requirements, respectively. The average transfusion amount in units per day according to indications of ECMO is represented in **FIGURE 2**. The transfusion requirements of RBC, FFP, and PLT were the highest in patients who received ECMO support following cardiac surgery.

Discussion

This study identified severe pre-ECMO thrombocytopenia as an independent predictor of in-hospital mortality in patients who underwent VA ECMO. This finding is in line with a previous study in which a criterion for pre-ECMO platelet of <100 × 10^3/μL was adopted in predicting in-hospital mortality.[18] However, in this study, the multivariate analysis revealed that platelet counts of 50-100 × 10^3/μL (moderate thrombocytopenia) and 100-140 × 10^3/μL (mild thrombocytopenia) did not have a negative impact on in-hospital survival outcomes compared with normal

TABLE 2. Univariate and multivariate Cox regression analyses for in-hospital mortality[a]

	Univariate analysis		Multivariate analysis	
	HR (95% CI)	*P*	HR (95% CI)	*P*
Age	1.019 (1.005-1.032)	.006	1.022 (1.008-1.036)	.002
Pre-ECMO Hb	0.989 (0.982-0.997)	.005	0.997 (0.989-1.005)	.490
Thrombocytopenia (reference: normal platelet count)				
Mild thrombocytopenia	1.065 (0.545-2.079)	.883	0.883 (0.434-1.794)	.730
Moderate thrombocytopenia	1.115 (0.611-2.034)	.980	0.992 (0.529-1.862)	.980
Severe thrombocytopenia	5.427 (3.286-8.963)	<.001	3.770 (2.127-6.683)	<.001
Pre-ECMO cardiac arrest	2.235 (1.513-3.301)	<.001	2.167 (1.453-3.232)	<.001
pH	0.724 (0.655-0.799)	<.001	0.833 (0.720-0.964)	.014
APACHE II score at ICU admission	1.022 (0.996-1.049)	.093		
SOFA score at ICU admission	1.124 (1.077-1.174)	<.001		
ECMO indication (Reference: Cardiogenic shock—others)				
Bridge to transplant	0.448 (0.163-1.233)	.120		
ECPR	1.797 (0.925-3.488)	.083		
Post-cardiac surgery	1.859 (0.789-4.384)	.156		
Cardiogenic shock, ACS	0.394 (0.150-1.035)	.059		
Cardiogenic shock, acute myocarditis	0.325 (0.071-1.487)	.147		
RBC transfusions (units/day)	1.062 (1.043-1.082)	<.001	1.048 (0.986-1.114)	.129
FFP transfusions (units/day)	1.079 (1.049-1.110)	<.001	0.985 (0.904-1.074)	.733
PLT transfusion > 8 (units/day)	1.377 (0.902-2.101)	.138		

ACS, acute coronary syndrome; APACHE, Acute Physiology and Chronic Health Evaluation; ECMO, extracorporeal membrane oxygenation; ECPR, extracorporeal cardiopulmonary resuscitation; FFP, fresh frozen plasma; Hb, hemoglobin; HR, hazard ratio; ICU, intensive care unit; PLT, platelet; RBC, red blood cell; SOFA, Sequential Organ Failure Assessment; .

[a]*Variables with* P < *.05 in univariate analysis were subjected to multivariate analysis. Multivariate cox regression analysis was set with entry and removal* P *values of .05 and .1, respectively. The multivariate analysis did not include the SOFA score because the criteria included* PaO_2 *and platelet count, thereby violating the independence among the analyzed variables.*

FIGURE 1. Kaplan-Meier cumulative survival curves according to the severity of thrombocytopenia (log-rank test P <.001) (A) and daily average platelet transfusion (log-rank test P =.130) (B). ECMO, extracorporeal membrane oxygenation.

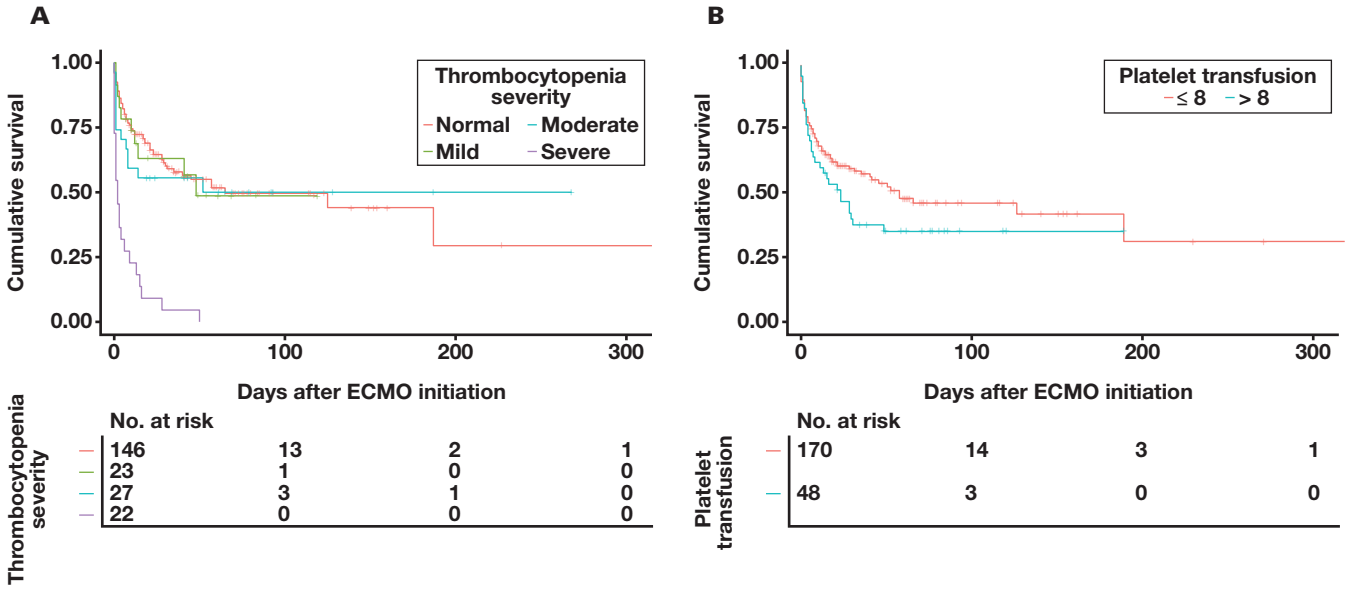

TABLE 3. Thrombotic or hemorrhagic complications according to thrombocytopenia severity

	Total (n = 218)	Thrombocytopenia				P
		Normal (n = 146)	Mild (n = 23)	Moderate (n = 27)	Severe (n = 22)	
Pulmonary hemorrhage (n = 8)	3.7% (8)	62.5% (5)	12.5% (1)	0% (0)	25.0% (2)	.405
CNS infarction (n = 10)	4.6% (10)	40.0% (4)	30.0% (3)	30.0% (3)	0% (0)	.035
CNS hemorrhage (n = 4)	1.8% (4)	50.0% (2)	25.0% (1)	25.0% (1)	0% (0)	.590
Surgical site bleeding (n = 15)	6.9% (15)	46.7% (7)	20.0% (3)	20.0% (3)	13.3% (2)	.351
Hemolysis (n = 2)	0.9% (2)	50.0% (1)	50.0% (1)	0% (0)	0% (0)	.318
GI bleeding (n = 4)	1.8% (4)	50.0% (2)	25.0% (1)	0% (0)	25.0% (1)	.497
DIC (n = 12)	5.5% (12)	58.3% (7)	16.7% (2)	8.3% (1)	16.7% (2)	.728
Cannula site bleeding (n = 46)	21.1% (46)	71.7% (33)	10.9% (5)	6.5% (3)	10.9% (5)	.603
Retroperitoneal bleeding (n = 7)	3.2% (7)	100.0% (7)	0% (0)	0% (0)	0% (0)	.920
PTE (n = 7)	3.2% (7)	85.7% (6)	0% (0)	0% (0)	14.3% (1)	.539

CNS, central nervous system; DIC, disseminated intravascular coagulation; GI, gastrointestinal; PTE, pulmonary thromboembolism.

platelet count. Therefore, we suggest that classifying thrombocytopenia into 2 categories, severe (platelet count <50 × 10^3/μL) and nonsevere (platelet count ≥50 × 10^3/μL), may be useful in risk stratification for VA ECMO patients.

Severe thrombocytopenia is prevalent in patients treated with ECMO.[7] It seems obvious that patients with low platelet counts are vulnerable to ECMO support, and well-known complications include bleeding and thromboembolic events. Interestingly, Opfermann et al[17] reported that thrombocytopenia also reflects conditions associated with poor outcomes, such as multiple organ failure and sepsis in patients receiving ECMO after cardiac surgery. This indicates that identifying pre-ECMO thrombocytopenia in risk stratification can be beneficial because a low platelet count indicates not only the potential risk of bleeding and thrombotic complications but also other poor outcome-related conditions.

Consistent with this, the results of our study demonstrated that thrombotic or hemorrhagic complications were not associated with the severity of thrombocytopenia in patients undergoing VA ECMO except for CNS infarction. However, none of the patients with severe pre-ECMO thrombocytopenia experienced CNS infarction, revealing that severe pre-ECMO thrombocytopenia was not associated with an increase in thrombotic or bleeding complications. Additionally, it implies that thrombotic or bleeding complications were not implicated in the negative impa m,./0c1t of severe thrombocytopenia on in-hospital survival. Further investigations are needed to elucidate the underlying mechanisms of thrombocytopenia in patients receiving ECMO.

In addition to thrombocytopenia, age, pH, and pre-ECMO cardiac arrest were associated with poor outcomes. Similar findings have been reported for pre-ECMO cardiac arrest in respiratory ECMO and ECMO for cardiogenic shock, where survival prediction models implement pre-ECMO as a prognostic factor.[15,16] The high prevalence of post–cardiac arrest sequelae such as brain injury and extracerebral organ dysfunction[24–26] may have negatively influenced the survival outcomes of patients receiving VA ECMO.

TABLE 4. Stepwise multiple linear regression analysis of predictors of transfusion requirements

	Unstandardized coefficient			Standardized coefficient		
	B	SE	95% CI	Beta	t	*P*
RBC						
(Constant)	22.36	3.57	15.32-29.40		6.26	<.001
SaO_2	–0.11	0.03	–0.17 to –0.05	–0.23	–3.54	<.001
Pre-ECMO Hb	–0.53	0.20	–0.93 to –0.13	–0.17	–2.63	.009
Days on ECMO	–0.21	0.07	–0.35 to –0.06	–0.19	–2.81	.005
ECMO indication: post cardiac surgery	5.20	2.02	1.22-9.17	0.16	2.57	.011
FFP						
(Constant)	6.04	2.21	1.69-10.40		2.74	.007
Days on ECMO	–0.17	0.05	–0.26 to –0.07	–0.23	–3.44	<.001
ECMO indication: post cardiac surgery	3.84	1.37	1.14-6.55	0.18	2.80	.006
SOFA score	0.19	0.08	0.04-0.34	0.16	2.44	.016
Not immunocompromised	–4.54	2.03	–8.53 to –0.54	–0.15	–2.24	.026
PLT						
(Constant)	7.03	3.20	0.72-13.34		2.20	.029
Pre-ECMO PLT	–0.01	0.00	–0.02-0.00	–0.18	–2.87	<.001
ECMO indication: bridge to transplant	6.26	1.34	3.61-8.90	0.31	4.67	<.001
ECMO indication: post cardiac surgery	6.99	1.55	3.92-10.05	0.30	4.50	<.001
ECMO indication: ECPR	7.91	2.33	3.31-12.51	0.63	3.39	<.001
Pre-ECMO cardiac arrest	5.68	2.29	1.17-10.19	0.45	2.48	.014
Not immunocompromised	–7.95	2.14	–12.17 to –3.73	–0.23	–3.72	<.001

ECMO, extracorporeal membrane oxygenation; ECPR, extracorporeal cardiopulmonary resuscitation; FFP, fresh frozen plasma; Hb, hemoglobin; PLT, platelet; RBC, red blood cell; SaO_2, oxygen saturation; SOFA, Sequential Organ Failure Assessment.

FIGURE 2. Average transfusion in unit/day according to the type of ECMO indications. ACS, acute coronary syndrome; ECMO, extracorporeal membrane oxygenation; ECPR, extracorporeal cardiopulmonary resuscitation; FFP, fresh frozen plasma; PLT, platelet; RBC, red blood cell.

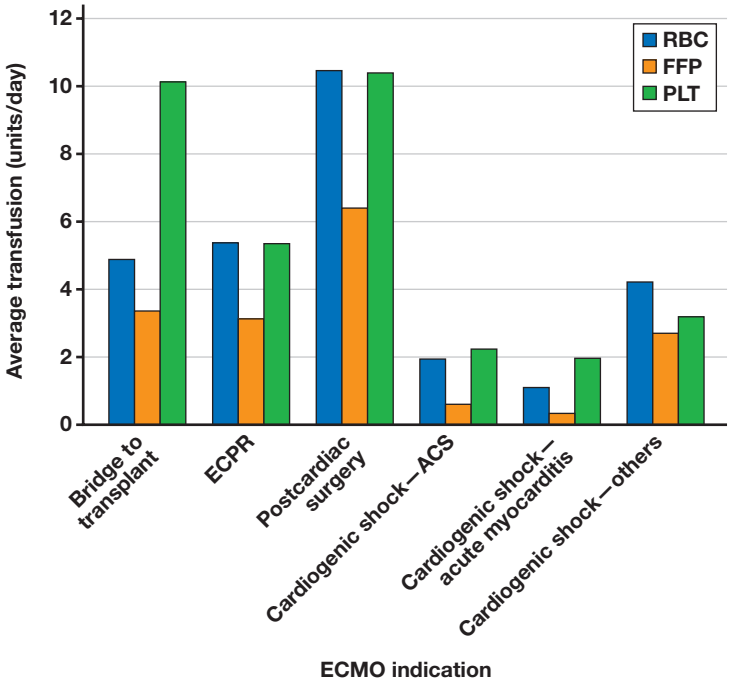

An observational study of 188 VA ECMO patients by Mazzeffi et al[22] demonstrated that patients who received 4 or more units of apheresis platelets during ECMO support were associated with increased in-hospital mortality, whereas patients who received 1 to 3 units were not associated with in-hospital mortality compared with those who did not receive any. Considering that 1 unit of apheresis platelets is equivalent to 6 to 8 units of platelet concentrates, it can be interpreted as using a cutoff of 24 units or more. As the authors of the study noted, this finding may be related to extremely ill patients suffering more severe illness and thrombocytopenia or in part to adverse transfusion reaction caused by platelet transfusion. The findings of our study showed that the amount of daily platelet transfusion and transfusion above 8 units/day were not associated with in-hospital mortality. Taken together, although the amount of average daily platelet transfusion can be managed regarding the patient's transfusion requirement, caution is needed when the total volume of transfusion accumulates during ECMO support.

Previous studies have investigated the prognostic value of SOFA score in patients receiving ECMO for respiratory failure or refractory cardiogenic shock.[15,16,27-29] Our findings demonstrated that the SOFA score at ICU admission was predictive of in-hospital survival; however, the APACHE II score was not associated with in-hospital mortality. Similarly, a large international cohort study of 3846 patients reported that the SOFA score at ICU admission performed better than APACHE II in predicting the survival of VA ECMO patients.[16] The authors proposed a prediction model for VA ECMO use in cardiogenic shock, the Survival After Venoarterial ECMO (SAVE) score, which demonstrated better performance than the SOFA and APACHE II scores. In addition to SOFA and APACHE II scores, a study by Treml et al[30] on 358 patients receiving ECMO support identified Simplified Acute Physiology Score III (SAPS III) as an independent predictor for 3-month mortality, whereas SOFA score was not. The heterogeneity in literature implies the need for further evaluation. A recent systematic review of 58 ECMO mortality prediction models, including the SAVE and Respiratory ECMO Survival Prediction (RESP) scores, claimed that only moderate performance models were observed.[31] Additionally, currently available models seem unsuitable for guiding decision-making before the establishment of ECMO because predicted mortality is conditional on having already initiated ECMO.[31] Therefore, the development of new prediction models is needed, and we believe that pre-ECMO thrombocytopenia severity may have prognostic value.

This study identified several pre-ECMO variables and the type of ECMO indication as predictors for transfusion requirements. However, as this study was conducted in a single center, further assessment is needed to verify the predictive value of these variables. Nevertheless, the findings of our study demonstrated that low pre-ECMO Hb and platelets were predictive of increased transfusion requirements of RBCs and PLTs, respectively, as expected. Additionally, these findings show that the type of indication for ECMO was associated with transfusion requirements. These findings can be used to prepare or reserve blood products in advance, so they may be provided in a timely manner when an increased blood requirement is expected.

This study has several limitations. First, the retrospective design makes it prone to biases inherent in retrospective observational studies. Second, this study was conducted at a single center, which requires further external validation. Third, patients with all indications for VA ECMO were analyzed; therefore, the nature of pre-ECMO thrombocytopenia may vary among patients who have undergone ECMO. In addition, this study did not include comorbidities and the underlying risks may vary among patients. However, APACHE II and SOFA scores were used to assess the severity of illness at ICU admission. Finally, it is known that decreased platelet function during ECMO results in a significant increase in transfusion requirement.[32] However, in this study, only platelet counts were assessed. Therefore, the ability to discern the impact of impaired platelet function from the variables assessed is limited.

In conclusion, our study demonstrated pre-ECMO thrombocytopenia as a factor for predicting the outcomes of patients undergoing VA ECMO. Additionally, our study showed that the amount of platelet transfusion per day was not associated with in-hospital mortality. Further, our study identified predictive variables of increased transfusion requirements in RBC, FFP, and PLT.

Conflict of Interest Disclosure

The authors have nothing to disclose.

Data Availability

The datasets generated and/or analyzed during this study are available from the corresponding author on reasonable request.

REFERENCES

1. Guglin M, Zucker MJ, Bazan VM, et al. Venoarterial ECMO for adults: JACC scientific expert panel. *J Am Coll Cardiol.* 2019;73(6):698-716. doi:10.1016/j.jacc.2018.11.038
2. Dalton HJ, Reeder R, Garcia-Filion P, et al, Eunice Kennedy Shriver National Institute of Child Health and Human Development Collaborative Pediatric Critical Care Research Network. Factors associated with bleeding and thrombosis in children receiving extracorporeal membrane oxygenation. *Am J Respir Crit Care Med.* 2017;196(6):762-771. doi:10.1164/rccm.201609-1945OC
3. Thomas J, Kostousov V, Teruya J. Bleeding and thrombotic complications in the use of extracorporeal membrane oxygenation. *Semin Thromb Hemost.* 2018;44(1):20-29. doi:10.1055/s-0037-1606179
4. Balle CM, Jeppesen AN, Christensen S, Hvas AM. Platelet function during extracorporeal membrane oxygenation in adult patients: a systematic review. *Front Cardiovasc Med*. 2018;5:157. doi:10.3389/fcvm.2018.00157
5. Chen Z, Mondal NK, Zheng S, et al. High shear induces platelet dysfunction leading to enhanced thrombotic propensity and diminished hemostatic capacity. *Platelets*. 2019;30(1):112-119. doi:10.1080/09537104.2017.1384542
6. Haneya A, Philipp A, Diez C, et al. Comparison of two different minimized extracorporeal circulation systems: hematological effects after coronary surgery. *ASAIO J.* 2009;55(6):592-597. doi:10.1097/MAT.0b013e3181be2f5c
7. Jiritano F, Serraino GF, Ten Cate H, et al. Platelets and extracorporeal membrane oxygenation in adult patients: a systematic review and meta-analysis. *Intensive Care Med.* 2020;46(6):1154-1169. doi:10.1007/s00134-020-06031-4
8. Oliver WC. Anticoagulation and coagulation management for ECMO. *Semin Cardiothorac Vasc Anesth.* 2009;13(3):154-175. doi:10.1177/1089253209347384
9. Peek GJ, Firmin RK. The inflammatory and coagulative response to prolonged extracorporeal membrane oxygenation. *ASAIO J.* 1999;45(4):250-263. doi:10.1097/00002480-199907000-00003
10. Squiccimarro E, Jiritano F, Serraino GF, Ten Cate H, Paparella D, Lorusso R. Quantitative and qualitative platelet derangements

in cardiac surgery and extracorporeal life support. *J Clin Med*. 2021;10(4):615. doi:10.3390/jcm10040615

11. Ellouze O, Abbad X, Constandache T, et al. Risk factors of bleeding in patients undergoing venoarterial extracorporeal membrane oxygenation. *Ann Thorac Surg.* 2021;111(2):623-628. doi:10.1016/j.athoracsur.2020.02.012
12. Cheng R, Hachamovitch R, Kittleson M, et al. Complications of extracorporeal membrane oxygenation for treatment of cardiogenic shock and cardiac arrest: a meta-analysis of 1,866 adult patients. *Ann Thorac Surg.* 2014;97(2):610-616. doi:10.1016/j.athoracsur.2013.09.008
13. Lo Coco V, Lorusso R, Raffa GM, et al. Clinical complications during veno-arterial extracorporeal membrane oxygenation in post-cardiotomy and non post-cardiotomy shock: still the Achille's heel. *J Thorac Dis*. 2018;10(12):6993-7004. doi:10.21037/jtd.2018.11.103
14. Mazzeffi M, Greenwood J, Tanaka K, et al. Bleeding, transfusion, and mortality on extracorporeal life support: ECLS Working Group on Thrombosis and Hemostasis. *Ann Thorac Surg.* 2016;101(2):682-689. doi:10.1016/j.athoracsur.2015.07.046
15. Schmidt M, Bailey M, Sheldrake J, et al. Predicting survival after extracorporeal membrane oxygenation for severe acute respiratory failure. The Respiratory Extracorporeal Membrane Oxygenation Survival Prediction (RESP) score. *Am J Respir Crit Care Med.* 2014;189(11):1374-1382. doi:10.1164/rccm.201311-2023OC
16. Schmidt M, Burrell A, Roberts L, et al. Predicting survival after ECMO for refractory cardiogenic shock: the survival after veno-arterial-ECMO (SAVE)-score. *Eur Heart J.* 2015;36(33):2246-2256. doi:10.1093/eurheartj/ehv194
17. Opfermann P, Bevilacqua M, Felli A, et al. Prognostic impact of persistent thrombocytopenia during extracorporeal membrane oxygenation: a retrospective analysis of prospectively collected data from a cohort of patients with left ventricular dysfunction after cardiac surgery. *Crit Care Med.* 2016;44(12):e1208-e1218. doi:10.1097/CCM.0000000000001964
18. Wang L, Yang F, Wang X, et al. Predicting mortality in patients undergoing VA-ECMO after coronary artery bypass grafting: the RE-MEMBER score. *Crit Care.* 2019;23(1):11. doi:10.1186/s13054-019-2307-y
19. Wang L, Shao J, Shao C, Wang H, Jia M, Hou X. The relative early decrease in platelet count is associated with mortality in post-cardiotomy patients undergoing venoarterial extracorporeal membrane oxygenation. *Front Med (Lausanne)*. 2021;8:733946. doi:10.3389/fmed.2021.733946
20. Extracorporeal Life Support Organization (ELSO) General Guidelines for all ECLS Cases. version 1.4. Accessed March 10, 2023. https://www.elso.org/ecmo-resources/elso-ecmo-guidelines.aspx
21. Qin CX, Yesantharao LV, Merkel KR, et al. Blood utilization and clinical outcomes in extracorporeal membrane oxygenation patients. *Anesth Analg.* 2020;131(3):901-908. doi:10.1213/ANE.0000000000004807
22. Mazzeffi M, Rabin J, Deatrick K, et al. Platelet transfusion and in-hospital mortality in veno-arterial extracorporeal membrane oxygenation patients. *ASAIO J.* 2022;68(10):1249-1255. doi:10.1097/MAT.0000000000001643
23. Yeo HJ, Cho WH, Kim D. Learning curve for multidisciplinary team setup in veno-venous extracorporeal membrane oxygenation for acute respiratory failure. *Perfusion.* 2019;34(1_suppl):30-38. doi:10.1177/0267659119827424
24. Mongardon N, Dumas F, Ricome S, et al. Postcardiac arrest syndrome: from immediate resuscitation to long-term outcome. *Ann Intensive Care.* 2011;1(1):45. doi:10.1186/2110-5820-1-45
25. Perkins GD, Callaway CW, Haywood K, et al. Brain injury after cardiac arrest. *Lancet.* 2021;398(10307):1269-1278. doi:10.1016/S0140-6736(21)00953-3
26. Roberts BW, Kilgannon JH, Chansky ME, et al. Multiple organ dysfunction after return of spontaneous circulation in postcardiac arrest syndrome. *Crit Care Med.* 2013;41(6):1492-1501. doi:10.1097/CCM.0b013e31828a39e9
27. Muller G, Flecher E, Lebreton G, et al. The ENCOURAGE mortality risk score and analysis of long-term outcomes after VA-ECMO for acute myocardial infarction with cardiogenic shock. *Intensive Care Med.* 2016;42(3):370-378. doi:10.1007/s00134-016-4223-9
28. Roch A, Hraiech S, Masson E, et al. Outcome of acute respiratory distress syndrome patients treated with extracorporeal membrane oxygenation and brought to a referral center. *Intensive Care Med.* 2014;40(1):74-83. doi:10.1007/s00134-013-3135-1
29. Schmidt M, Zogheib E, Rozé H, et al. The PRESERVE mortality risk score and analysis of long-term outcomes after extracorporeal membrane oxygenation for severe acute respiratory distress syndrome. *Intensive Care Med.* 2013;39(10):1704-1713. doi:10.1007/s00134-013-3037-2
30. Treml B, Breitkopf R, Bukumirić Z, Bachler M, Boesch J, Rajsic S. ECMO Predictors of mortality: a 10-year referral centre sxperience. *J Clin Med*. 2022;11(5):1224. doi:10.3390/jcm11051224
31. Pladet LCA, Barten JMM, Vernooij LM, et al. Prognostic models for mortality risk in patients requiring ECMO. *Intensive Care Med.* 2023;49(2):131-141. doi:10.1007/s00134-022-06947-z
32. Tauber H, Streif W, Fritz J, et al. Predicting transfusion requirements during extracorporeal membrane oxygenation. *J Cardiothorac Vasc Anesth.* 2016;30(3):692-701. doi:10.1053/j.jvca.2016.01.009

An observational association study between maternal homocysteine and pregnancy complications or perinatal outcomes with established trimester-specific reference intervals in pregnant women

Guodong Tang, BS[1,2,5], Shaofei Su, PhD[3], Yifan Lu, MS[1,2], Lanlan Meng, MS[1,2], Lican Han, BS[1,2], Zhengwen Xu, BS[1,2], Lin Liu, BS[1,2], Jiazi Zeng, BS[1,2], Lu Chen, BS[1,2], Jing Wang, MS[1,2], Yue Zhang, BS[4], Yanhong Zhai, MD[1,2], Zheng Cao, PhD[1,2]

[1]Department of Laboratory Medicine, [2]Center of Clinical Mass Spectrometry, [3]Central Laboratory, and [4]Information Center, Beijing Obstetrics and Gynecology Hospital, Capital Medical University. Beijing Maternal and Child Health Care Hospital, Beijing, China; [5]Department of Clinical Laboratory, Beijing Chao-yang Hospital, Capital Medical University, Beijing, China. Corresponding author: Zheng Cao; zhengcao2011@ccmu.edu.cn

Key words: homocysteine; pregnancy; population-based; cohort study; outcome; reference interval

Abbreviations: Hcy, homocysteine; RI, reference interval; PE, preeclampsia; GH, gestational hypertension; GDM, gestational diabetes mellitus; ICP, intrahepatic cholestasis of pregnancy; PPH, postpartum hemorrhage; CV, coefficient of variation; BMI, body mass index; OR, odds ratio; URL, upper reference limit

Laboratory Medicine 2024;55:355-360; https://doi.org/10.1093/labmed/lmad092

ABSTRACT

Background: Elevated homocysteine (Hcy) level during pregnancy is positively associated with various gestational-specific diseases. However, there is no uniform standard for the reference interval (RI) of Hcy in pregnancy.

Methods: From January 2017 to January 2019, 14,530 singleton pregnant women registered at our institute were included for the establishment of trimester-specific RIs of Hcy with both the nonparametric approach and the indirect Hoffmann method, followed by pregnancy outcome association analysis conducted with logistic regression.

Results: The serum Hcy level in the nonpregnant group was significantly higher than that of pregnant women. A relatively decreased Hcy concentration was observed in the second trimester when compared with that of the first or third trimester. The direct RIs of Hcy in the first or third, and second trimesters were 4.6 to 8.0 mmol/L (merged) and 4.0 to 6.4 mmol/L, respectively, which showed no significant difference compared with the RI derived from the indirect Hoffmann method. In the subsequent risk analysis, the first trimester Hcy was found to be negatively associated with GDM development; whereas the third trimester Hcy conferred increased risk of postpartum hemorrhage after delivery.

Conclusion: Having established trimester-specific RIs, our study sheds light on the complicated roles of Hcy in pregnancy-related complications.

Introduction

Homocysteine (Hcy) is a sulfur-containing amino acid that is formed during the metabolism of methionine to cysteine, serving as the most important methyl group donor in the human body.[1] As a key monitoring indicator of human health, an abnormally elevated level of Hcy is associated with increased risks for various cardiovascular diseases.[2] Due to the increase of circulating fluid or blood volume, Hcy concentration in pregnancy has been shown to be lower than that of nonpregnant controls, suggesting the clinical need to establish Hcy reference intervals (RIs) in the pregnant population.[3] However, whether there is a distinction in Hcy levels among different trimesters remains controversial.[3-6]

It has been reported that elevated maternal Hcy level typically introduced by poor folate status was associated with a variety of perinatal complications and postpartum syndromes.[7-12] For instance, in a case-control study, significantly elevated maternal serum Hcy was observed in patients diagnosed with preeclampsia (PE), whereas the folate and vitamin B12 levels in PE patients were essentially the same as normal pregnancy.[13,14] In another retrospective cohort study, a high level of Hcy in the first trimester was found to be an independent risk factor for severe PE, but it is not a helpful marker for predicting the subsequent development of gestational hypertension (GH) or mild PE.[15] A moderately positive correlation between plasma total Hcy level and gestational diabetes mellitus (GDM) was reported in a Chinese Han population.[16] A significant association was even observed between increased Hcy level and a previous history of GDM in pregnant women.[17] In contrast, in a prospective study including 243 pregnant women, an association between hyperhomocysteinemia and GDM could not be demonstrated.[12] Other studies have shown that maternal Hcy concentration was inversely

associated with neonatal weights.[18,19] However, few studies to date have systematically evaluated the impacts of maternal Hcy levels on the risks of developing adverse pregnancy complications or outcomes.

The traditional method of RI establishment requires at least 120 healthy subjects in whom there is no standard definition for absolute "heathy status." It is also difficult for laboratory professionals to rule out all subclinical diseases and abnormalities that may affect analysis results. The indirect (Hoffmann) method is a method proposed by Hoffmann to screen the normal population based on the cumulative probability distribution of data so as to establish the reference interval,[20,21] with no requirement of recruiting healthy subjects. Whether the Hoffmann method is suitable for the estimation of Hcy RIs in pregnant women still needs to be confirmed.

To fill these knowledge gaps, we conducted a population-based cohort study, focusing on the establishment of instrument-specific gestational RIs of Hcy and the associations between Hcy and maternal/fetal risks of peri- and postpartum complications.

Materials and Methods

Subjects and Laboratory Data

To establish the trimester-specific RIs of Hcy, 150 healthy singleton pregnant women (aged 25 to 40) who gave live birth at our institute and presented normal pregnancy test results (ie, routine blood, urine, and biochemical tests) and 150 nonpregnant healthy controls with matching ages were enrolled. The selection and exclusion criteria were as previous described[22] (see Supplementary Methods).

For the association study, the first and third trimester Hcy laboratory results as well as the corresponding pregnancy/delivery outcomes were retrieved from the digital history records of the women who were registered at the Beijing Obstetrics and Gynecology Hospital with regular antenatal checkups. As a result, from October 2018 to September 2020, a total of 14,530 eligible singleton pregnant women were included in the study. Considering the completeness and availability of the medical records, the following peri- and postpartum complications or adverse outcomes were involved for the subsequent risk association analyses: gestational hypertension (GH), gestational diabetes mellitus (GDM), preeclampsia (PE), intrahepatic cholestasis of pregnancy (ICP), macrosomia, and postpartum hemorrhage (PPH), the definitions of which are provided in Supplementary Table 1.

The study protocol was approved by the Ethics Committee of Beijing Obstetrics and Gynecology Hospital (2022-KY-007-02). The ethics committee waived the requirement for informed consent from participants because all Hcy tests are part of routine antenatal care during pregnancy. All the laboratory data were anonymous before use.

Hcy Measurement Method

Serum Hcy levels were assayed on the fully automated ARCHITECT ci16200 Integrated System Chemistry/Immunology Analyzer (Abbott) with the Homocysteine Assay Kit (enzymatic cycling method). The limit of quantitation for the serum Hcy assay was 0.01 mmol/L. The intra-assay coefficient of variation (CV) of serum Hcy was 3.8%; the interassay CV was 5.3%. The serum samples of the subjects were stored at 4°C for less than 24 hours or at −20°C for longer time storage (less than 1 month) before testing. The ARCHITECT homocysteine assay is a 1-step immunoassay for the quantitative determination of total L-homocysteine in human serum or plasma. Bound or dimerized Hcy (the oxidized form) is reduced by dithiothreitol to free Hcy, which is subsequently converted to S-adenosyl homocysteine by the action of the recombinant enzyme S-adenosyl homocysteine hydrolase. The S-adenosyl homocysteine then competes with acridinium-labeled S-adenosyl cysteine for particle-bound monoclonal antibody. An indirect relationship exists between the amount of homocysteine in the sample and the relative light units detected by the ARCHITECT iSystem optics, which is used to calculate the serum concentration of Hcy.

Statistical Analysis

The normality of quantitative data was tested by Kolmogorov-Smirnov test. The standard deviation was used for descriptive statistics and *t*-test was used for comparison between the 2 groups. Descriptive statistics were performed by interquartile spacing for data that did not conform to normal distribution, and rank-sum test was used for comparison between groups. Multivariate logistic regression analysis was used to analyze odds ratios (ORs) and 95% CIs with maternal age and prepregnancy body mass index (BMI) adjusted as confounders. Basically, the 2 variables of age and prepregnancy BMI were included as covariates into the logistic regression analysis to calculate the resulting OR and *P* values for the adjusted risk relationship between serum Hcy and pregnancy outcomes. Outlying values were tested by Tukey's method, in which outlying values were defined as less than Q1−1.5 × interquartile range (IQR) or more than Q3−1.5 × IQR (Q1 is the 25th percentage, Q3 the 75th percentage and the IQR is Q3−Q1). The Mann-Whitney *U*-test was used to detect the statistical significance of Hcy in the first and third trimester, and $P < .05$ was considered statistically significant. The above data analyses were performed using SPSS 22.0 software.

To estimate the trimester-specific RIs using the direct method, nonparametric analysis was used with the Hcy testing results of the 150 healthy singleton pregnant women. The 2.5th and 97.5th percentiles were used as the lower and upper limits of RIs, respectively. The Hoffmann method used to indirectly calculate the reference intervals of Hcy in pregnancy was as previously described.[21,22] The approach for statistical testing of mean difference between subgroups is based on the proportion criterion developed by Lahti.[15] Briefly, the lower limit (2.5th percentile) and upper limit (97.5th percentile) were first calculated using data covering 2 neighboring subgroups. Next, the outlier was determined as proportions of the subgroup distribution outside reference limits established by combining neighboring subgroups. If at least 1 of the 4 proportions of the subgroups outside the common reference limits exceeded or was equal to 4.1%, or laid below or was equal to 0.9%, partitioning was considered necessary.[23]

Results

As shown by the boxplot in **FIGURE 1**, the serum Hcy level in the nonpregnant control women was significantly higher than that of pregnant women in the first, second, or third trimester, with medians (25th-75th percentile) of 8.6 (7.3-10.3), 5.0 (4.6-5.4), 6.3 (5.5-6.8), and 6.0 (5.4-6.7) mmol/L, respectively. By contrast, the Hcy level was essentially unchanged between the first and third trimesters but was significantly decreased in the second trimester (**FIGURE 1**). The Hcy RI of the first and third trimester merged using the Lahti method (**TABLE 1**) was 4.6-8.0 mmol/L compared with the RI of 3.9-9.1 mmol/L derived from the Hoffmann method. There was no significant difference between the

observed RI of the healthy women and the RIs calculated by Hoffmann's method (absolute difference percentage smaller than reference change value percentage), suggesting the validity of the indirect method of Hcy RI estimation in pregnancy. The second trimester Hcy RI, which was not mergeable with the other trimesters, was estimated as 4.0-6.4 mmol/L by the direct method (**TABLE 1**).

FIGURE 1. Box plots representing the serum homocysteine level of nonpregnant and pregnant women in the first, second, or third trimester. The homocysteine concentrations of different patient groups were presented as median (25th-75th percentile). *P < .001; NS, not significant.

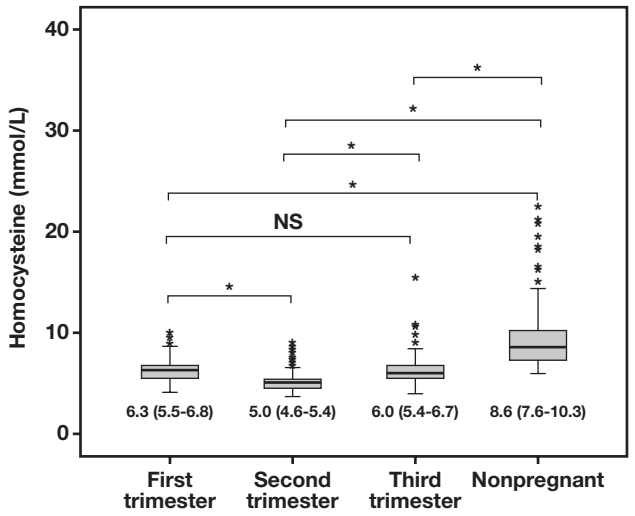

Given the onset time of various pregnancy diseases, the multivariate logistic regression analysis to estimate the risks of GDM, GH, PE, and ICP was carried out using first trimester Hcy; the analysis for macrosomia and PPH was conducted using both first and third trimester Hcy. The baseline characteristics of age and prepregnancy BMI and the medians of Hcy levels in different complication groups are summarized in **TABLE 2**, showing that the first trimester Hcy was significant decreased in the GDM and macrosomia groups. However, in the patients who experienced PPH, the third-trimester Hcy level was significantly elevated. In the subsequent logistic regression analysis, the OR values were calculated with cutoffs set around the upper reference limit (URL) of Hcy. The Hcy cutoff values used in the multivariate logistic regression analysis, as well as the number and percentage of the Hcy data points greater than the corresponding cutoffs, are listed in Supplementary Table 2.

Interestingly, as shown in **TABLE 3**, the first trimester Hcy was negatively associated with the risk of GDM development, with ORs ranged

TABLE 1. Trimester-specific reference intervals of serum homocysteine using both direct and indirect methods

Trimester[a]	Trimester-specific RIs, mmol/L		Absolute difference, %	RCV, %
	Observed RI	Hoffmann RI		
First or third	4.6-8.0	3.9-9.1	13.8-15.2	17.3
Second	4.0-6.4	—	—	—

RCV, reference change value; RI, reference interval.
[a]First trimester is 1 to 12 gestational weeks (GWs); second trimester, 13 to 28 GWs; third trimester, 29 to 40 GWs.

TABLE 2. Demographic data and basic statistics of the serum homocysteine in patients with different pregnancy complications or outcomes[a]

	Age, y	Prepregnancy BMI, kg/m^2	Hcy, mmol/L[b]	Hcy, mmol/L[c]
GDM positive (n = 1075, 7.3%)	33 (30-36)	23.01 (20.94-25.63)	6.6 (6.0-7.4)	—
GDM negative (n = 13,455)	31 (29-34)	21.11 (19.49-23.31)	6.8 (6.1-7.7)	—
P	<.001	<.001	<.001	—
GH positive (n = 276, 1.8%)	31 (29-35)	23.14 (20.82-26.00)	6.8 (6.0-7.6)	—
GH negative (n = 14,254)	31 (29-34)	21.23 (19.53-23.44)	6.8 (6.1-7.7)	—
P	.123	<.001	.172	—
PE positive (n = 554, 3.8%)	32 (29-35)	24.09 (21.36-27.04)	6.9 (6.1-7.7)	—
PE negative (n = 13,976)	31 (29-34)	21.22 (19.53-23.34)	6.8 (6.1-7.7)	—
P	<.001	<.001	.193	—
ICP positive (n = 37, 0.2%)	31 (29-35)	20.96 (19.20-23.52)	6.9 (6.5-7.9)	—
ICP negative (n = 14,493)	31 (29-34)	21.26 (19.53-23.44)	6.8 (6.1-7.7)	—
P	.497	.476	.219	—
Macrosomia positive (n = 258, 1.7%)	32 (30-35)	22.90 (21.22-25.36)	6.5 (5.9-7.4)	6.1 (5.4-6.9)
Macrosomia negative (n = 14,272)	31 (29-34)	21.23 (19.53-23.44)	6.8 (6.1-7.7)	6.0 (5.4-6.9)
P	<.001	<.001	.006	.378
PPH positive (n = 1116, 7.6%)	32 (29-35)	22.03 (20.04-24.46)	6.8 (6.1-7.6)	6.2 (5.4-7.1)
PPH negative (n = 13,414)	31 (29-34)	21.22 (19.53-21.38)	6.8 (6.1-7.7)	6.0 (5.3-6.9)
P	<.001	<.001	.223	<.001

BMI, body mass index; GDM, gestational diabetes mellitus; GH, gestational hypertension; Hcy, homocysteine; ICP, intrahepatic cholestasis of pregnancy; PE, preeclampsia; PPH, postpartum hemorrhage.
[a]All the numerical values were presented as median (25th-75th percentile). P < .05 *is considered significant.*
[b]First trimester.
[c]Third trimester.

TABLE 3. Logistic regression analysis of serum Hcy for the risks of pregnancy complications and adverse pregnancy outcomes[a]

		GDM		GH		PE	
		OR (95% CI)	*P*	OR (95% CI)	*P*	OR (95% CI)	*P*
Hcy[b]	80% URL	0.74 (0.65-0.84)	<.01	0.83 (0.65-1.06)	.14	1.14 (0.95-1.36)	.16
	85% URL	0.70 (0.62-0.80)	<.01	0.90 (0.71-1.15)	.40	1.13 (0.95-1.34)	.17
	90% URL	0.68 (0.59-0.79)	<.01	0.80 (0.61-1.03)	.08	1.10 (0.92-1.31)	.31
	95% URL	0.70 (0.60-0.82)	<.01	0.85 (0.64-1.14)	.28	1.07 (0.88-1.30)	.49
	100% URL	0.73 (0.61-0.87)	<.01	0.72 (0.51-1.02)	.06	1.15 (0.93-1.43)	.20
	105% URL	0.67 (0.54-0.83)	<.01	0.68 (0.45-1.03)	.07	1.09 (0.84-1.40)	.51
	110% URL	0.53 (0.40-0.70)	<.01	0.58 (0.34-0.98)	.04	1.23 (0.93-1.64)	.15
	115% URL	0.52 (0.37-0.73)	<.01	0.71 (0.40-1.24)	.23	1.10 (0.78-1.54)	.60
	120% URL	0.43 (0.28-0.66)	<.01	0.72 (0.38-1.39)	.33	1.04 (0.70-1.55)	.86
Hcy[c]	80% URL	—	—	—	—	—	—
	85% URL	—	—	—	—	—	—
	90% URL	—	—	—	—	—	—
	95% URL	—	—	—	—	—	—
	100% URL	—	—	—	—	—	—
	105% URL	—	—	—	—	—	—
	110% URL	—	—	—	—	—	—
	115% URL	—	—	—	—	—	—
	120% URL	—	—	—	—	—	—
		ICP		Macrosomia		PPH	
		OR (95% CI)	*P*	OR (95% CI)	*P*	OR (95% CI)	*P*
Hcy[b]	80% URL	1.93 (0.91-4.10)	.09	0.67 (0.52-0.86)	<.01	0.95 (0.83-1.07)	.39
	85% URL	1.16 (0.61-2.21)	.66	0.73 (0.57-0.94)	.01	0.97 (0.85-1.09)	.57
	90% URL	1.14 (0.58-2.21)	.70	0.76 (0.58-1.00)	.05	0.92 (0.80-1.04)	.19
	95% URL	1.45 (0.73-2.88)	.30	0.75 (0.55-1.02)	.06	0.92 (0.80-1.07)	.29
	100% URL	1.11 (0.48-2.52)	.81	0.67 (0.46-0.96)	.03	0.89 (0.75-1.05)	.17
	105% URL	0.65 (0.20-2.13)	.48	0.78 (0.51-1.17)	.23	0.87 (0.71-1.06)	.16
	110% URL	0.62 (0.15-2.59)	.51	0.86 (0.54-1.37)	.53	0.87 (0.69-1.10)	.24
	115% URL	0.43 (0.06-3.17)	.41	0.84 (0.48-1.44)	.52	0.81 (0.61-1.07)	.14
	120% URL	0.61 (0.08-4.44)	.62	0.71 (0.63-1.39)	.32	0.79 (0.57-1.09)	.15
Hcy[c]	80% URL	—	—	1.00 (0.78-1.30)	.96	1.32 (1.16-1.49)	<.01
	85% URL	—	—	1.01 (0.76-1.34)	.93	1.30 (1.14-1.49)	<.01
	90% URL	—	—	1.10 (0.80-1.49)	.57	1.24 (1.07-1.45)	<.01
	95% URL	—	—	1.16 (0.82-1.64)	.42	1.25 (1.05-1.48)	.01
	100% URL	—	—	1.04 (0.68-1.57)	.87	1.36 (1.12-1.65)	<.01
	105% URL	—	—	1.03 (0.63-1.67)	.91	1.43 (1.15-1.78)	<.01
	110% URL	—	—	0.84 (0.46-1.56)	.59	1.35 (1.04-1.74)	.02
	115% URL	—	—	0.95 (0.48-1.86)	.87	1.39 (1.03-1.86)	.03
	120% URL	—	—	1.08 (0.53-2.21)	.83	1.30 (0.93-1.82)	.13

BMI, body mass index; GDM, gestational diabetes mellitus; GH, gestational hypertension; Hcy, homocysteine; ICP, intrahepatic cholestasis of pregnancy; OR, odds ratio; PE, preeclampsia; PPH, postpartum hemorrhage; URL, upper reference limit.
[a]*P < .05 is considered significant.*
[b]*First trimester.*
[c]*Third trimester.*

between 0.43 (95% CI, 0.28-0.66) and 0.74 (95% CI, 0.65-0.84) when the cutoffs were set at 80% to 120% URLs of Hcy. In contrast, the third-trimester Hcy posed moderately increased risk in women suffering PPH after delivery (**TABLE 3**).

Discussion

The Hoffmann method that has been widely adopted to determine the RIs of clinical laboratory tests does not require additional effort to recruit and collect samples from healthy people. It has also been applied

to situations where it would be difficult to obtain samples (such as cerebrospinal fluid) from healthy subjects.[24,25] To the best of our knowledge, the Hoffman method was used in our study for the first time to estimate trimester-specific Hcy RIs, further proving its merit and validity in the pregnant population.

As shown in **FIGURE 1**, serum Hcy was decreased naturally in pregnancy compared with nonpregnant controls. Second trimester Hcy concentration was the lowest of all 3 trimesters, which is consistent with other reports from previous studies.[3,26] It is associated with a physiological decline in albumin during pregnancy and also with folic acid supplementation.[27] The decrease in Hcy level during normal pregnancy is helpful to maintain the integrity of maternal vascular endothelial cells and the elasticity of coronary arteries.[5,6] Therefore, given the influence of multidimensional information such as age, diet, and prepregnancy BMI, it is of great clinical value to formulate a reasonable RI for Hcy during pregnancy through a large-sample sized study.

Further, our study showed that serum Hcy level was negatively associated with GDM (**TABLE 3**). The higher the Hcy level in the first trimester, the lower the risk of GDM development observed. Robillon et al[28] found that plasma Hcy concentration was significantly reduced in patients with type 1 diabetes with virtually no microvascular complications, which they believed was attributed to renal hyperperfusion. Renal hyperperfusion in early diabetes has been reported to lead to increased catabolism of homocysteine.[29] In another study, it was shown that the patients with albuminuria diabetes had lower Hcy than matched control subjects. In addition, in their univariate and multivariate analyses, Hcy was negatively associated with blood glucose levels in the diabetic group.[30] However, the mechanism behind the negative association between first trimester Hcy level and GDM development remains unclear and requires further clinical and biological investigations.

Although this is a large-sized population-based cohort study that rendered significant statistical power to the subsequent association analysis, a few limitations still exist. First, our work is a single-center study that lacks ethnic background diversity. Studies involving multiple centers and other populations in different regions would be more comprehensive and representative. Second, the gravidity, parity, and folic acid supplementation that may be contributive to the prevalence of variable pregnancy complications were not included or available in this analysis.

Conclusion

In this population-based cohort study, trimester-specific RIs of Hcy were established with both direct observational and indirection Hoffmann methods. Further, first-trimester Hcy was found to be negatively associated in GDM development, whereas third-trimester Hcy indicated increased risk of PPH after delivery. Our results have shed light on the complicated roles of Hcy in pregnancy-related complications.

Funding

This work was supported by the Training Fund for Open Projects at Clinical Institutes and Departments of Capital Medical University (CCMU2022ZKYXZ006), the Beijing Municipal Administration of Hospitals Incubating Program (No. PX2020060), and Beijing Obstetrics and Gynecology Hospital, Capital Medical University, Beijing Maternal and Child Health Care Hospital "Discipline Backbone" Plan Special Funds (No. XKGG201802). The funding bodies did not take part in the design of the study, the collection, analysis, or interpretation of the data, nor manuscript writing.

Conflict of Interest Disclosure

The authors have nothing to disclose.

Data Availability

According to the patients' verbal consent, their relevant demographic and medical records are only available from the corresponding author on reasonable request.

REFERENCES

1. Hague WM. Homocysteine and pregnancy. *Best Pract Res Clin Obstet Gynaecol.* 2003;17(3):459-469. https://doi.org/10.1016/s1521-6934(03)00009-9
2. Sukumar N, Adaikalakoteswari A, Venkataraman H, Maheswaran H, Saravanan P. Vitamin B12 status in women of childbearing age in the UK and its relationship with national nutrient intake guidelines: results from two national diet and nutrition surveys. *BMJ Open*. 2016;6(8):e011247. https://doi.org/10.1136/bmjopen-2016-011247
3. Walker MC, Smith GN, Perkins SL, Keely EJ, Garner PR. Changes in homocysteine levels during normal pregnancy. *Am J Obstet Gynecol.* 1999;180(3 pt 1):660-664. https://doi.org/10.1016/s0002-9378(99)70269-3
4. Holmes VA, Wallace JM, Alexander HD, et al. Homocysteine is lower in the third trimester of pregnancy in women with enhanced folate status from continued folic acid supplementation. *Clin Chem.* 2005;51(3):629-634. https://doi.org/10.1373/clinchem.2004.032698
5. Dai C, Fei Y, Li J, Shi Y, Yang X. A novel review of homocysteine and pregnancy complications. *Biomed Res Int.* 2021;2021:6652231. https://doi.org/10.1155/2021/6652231
6. Yang Y, Jiang H, Tang A, Xiang Z. Changes of serum homocysteine levels during pregnancy and the establishment of reference intervals in pregnant Chinese women. *Clin Chim Acta.* 2019;489:1-4. https://doi.org/10.1016/j.cca.2018.11.026
7. Li J, Leng J, Li W, et al. Roles of insulin resistance and beta cell dysfunction in macrosomia among Chinese women with gestational diabetes mellitus. *Prim Care Diabetes*. 2018;12(6):565-573. https://doi.org/10.1016/j.pcd.2018.07.010
8. Seghieri G, Breschi MC, Anichini R, et al. Serum homocysteine levels are increased in women with gestational diabetes mellitus. *Metabolism*. 2003;52(6):720-723. https://doi.org/10.1016/s0026-0495(03)00032-5
9. Guven MA, Kilinc M, Batukan C, Ekerbicer HC, Aksu T. Elevated second trimester serum homocysteine levels in women with gestational diabetes mellitus. *Arch Gynecol Obstet.* 2006;274(6):333-337. https://doi.org/10.1007/s00404-006-0191-6
10. Idzior-Waluś B, Cyganek K, Sztefko K, et al. Total plasma homocysteine correlates in women with gestational diabetes. *Arch Gynecol Obstet.* 2008;278(4):309-313. https://doi.org/10.1007/s00404-008-0571-1
11. López-Quesada E, Antònia Vilaseca M, Gómez E, Lailla JM. Are plasma total homocysteine and other amino acids associated with glucose intolerance in uncomplicated pregnancies and preeclampsia? *Eur J Obstet Gynecol Reprod Biol.* 2005;119(1):36-41. https://doi.org/10.1016/j.ejogrb.2004.01.046
12. Mascarenhas M, Habeebullah S, Sridhar MG. Revisiting the role of first trimester homocysteine as an index of maternal and fetal outcome. *J Pregnancy*. 2014;2014:123024. https://doi.org/10.1155/2014/123024

13. Kulkarni A, Mehendale S, Pisal H, et al. Association of omega-3 fatty acids and homocysteine concentrations in pre-eclampsia. *Clin Nutr.* 2011;30(1):60-64. https://doi.org/10.1016/j.clnu.2010.07.007
14. Serrano NC, Quintero-Lesmes DC, Becerra-Bayona S, et al. Association of pre-eclampsia risk with maternal levels of folate, homocysteine and vitamin B12 in Colombia: a case-control study. *PLoS One.* 2018;13(12):e0208137. https://doi.org/10.1371/journal.pone.0208137
15. Sun F, Qian W, Zhang C, Fan J-X, Huang H-F. Correlation of maternal serum homocysteine in the first trimester with the development of gestational hypertension and preeclampsia. *Med Sci Monit.* 2017;23:5396-5401. https://doi.org/10.12659/msm.905055
16. Deng M, Zhou J, Tang Z, et al. The correlation between plasma total homocysteine level and gestational diabetes mellitus in a Chinese Han population. *Sci Rep.* 2020;10(1):18679. https://doi.org/10.1038/s41598-020-75797-w
17. Alatab S, Fakhrzadeh H, Sharifi F, et al. Correlation of serum homocysteine and previous history of gestational diabetes mellitus. *J Diabetes Metab Disord*. 2013;12:34. https://doi.org/10.1186/2251-6581-12-34
18. Yajnik CS, Deshpande SS, Panchanadikar AV, et al. Maternal total homocysteine concentration and neonatal size in India. *Asia Pac J Clin Nutr.* 2005;14(2):179-181.
19. Takimoto H, Mito N, Umegaki K, et al. Relationship between dietary folate intakes, maternal plasma total homocysteine and B-vitamins during pregnancy and fetal growth in Japan. *Eur J Nutr.* 2007;46(5):300-306. https://doi.org/10.1007/s00394-007-0667-6
20. Hoffmann RG. Statistics in the practice of medicine. *JAMA.* 1963;185:864-873. https://doi.org/10.1001/jama.1963.03060110068020
21. Hoffmann G, Lichtinghagen R, Wosniok W. Simple estimation of reference intervals from routine laboratory data. *J Lab Med*. 2016;39(6):389-402. https://doi.org/10.1515/labmed-2015-0104
22. Lu Y, Jia Z, Su S, et al. Establishment of trimester-specific reference intervals of serum lipids and the associations with pregnancy complications and adverse perinatal outcomes: a population-based prospective study. *Ann Med.* 2021;53(1):1632-1641. https://doi.org/10.1080/07853890.2021.1974082
23. Lahti A, Hyltoft Petersen P, Boyd JC, Fraser CG, Jørgensen N. Objective criteria for partitioning Gaussian-distributed reference values into subgroups. *Clin Chem.* 2002;48(2):338-352.
24. Liu J, Zhan S, Jia Y, et al. Retinol and α-tocopherol in pregnancy: establishment of reference intervals and associations with CBC. *Matern Child Nutr.* 2020;16(3):e12975. https://doi.org/10.1111/mcn.12975
25. Han L, Zheng W, Zhai Y, et al. Reference intervals of trimester-specific thyroid stimulating hormone and free thyroxine in Chinese women established by experimental and statistical methods. *J Clin Lab Anal.* 2018;32(4):e22344. https://doi.org/10.1002/jcla.22344
26. Hogg BB, Tamura T, Johnston KE, Dubard MB, Goldenberg RL. Second-trimester plasma homocysteine levels and pregnancy-induced hypertension, preeclampsia, and intrauterine growth restriction. *Am J Obstet Gynecol.* 2000;183(4):805-809. https://doi.org/10.1067/mob.2000.109044
27. Singh U, Gupta HP, Singh RK, et al. A study of changes in homocysteine levels during normal pregnancy and pre-eclampsia. *J Indian Med Assoc.* 2008;106(8):503-505.
28. Robillon JF, Canivet B, Candito M, et al. Type 1 diabetes mellitus and homocyst(e)ine. *Diabete Metab*. 1994;20(5):494-496.
29. Cronin CC, McPartlin JM, Barry DG, Ferriss JB, Scott JM, Weir DG. Plasma homocysteine concentrations in patients with type 1 diabetes. *Diabetes Care.* 1998;21(11):1843-1847. https://doi.org/10.2337/diacare.21.11.1843
30. Mazza A, Bossone E, Mazza F, Distante A. Reduced serum homocysteine levels in type 2 diabetes. *Nutr Metab Cardiovasc Dis.* 2005;15(2):118-124. https://doi.org/10.1016/j.numecd.2004.03.001

Alteration of circulating miRNAs during myocardial infarction and association with lipid levels

Aybike Sena Ozuynuk-Ertugrul, MSc[1,2], Berkay Ekici, MD[3], Aycan Fahri Erkan, MD[3], Neslihan Coban, PhD[1]

[1]Department of Genetics, Aziz Sancar Institute of Experimental Medicine, Istanbul University, Istanbul, Turkey; [2]Institute of Graduate Studies in Health Sciences, Istanbul University, Istanbul, Turkey; [3]Department of Cardiology, Faculty of Medicine, Ufuk University, Ankara, Turkey. Corresponding author: Neslihan Coban; neslic@istanbul.edu.tr

Key words: miR-126-3p, miR-210-3p, let-7g-5p, biomarker, coronary artery disease, myocardial infarction

Abbreviations: CAD, coronary artery disease; SAP, stable angina pectoris; UAP, unstable angina pectoris; MI, myocardial infarction; AMI, acute myocardial infarction; TC, total cholesterol; TG, triglycerides; CK-MB, creatine kinase–myocardial band; cTnI, cardiac troponin I; TyG, triglyceride-glucose; DAVID, Database for Annotation, Visualization, and Integrated Discovery; GO, gene ontology; KEGG, Kyoto Encyclopedia of Genes and Genomes; GAD, Genetic Association Database; T2DM, type 2 diabetes mellitus; ECs, endothelial cells; STEMI, ST-segment elevation myocardial infarction; NCCP, noncardiac chest pain; SIS, segment stenosis score; NSTEMI, non–ST-elevated MI; HUNT, Nord-Trøndelag Healthy

Laboratory Medicine 2024;55:361-372; https://doi.org/10.1093/labmed/lmad094

ABSTRACT

Background: Increasing mortality and morbidity of coronary artery disease (CAD) highlight the emerging need for novel noninvasive markers such as circulating microRNAs (miRNAs).

Objective: To evaluate the circulating levels of miR-126-3p, miR-210-3p, let-7g-5p, and miR-326, and their associations with known contributors to CAD, in CAD subgroups.

Methods: We divided the cohort into 4 groups: non-CAD controls (≤30% stenosis; n = 55), and patients with stable angina pectoris (SAP; n = 48), unstable AP (UAP; n = 46), and myocardial infarction (MI; n = 36). The circulating levels of miR-126-3p, miR-210-3p, let-7g-5p, and miR-326 were determined using TaqMan Advanced miRNA Assays in serum specimens.

Results: Circulating miR-126-3p levels were lower in the MI and UAP groups, compared with the non-CAD group, whereas miR-210-3p circulating levels were lower in the MI group than others. The levels of circulating let-7g-5p were shown to be useful for distinguishing UAP from MI, and there were substantial differences in circulating let-7g-5p levels between the UAP and MI groups. Moreover, lipid levels and ratios were lower in individuals with high circulating miR-126-3p and miR-210-3p levels.

Conclusions: The study results suggest that circulating miR-126-3p, miR-210-3p, and let-7g-5p are differentiated between different clinical presentations of CAD and associated with lipid levels, which are important risk factors and determinants of CAD.

Introduction

Atherosclerosis is a process that involves the accumulation of lipids, cells (macrophages, T lymphocytes, and smooth muscle cells), and the extracellular matrix after endothelial dysfunction.[1] Coronary artery disease (CAD), which results from the formation of atherosclerotic plaque and chronic inflammation, is one of the cardiovascular diseases (CVD), and CVD remains the leading cause of mortality globally.[2] CAD has a latency period of many years and has different clinical presentations, such as stable angina pectoris (SAP), unstable angina pectoris (UAP), and myocardial infarction (MI). Angina pectoris is defined as substernal chest pain, pressure, or discomfort typically exacerbated by exertion or emotional stress. In SAP and UAP, which are subgroups of angina pectoris, coronary arteries narrow partially.[3] MI (or acute myocardial infarction [AMI]), another common result of atherosclerosis, blocks blood flow to the heart due to a blood clot in the atheroma plaque rupture area. As a result of MI, heart muscles, heart walls, and heart valves are severely damaged by arrhythmia.[4]

miRNAs are short noncoding RNAs, approximately 22 nucleotides in length, that regulate gene expression posttranscriptionally.[5] Differentially expressed miRNAs are important in CAD pathogenesis.[6] Circulating miRNAs are stably present in biological fluids such as serum, plasma, and urine; therefore, their use as prognostic and diagnostic noninvasive biomarkers is thought to be possible.[7] Circulating miRNAs exhibit greater stability than cellular miRNAs, which can be attributed to their association with AGO2 or their presence within extracellular vesicles, such as exosomes and microvesicles.[8] Previous studies, such as one by Altesha et al,[9] which investigated the functionality of miRNAs as biomarkers, presented promising results. In other previous studies, such as one by Wang L et al,[10] circulating levels of miRNAs such as miR-1, miR-133, and miR-208 were found to differ between patients with

CAD and control individuals. The findings of several studies[11-13] have shown that circulating miR-126-3p, miR-210-3p, let-7g-5p, and miR-326 appear to be differentially expressed miRNAs in patients with CAD compared with controls.

This study aimed to examine and compare the circulating levels of miR-126-3p, miR-210-3p, miR-326, and let-7g-5p in the serum specimens of patients with SAP, UAP, and MI, and controls in the non-CAD group. Also, we investigated the correlations between miRNA levels and well-known risk factors of CAD, such as serum lipid levels. Lastly, we evaluated the putative target genes of miR-126-3p, miR-326, miR-210-3p, and let-7g-5p by their possible contribution mechanism to CAD pathogenesis.

Methods

Study Population and Measurement of Risk Factors

In total, 185 study participants were recruited for and enrolled in the Cardiology Department of Ufuk University, Faculty of Medicine between September 1, 2015, and September 1, 2017, as defined previously.[14] These individuals were sorted into the following groups as follows: non-CAD controls (≤30% stenosis; n = 55), SAP (n = 48); UAP (n = 46), and MI (n = 36). We obtained written informed consent from all participants. The specimen collection and analysis processes were conducted in compliance with the ethical guidelines of the Declaration of Helsinki and approved by the Institutional Review Board of Istanbul University (approval date: August 17, 2015; No. 1542). Measurement of CAD risk factors (fasting glucose, total cholesterol [TC], low-density lipoprotein cholesterol [LDL-C], fasting triglycerides [TG], high-density lipoprotein cholesterol [HDL-C], and hemoglobin) and MI markers (creatine kinase–myocardial band [CK-MB] and cardiac troponin I [cTnI]) were taken, and the TC/HDL-C, LDL-C/HDL-C, and $\log_{10}$(TG/HDL-C) ratios, as well as the triglyceride-glucose (TyG) index, were calculated, as previously described.[14]

miRNA Extraction and Determination of miRNA Expression Levels by Quantitative RT-PCR

We performed miRNA isolation from the 100 µL of serum specimens from the individuals recruited in the study, using the miRNeasy Serum/Plasma Kit (QIAGEN) according to manufacturer instructions. The quantity and quality of the isolated miRNA specimens were assessed using the NanoDrop 2000 Spectrophotometer (Thermo Fisher Scientific). miRNA specimens were diluted into 7.5 ng/µL. Also, 4 µL (50 pM) of 5′ phosphorylated synthetic miR-39 from *Caenorhabditis elegans* (cel-miR-39), which is used as an exogenous control miRNA, was added to each specimen before the cDNA synthesis procedure (Applied Biosystems Life Technologies). The cDNA synthesis was performed using the TaqMan Advanced miRNA cDNA Synthesis Kit (Applied Biosystems Life Technologies), following the manufacturer-provided instructions. We performed quantitative real-time polymerase chain reaction (qRT-PCR) using the TaqMan Advanced MicroRNA Assay Kit (Applied Biosystems Life Technologies). qRT-PCR testing was performed with 2.5 µL cDNA using the LightCycler480 Real-Time PCR System (F. Hoffman-La Roche).

We analyzed the resulting data using the comparative threshold cycle (Ct) method ($2^{-\Delta\Delta Ct}$ method) and reported the results as relative quantification values. For normalization of miR-126-3p (assay ID: 477887_mir, assay name: hsa-miR-126-3p), miR-210-3p (assay ID: 477970_mir, assay name: hsa-miR-210-3p), miR-326 (assay ID:478027_mir, assay name: hsa-miR-326), and let-7g-5p (assay ID:478580_mir, assay name: hsa-let-7g-5p) expressions, we used cel-miR-39-3p (assay ID: 478293_mir, assay name: cel-miR-39-3p) as the exogenous control. Circulating levels of miR-126-3p, miR-210-3p, and cel-miR-39-3p were examined in serum specimens from the male and female subjects in the non-CAD (n = 55), SAP (n = 48), UAP (n = 46) and MI (n = 36) groups. Meanwhile, let-7g-5p and miR-326 levels were examined in the serum specimens of male subjects (non-CAD group, n = 20; SAP, n = 19; UAP, n = 14; and MI, n = 26).

Bioinformatic Analysis

We utilized the miRWalk, miRDB, miRMap, RNA22, and DIANA MicroT-CDS databases to determine putative miRNA target genes.[15-19] The miRNA-target gene interaction pairings were chosen if at least 2 of the 5 databases predicted them. The Database for Annotation, Visualization, and Integrated Discovery (DAVID; version 6.8) was used to perform a functional analysis of the target genes to deduce their putative functions.[20] Further, we used Enrichr, a web-based tool, to perform gene ontology (GO) annotations on the miRNA target genes we had obtained.[21] ClueGO software was utilized for the pathway analysis of the putative target genes of the miRNAs using the Kyoto Encyclopedia of Genes and Genomes (KEGG) database.[22] The relevancy of a biological pathway/term to the predicted miRNA target genes was determined using the Fisher exact test. The corrected *P* values of significant pathways/terms were <.05 (Benjamini-Hochberg procedure). Target genes associated with CVD were obtained from the Genetic Association Database (GAD) (update from August 2014; accessed March 2020) and Malacards database[23] (version 1.05; accessed March 2020), as previously described.[24]

Statistical Analyses

Categorical variables were analyzed using χ^2 testing. The ANOVA test was used for the comparison of continuous variables between groups. Due to skewed distributions of HDL, TG, HbA1c, and fasting glucose parameters, we used the nonparametric Kruskal-Wallis test for these variables. Categorical variables were reported as percentages, whereas quantitative variables were presented as mean (SD) values. We performed Kruskal-Wallis testing to analyze the difference in serum miRNA expression between groups. Spearman rank correlation analysis was used to examine the correlations between miRNAs and biochemical variables. For the formation of tertile groups (T1, T2, and T3), we divided the study population into 3 equal groups, using 33.3th and 66.6th percentile values of circulating miRNA levels as cut-off values for each miRNA separately. The analyses using tertile groups were conducted using T1 and T3. T1 of miRNAs represents individuals with low expression of miRNAs, whereas the T3 group was formed with individuals with high expression of miRNAs. We used the ROC curve to determine the ability to discriminate between groups and also calculated the AUC. Statistical analyses were conducted using SPSS (version 23.0; SPSS) and GraphPad Prism (version 8; GraphPad Software). For all tests, P <.05 was evaluated as being statistically significant.

Results

Baseline Characteristics of Study Subjects

Of the enrolled 185 subjects, 55 were in the non-CAD control group (mean age [SD], 65.4 [8.9] years), 48 had been diagnosed with SAP (mean

FIGURE 1. Circulating levels of miR-126-3p, miR-210-3p, miR-326, and let-7g-5p. A, The circulating levels of miR-126-3p were significantly different in the myocardial infarction (MI) and unstable angina pectoris (UAP) groups, compared with control individuals from the non–coronary artery disease (CAD) group. In pairwise comparisons other than UAP vs control and MI vs control, the circulating levels of miR-126-3p were not significantly different. B, In pairwise comparisons, the circulating levels of miR-210-3p were significantly different in the MI group compared with the UAP, SAP, and non-CAD control groups. C, In pairwise comparisons, the circulating levels of let-7g-5p were significantly different in the MI group compared to the UAP group. D, The circulating levels of miR-326 were not significantly different between groups.

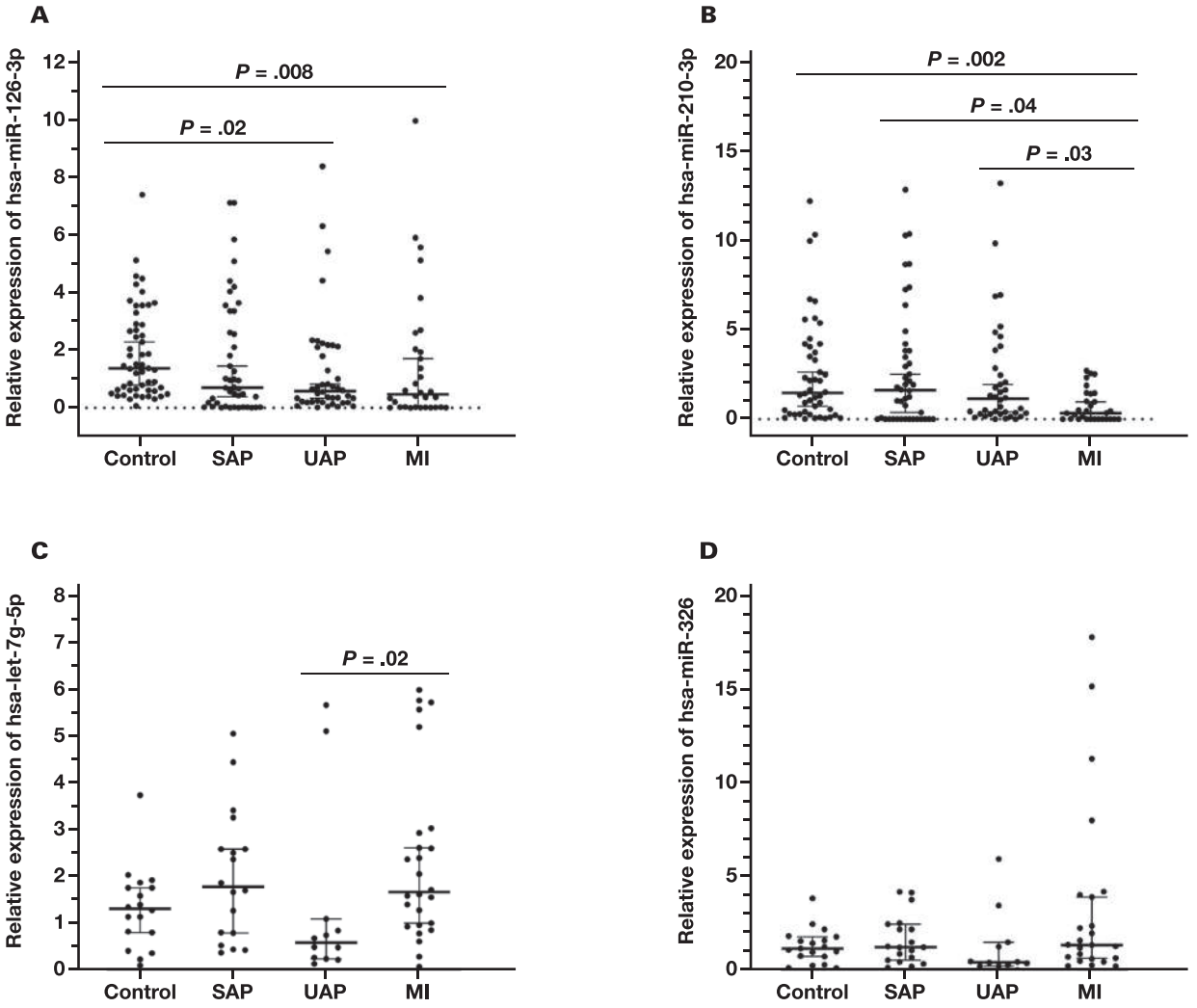

age, 52.0 [5.7] years), 46 had been diagnosed with UAP (mean age, 62.2 [12.8] years), and 36 had been diagnosed with MI (mean age, 54.0 [8.5] years). The baseline characteristics of the groups are shown in Supplemental Table S1. CAD family history significantly differed among groups, in addition to the levels of serum lipids, fasting glucose, CK-MB, and cTn-I. The prevalence of type 2 diabetes mellitus (T2DM), obesity, and hypertension was not different among the groups. Also, the frequencies of lipid-lowering drug usage, current smoking status, and use of antidiabetic drugs were not significantly different between groups (Supplemental Table S1).

Expression Levels of Circulating miR-126-3p, miR-210-3p, miR-326, and let-7g-5p

The circulating levels of miR-126-3p and miR-210-3p were successfully determined in 171 individuals (non-CAD, n = 53; SAP, n = 44; UAP, n = 42; and MI, n = 32); let-7g-5p and miR-326 levels were determined in 74 male subjects (non-CAD, n = 18; SAP, n = 18; UAP, n = 12; and MI, n = 26) using qRT-PCR. The expression levels of miR-126-3p and miR-210-3p in 14 individuals, as well as let-7g-5p and miR-326 levels in 5 men, could not be determined due to issues with the quality of their RNA specimens.

Pairwise comparisons were made in the non-CAD, SAP, UAP, and MI groups. The levels of miR-126-3p expression were to be significantly decreased in the MI group, compared with the non-CAD group (P = .008; **FIGURE 1A**). Also, the expression of miR-126-3p was lower in the UAP group, compared with non-CAD controls (P = .02; **FIGURE 1A**). When we analyzed circulating miR-210-3p levels, we discovered that the expression levels were lower in the MI group, compared with those levels in the UAP, SAP, and non-CAD control groups (P = .03, P = .04, and P = .002, respectively; **FIGURE 1B**). When we compared the circulating levels of let-7g-5p between selected groups, we found that the levels were significantly differentiated

TABLE 1. High and low expression tertiles of miRNAs and clinical presentations of CAD

Variable	Group, % (No.)				χ^2 *P* value	Multivariate logistic regression [OR (95% CI); *P* value][a]			
	Non-CAD	SAP	UAP	MI		Non-CAD vs SAP	Non-CAD vs UAP		Non-CAD vs MI
Low miR-126-3p expression	23.3 (7)	53.5 (16)[b]	62.1 (18)[c]	64.0 (16)[d]	**.006**	Reference: 1.00			
High miR-126-3p expression	76.7 (23)	46.7 (14)	37.9 (11)	36.0 (9)		0.014 (0.001-0.351); ***P* = .01**	0.042 (0.007-0.263) ***P* = .001**		0.040 (0.004-0.377) ***P* = .005**
	Non-CAD	SAP	UAP	MI		Non-CAD vs MI	SAP vs MI	UAP vs MI	Non-MI vs MI
Low miR-210-3p expression	36.4 (12)	46.9 (15)	50.0 (11)	78.9 (15)[e-h]	**.03**	Reference: 1.00			
High miR-210-3p expression	63.6 (21)	53.1 (17)	50.0 (11)	21.1 (4)		0.046 (0.005-0.394) ***P* = .005**	0.220 (0.039-1.232) *P* = .09	0.575 (0.111-2.696) *P* = .51	0.230 (0.067-0.797) ***P* = .02**
	Non-CAD	**SAP**	**UAP**	**MI**		**Non-MI vs MI[i]**			
Low let-7g-5p expression	66.6 (6)	42.9 (6)	80.0 (8)	25.0 (4)[j,k]	**.03**	Reference: 1.00			
High let-7g-5p expression	33.3 (3)	57.1 (8)	20.0 (2)	75.0 (12)		4.562 (1.182-17.608) ***P* = .03**			
	Non-CAD	SAP	UAP	MI					
Low miR-326 expression	40.0 (4)	41.7 (5)	80.0 (8)	38.9 (7)	.16				
High miR-326 expression	60.0 (6)	58.3 (7)	20.0 (2)	61.1 (11)					

CAD, coronary artery disease; MI, myocardial infarction; SAP, stable angina pectoris; UAP, unstable angina pectoris.
[a]*Logistic regression analysis adjusted for age and sex.*
[b]*Control vs SAP;* P = *.02.*
[c]*Control vs UAP;* P = *.003.*
[d]*Control vs MI;* P = *.002.*
[e]*Control vs MI;* P = *.003.*
[f]*SAP vs MI;* P = *.02.*
[g]*UAP vs MI;* P = *.06.*
[h]*Non-MI vs MI;* P = *.01.*
[i]*Logistic regression analysis adjusted for age.*
[j]*UAP vs MI;* P = *.01.*
[k]*Non-MI vs MI;* P = *.02.*

between UAP and MI groups (*P* = .02; **FIGURE 1C**). There was no statistically significant difference between groups regarding circulating miR-326 levels (**FIGURE 1D**).

Clinical Presentation and Low and High Expressions of miRNA

Next, we divided the study population into tertiles as T1, T2, and T3, according to the expression levels of miRNAs, to better identify the associations and to eliminate the bias that takes root from outliers. The clinical presentation of CAD was examined in high and low expression tertiles of miR-126-3p, miR-210-3p, and let-7g-5p, and the distributions of patients between groups were significantly different (**TABLE 1**). Moreover, the SAP, UAP, and MI groups were predominantly in the low expression tertile of miR-126-3p, compared with controls in pairwise comparisons (**TABLE 1**). These results were also statistically significant in the logistic regression analysis adjusted to age and sex (**TABLE 1**).

When the T1 and T3 of miR-210-3p were compared between groups, the MI group was found predominantly in the low-expression tertile, compared with the control, SAP, and UAP groups, in pairwise comparisons. Moreover, when individuals were compared according to MI status, patients without MI were more prevalent in certain high-expression tertile groups compared to patients with MI (**TABLE 1**). However, the differences between control and MI groups and non-MI vs MI were found to be statistically significant in the logistic regression analysis adjusted to age and sex (**TABLE 1**). Still, we found the high expression tertile of let-7g-5p to be more prevalent in the MI group compared to the UAP and non-MI groups (control, SAP, and UAP; **TABLE 1**). Also, high expression of let-7g-5p increased the risk for MI in the logistic regression analysis adjusted for age (**TABLE 1**). There was no statistically significant difference between clinical presentation and tertiles of miR-326 (**TABLE 1**).

The Diagnostic Accuracy of miR-126-3p, miR-210-3p, and let-7g-5p

To evaluate the sensitivity and specificity of miR-126-3p, miR-210-3p, and let-7g-5p for diagnosing SAP, UAP, and MI, the AUC value was calculated using ROC curves (Supplemental Figure 1). As shown in **FIGURE 2**, miR-126-3p has a moderate power for distinguishing the MI group from the non-CAD group with the AUC value of 0.673 (95% CI, 0.547-0.812). The sensitivity and specificity of miR-126-3p for the MI group vs non-CAD controls were determined to be 59.4% sensitivity and 77.4% specificity, with a 0.60 cut-off. The AUC of miR-210-3p for the distinction of MI and non-CAD controls was found to be 0.751 (63.3% sensitivity and 71.7% specificity with 0.50 cut-off; *P* < .001; **FIGURE 2**).

We also performed ROC curve analyses using the crucial MI risk factors of TG/HDL ratio and presence of diabetes mellitus (DM), to better test the power of miRNAs. The cut-off value for TG/HDL ratio was determined to be ≥4.0, according to previous study reports, such as one by Chen et al.[25] The AUC value was found to be 0.871 for the model

FIGURE 2. Sensitivity and specificity of circulating miR-126-3p and miR-210-3p. ROC curve analyses were performed to determine the discriminative ability of miR-126-3p and miR-210-3p among non–coronary artery disease (CAD) and myocardial infarction (MI) groups.

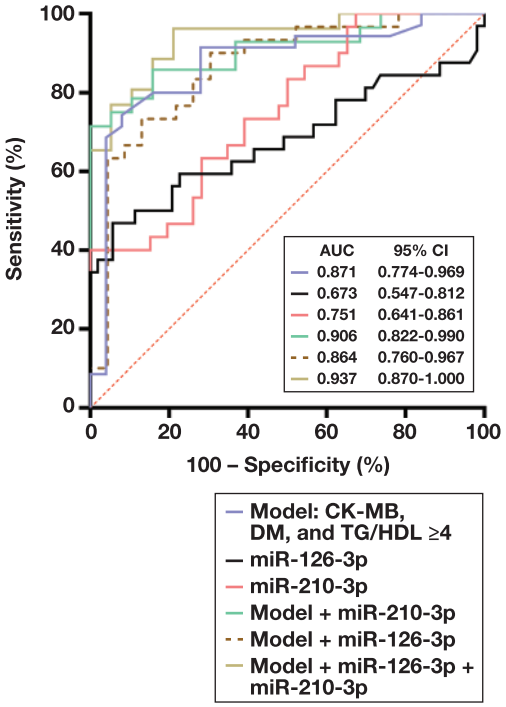

of CK-MB, TG/HDL ratio ≥4, and DM (**FIGURE 2**). When the model and miR-210-3p were evaluated together, the discrimination of MI from non-CAD was better (AUC, 0.906; 95% CI, 0.822-0.990; **FIGURE 2**). The discriminating power was best in the model, including CK-MB, DM, TG/HDL ≥4, miR-210-3p, and miR-126-3p, together with the AUC value of 0.937 (**FIGURE 2**). When the diagnostic accuracy of let-7g-5p for distinguishing UAP from MI was evaluated using ROC curve analysis, the AUC value was found to be 0.776 (95% CI, 0.593-0.959), with 84.6% sensitivity and 75% specificity (cut-off, 0.85) (Supplemental Figure 1).

Associations Between Clinical and Biochemical Parameters and Circulating miRNA Levels

The associations between clinical and biochemical parameters and tertile groups of miRNAs were evaluated in the study population, as divided into the control, SAP, UAP, and MI groups. We discovered that the stenosis percentage differs between T1 and T3 of miR-126-3p and miR-210-3p in the study population (**FIGURE 3**). Also, plasma lipid levels were associated with tertiles of miR-210-3p and miR-126-3p (**FIGURE 3**). In addition, a negative correlation was observed between CK-MB and miR-210-3p in the study population (r = –0.262; P = .007). Individuals in the low miR-210-3p tertile have shown significantly higher CK-MB levels (P = .01) and higher cTnI levels with borderline statistical significance (P = .08). The high miR-210-3p expression tertile had lower LDL-C levels in the study population and control groups (**FIGURE 3**), whereas the TG levels of the same tertile were lower in the study population, SAP, and UAP groups (**FIGURE 3**). Similarly, the low-expression tertiles of miR-126-3p and miR-210-3p have shown higher LDL-C/HDL-C and TC/HDL-C ratios in the subgroups (**FIGURE 3**). Also, miR-210-3p expression levels were significantly associated with the TyG index in the study population and UAP groups.

In Silico Analyses of miR-126-3p, miR-210-3p, and let-7g-5p

In bioinformatic analyses, 105, 244, 460, 1318, and 21 putative targets were found in DIANA MicroT-CDS, RNA22, miRMap, miRWalk, and miRDB databases, respectively, for miR-126-3p. In total, 158 of these genes were intersected in 2 of the databases, and 31 predicted genes were common in 3 databases. When the relationship of these putative targets with the CVD was evaluated, 49 and 3 of the target genes intersecting in the 2 databases were found to be associated in GAD and Malacards, respectively (Supplemental File). We discovered that 14 and 2 of the predicted target genes intersecting in 3 of the databases mentioned earlier herein were CVD-associated genes in GAD and Malacards, respectively (Supplemental File). Putative targets of miR-126-3p that intersected in 2 of the databases were found to be significantly enriched in the HIF-1 signaling pathway, FoxO signaling pathway, mTOR signaling pathway, AMPK signaling pathway, insulin signaling pathways, autophagy, and T2DM KEGG terms, along with others (**FIGURE 4A**; Supplemental File).

The bioinformatic analysis revealed 11044, 1203, 2164, 184, and 84 putative target genes in RNA22, miRMap, miRWalk, DIANA MicroT-CDS, and miRDB databases, respectively, for miR-210-3p. In total, 2221 of these target genes were intersected in 2 of the databases mentioned earlier herein, and 287 predicted genes were intersected in 3 databases. In the analysis of the DAVID bioinformatics tool, 612 predicted target genes in 2 databases were enriched in cardiovascular GAD disease class by 1.1-fold (adjusted P = .001) (Supplemental File). In all, 33 genes were associated with CHD, AMI, and MI in the Malacards database (Supplemental File). When the genes common in 3 of the 5 databases were evaluated for their relationship to CVD development, 87 and 4 were associated with CVD in GAD and Malacards, respectively (Supplemental File). In pathway analysis for the putative targets of miR-210-3p, we found that target genes were enriched significantly in CAD-related KEGG pathways such as vascular smooth muscle contraction, the insulin signaling pathway, the AMPK signaling pathway, and autophagy (**FIGURE 4B**; Supplemental File).

We found 3545, 13914, 2956, 1370, and 174 putative target genes for let-7g-5p in miRMap, RNA22, DIANA MicroT-CDS, and mirDB databases, respectively. In total, 4714 of these targets intersected in the results of at least 2 databases, and 1206 of these target genes are associated with CVD according to the GAD, whereas 62 are associated with CHD, AMI, and MI in the Malacards database. Moreover, in the analysis conducted using the DAVID bioinformatics tool, putative targets intersecting in 2 databases were enriched in GAD cardiovascular diseases and metabolic diseases by 1.1-fold change (adjusted P value [Benjamini-Hochberg method] = 4.2×10^{-7} and 4.2×10^{-7}, respectively]. Also, putative target genes of the let-7g-5p were enriched in the MAPK signaling pathway, TGF-β signaling pathway, cGMP-PKG signaling pathway, and ABC transporters KEGG terms (P < .05 Benjamini-Hochberg corrected; Supplemental File).

Discussion

There is an ongoing investigation for the identification of noninvasive biomarkers that will make it possible to diagnose and elucidate the prognosis of CAD. In this study, we found that circulating miR-126-3p

FIGURE 3. Expression tertiles of miR-126-3p and miR-210-3p are associated with clinical parameters. The stenosis percentage (A) is lower in the high tertiles of miR-126-3p and miR-210-3p. LDL-C (B), TG levels (C), LDL-C/HDL-C (D), TC/HDL-C ratios (E), and triglyceride-glucose (TyG; F) index were lower in the high miR-210-3p expression tertile in the subgroups. In the study population, LDL-C level and TC/HDL-C ratio were lower in the high miR-126-3p expression tertile.

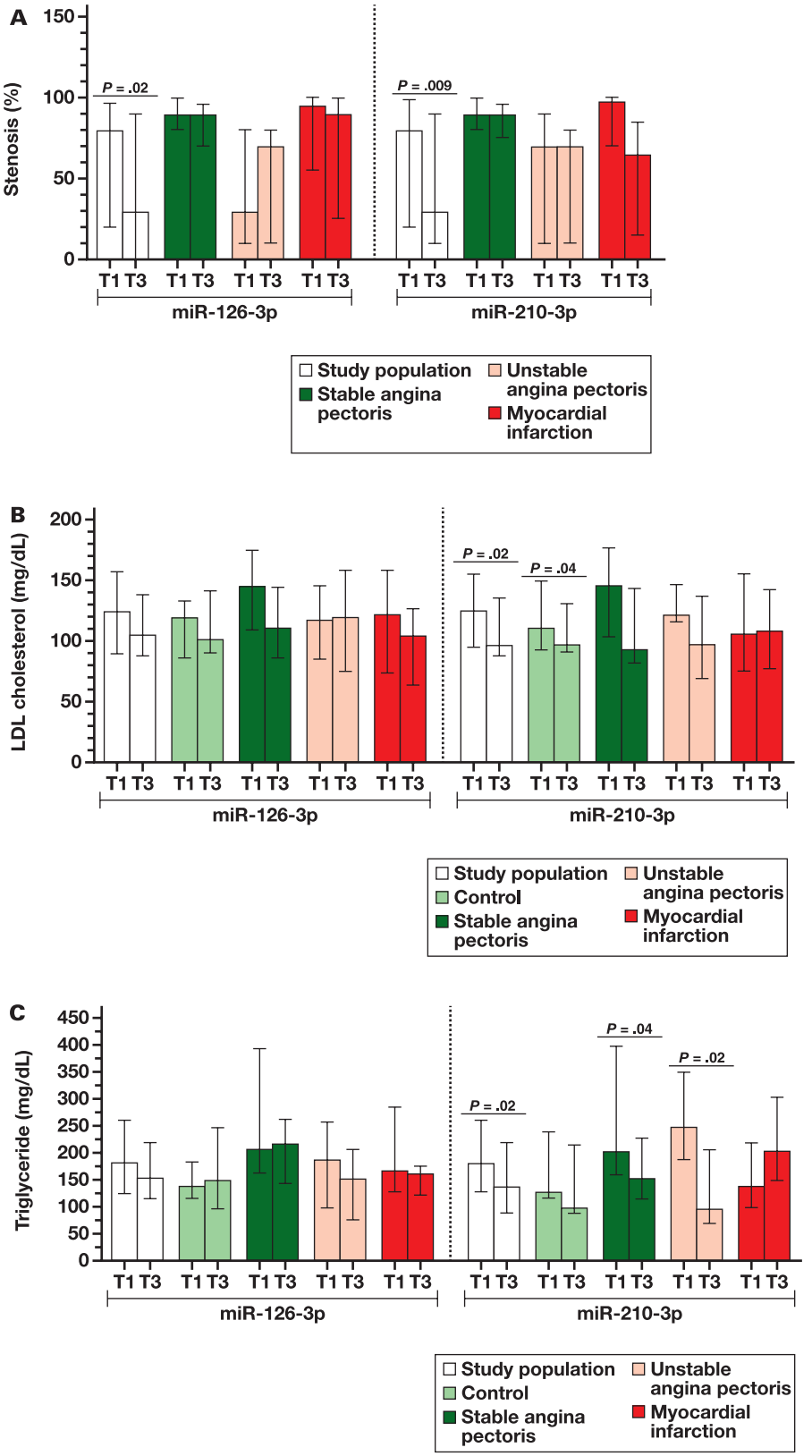

FIGURE 3. (cont)

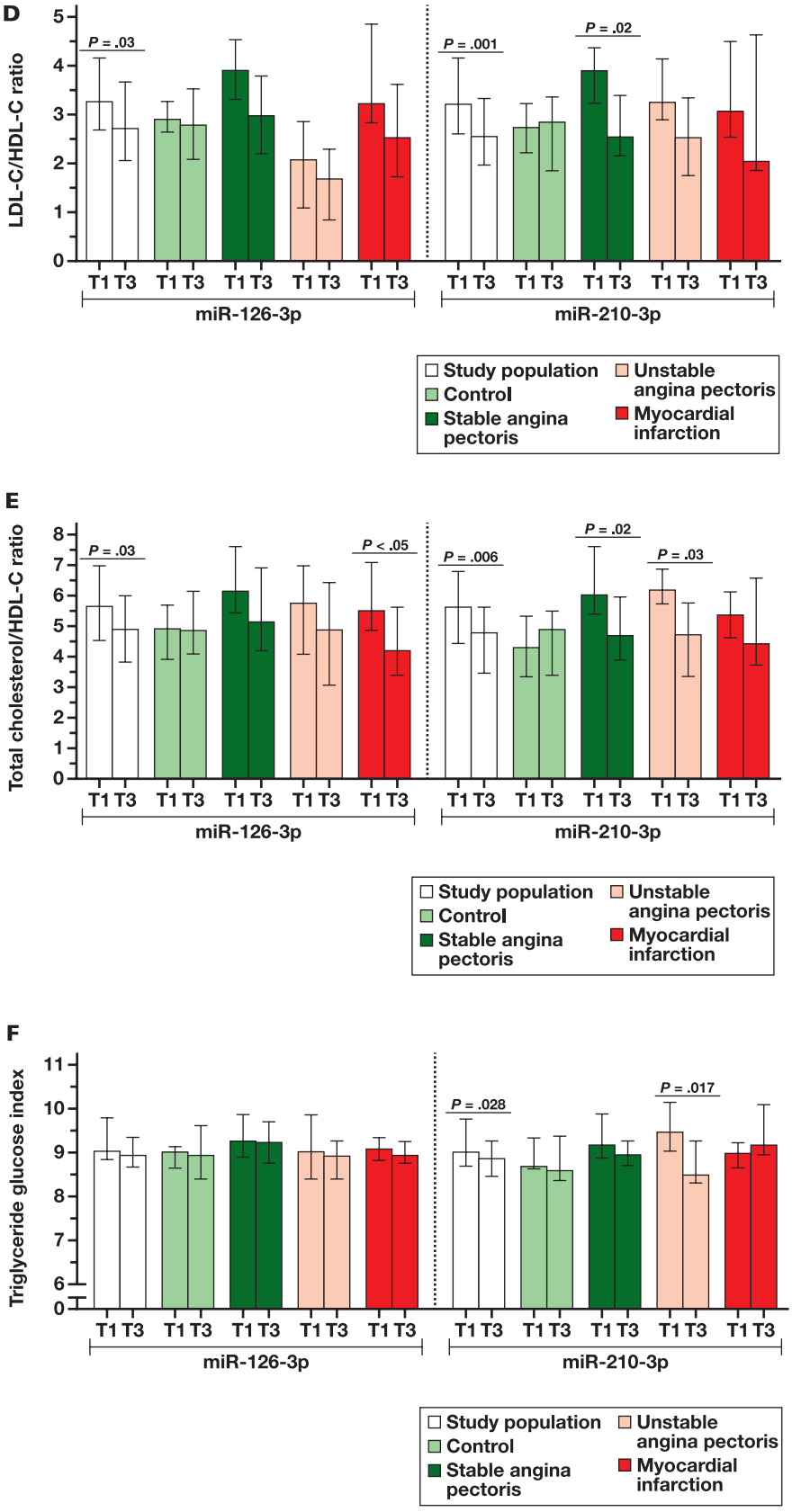

FIGURE 4. **Kyoto Encyclopedia of Genes and Genomes (KEGG) pathway analyses. Pathway analyses were performed using the miRNA target genes we retrieved using the KEGG database terms by utilizing ClueGO. The Fisher exact test (adjusted using the Benjamini-Hochberg procedure) was used to assess the relevance of a biological pathway/term to the putative miRNA target genes. The top 20 pathways that putative target genes of miR-126-3p (A) and miR-210-3p (B) enriched were given. The numbers after the bars indicate the number of predicted targets of miRNAs in the pathway. *$P \leq .05$; **$P \leq .01$.**

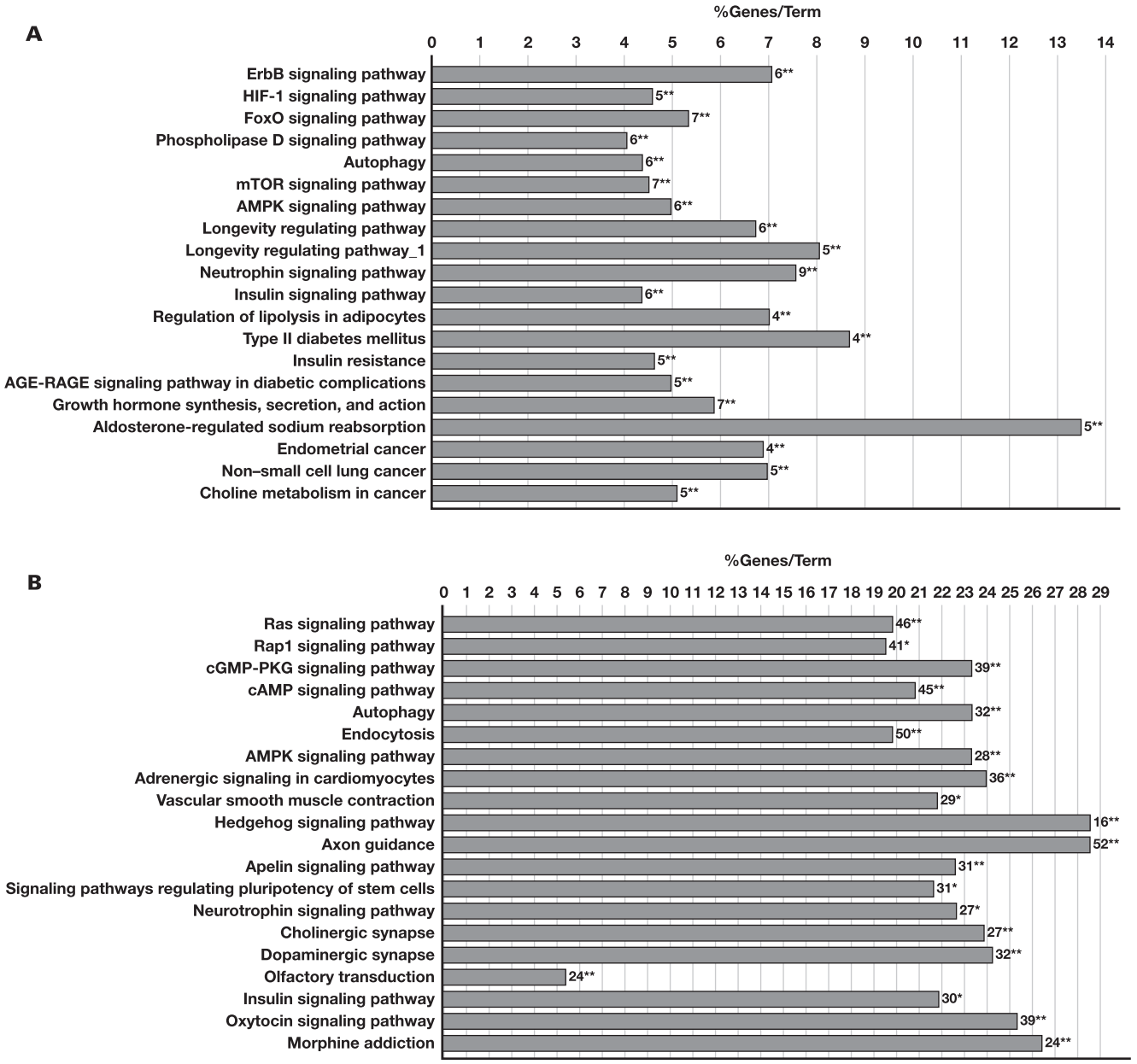

is downregulated significantly in patients with MI and UAP, compared with non-CAD controls. Also, circulating levels of miR-210-3p were downregulated significantly in the MI group, compared with the non-CAD control, SAP, and UAP groups. Circulating let-7g-5p was found at higher levels in the MI group, compared with the UAP group. Moreover, miR-210-3p and miR-126-3p were associated closely with serum lipid levels (**FIGURE 5**).

In the continuing search for a novel biomarker for CAD, miR-126-3p was one of the miRNAs examined. As previously demonstrated, the impact of miR-126 is influenced by the source of miR-126 and the specific mature strand (-3p or -5p) that is involved, as in atherosclerosis and angiogenesis processes.[26,27] For instance, miR-126-3p mainly exhibits atheroprotective features on endothelial cells (ECs) through suppressing inflammation, whereas miR-126-5p primarily increases the proliferation of ECs and reducing atherosclerosis.[26] These features highlight the functional complexity of this miRNA. As was comprehensively reviewed by Yu et al,[28] miR-126-3p is associated with vascular or related diseases. Endothelial cells exhibit high levels of miR-126, which helps to preserve vascular integrity and promote angiogenesis.[29]

In a mouse model, genetic deletion of miR-126 resulted in the embryonic death of some mice related to vascular leakage, and the remaining mice had pathologies associated with angiogenesis deficiencies.[30]

FIGURE 5. **Graphical abstract. Individuals who underwent coronary angiography were grouped as controls not having non–coronary artery disease (CAD), as well as patients with stable angina pectoris (SAP), unstable angina pectoris (UAP), and myocardial infarction (MI). The circulating levels of miR-126-3p, miR-210-3p, let-7g-5p, and miR-326 were determined in serum specimens. The circulating levels of miR-126-3p were lower in the MI and UAP groups compared to the non-CAD group; circulating miR-210-3p levels were at lower levels in the MI group than others. The levels of let-7g-5p were significantly different between the UAP and MI groups. To evaluate the sensitivity and specificity of miR-126-3p, miR-210-3p, and let-7g-5p for diagnosing SAP, UAP, and MI, the AUC value was calculated using ROC curves. The AUC of miR-210-3p for the distinction of MI and non-CAD controls was found to be 0.751 (63.3% sensitivity and 71.7% specificity). The discrimination power was best in the model that includes creatine kinase–myocardial band (CK-MB), diabetes mellitus (DM), TG/HDL >4, miR-210-3p, and miR-126-3p with an AUC value of 0.927. Moreover, lipid levels, lipid ratios, and stenosis percentage were lower in individuals with high circulating miR-126-3p and miR-210-3p levels. The illustration was created via BioRender.com.**

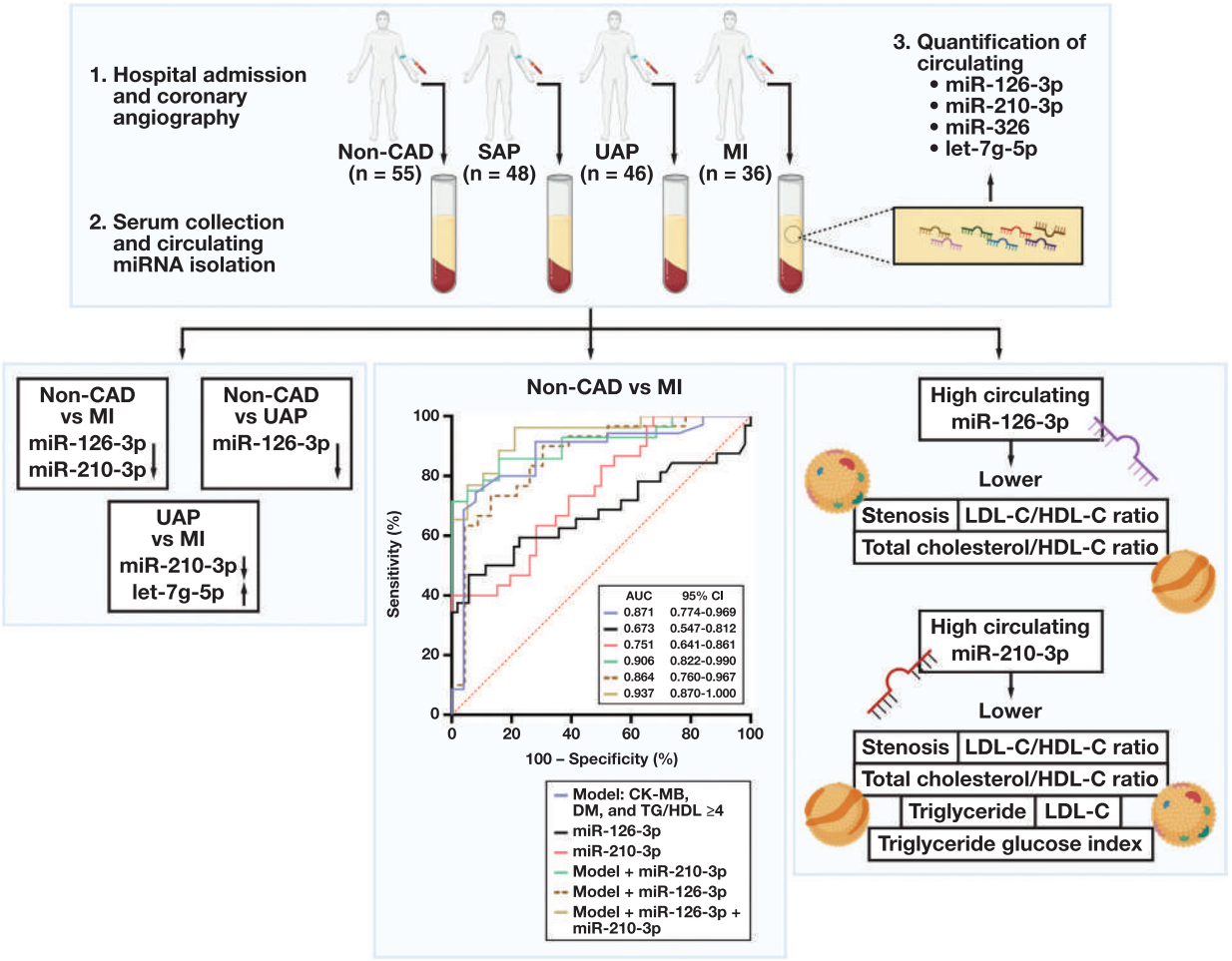

Moreover, overexpression of miR-126 attenuated atherosclerotic plaque progression in APOE$^{-/-}$ mice fed a high-fat diet.[31] Circulating levels of miR-126-3p were examined in ACS groups, and related studies were concluded with rather contradicting results.[31-34] In some previous studies, such as that by Wang et al,[33] circulating levels of miR-126-3p decreased in patients with CAD, compared with controls, whereas others[31,32,34] reported increased circulating levels.

In the present study, we determined that circulating miR-126-3p levels were lower in the MI and UAP groups, compared with the control group. Moreover, the high-expression tertile was more prevalent in the control group than in the SAP, UAP, and MI groups, and stenosis was lower in the high-expression tertile. In line with this finding, Fichtlscherer et al[35] showed that circulating miR-126-3p levels are downregulated in patients with CAD compared to healthy controls.

miR-210-3p and miR-210-5p are the hypoxia-inducible miRNAs (hypoxamiRs) regulated by HIF-1α in the hypoxic environment.[36] miR-210 regulates cell survival, proliferation, apoptosis, differentiation, and other physiological functions by controlling its downstream target genes after hypoxia. According to the results from recent studies, such as one by Diao et al,[37] miR-210-3p is elevated in hypoxic cardiomyocytes and demonstrates cytoprotective features. In addition, Qiao et al[38] showed that in macrophages, high miR-210-3p levels inhibit lipid accumulation and NF-κB-mediated inflammation by suppressing IGF2 in atherosclerosis. Also, improved plaque stability was established with the increased expression of miR-210 through APC inhibition and increased VSMC survival.[39]

miR-210-3p is evaluated as a potential biomarker in studies related to hypoxia, preeclampsia, cancer, and stroke, with better reliability and repeatability in circulation.[40-42] From the perspective of CVDs, miR-210-3p levels in whole-blood specimens from 16 patients with CAD were increased, compared with 16 controls.[43] In another study,[44] plasma levels of miR-210-3p were upregulated in 9 patients with diabetes and CVD, compared with 6 patients who had diabetes but no CVD.

In contrast, Qin et al[45] showed that miR-210 levels were negatively correlated with the cardiac damage marker cTnI, a well-known marker upregulated in MI and cardiac damage. In line with Qin et al, in the present study we observed a negative correlation between miR-210-3p and CK-MB, which is also a well-known marker in MI, and higher CK-MB and cTnI levels in the low miR-210-3p tertile, compared with the high miR-210-3p tertile. In a microarray analysis conducted on patients with MI and healthy controls, Rincón et al[46] demonstrated that circulating miR-210-3p levels are downregulated in patients with MI. In the present study, decreased circulating levels of miR-210-3p were observed in the MI group, compared with the SAP, UAP, and non-CAD groups; also, the stenosis percentage was lower in the high miR-210-3p tertile.

Zeller et al[47] compared the circulating miR-210-3p levels on admission, and after 3 and 6 hours of admission, in 29 patients with ST-segment elevation MI (STEMI) and 63 controls with noncardiac chest pain (NCCP). These coauthors found that miR-210-3p levels are increased within 6 hours, although it was not specified whether there is a difference in miR-210-3p levels between the STEMI group and NCCP control group on admission. The gradual increase in the abundance of miR-210-3p highlights the importance of the specimen collection timeline. Other studies investigate the relation of miR-210 to the presence of CAD. However, we could not compare those findings with ours because the examined strand of the miR-210 (-3p or -5p) is not specified, which complicates the assessment of the results. To our knowledge, our study is the first in the literature to show the downregulation of circulating miR-210-3p in patients with MI compared to non-CAD controls, patients with SAP, and patients with UAP.

The molecular function and the target genes of let-7g-5p were previously studied in vivo and in vitro. Previous study findings demonstrated evidence for let-7g-5p reducing macrophage foam cell formation by inhibiting canonical and noncanonical NF-κB signaling pathways and reducing inflammatory and apoptotic responses. Also, in a few studies, the association between the circulating levels of let-7g-5p and the presence and severity of CAD was previously investigated. The circulating levels of let-7g-5p were associated with the segment stenosis score (SIS): this scoring system evaluates the severity of coronary atherosclerosis.[48] In this study, it has been found that patients with severe atherosclerosis have lower circulating let-7g-5p.[48] In line with this finding, serum let-7g-5p levels decreased during acute non–ST-elevated MI (NSTEMI), compared with a control group, in a study conducted by Mompeón et al.[49]

As a part of the HUNT (Nord-Trøndelag Healthy) study, Bye et al[50] have shown that circulating let-7g-5p levels are decreased in patients with AMI, compared with healthy controls. In contrast, Velle-Forbord et al[13] have shown that circulating levels of let-7g-5p are increased in patients with fatal MI compared to controls, as a part of the HUNT study. In the present study, although there was no difference between non-CAD controls and the MI group, the UAP group showed significantly lower circulating levels than the MI group. The contradicting results on the circulating levels of the examined miRNAs as a diagnostic marker indicate the need for analysis in larger study groups. The vast diversity and minimal overlap of aberrant miRNA expression patterns in different studies may be due to patient group, type of specimen, study design, various detection methods, and specimen collection procedures, as well as race and ethnicity.

The risk factors of CAD, such as low HDL-C, high LDL-C, and TG levels, were well defined among the lipid ratios, which were determined as CVD risk indicators. In addition to blood lipid levels, the LDL-C/HDL-C, TC/HDL-C, and TG/HDL-C ratios are thought to be markers of cardiovascular disorders because an imbalance in the cholesterol transported by protective and atherogenic lipoproteins might indicate a higher risk of CVD.[51] Nam et al[52] suggest that the TC/HDL-C and LDL-C/HDL-C ratios are more potent markers of CAD risk than LDL and HDL levels only. In a previous study,[53] patients with CAD and high LDL-C levels had considerably lower levels of miR-126-3p. In line with this finding, although it did not reach statistical significance, the high miR-126-3p tertile showed lower LDL-C levels. In addition, the LDL-C/HDL-C and TC/HDL-C ratios were significantly lower in the high miR-126-3p tertile. Further, in this study, we found that LDL-C, TG, TC/HDL-C, LDL-C/HDL-C ratios, and TyG index are at lower levels in the high miR-210-3p tertile in several groups. Qiao et al[38] demonstrated that miR-210-3p was negatively correlated with TG and TC levels, which is in line with our results. These findings point out the associations between the miRNAs and CAD risk factors and therefore highlight the importance of miRNAs as a potential target for the disease.

The results of our bioinformatics analyses have shown that putative target genes of miR-210-3p intersecting in 2 of the analyzed databases are significantly enriched in cardiovascular GAD disease class by 1.1-fold, whereas putative targets of let-7g-5p are enriched in metabolic diseases and CVD GAD classes significantly. The biological processes and the KEGG pathways that these putative targets have enriched are linked to the CAD pathological process. We found that putative targets of miR-210-3p and miR-126-3p are enriched in CAD-related KEGG pathways such as AMPK signaling, autophagy, and insulin signaling.

Several limitations must be taken into account. In this study, the size of the subgroups of CAD prevented us from considering the status of patients regarding use of lipid-lowering and antidiabetic drugs. Because miRNAs could also be bound to lipoprotein particles such as HDL, in future studies, status of usage of lipid-lowering drugs should be considered.

Conclusions

Our study results indicate that miR-126-3p and miR-210-3p can discriminate individuals belonging in the non-CAD group from those with UAP and MI, whereas levels of circulating let-7g-5p significantly discriminate UAP from MI. However, it is crucial to remember that conflicting findings from previous studies emphasize the need for further research to enable full comprehension of the potential function of miRNAs as diagnostic and/or prognostic biomarkers. Therefore, it is imperative to conduct more clinical validation studies to determine the clinical relevance of miRNAs and further functional studies to enlighten their role in the development of SAP, UAP, and MI.

Funding

This study was funded by the Scientific Research Projects Coordination Unit of Istanbul University (project numbers: 37688 and 28984).

Conflict of Interest Disclosure

The authors have nothing to disclose.

REFERENCES

1. Mallat Z, Corbaz A, Scoazec A, et al. Expression of interleukin-18 in human atherosclerotic plaques and relation to plaque instability. *Circulation.* 2001;104(14):1598-1603. https://doi.org/10.1161/hc3901.096721

2. Malakar AK, Choudhury D, Halder B, Paul P, Uddin A, Chakraborty S. A review on coronary artery disease, its risk factors, and therapeutics. *J Cell Physiol.* 2019;234(10):16812-16823. https://doi.org/10.1002/jcp.28350
3. Kloner RA, Chaitman B. Angina and its management. *J Cardiovasc Pharmacol Ther.* 2017;22(3):199-209. https://doi.org/10.1177/1074248416679733
4. Lu L, Liu M, Sun R, Zheng Y, Zhang P. Myocardial infarction: symptoms and treatments. *Cell Biochem Biophys.* 2015;72(3):865-867. https://doi.org/10.1007/s12013-015-0553-4
5. Bartel DP. MicroRNAs: genomics, biogenesis, mechanism, and function. *Cell.* 2004;116(2):281-297. https://doi.org/10.1016/s0092-8674(04)00045-5
6. Sun X, Sit A, Feinberg MW. Role of miR-181 family in regulating vascular inflammation and immunity. *Trends Cardiovasc Med.* 2014;24(3):105-112. https://doi.org/10.1016/j.tcm.2013.09.002
7. Fazmin IT, Achercouk Z, Edling CE, Said A, Jeevaratnam K. Circulating microRNA as a biomarker for coronary artery disease. *Biomolecules*. 2020;10(10):1354. https://doi.org/10.3390/biom10101354
8. O'Brien J, Hayder H, Zayed Y, Peng C. Overview of microRNA biogenesis, mechanisms of actions, and circulation. *Front Endocrinol (Lausanne)*. 2018;9:402. https://doi.org/10.3389/fendo.2018.00402
9. Altesha MA, Ni T, Khan A, Liu K, Zheng X. Circular RNA in cardiovascular disease. *J Cell Physiol.* 2019;234(5):5588-5600. https://doi.org/10.1002/jcp.27384
10. Wang L, Jin Y. Noncoding RNAs as biomarkers for acute coronary syndrome. *Biomed Res Int.* 2020;2020:3298696. https://doi.org/10.1155/2020/3298696
11. Guan Y, Song X, Sun W, Wang Y, Liu B. Effect of hypoxia-induced microRNA-210 expression on cardiovascular disease and the underlying mechanism. *Oxid Med Cell Longev*. 2019;2019:4727283. https://doi.org/10.1155/2019/4727283
12. Li H-Y, Zhao X, Liu Y-Z, et al. Plasma microRNA-126-5p is associated with the complexity and severity of coronary artery disease in patients with stable angina pectoris. *Cell Physiol Biochem.* 2016;39(3):837-846. https://doi.org/10.1159/000447794
13. Velle-Forbord T, Eidlaug M, Debik J, et al. Circulating microRNAs as predictive biomarkers of myocardial infarction: Evidence from the HUNT study. *Atherosclerosis.* 2019;289:1-7. https://doi.org/10.1016/j.atherosclerosis.2019.07.024
14. Ozuynuk AS, Erkan AF, Dogan N, et al. Examining the effects of the *CLU* and *APOE* polymorphisms' combination on coronary artery disease complexed with type 2 diabetes mellitus. *J Diabetes Complications.* 2022;36(1):108078. https://doi.org/10.1016/j.jdiacomp.2021.108078
15. Miranda KC, Huynh T, Tay Y, et al. A pattern-based method for the identification of microRNA binding sites and their corresponding heteroduplexes. *Cell.* 2006;126(6):1203-1217. https://doi.org/10.1016/j.cell.2006.07.031
16. Paraskevopoulou MD, Georgakilas G, Kostoulas N, et al. DIANA-microT web server v5.0: service integration into miRNA functional analysis workflows. *Nucleic Acids Res.* 2013;41(Web Server issue):W169-W173. https://doi.org/10.1093/nar/gkt393
17. Vejnar CE, Zdobnov EM. MiRmap: comprehensive prediction of microRNA target repression strength. *Nucleic Acids Res.* 2012;40(22):11673-11683. https://doi.org/10.1093/nar/gks901
18. Chen Y, Wang X. miRDB: an online database for prediction of functional microRNA targets. *Nucleic Acids Res.* 2020;48(D1):D127-D131. https://doi.org/10.1093/nar/gkz757
19. Dweep H, Gretz N. miRWalk2.0: a comprehensive atlas of microRNA-target interactions. *Nat Methods.* 2015;12(8):697. https://doi.org/10.1038/nmeth.3485
20. Huang DW, Sherman BT, Lempicki RA. Bioinformatics enrichment tools: paths toward the comprehensive functional analysis of large gene lists. *Nucleic Acids Res.* 2009;37(1):1-13.
21. Chen EY, Tan CM, Kou Y, et al. Enrichr: interactive and collaborative HTML5 gene list enrichment analysis tool. *BMC Bioinf.* 2013;14:128. https://doi.org/10.1186/1471-2105-14-128
22. Bindea G, Mlecnik B, Hackl H, et al. ClueGO: a Cytoscape plug-in to decipher functionally grouped gene ontology and pathway annotation networks. *Bioinformatics.* 2009;25(8):1091-1093. https://doi.org/10.1093/bioinformatics/btp101
23. Rappaport N, Nativ N, Stelzer G, et al. MalaCards: an integrated compendium for diseases and their annotation. *Database (Oxford)*. 2013;2013:bat018. https://doi.org/10.1093/database/bat018
24. Coban N, Ozuynuk AS, Erkan AF, Guclu-Geyik F, Ekici B. Levels of miR-130b-5p in peripheral blood are associated with severity of coronary artery disease. *Mol Biol Rep.* 2021;48(12):7719-7732. https://doi.org/10.1007/s11033-021-06780-5
25. Chen Y, Chang Z, Liu Y, et al. Triglyceride to high-density lipoprotein cholesterol ratio and cardiovascular events in the general population: a systematic review and meta-analysis of cohort studies. *Nutr Metab Cardiovasc Dis.* 2022;32(2):318-329. https://doi.org/10.1016/j.numecd.2021.11.005
26. Boon RA, Dimmeler S. MicroRNA-126 in atherosclerosis. *Arterioscler Thromb Vasc Biol.* 2014;34(7):e15-e16. https://doi.org/10.1161/ATVBAHA.114.303572
27. Zhou Q, Anderson C, Hanus J, et al. Strand and cell type-specific function of microRNA-126 in angiogenesis. *Mol Ther.* 2016;24(10):1823-1835. https://doi.org/10.1038/mt.2016.108
28. Yu B, Jiang Y, Wang X, Wang S. An integrated hypothesis for miR-126 in vascular disease. *Med Res Arch*. 2020;8(5):2133.
29. Fish JE, Santoro MM, Morton SU, et al. miR-126 regulates angiogenic signaling and vascular integrity. *Dev Cell.* 2008;15(2):272-284. https://doi.org/10.1016/j.devcel.2008.07.008
30. Wang S, Aurora AB, Johnson BA, et al. The endothelial-specific microRNA miR-126 governs vascular integrity and angiogenesis. *Dev Cell.* 2008;15(2):261-271. https://doi.org/10.1016/j.devcel.2008.07.002
31. Fan J-L, Zhang L, Bo X-H. MiR-126 on mice with coronary artery disease by targeting S1PR2. *Eur Rev Med Pharmacol Sci.* 2020;24(2):893-904. https://doi.org/10.26355/eurrev_202001_20074
32. Zhelankin AV, Stonogina DA, Vasiliev SV, et al. Circulating extracellular miRNA analysis in patients with stable CAD and acute coronary syndromes. *Biomolecules*. 2021;11(7):962. https://doi.org/10.3390/biom11070962
33. Wang J-N, Yan Y-Y, Guo Z-Y, Jiang Y-J, Liu L-L, Liu B. Negative association of circulating microRNA-126 with high-sensitive C-reactive protein and vascular cell adhesion molecule-1 in patients with coronary artery disease following percutaneous coronary intervention. *Chin Med J (Engl).* 2016;129(23):2786-2791. https://doi.org/10.4103/0366-6999.194645
34. He Y, Zhong J, Huang S, et al. Elevated circulating miR-126-3p expression in patients with acute myocardial infarction: its diagnostic value. *Int J Clin Exp Pathol*. 2017;10(11):11051-11056.
35. Fichtlscherer S, De Rosa S, Fox H, et al. Circulating microRNAs in patients with coronary artery disease. *Circ Res.* 2010;107(5):677-684. https://doi.org/10.1161/CIRCRESAHA.109.215566
36. Zaccagnini G, Greco S, Voellenkle C, Gaetano C, Martelli F. miR-210 hypoxamiR in angiogenesis and diabetes. *Antioxid Redox Signal.* 2021;36(10-12):685-706. https://doi.org/10.1089/ars.2021.0200
37. Diao H, Liu B, Shi Y, et al. MicroRNA-210 alleviates oxidative stress-associated cardiomyocyte apoptosis by regulating BNIP3. *Biosci Biotechnol Biochem.* 2017;81(9):1712-1720. https://doi.org/10.1080/09168451.2017.1343118
38. Qiao X-R, Wang L, Liu M, Tian Y, Chen T. MiR-210-3p attenuates lipid accumulation and inflammation in atherosclerosis by repressing IGF2. *Biosci Biotechnol Biochem.* 2020;84(2):321-329. https://doi.org/10.1080/09168451.2019.1685370
39. Eken SM, Jin H, Chernogubova E, et al. MicroRNA-210 enhances fibrous cap stability in advanced atherosclerotic

lesions. *Circ Res.* 2017;120(4):633-644. https://doi.org/10.1161/CIRCRESAHA.116.309318

40. Nejad RMA, Saeidi K, Gharbi S, Salari Z, Saleh-Gohari N. Quantification of circulating miR-517c-3p and miR-210-3p levels in preeclampsia. *Pregnancy Hypertens*. 2019;16:75-78. https://doi.org/10.1016/j.preghy.2019.03.004
41. Świtlik WZ, Karbownik MS, Suwalski M, Kozak J, Szemraj J. Serum miR-210-3p as a potential noninvasive biomarker of lung adenocarcinoma: a preliminary study. *Genet Test Mol Biomarkers.* 2019;23(5):353-358. https://doi.org/10.1089/gtmb.2018.0275
42. Rahmati M, Ferns GA, Mobarra N. The lower expression of circulating miR-210 and elevated serum levels of HIF-1α in ischemic stroke; possible markers for diagnosis and disease prediction. *J Clin Lab Anal.* 2021;35(12):e24073. https://doi.org/10.1002/jcla.24073
43. Patterson AJ, Song MA, Choe D, Xiao D, Foster G, Zhang L. Early detection of coronary artery disease by micro-RNA analysis in asymptomatic patients stratified by coronary CT angiography. *Diagnostics (Basel)*. 2020;10(11):875. https://doi.org/10.3390/diagnostics10110875
44. Mihaleva I, Kyurkchiyan S, Dodova R, et al. MiRNA expression analysis emphasized the role of miR-424 in diabetic cardiovascular complications. *Int J Diabetes Dev Ctries*. 2021;41(4):579-585. https://doi.org/10.1007/s13410-021-00934-8
45. Qin X, Chang F, Wang Z, Jiang W. Correlation of circulating pro-angiogenic miRNAs with cardiotoxicity induced by epirubicin/cyclophosphamide followed by docetaxel in patients with breast cancer. *Cancer Biomark.* 2018;23(4):473-484. https://doi.org/10.3233/CBM-181301
46. Rincón LM, Rodríguez-Serrano M, Conde E, et al. Serum microRNAs are key predictors of long-term heart failure and cardiovascular death after myocardial infarction. *ESC Heart Fail*. 2022;9(5):3367-3379. https://doi.org/10.1002/ehf2.13919
47. Zeller T, Keller T, Ojeda F, et al. Assessment of microRNAs in patients with unstable angina pectoris. *Eur Heart J.* 2014;35(31):2106-2114. https://doi.org/10.1093/eurheartj/ehu151
48. de Gonzalo-Calvo D, Vilades D, Martínez-Camblor P, et al. Circulating microRNAs in suspected stable coronary artery disease: a coronary computed tomography angiography study. *J Intern Med.* 2019;286(3):341-355. https://doi.org/10.1111/joim.12921
49. Mompeón A, Pérez-Cremades D, Paes AB, et al. Circulating miRNA fingerprint and endothelial function in myocardial infarction: comparison at acute event and one-year follow-up. *Cells*. 2022;11(11):1823. https://doi.org/10.3390/cells11111823
50. Bye A, Røsjø H, Nauman J, et al. Circulating microRNAs predict future fatal myocardial infarction in healthy individuals – The *HUNT* study. *J Mol Cell Cardiol.* 2016;97:162-168. https://doi.org/10.1016/j.yjmcc.2016.05.009
51. Millán J, Pintó X, Muñoz A, et al. Lipoprotein ratios: Physiological significance and clinical usefulness in cardiovascular prevention. *Vasc Health Risk Manag.* 2009;5:757-765.
52. Nam B-H, Kannel WB, D'Agostino RB. Search for an optimal atherogenic lipid risk profile: from the Framingham Study. *Am J Cardiol.* 2006;97(3):372-375. https://doi.org/10.1016/j.amjcard.2005.08.055
53. Sun X, Zhang M, Sanagawa A, et al. Circulating microRNA-126 in patients with coronary artery disease: correlation with LDL cholesterol. *Thromb J*. 2012;10(1):16. https://doi.org/10.1186/1477-9560-10-16

IgA is the predominant isotype of anti-β2 glycoprotein I in patients with COVID-19

Sarra Melayah, MD,[1,2,3] Nouha Omrani, MS,[4] Hela Alouini, MS,[2] Mariam Ghozzi, MD,[1,2,5] Sawssen Mrad, MD,[6] Mohamed Boussarsar, PhD,[7] Houda Chaouch, PhD,[8] Wissem Hachfi, PhD,[8] Amel Letaief, PhD,[8] Amani Mankaï, PhD,[1,9,10] Ibtissem Ghedira, PhD[1,2]

[1]Laboratory of Immunology, Farhat Hached University Hospital, Sousse, Tunisia; [2]Department of Immunology, Faculty of Pharmacy, University of Monastir, Monastir, Tunisia; [3]LR12SP11, Department of Biochemistry, Sahloul University Hospital, Sousse, Tunisia; [4]Faculty of Sciences of Tunis, University of Tunis El Manar, Tunis, Tunisia; [5]LR14SP02, Research Unit "Epidemiology and Immunogenetics of Viral Infections," Sahloul University Hospital, Sousse, Tunisia; [6]Laboratory of Biochemistry and Departments of [7]Medical Intensive Care and [8]Infectious Diseases, Farhat Hached University Hospital, Sousse, Tunisia; [9]High School of Sciences and Techniques of Health, University of Tunis El Manar, Tunis, Tunisia; [10]Research Unit "Obesity: Etiopathology and Treatment, UR18ES01," National Institute of Nutrition and Food Technology, Tunis, Tunisia.
Corresponding author: Sarra Melayah; sarra.125@hotmail.fr

Key words: antiphospholipid antibodies; anticardiolipin antibodies; anti-β2 glycoprotein I antibodies; COVID-19; adults; autoimmunity

Abbreviations: aPL, antiphospholipid antibodies; aCL, anticardiolipin antibodies; aβ2GPI, anti-β2 glycoprotein I antibodies; Ig, immunoglobulin; LA, lupus anticoagulant; APS, antiphospholipid syndrome; ASCA, anti-*Saccharomyces cerevisiae* antibodies; CRP, C-reactive protein; ICU, intensive care unit; ELISA, enzyme-linked immunosorbent assay; SpO_2, peripheral oxygen saturation; RA, rheumatoid arthritis

Laboratory Medicine 2024;55:373-379; https://doi.org/10.1093/labmed/lmad097

ABSTRACT

Objective: The aim of this research was to determine the frequency of antiphospholipid antibodies (aPL) in patients with COVID-19.

Methods: The frequency and titers of anticardiolipin antibodies (aCL) and anti-β2 glycoprotein I antibodies (aβ2GPI) were determined in sera of adult patients hospitalized with COVID-19. Immunoglobulin (Ig)G, IgA, IgM aCL, and aβ2GPI were measured using enzyme-linked immunosorbent assay.

Results: Eighty-three patients were included in the study. The mean age of patients was 62 ± 13.9 years, ranging from 23 to 86 years. Stratification according to severity of infection divided patients in 2 groups: 45 patients with moderate infection and 38 patients with critical or severe infection. Out of the 83 patients suffering from COVID-19, aPL (aCL or aβ2GPI) were detected in 24 patients (28.9%). IgG, IgA and IgM aβ2GPI were positive in 2.4%, 16.9% and 8.4%, respectively. IgG, IgA and IgM aCL showed positivity in 7.2%, 0%, and 4.8%, respectively. The frequency of aPL was 36.8% in patients with critical/severe infection and 22.2% in patients with moderate infection. In critical/severe patients, the frequency of aβ2GPI was significantly higher than aCL (34.2% vs 13.2%, $P = .03$) and aβ2GPI-IgA were significantly more frequent than aβ2GPI-IgG (21.1% vs 2.6%, $P = .028$).

Conclusion: In this cross-sectional study, aPL and particularly aβ2GPI-IgA were common in patients with COVID-19.

Introduction

COVID-19 is an infectious disease induced by SARS-CoV-2.[1] The clinical picture of COVID-19 includes many manifestations that are frequently described in autoimmune diseases such as several extrapulmonary manifestations.[2] SARS-CoV-2 is now considered to be a trigger of autoimmunity[3,4] and is able to induce severe immunopathology.[5,6] Moreover, high incidence of autoimmune diseases after SARS-CoV-2 infection has been reported.[7-9] Likewise, new-onset autoantibodies in patients with COVID-19 have been reported and were positively correlated with anti-SARS-CoV-2 antibodies.[10]

Antiphospholipid antibodies (aPL) include a panel of autoantibodies directed against anionic phospholipids or protein-phospholipid complexes.[11] Three main types of antibodies are described: anticardiolipin antibodies (aCL), anti-β2 glycoprotein I antibodies (aβ2GPI), and lupus anticoagulant (LA). These antibodies occur not only in antiphospholipid syndrome (APS) but also in autoimmune diseases, malignancies, and infections.[12] It is acknowledged that infection could induce aPL production.[13] Our research has previously demonstrated a high frequency of aPL in chronic hepatitis C patients.[14] Indeed, the initial immune response to viral antigen could expand to self-proteins through common recognition and epitope spreading. Otherwise, molecular mimicry between viral epitopes and autoantigens will lead to loss of tolerance and induction of autoimmunity.[15] A strong inflammation will accelerate this phenomenon, and in COVID-19 a cytokine storm has widely been described.[16-18]

We have previously demonstrated a high frequency of aPL, especially aβ2GPI, in many diseases that share clinical manifestations with

COVID-19.[14,19-23] Thus, the objective of our study was to investigate the frequency of aPL (aβ2GPI and aCL) in a cohort of COVID-19 patients.

Materials and Methods

Patients

A cross-sectional study that included 83 hospitalized adult patients affected by COVID-19 in Farhat Hached Hospital of Sousse, Tunisia, was conducted. The criteria for inclusion were any consecutive patient older than 18 years, tested positive for SARS-CoV-2 on nasopharyngeal swab samples by reverse transcription-polymerase chain reaction, and who required hospital admission. Collection of patient samples was conducted from March 2021 to July 2022. All samples were obtained in the first 24 hours of hospital admission. Demographic, epidemiological, clinical data, medical history, and laboratory results were extracted from medical records. The research team accessed the database first on April 1, 2021. Patients with incomplete medical records were excluded from the study.

Patients were subdivided into 2 groups: moderate and severe/critical illness according to World Health Organization guidelines.[24] Classification of patients was based on clinical symptoms, respiratory rate, oxygen saturation, pneumonia severity, and the need of invasive ventilation. Moderate disease included patients with evidence of pneumonia but no signs of severe pneumonia (peripheral oxygen saturation [SpO_2] ≥90% on room air). Severe cases included clinical signs of pneumonia and respiratory rate >30 breaths/min or SpO_2 <90% on room air. Critical cases were patients with acute respiratory distress syndrome (Berlin definition),[25] sepsis, or septic shock.

All hospitalized patients or the next of kin for patients who were admitted in the intensive care unit (ICU) gave their written informed consent. Our study was approved by the ethics committee of the University Hospital of Farhat Hached.

Biological Biomarkers

C-reactive protein (CRP), white blood cell count, platelet count, hemoglobin, prothrombin time, aspartate aminotransferase, alanine aminotransferase, total bilirubin, and direct bilirubin were evaluated on the same date of serum sampling for aPL. The D-dimer was carried out for only a few patients due to the lack of reagents, especially during the first period of the pandemic, so we did not include this parameter in the study.

Serum Antiphospholipid Antibodies Determination

Serum samples were assayed for aCL- and aβ2GPI-IgG, IgA, and IgM using an enzyme-linked immunosorbent assay (ELISA) (Orgentec Diagnostika). The determination was based on an indirect ELISA with the following steps: specific antibodies contained in the patient sample bind to the antigen coated on the surface of the reaction wells. After incubation, a first washing step removes unbound and unspecifically bound serum components. Subsequently added enzyme conjugate binds the immobilized antigen-antibody complexes. After incubation, a second washing step removes unbound enzyme conjugate. Adding TMB Substrate Solution (3,3',5,5'- tetramethylbenzine) leads to hydrolization of substrate, forming a blue-colored product. Addition of an acid stops the reaction, generating a yellow end-product. The color intensity correlates with the concentration of antigen-antibody complexes and can be measured at 450 nm by spectrophotometer.

Normal values were as follows: 10 U/mL for aCL-IgG and IgA, 7 U/mL for aCL-IgM, and 8 U/mL for IgG, IgM, and IgA aβ2GPI based on the manufacturer's recommendations.

Statistical Analysis

All statistical analysis were performed using SPSS software, version 22. Continuous variables were expressed as means and SDs and medians and IQRs according to their distribution. Categorial variables were expressed as numbers and percentages. The variables were tested for normality using the Kolmogorov-Smirnov test with Lilliefors adjustment. Where appropriate, the χ^2 test, Fisher's exact test, or Mann-Whitney test were used for the comparison of frequencies. To compare variables reported with means, we used the parametric Student *t*-test and for variables reported with medians, we used Mann-Whitney test. A *P* value lower than .05 was considered to be statistically significant.

Results

General Characteristics

A total of 83 hospitalized COVID-19 patients (44 men and 39 women with a mean age of 62 ± 13.9 years) were enrolled in this study. Overview of the characteristics of the patients, including demographic features, medical history, comorbidities, and symptoms at hospital admission, are summarized in **TABLE 1**. Most of the patients were over the age of 60 years (60.2% vs 39.8%; *P* = .008). Sixty-seven patients out of 83 (80.7%) suffered from chronic diseases. Among them, 46 (68.6%) had at least 2 chronic diseases. Seven patients (8.4%) had autoimmune diseases. Specifically, 6 patients (7.2%) had type 1 diabetes and 1 patient suffered from systemic lupus erythematosus and rheumatoid arthritis (RA). Liver abnormalities were observed in 37.8% of the patients (28.9% had cytolysis and 19.6% had hyperbilirubinemia). No thrombotic events were observed at the time of aPL measurements. Disease severity was moderate in 45 patients (54.2%) and severe or critical in 38 patients (45.8%). Twenty-four patients (28.9%) were admitted to the ICU.

Frequency of Antiphospholipid Antibodies

The frequency of aPL (aCL or aβ2GPI) in the study population was 28.9% (n = 24). Among these 24 patients, 19 (22.9%) had only 1 positive antibody and 5 (6%) had 2 or more antibodies. aβ2GPI were significantly more frequent than aCL (25.3% vs 9.6%; *P* = .008). aβ2GPI-IgA was the most detected antibody (16.9%), followed by aβ2GPI-IgM (8.4%) and aCL-IgG (7.2%). Thirteen patients (15.7%) were positive for aβ2GPI-IgA and negative for other aPL (isolated aβ2GPI-IgA) (**TABLE 2**).

FIGURE 1 illustrates the mean titers of aCL (1A) and aβ2GPI (1B) in overall, moderate, and severe/critical COVID-19 patients. No significant differences were noted for the mean titers of each isotype of aCL or aβ2GPI between the 2 groups of COVID-19 patients.

COVID-19 Severity and Antiphospholipid Antibodies

Among the 38 patients with a critical or severe form of COVID-19, 14 (36.8%) had aPL (aCL and/or aβ2GPI), whereas among the 45 patients with a moderate form of COVID-19, 10 (22.2%) had aPL. In patients with a critical/severe form of the disease, 34.2% of cases had aβ2GPI and 13.2% had aCL (*P* = .03) and aβ2GPI-IgA was significantly more frequent than aβ2GPI-IgG (21.1% vs 2.6%, *P* = .028). Patients with moderate COVID-19 had 17.8% aβ2GPI and 6.7% had aCL. No significant

TABLE 1. General characteristics of COVID-19 patients (n = 82)

Characteristics	Results
Demographic characteristics	
Sex ratio (M/F)	1.1 (44/39)
Mean age ± SD, y	62 ± 13.9
Age range, y	23-86
Medical history/comorbidity, n (%)	
Diabetes mellitus	40 (48.2)
Hypertension	25 (30.1)
Coronary heart disease	9 (10.8)
Pulmonary disease	5 (6)
Chronic kidney disease	5 (6)
Cancer	4 (4.8)
Thrombotic event	0
Symptoms at hospital admission, n (%)	
Fever	44 (53)
Cough	56 (67.5)
Dyspnea	38 (45.8)
Asthenia	47 (56.6)
Myalgia	21 (25.3)
Headache	21 (25.3
Ageusia	7 (8.4)
Disease severity status, n (%)	
Moderate	45 (54.2)
Critical/severe	38 (45.8)
Laboratory parameters	
C-reactive protein, mg/dL, median (IQR)	68.5 (39.2-123)
White cell count, × 10^3/µL, median (IQR)	7.8 (5.9-11.2)
Platelet count, × 10^3/µL, median (IQR)	233.5 (167-302)
Hemoglobin, g/dL, median (IQR)	12.9 (10.6-14.2)
Prothrombin time, %, median (IQR)	78 (62.5-85)
ASAT, U/L, mean ± SD	35 ± 18
ALAT, U/L, mean ± SD	33 ± 29
Total bilirubin, µmol/L, mean ± SD	30 ± 8
Direct bilirubin, µmol/L, mean ± SD	11 ± 2

ALAT, alanine aminotransferase; ASAT, aspartate aminotransferase.

differences were noted for the different aCL and aβ2GPI isotypes between the 2 groups of patients (**TABLE 2**).

Comparison Between aPL Positive and aPL Negative Patients

Compared with patients without aPL, aPL-positive patients did not show significant differences in age, sex, preexisting comorbidities, severity of the disease, or laboratory parameters except for hemoglobin and direct bilirubin levels (**TABLE 3**).

Discussion

In the present study, we demonstrated a high frequency of aPL (aCL or aβ2GPI) in COVID-19 patients. This frequency (28.9%) is similar to that (34.7%) found by Gasparini et al[26] who conducted a similar study to ours. In fact, they evaluated aCL and aβ2GPI of 3 isotypes (IgG, IgA, IgM) but not LA or antiphosphatidylserine antibodies.

aβ2GPI-IgA were the most frequent aPL in our study. This result confirms those of previously reported studies.[26-31] The frequency of aβ2GPI-IgA in our study was similar to that found by Serrano et al[27] (16.9% and 15%, respectively). In our group of patients with critical/severe COVID-19, the frequency of aβ2GPI-IgA was similar to that of Xiao et al[28] (21.1% and 28.8%, respectively) and Bnina et al[31] (21.1% and 24%, respectively).[31] Xiao et al[28] demonstrated also that aCL-IgA (25.8%) were frequent in COVID-19 patients and Zeng et al[32] found that 28.7% of COVID-19 patients had aCL-IgA, whereas in our study aCL-IgA were not detected. This discrepancy could be explained by the difference between the epidemiological characteristics of patients included and the methods used for aCL measurement.

In the critical/severe COVID-19 group, aβ2GPI-IgA, which is considered an extracriteria aPL, was significantly more frequent than aβ2GPI-IgG (21.1% vs 2.6%, P = .028). Similarly, it has been reported that total serum IgA, but not IgG, is elevated in severe COVID-19.[33] The predominance of the IgA isotype of aβ2GPI in our study and in other studies[26-29] and the reported high frequency of aCL-IgA[28,32] could be explained by the fact that SARS-CoV-2 is implicated in mucosal damage, as it affects mainly lung and intestinal mucosa. Thus, the production of IgA[34,35] may be secondary to the break of mucosal immune tolerance. Interestingly, a relationship between the intestinal immune axis for IgA production and the gene TIMELESS has been reported in COVID-19.[36] Moreover, in all our previous studies on aPL, IgA was the predominant isotype of aβ2GPI (**TABLE 4**).

We found that the frequency of aβ2GPI-IgM was 8.4% in patients with COVID-19. Interestingly, this frequency was 15.8% in the critical/severe COVID-19 group vs 2.2% in the moderate COVID-19 group, and the difference between the 2 groups was near to the threshold of significance (P = .06). Similarly to our findings, Sadeghi et al[39] showed that the frequency of aβ2GPI-IgM was higher in patients admitted to the ICU compared with non-ICU patients (10.5% vs 0%; P = .05). They demonstrated that aβ2GPI-IgM were near levels showing significant association based on Sequential Organ Failure Assessment score. Moreover, in a study conducted in 172 patients hospitalized with COVID-19 measuring 8 types of aPL, the authors detected aCL-IgM in 23% of samples and titers of aCL-IgM correlated with neutrophil hyperactivity, including the release of neutrophil extracellular traps, higher platelet counts, more severe respiratory disease, and lower clinical estimated glomerular filtration rate.[40] Further studies are needed to clarify the pathogenic role of aPL-IgM in COVID-19 patients.

The role of aPL in the risk for thrombosis in COVID-19 is still controversial.[41] Some studies demonstrated an association between aPL and thrombosis.[28,29,42] Xiao et al[28] found that in patients with multiple antibody positivity, the most common profile was the presence of both aβ2GPI-IgA and aCL-IgA. They also reported that in patients with such antibody profile, the incidence of cerebral infarction was significantly higher than in those who were negative for aPL. None of our patients had thrombotic events. Likewise, in other studies, no correlation between the presence of aPL and thromboembolic manifestations was found.[26,27,43,44] Besides, our mean level of aPL is low and similar to those previously described.[27,29,33,43,44] In fact, titers of aPL have been described to be lower in COVID-19 than in APS.[43] Otherwise, unlike in APS, most COVID-19 patients had only 1 type of aPL.[26] In our study,

TABLE 2. Frequencies of aCL and aβ_2GPI in COVID-19 patients

	Patients with COVID-19 (n = 83), n (%)	Patients with critical/severe COVID-19 (n = 38), n (%)	Patients with moderate COVID-19 (n = 45), n (%)	*P*[a]
aCL or aβ2GPI	24 (28.9)	14 (36.8)	10 (22.2)	.1
aCL (IgG, IgA, or IgM)	8 (9.6)[b]	5 (13.2)[d]	3 (6.7)	.5
aCL-IgG	6 (7.2)	4 (10.5)	2 (4.4)	.5
aCL-IgA	0	0	0	-
aCL-IgM	4 (4.8)	3 (7.9)	1 (2.2)	.5
aβ2GPI (IgG, IgA, or IgM)	21 (25.3)[b]	13 (34.2)[d]	8 (17.8)	.08
aβ2GPI-IgG	2 (2.4)[c]	1 (2.6)[e]	1 (2.2)	1
aβ2GPI-IgA	14 (16.9)[c]	8 (21.1)[e]	6 (13.3)	.35
aβ2GPI-IgM	7 (8.4)	6 (15.8)	1 (2.2)	.06
aCL and aβ2GPI	5 (6)	4 (10.5)	1 (2.2)	.26
Single antibody	19 (22.9)[f]	10 (26.3)	9 (20)[g]	.49
Multiple antibodies	5 (6)[f]	4 (10.5)	1 (2.2)[g]	.26
Isolated aβ2GPI-IgA	13 (15.7)	7 (18.4)	6 (13.3)	.5

aβ2GPI, anti-β2 glycoprotein I antibodies; aCL, anticardiolipin antibodies.
[a]*Comparison of patients with critical/severe COVID-19 vs patients with moderate COVID-19.*
[b]*Comparison between aβ2GPI (IgG, IgA, or IgM) and aCL (IgG, IgA, or IgM) in COVID-19 patients,* P = *.008.*
[c]*Comparison between aβ2GPI-IgA and aβ2GPI-IgG in COVID-19 patients,* P = *.002.*
[d]*Comparison between aβ2GPI (IgG, IgA, or IgM) and aCL (IgG, IgA, or IgM) in critical/severe COVID-19 patients,* P = *.03.*
[e]*Comparison between aβ2GPI-IgA vs aβ2GPI-IgG in critical/severe COVID-19 patients,* P = *.028.*
[f]*Comparison between single antibody and multiple antibodies in COVID-19 patients,* P = *.002.*
[g]*Comparison between single antibody vs multiple antibodies in patients with moderate COVID-19,* P = *.007.*

FIGURE 1. Mean titers of anticardiolipin antibodies (aCL) (A) and anti-β2 glycoprotein I antibodies (aβ_2GPI) (B) in COVID-19 patients. aCL, anticardiolipin antibodies; aβ2GPI, anti-beta 2-glycoprotein I antibodies.

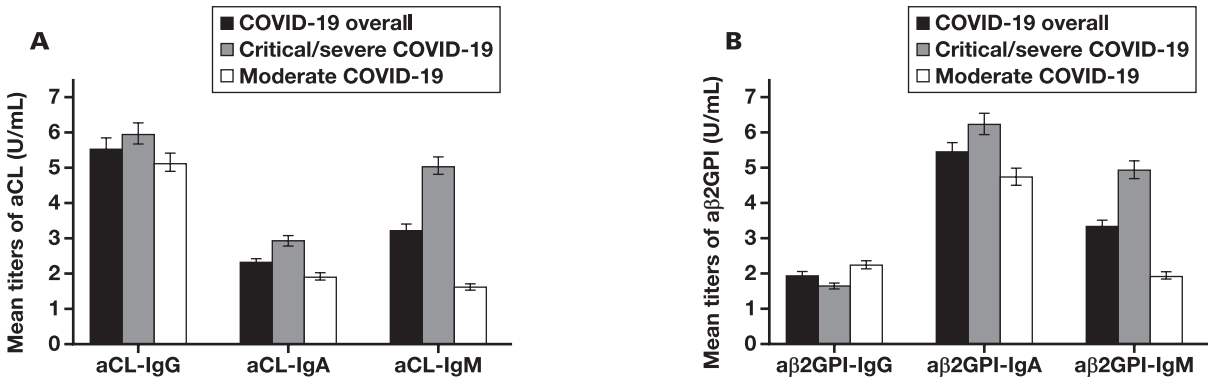

single antibody positivity was significantly more frequent than multiple antibody positivity (22.9% vs 6%, *P* = .002), whereas triple aPL positivity is more predictive of thrombosis.[41] It has also been demonstrated that aβ2GPI in COVID-19 are not directed against domain 1 as in APS but they recognize domains 4 and 5.[43] Domain 4 and 5 are not associated with APS and are not pathogenic.[45] In COVID-19, aPL are not the main factor of thrombophilic microangiopathy.[45,46] aPL in COVID-19 may be considered as bystander but not pathogenic antibodies.[45] So aβ2GPI that we and others detected in COVID-19 patients could be implicated in manifestations other than those described in APS.

aβ2GPI could induce articular manifestations in acute COVID-19 or during post-COVID-19 syndrome. In our study, due to the critical condition of patients admitted to the ICU, looking for articular manifestations could not be performed. However, it has been reported that joint pain is one of the most common symptoms in patients with COVID-19 (27.3%) and it is one of the persistent symptoms after acute COVID-19.[47] In fact, arthralgia has been described in 62% of patients with post-COVID-19 syndrome[48] and arthritis in 37%.[49] We had previously found a high frequency of aβ2GPI in another viral disease in which articular manifestations are frequent. In fact, in our chronic hepatitis C patients, the frequency of aβ2GPI and particularly of IgA isotype was significantly higher in patients than in the control group (38.5% vs 7.8%, $P < 10^{-6}$).[14] The aβ2GPI that we detected in this study could be anti-*Saccharomyces cerevisiae* antibodies (ASCA). Indeed, *S cerevisiae* has common epitopes with β2GPI.[50] We have previously detected ASCA in 15.9% of our patients with severe COVID-19.[51] Fascinatingly, cross-reactive epitopes have been discovered both between *S cerevisiae* and SARS-CoV-2[52] and *S cerevisiae* and autoantigens of rheumatoid arthritis (RA).[53] Also, we have demonstrated that 26.7% of patients with RA have aβ2GPI-IgA, and we have hypothesized that aβ2GPI-IgA are both the

TABLE 3. Comparison of demographic, clinical characteristics, and laboratory findings according to aPL positivity[a]

	aPL positive patients (n = 24)	aPL negative patients (n = 59)	*P*
Mean age ± SD, y	64 ± 14.9	61 ± 13.4	.3
Male, n (%)	11 (45.8)	33 (55.9)	.4
Preexisting comorbidities, n (%)			
Diabetes mellitus	9 (37.5)	31 (52.5)	.2
Hypertension	6 (25)	19 (32.2)	.5
Coronary heart disease	2 (8.3)	7 (11.9)	.9
Autoimmune diseases	2 (8.3)	5 (8.5)	1
Disease severity status, n (%)			
Moderate	10 (41.7)	35 (59.3)	.14
Critical/severe	14 (58.3)	24 (40.7)	.14
Laboratory parameters, median (IQR)			
C-reactive protein, mg/dL	90 (34.75-120.7)	61 (39.2-126)	.56
White blood cell count, $\times 10^3$/µL	7.4 (5.9-16.4)	8.3 (5.9-11.1)	.85
Platelet count, $\times 10^3$/µL	194 (140-287)	243 (176.5-313)	.17
Hemoglobin, g/L	11.9 (10-13)	13.25 (10.9-14.4)	**.04**
Prothrombin time, %	68 (60-83)	78 (62.7-85.2)	.8
ASAT, U/L, mean ± SD	38.5 ± 18.4	32.2 ± 17.6	.15
ALAT, U/L, mean ± SD	40.4 ± 43.8	30.2 ± 21.2	.28
Total bilirubin, µmol/L, mean ± SD	15.6 ± 13.1	11.8 ± 5.7	.18
Direct bilirubin, µmol/L, mean ± SD	4.5 ± 3.6	2.8 ± 2	**.03**

ALAT, alanine aminotransferase; aPL, antiphospholipid antibodies; ASAT, aspartate aminotransferase.
[a]*Bold values indicate significance.*

TABLE 4. Predominance of aβ2GPI-IgA in our previous studies

Authors	Diseases	aβ2GPI-IgG, %	aβ2GPI-IgA, %	aβ2GPI-IgM, %
Mankaï et al, 2012[19]	Celiac disease	1.6	14.3	1.6
Mankaï et al, 2013[37]	Systemic lupus erythematosus	19.8	50.9	—
Mankaï et al, 2015[20]	Primary biliary cholangitis	12.5	62.5	21.2
Mankaï et al, 2016[38]	Antiphospholipid syndrome	22	83.1	—
Melayah et al, 2020[21]	Rheumatoid arthritis	6.7	26.7	5.6
Manka ï et al, 2022[22]	Hashimoto's thyroiditis	5	27.3	8.6
Melayah et al, 2022[14]	Chronic hepatitis C	7.3	38.5	9.4
Melayah et al, 2023[23]	Articular manifestations	5.4	20.4	2.9

aβ2GPI, anti-β2 glycoprotein I antibodies.

cause and the consequence of arthritis in RA.[21] It is worthy to note that β2GPI is a ubiquitous protein present in joints.[54] *S cerevisiae* also has common epitopes with β2GPI.[50] By the way, we reported that 20.5% of patients with RA had ASCA-IgG.[55] So, could we imagine that in COVID-19 patients, aβ2GPI-IgA bind to *S cerevisiae* or to SARS-CoV-2, which could migrate from the gut to the articulation via the vascular compartment as a consequence of a leaky intestinal wall[56] resulting in gut microbiota dysbiosis[57]? Because in COVID-19 complement activation includes not only classical but also an alternative pathway[58] and aβ2GPI are of the IgA isotype, an alternative pathway is activated and subsequently inflammation and articular damage take place.

aβ2GPI could also be implicated in hepatic manifestations of COVID-19. In fact, liver injury is now recognized as an extrapulmonary manifestation of severe COVID-19.[59-61] Otherwise, SARS-CoV-2 was detected in the liver of patients who died from COVID-19.[62] Moreover, liver function abnormalities were seen in 19% of COVID-19 patients and were associated with disease severity.[63] Furthermore, gammaglutamyl transferase, a diagnostic biomarker of cholangiocyte injury, has been reported to be elevated in 54% of COVID-19 patients.[64] Interestingly, β2GPI, which is a ubiquitous protein and is highly expressed in the liver, and not only do β2GPI and SARS-CoV-2 have cross-reactive epitopes with *S cerevisiae* but also SARS-CoV-2 has common epitopes with the main auto-antigen (M2) of primary biliary cholangitis.[65] So we could imagine that aβ2GPI will bind to β2GPI expressed in the liver or to *S cerevisiae* that migrated from the intestine to the liver because of a leaky gut. The result of this mechanism will be complement activation and inflammation such as we explained above for articular manifestations.

We acknowledge that our study has some limitations. First, it is not a prospective study, so we do not have data on the evolution of aPL over time. Second, LA was not performed. Third, we did not follow

patients for the possible new onset of autoimmune diseases in the post-COVID-19 period.

In conclusion, we demonstrated herein a high frequency of aβ2GPI-IgA in COVID-19 patients.

Conflict of Interest Disclosure

The authors have nothing to disclose.

REFERENCES

1. Wu F, Zhao S, Yu B, et al. A new coronavirus associated with human respiratory disease in China. *Nature.* 2020;579(7798):265-269. https://doi.org/10.1038/s41586-020-2008-3
2. Gupta A, Madhavan MV, Sehgal K, et al. Extrapulmonary manifestations of COVID-19. *Nat Med.* 2020;26(7):1017-1032. https://doi.org/10.1038/s41591-020-0968-3
3. Dotan A, Muller S, Kanduc D, David P, Halpert G, Shoenfeld Y. The SARS-CoV-2 as an instrumental trigger of autoimmunity. *Autoimmun Rev.* 2021;20(4):102792. https://doi.org/10.1016/j.autrev.2021.102792
4. Kocivnik N, Velnar T. A review pertaining to SARS-CoV-2 and autoimmune diseases: what is the connection? *Life (Basel)*. 2022;12(11):1918. https://doi.org/10.3390/life12111918
5. Brodin P. Immune determinants of COVID-19 disease presentation and severity. *Nat Med.* 2021;27(1):28-33. https://doi.org/10.1038/s41591-020-01202-8
6. Arish M, Qian W, Narasimhan H, Sun J. COVID-19 immunopathology: from acute diseases to chronic sequelae. *J Med Virol.* 2023;95(1):28122. https://doi.org/10.1002/jmv.28122
7. Putry BO, Khairunnisa N, Balga HM, et al. Can SARS-CoV-2 trigger new onset of autoimmune disease in adults? A case-based review. *Heliyon*. 2022;8(11):e11328. https://doi.org/10.1016/j.heliyon.2022.e11328
8. Yazdanpanah N, Rezaei N. Autoimmune complications of COVID-19. *J Med Virol.* 2022;94(1):54-62. https://doi.org/10.1002/jmv.27292
9. Bizjak M, Emeršič N, Zajc Avramovič M, et al. High incidence of multisystem inflammatory syndrome and other autoimmune diseases after SARS-CoV-2 infection compared to COVID-19 vaccination in children and adolescents in south central Europe. *Clin Exp Rheumatol.* 2023;41(5):1183-1191. https://doi.org/10.55563/clinexprheumatol/i1l2xn
10. Chang SE, Feng A, Meng W, et al. New-onset IgG autoantibodies in hospitalized patients with COVID-19. *Nat Commun.* 2021;12(1):5417. https://doi.org/10.1038/s41467-021-25509-3
11. Barreno-Rocha SG, Guzmán-Silahua S, Rodríguez-Dávila SD, et al. Antiphospholipid antibodies and lipids in hematological malignancies. *Int J Mol Sci.* 2022;23(8):4151. https://doi.org/10.3390/ijms23084151
12. Gómez-Puerta JA, Cervera R. Diagnosis and classification of the antiphospholipid syndrome. *J Autoimmun.* 2014;48-49(7):20-25. https://doi.org/10.1016/j.jaut.2014.01.006
13. Mendoza-Pinto C, García-Carrasco M, Cervera R. Role of infectious diseases in the antiphospholipid syndrome (including its catastrophic variant). *Curr Rheumatol Rep.* 2018;20(10):62. https://doi.org/10.1007/s11926-018-0773-x
14. Melayah S, Kallala O, Ben Ahmed M, et al. IgA anti-beta-2 glycoprotein I antibodies in chronic hepatitis C. *Arab J Gastroenterol*. 2022;23(1):26-31. https://doi.org/10.1016/j.ajg.2021.12.003
15. Fujinami RS, von Herrath MG, Christen U, Whitton JL. Molecular mimicry, bystander activation, or viral persistence: infections and autoimmune disease. *Clin Microbiol Rev.* 2006;19(1):80-94. https://doi.org/10.1128/CMR.19.1.80-94.2006
16. Rondovic G, Djordjevic D, Udovicic I, et al. From cytokine storm to cytokine breeze: did lessons learned from immunopathogenesis improve immunomodulatory treatment of moderate-to-severe COVID-19? *Biomedicines*. 2022;10(10):2620. https://doi.org/10.3390/biomedicines10102620
17. Liu Y, Sawalha AH, Lu Q. COVID-19 and autoimmune diseases. *Curr Opin Rheumatol.* 2021;33(2):155-162. https://doi.org/10.1097/bor.0000000000000776
18. Zanza C, Romenskaya T, Manetti AC, et al. Cytokine storm in COVID-19: immunopathogenesis and therapy. *Medicina (Kaunas)*. 2022;58(2):144. https://doi.org/10.3390/medicina58020144
19. Mankaï A, Achour A, Thabet Y, Manoubia W, Sakly W, Ghedira I. Anticardiolipin and anti-beta 2-glycoprotein I antibodies in celiac disease. *Pathol Biol (Paris).* 2012;60(5):291-295. https://doi.org/10.1016/j.patbio.2011.07.003
20. Mankaï A, Manoubi W, Ghozzi M, Melayah S, Sakly W, Ghedira I. High frequency of antiphospholipid antibodies in primary biliary cirrhosis. *J Clin Lab Anal.* 2015;29(1):32-36. https://doi.org/10.1002/jcla.21723
21. Melayah S, Changuel M, Mankaï A, Ghedira I. IgA is the predominant isotype of anti-β2 glycoprotein I antibodies in rheumatoid arthritis. *J Clin Lab Anal.* 2020;34(6):e23217. https://doi.org/10.1002/jcla.23217
22. Mankaï A, Melayah S, Bousetta S, Ghozzi M, Yacoub-Jemni S, Ghedira I. Antiphospholipid antibodies in autoimmune thyroid diseases. *J Clin Lab Anal.* 2022;36(12):e24788. https://doi.org/10.1002/jcla.24788
23. Melayah S, Ghozzi M, Ghedira I, Mankaï A. Anticardiolipin and anti-beta 2-glycoprotein I antibodies in patients with unexplained articular manifestations. *J Clin Lab Anal.* 2023;37(1):e24812. https://doi.org/10.1002/jcla.24812
24. World Health Organization. COVID-19 clinical management: living guidance WHO; 1-81. Accessed November 23, 2021. https://www.who.int/publicationsdetail-redirect/WHO-2019-nCoV-clinical-2021-1%0Ahttp:// files/20/WHO-2019-nCoV-clinical-2021-1.html
25. Ranieri VM, Rubenfeld GD, Thompson BT, et al; ARDS Definition Task Force. Acute respiratory distress syndrome: the Berlin definition. *JAMA.* 2012;307(23):2526-2533. https://doi.org/10.1001/jama.2012.5669
26. Gasparini G, Canepa P, Verdiani S, et al. A retrospective study on the prevalence of anti-phospholipid antibodies, thrombotic events and cutaneous signs of vasculopathy in 173 hospitalized COVID-19 patients. *Int J Immunopathol Pharmacol.* 2021;35:20587384211042115. https://doi.org/10.1177/20587384211042115
27. Serrano M, Espinosa G, Lalueza A, et al; APS-COVID 19 Study Group/European Forum on Antiphospholipid Antibodies. Beta-2-glycoprotein-i deficiency could precipitate an antiphospholipid syndrome-like prothrombotic situation in patients with coronavirus disease 2019. *ACR Open Rheumatol*. 2021;3(4):267-276. https://doi.org/10.1002/acr2.11245
28. Xiao M, Zhang Y, Zhang S, et al. Antiphospholipid antibodies in critically ill patients with COVID-19. *Arthritis Rheumatol*. 2020;72(12):1998-2004. https://doi.org/10.1002/art.41425
29. Gil-Etayo FJ, Garcinuño S, Lalueza A, et al. Anti-phospholipid antibodies and COVID-19 thrombosis: a co-star, not a supporting actor. *Biomedicines*. 2021;9(8):899. https://doi.org/10.3390/biomedicines9080899
30. Garcia-Arellano G, Camacho-Ortiz A, Moreno-Arquieta IA, et al. Anticardiolipin and anti-beta-2 glycoprotein I antibodies in patients with moderate or severe COVID-19. *Am J Med Sci.* 2023;365(2):215-217. https://doi.org/10.1016/j.amjms.2022.10.012
31. Bnina AB, Dhia RB, Gnaba S, et al. Assessment of antiphospholipid antibodies profiles based on severity of COVID-19 pneumonia. *Pan Afr Med J*. 2022;42:110. https://doi.org/10.11604/pamj.2022.42.110.33020
32. Zeng H, Cai M, Xue H, Xie W, Long X. Prevalence and coagulation correlation of anticardiolipin antibodies in patients with COVID-19. *Medicine (Baltimore).* 2022;101(41):e31040. https://doi.org/10.1097/MD.0000000000031040

33. Hasan Ali O, Bomze D, Risch L, et al. Severe coronavirus disease 2019 (COVID-19) is associated with elevated serum immunoglobulin (Ig) A and antiphospholipid IgA antibodies. *Clin Infect Dis.* 2021;73(9):e2869-e2874. https://doi.org/10.1093/cid/ciaa1496

34. Padoan A, Sciacovelli L, Basso D, et al. IgA-Ab response to spike glycoprotein of SARS-CoV-2 in patients with COVID-19: a longitudinal study. *Clin Chim Acta.* 2020;507(12):164-166. https://doi.org/10.1016/j.cca.2020.04.026

35. Yu HQ, Sun BQ, Fang ZF, et al. Distinct features of SARS-CoV-2-specific IgA response in COVID-19 patients. *Eur Respir J.* 2020;56(2):2001526. https://doi.org/10.1183/13993003.01526-2020

36. Zhang W, Di L, Liu Z, et al. TIMELESS is a key gene mediating thrombogenesis in COVID-19 and antiphospholipid syndrome. *Sci Rep.* 2022;12(1):17248. https://doi.org/10.1038/s41598-022-21694-3

37. Mankaï A, Sakly W, Thabet Y, Achour A, Manoubi W, Ghedira I. Anti-*Saccharomyces cerevisiae* antibodies in patients with systemic lupus erythematosus. *Rheumatol Int.* 2013;33(3):665-669. https://doi.org/10.1007/s00296-012-2431-3

38. Mankaï A, Layouni S, Ghedira I. Anti *Saccharomyces cerevisiae* antibodies in patients with anti-β2 glycoprotein I antibodies. *J Clin Lab Anal.* 2016;30(6):818-822. https://doi.org/10.1002/jcla.21942

39. Sadeghi A, Hasanlu M, Feyzi A, Mansori K, Ghodrati S, Parsamanesh N. Evaluating the relationship between antiphospholipid antibodies and COVID-19 severity. *DNA Cell Biol.* 2023;42(1):65-71. https://doi.org/10.1089/dna.2022.0293

40. Zuo Y, Estes SK, Ali RA, et al. Prothrombotic autoantibodies in serum from patients hospitalized with COVID-19. *Sci Transl Med.* 2020;12(570):eabd3876. https://doi.org/10.1126/scitranslmed.abd3876

41. Wang X, Gkrouzman E, Andrade DCO, et al, APS ACTION. COVID-19 and antiphospholipid antibodies: a position statement and management guidance from AntiPhospholipid Syndrome Alliance for Clinical Trials and InternatiOnal Networking (APS ACTION). *Lupus.* 2021;30(14):2276-2285. https://doi.org/10.1177/09612033211062523

42. Zhang Y, Cao W, Jiang W, et al. Profile of natural anticoagulant, coagulant factor and anti-phospholipid antibody in critically ill COVID-19 patients. *J Thromb Thrombolysis.* 2020;50(3):580-586. https://doi.org/10.1007/s11239-020-02182-9

43. Borghi MO, Beltagy A, Garrafa E, et al. Anti-phospholipid antibodies in COVID-19 are different from those detectable in the anti-phospholipid syndrome. *Front Immunol.* 2020;11:584241. https://doi.org/10.3389/fimmu.2020.584241

44. Gatto M, Perricone C, Tonello M, et al. Frequency and clinical correlates of antiphospholipid antibodies arising in patients with SARS-CoV-2 infection: findings from a multicentre study on 122 cases. *Clin Exp Rheumatol.* 2020;38(4):754-759.

45. Meroni PL, Borghi MO. Antiphospholipid antibody assays in 2021: looking for a predictive value in addition to a diagnostic one. *Front Immunol.* 2021;12:726820. https://doi.org/10.3389/fimmu.2021.726820

46. Meroni PL, Borghi MO. Antiphospholipid antibodies and COVID-19 thrombotic vasculopathy: one swallow does not make a summer. *Ann Rheum Dis.* 2021;80(9):1105-1107. https://doi.org/10.1136/annrheumdis-2021-220520

47. Carfì A, Bernabei R, Landi F; Gemelli Against COVID-19 Post-Acute Care Study Group. Persistent symptoms in patients after acute COVID-19. *JAMA.* 2020;324(6):603-605. https://doi.org/10.1001/jama.2020.12603

48. Anaya JM, Rojas M, Salinas ML, et al; Post-COVID Study Group. Post-COVID syndrome: a case series and comprehensive review. *Autoimmun Rev.* 2021;20(11):102947. https://doi.org/10.1016/j.autrev.2021.102947

49. Taha SI, Samaan SF, Ibrahim RA, El-Sehsah EM, Youssef MK. Post-COVID-19 arthritis: is it hyperinflammation or autoimmunity? *Eur Cytokine Netw.* 2021;32(4):83-88. https://doi.org/10.1684/ecn.2021.0471

50. Krause I, Blank M, Cervera R, et al. Cross-reactive epitopes on beta2-glycoprotein-I and *Saccharomyces cerevisiae* in patients with the antiphospholipid syndrome. *Ann N Y Acad Sci.* 2007;1108(1):481-488. https://doi.org/10.1196/annals.1422.051

51. Melayah S, Mankaï A, Jemni M, et al. Anti-*Saccharomyces cerevisiae* antibodies in patients with COVID-19. *Arab J Gastroenterol*. 2022;23(4):241-245. https://doi.org/10.1016/j.ajg.2022.07.001

52. Serrano P, Johnson MA, Chatterjee A, et al. Nuclear magnetic resonance structure of the nucleic acid-binding domain of severe acute respiratory syndrome coronavirus nonstructural protein 3. *J Virol.* 2009;83(24):12998-13008. https://doi.org/10.1128/JVI.01253-09

53. Rinaldi M, Perricone R, Blank M, Perricone C, Shoenfeld Y. Anti-*Saccharomyces cerevisiae* autoantibodies in autoimmune diseases: from bread baking to autoimmunity. *Clin Rev Allergy Immunol.* 2013;45(2):152-161. https://doi.org/10.1007/s12016-012-8344-9

54. Blank M, Shoenfeld Y. Beta-2-glycoprotein-I, infections, antiphospholipid syndrome and therapeutic considerations. *Clin Immunol.* 2004;112(2):190-199. https://doi.org/10.1016/j.clim.2004.02.018

55. Melayah S, Ghozzi M, Jemni M, Sakly N, Ghedira I, Mankaï A. Anti-*Saccharomyces cerevisiae* antibodies in rheumatoid arthritis. *Lab Med*. 2022;53(6):585-589. https://doi.org/10.1093/labmed/lmac054

56. Cardinale V, Capurso G, Ianiro G, Gasbarrini A, Arcidiacono PG, Alvaro D. Intestinal permeability changes with bacterial translocation as key events modulating systemic host immune response to SARS-CoV-2: a working hypothesis. *Dig Liver Dis.* 2020;52(12):1383-1389. https://doi.org/10.1016/j.dld.2020.09.009

57. Zuo T, Zhang F, Lui GCY, et al. Alterations in gut microbiota of patients with COVID-19 during time of hospitalization. *Gastroenterology.* 2020;159(3):944-955.e8. https://doi.org/10.1053/j.gastro.2020.05.048

58. Macor P, Durigutto P, Mangogna A, et al. Multiple-organ complement deposition on vascular endothelium in COVID-19 patients. *Biomedicines*. 2021;9(8):1003. https://doi.org/10.3390/biomedicines9081003

59. Ekpanyapong S, Reddy KR. Liver and biliary tract disease in patients with coronavirus disease-2019 infection. *Gastroenterol Clin North Am.* 2023;52(1):13-36. https://doi.org/10.1016/j.gtc.2022.09.001

60. Georgakopoulou VE, Bali T, Adamantou M, et al. Acute hepatitis and liver injury in hospitalized patients with COVID-19 infection. *Exp Ther Med*. 2022;24(5):691. https://doi.org/10.3892/etm.2022.11627

61. Elmunzer BJ, Spitzer RL, Foster LD, et al; North American Alliance for the Study of Digestive Manifestations of COVID-19. Digestive manifestations in patients hospitalized with coronavirus disease 2019. *Clin Gastroenterol Hepatol.* 2021;19(7):1355-1365.e4. https://doi.org/10.1016/j.cgh.2020.09.041

62. Shankar P, Singh J, Joshi A, et al. Organ involvement in COVID-19: a molecular investigation of autopsied patients. *Microorganisms*. 2022;10(7):1333. https://doi.org/10.3390/microorganisms10071333

63. Mao R, Qiu Y, He JS, et al. Manifestations and prognosis of gastrointestinal and liver involvement in patients with COVID-19: a systematic review and meta-analysis. *Lancet Gastroenterol Hepatol*. 2020;5(7):667-678. https://doi.org/10.1016/S2468-1253(20)30126-6

64. Zhang C, Shi L, Wang FS. Liver injury in COVID-19: management and challenges. *Lancet Gastroenterol Hepatol*. 2020;5(5):428-430. https://doi.org/10.1016/S2468-1253(20)30057-1

65. Vojdani A, Kharrazian D. Potential antigenic cross-reactivity between SARS-CoV-2 and human tissue with a possible link to an increase in autoimmune diseases. *Clin Immunol.* 2020;217:108480. https://doi.org/10.1016/j.clim.2020.108480

Resazurin microplate test method for rapid determination of colistin resistance in carbapenem-resistant *Acinetobacter baumanii* isolates

Kubra Yildirim, PhD[1,2], Ece Simsek, PhD[1,2,3], Orhan Kocak, MSc[2], Serhat Bozkurt, MSc[2], Ozlem Koyuncu Ozyurt, MD[4], Ahmet Yilmaz Coban, PhD[1,2,3]

[1]Department of Nutrition and Dietetics, Faculty of Health Sciences, [2]Tuberculosis Research Center, [3]Department of Medical Biotechnology, Institute of Health Sciences, and [4]Department of Medical Microbiology, Faculty of Medicine, Akdeniz University, Antalya, Turkey. Corresponding author: ecesimsek@akdeniz.edu.tr

Key words: *Acinetobacter baumannii*, rapid antibiogram susceptibility test, resazurin, colistin, carbapenem resistance, colorimetric test

Abbreviations: CRAB, carbapenem-resistant *Acinetobacter baumannii*; EUCAST, European Committee on Antimicrobial Susceptibility Testing; BMD, broth microdilution test; BD, Becton, Dickinson and Company; CAMHB, cation-adjusted Mueller-Hinton broth; MIC; minimum inhibitory concentration; R, resistant; S, sensitive

Laboratory Medicine 2024;55:380-385; https://doi.org/10.1093/labmed/lmad099

ABSTRACT

Background: Colistin-resistant *Acinetobacter baumannii* isolates are extremely important pathogens for hospital-acquired infections.

Objective: To investigate the effectiveness of the resazurin microplate assay (REMA) for the rapid determination of colistin resistance.

Methods: Susceptibility for colistin was investigated in vitro by the broth microdilution method (BMD) and the resazurin microplate assay (REMA) on 106 carbapenem-resistant *Acinetobacter baumannii* isolates.

Results: The results of both test methods were compared, and the categorical agreement between them was found to be 100%. No minor, major, or very major discrepancy was observed between the 2 methods.

Conclusions: The most important advantages of REMA are that the results are obtained within 6 hours compared to the reference method, that it is easy to evaluate because it is colorimetric, and that the susceptibility result can be reported to the clinician on the same day as bacterial identification.

Introduction

Nosocomial infections remain a common problem. *Acinetobacter baumannii* is an opportunistic pathogen that is present in ventilator-associated pneumonia and septicemia, especially in intensive care units.[1] The high antibiotic resistance of *A baumanii* is the main reason for treatment failure. Increasing resistance, especially in important groups such as carbapenems and beta-lactams, limits the antimicrobial agents to be used in the treatment process.[2] According to World Health Organization data, increasing resistance rates of gram-negative bacteria require new drug-development strategies in creating effective treatments; carbapenem-resistant *A baumannii* (CRAB) infections are at the top of the list of pathogens that should be prioritized for treatment development.[3]

There are many challenges in the diagnosis and treatment of CRAB infections. These include diagnostic uncertainties, the limitation of rapid molecular tests in routine use, the need to optimize the dose of antimicrobials to be used to achieve pharmacokinetic and pharmacodynamic targets, and the fact that biofilm formations associated with CRAB infections are commonly associated with resistant phenotypes and increased virulence.[4] Antimicrobial agents frequently encountered in the treatment of CRAB infections are primarily polymyxins (colistin, polymyxin B), tetracyclines (eravacycline, minocycline, tigecycline), and β-lactams (ampicillin-sulbactam, carbapenems); however, increasing resistance problems when each is used by itself are worrisome.[4] Therefore, combination therapy with at least 2 in vitro active agents is recommended in treatment.[5]

In studies on treatment options, colistin has become the primary antimicrobial agent in combination treatments, due to its high activity in in vitro studies. Although the combination of colistin with a carbapenem drug such as meropenem initially appeared to increase the synergistic effect, studies have shown no significant difference in the results obtained from the use of colistin by itself.[4] Another recommended treatment

option is the use of ampicillin-sulbactam, colistin, and carbapenem in a triple combination, especially for patients who have previously received colistin and carbapenem combination therapy. Tigecycline is another antimicrobial agent reported to be used in combined treatment with colistin. However, it has been reported that the minimum inhibitory concentration (MIC) must be ≤2 mg/L for effective treatment. Despite this, a clinical breakpoint for *Acinetobacter* spp has not been determined by EUCAST (the European Committee on Antimicrobial Susceptibility Testing) or the Clinical and Laboratory Standards Institute (CLSI).[4]

Novel β-lactams such as cefiderocol and sulbactam-durlobactam show significant in vitro activity against several isolates. However, susceptibility breakpoints are variable or have not yet been established.[6] Especially in CRAB infections, colistin still maintains its importance as the first antibiotic used in the treatment steps.[7]

The reference method routinely used in the detection of colistin resistance is the broth microdilution test method (BMD).[8,9] However, the disadvantage of this reference method is its long wait period for results, such as 24 hours. Molecular methods provide rapid detection; however, these are disadvantageous due to their high cost and the lack of experience among many laboratory technicians in using them.

In recent years, colorimetric test methods have been developed for susceptibility testing of *Staphylococcus aureus*, *Mycobacterium tuberculosis*, and *Enterobactericales* groups. The use of these methods enables rapid detection of resistance. At the same time, the low cost of testing compared to molecular methods is one of the most important advantages of these tests.[10-12] The methods used are based on enzymatic properties such as nitrate reductase activity of bacteria, as well as dyes such as methylene blue and resazurin, which show the presence of living cells.

Therefore, in this study, we aimed to develop a modified test method. This method aims to a rapid detection by using resazurin dye in the determination of colistin resistance on CRAB isolates, which will provide a colorimetric evaluation advantage.

Methods

Bacterial Strains

A total of 106 CRAB (imipenem- and meropenem-resistant) isolates from blood cultures were tested in this study. Previously identified to the species level using the MALDI-TOF (Becton, Dickinson and Company [BD]), their carbapenem resistance was determined with the PHONEX (BD) system. *E coli* ATCC 25922 (colistin-susceptible) and *E coli* NCTC 13846 (colistin-resistant) (mcr-1–positive) were used as controls in the study.

Chemical Substances

The colistin-sulfate antibiotic was purchased in commercial powder form (Merck). Stock solutions of 4096 μg/mL were prepared by dissolving with distilled water and stored in small volumes at −80°C until the working day. Resazurin was purchased in commercial powder form (Merck). It was prepared at a concentration of 0.02% in distilled water. After sterilization by membrane filtration, the resulting solution was stored at 4°C until use.

Preparation of Media

In this study, commercially available cation-adjusted Mueller-Hinton broth (CAMHB) (BD) (calcium: 20-25 mg/L, magnesium: 10-12.5 mg/L) was used for the preparation of microdilution and resazurin plates. Bacteria were grown on blood agar media. Both media were in powder and prepared according to manufacturer recommendations.

Preparation of BMD and REMA Plates

The BMD test method recommended by CLSI was used as the reference method.[5] Control strains and clinical isolates were tested in CAMHB broth. Colistin concentrations were determined according to the quality control range specified by EUCAST and were prepared in concentrations of 16 to 0.5 μg/mL by 2-fold serial dilution.[9]

The first and the last wells were used as growth and sterility control wells in each plate, respectively. The prepared plates were stored at −80°C until used. Before experiments, they were removed from −80°C use, thawed, and brought to room temperature.

Preparation of Bacterial Inoculum

In BMD and REMA application, the bacterial inoculum was prepared from a fresh bacterial culture on blood agar by direct colony suspension method and adjusted to that of McFarland number 0.5, turbidity standard. The same bacterial inoculum was used for both methods.

Reference Antimicrobial Susceptibility Testing (BMD)

The bacterial suspension, adjusted to McFarland standard number 0.5 turbidity, was diluted 1:100 with CAMHB. It was then inoculated as 50 μL to all wells except the sterility well; next, the plates were incubated at mean (SD) 35°C (2°C) for 16 to 20 hours. After incubation, the lowest antibiotic concentration with no visible growth was recorded as the MIC value. According to EUCAST criteria, strains with a MIC of ≤2 μg/mL were colistin susceptible; strains with a MIC of >2 μg/mL were determined to be colistin resistant.[9]

Standardization of REMA

Standardization of the REMA was performed by using reference strains and 25 *A baumannii* isolates. The isolates were tested with McFarland number 0.5, McFarland number 1, and McFarland number 2 turbidity, with 50 μL bacterial suspension added to all wells. At the end of the 3-hour incubation, resazurin reagent was added every hour to all McFarland turbidities. After the addition of the reagent, the resulting mixture was incubated for 1 hour. The susceptibility results obtained with McFarland number 0.5 inoculum at the 6th hour of incubation were found to be 100% compatible with the BMD results.

Performance of REMA

As a result of the standardization study, bacterial inoculum for REMA was applied as 50 μL of McFarland number 0.5 turbidity. After incubation at 35°C for 5 hours, 30 μL resazurin was added to all wells and incubation was continued for 1 hour. When a color change from blue to red was observed in the antibiotic-free control wells, the MIC values were determined. The MIC is reported from the last well in which a color change was not seen. The MIC values were evaluated according to the recommendations of EUCAST and compared with the reference method.

Analysis of Results

Results were analyzed according to US Food and Drug Administration (FDA) criteria.[13] In the analysis, minor, major, and extremely major discrepancies and category and essential agreement were determined comparatively.

TABLE 1. MICs of colistin using the BMD method and results of the REMA

Isolate	Species	BMD MIC colistin (μg/mL)	REMA 6th-hour colistin (μg/mL)	Phenotype
Control 1	*E coli* NCTC 13846	4	4	R
Control 2	*E coli* ATCC 25922 *A baumanii*	2	2	S
1		>16	>16	R
2		2	≤0.5	S
3		≤0.5	≤0.5	S
4		0.5	0.5	S
5		1	≤0.5	S
6		1	≤0.5	S
7		≤0.5	≤0.5	S
8		≤0.5	≤0.5	S
9		≤0.5	≤0.5	S
10		≤0.5	≤0.5	S
11		1	≤0.5	S
12		1	≤0.5	S
13		16	16	R
14		≤0.5	≤0.5	S
15		0.5	≤0.5	S
16		≤0.5	≤0.5	S
17		≤0.5	≤0.5	S
18		≤0.5	≤0.5	S
19		4	4	R
20		2	2	S
21		≤0.5	≤0.5	S
22		≤0.5	≤0.5	S
23		≤0.5	≤0.5	S
24		≤0.5	≤0.5	S
25		≤0.5	≤0.5	S
26		≤0.5	≤0.5	S
27		≤0.5	≤0.5	S
28		≤0.5	≤0.5	S
29		2	2	S
30		≤0.5	≤0.5	S
31		≤0.5	≤0.5	S
32		2	2	S
33		≤0.5	≤0.5	S
34		≤0.5	≤0.5	S
35		≤0.5	≤0.5	S
36		≤0.5	≤0.5	S
37		≤0.5	≤0.5	S
38		≤0.5	≤0.5	S
39		≤0.5	≤0.5	S
40		≤0.5	≤0.5	S
41		2	1	S
42		16	16	R
43		16	16	R
44		>16	16	R
45		>16	16	R
46		1	1	S

TABLE 1. (cont)

Isolate	Species	BMD MIC colistin (µg/mL)	REMA 6th-hour colistin (µg/mL)	Phenotype
47		1	2	S
48		2	2	S
49		≤0.5	2	S
50		2	2	S
51		>16	>16	R
52		≤0.5	≤0.5	S
53		1	2	S
54		2	2	S
55		2	2	S
56		2	1	S
57		1	1	S
58		0.5	0.5	S
59		0.5	0.5	S
60		0.5	0.5	S
61		2	2	S
62		1	1	S
63		1	1	S
64		1	1	S
65		1	1	S
66		1	1	S
67		1	1	S
68		2	2	S
69		2	2	S
70		1	1	S
71		2	2	S
72		2	2	S
73		0.5	1	S
74		2	2	S
75		1	1	S
76		2	2	S
77		2	2	S
78		1	2	S
79		0.5	≤0.5	S
80		1	1	S
81		0.5	≤0.5	S
82		>16	16	R
83		0.5	0.5	S
84		0.5	≤0.5	S
85		0.5	≤0.5	S
86		0.5	≤0.5	S
87		0.5	1	S
88		0.5	1	S
89		1	0.5	S
90		≤0.5	0.5	S
91		0.5	1	S
92		0.5	1	S
93		2	0.5	S
94		0.5	0.5	S
95		0.5	0.5	S

TABLE 1. (cont)

Isolate	Species	BMD MIC colistin (μg/mL)	REMA 6th-hour colistin (μg/mL)	Phenotype
96		0.5	0.5	S
97		1	≤0.5	S
98		0,5	0.5	S
99		≤0.5	≤0.5	S
100		≤0.5	0.5	S
101		0.5	≤0.5	S
102		0.5	0.5	S
103		0.5	0.5	S
104		0.5	0.5	S
105		0.5	1	S
106		≤0.5	0.5	S

BMD, broth microdilution method; MIC, minimum inhibitory concentration; R, resistant; REMA, resazurin microplate assay; S, sensitive.

Results

A total of 106 CRAB isolates were studied for colistin resistance with the BMD and REMA. The study was carried out in duplicate. *E coli* ATCC 25922 (colistin-susceptible) and *E coli* NCTC 13846 (colistin-resistant) (mcr-1–positive) strains were used as control strains. MIC values in both methods were determined at 2 μg/mL for *E coli* ATCC 25922, and MIC was determined at 4 μg/mL for *E coli* NCTC 13846. According to the BMD test method, colistin MICs were determined as >16 μg/mL for 5 isolates, 16 μg/mL for 3 isolates, 4 μg/mL for 1 isolate, 2 μg/mL for 19 isolates, 1 μg/mL for 20 isolates, 0.5 μg/mL for 25 isolates, and ≤0.5 μg/mL for 33 isolates. According to the REMA, colistin MICs were determined as being >16 μg/mL for 2 isolates, 16 μg/mL for 6 isolates, 4 μg/mL for 1 isolate, 2 μg/mL for 19 isolates, 1 μg/mL for 19 isolates, 0.5 μg/mL for 17 isolates, and ≤0.5 μg/mL for 42 isolates. According to EUCAST criteria, 9 isolates were defined as colistin resistant and 97 isolates as colistin susceptible in both methods.

Although 3 of the resistant isolates had an MIC of >16 μg/mL in the BMD, the same isolates were found to have an MIC of 16 μg/mL in the REMA. Eight of the susceptible isolates yielded an MIC of 0.5 μg/mL in the BMD, and the MIC was ≤0.5 μg/mL in REMA. The results of both tests were compared and given in **TABLE 1**.

When the results were compared according to the criteria adopted by the FDA, the categorical agreement between both methods was found to be 100%.[13] There is no minor, major, or very major discrepancy between both methods.

Discussion

Increasing antibiotic resistance is a serious problem for *A baumannii* infections, which are common in hospitals, especially in intensive care units, as is the case with many other bacteria.[1] The limitation of antimicrobial drugs to be used in treatment due to resistance requires the development of new drug strategies.[14] There are many studies related to the drugs developed in recent years. However, the novel agents discussed therein are costly for many countries and limited in their effectiveness against multidrug-resistant *Acinetobacter* spp.[5] In studies conducted with cefiderocol, developed for the treatment of CRAB infections, its use by itself and in combination, compared with colistin, did not show the expected effect.[15] New β-lactams such as durlobactam have not received FDA approval; however, studies suggest that the sulbactam-durlobactam combination may have a significant role in treatment.[16] Therefore, colistin remains one of the most important agents in the treatment of CRAB infections.

The use of colistin by itself may cause resistance problems; however, study results have shown that its effectiveness increases when used together with a carbapenem agent, such as meropenem or imipenem. The type of treatment is mostly related to the diagnosis of the patient. In invasive CRAB infections, antibiotics such as ampicillin sulbactam and tigecycline are often added to the colistin combination.[4]

CLSI and EUCAST have made many updates over the years regarding the correct determination of colistin doses for use in treatment.[5] Due to difficulties with susceptibility testing, semiautomated antimicrobial susceptibility testers and gradient assays have been determined to significantly underestimate colistin resistance, and BMD is required to safely estimate susceptibility.[8,9]

Colistin resistance can be determined by molecular methods and the BMD method.[8] The cost of molecular methods is a disadvantage for many small laboratories. Also, the disadvantage of the BMD method is that it yields results after a long period of time, such as 24 hours, and there are differences in evaluations among the different people performing the testing.

In recent years, it has been reported that susceptibility results are obtained effectively and quickly with colorimetric tests for many bacterial groups. The development of colorimetric methods such as resazurin and nitrate reductase in *S aureus* and *M tuberculosis* has shown the advantages of providing an early diagnosis in achieving susceptibility results.[10,11]

In our study, colistin MIC values were determined colorimetrically in a short time period of 6 hours. Similarly, in another study, in which colistin resistance was determined with resazurin developed for *A baumannii* isolates, it was observed that colistin resistance could be detected within 4 hours of preparing a bacterial inoculum with McFarland number 3.5 turbidities.[17]

There are also other studies in the literature in which colistin susceptibility was determined with resazurin.[18] However, these studies were performed at a single concentration for colistin. In our study, all MIC ranges could be determined for colistin. During the study, deviations in MIC values were observed in the standardization experiments conducted in McFarland number 1 and McFarland number 2. It was observed that as the McFarland turbidity increased, the isolates that appeared to be

sensitive, via the BMD method, shifted to the resistance limit. The high McFarland turbidity was not used for the MIC determination because the MIC values detected were more than twice the sensitivity values defined for the BMD method.

The REMA was performed with some modifications to the BMD method recommended by CLSI. The use of resazurin dye, which provides visual identification of live microorganisms, is the advantage of colorimetric evaluation. The detectability of colistin MICs at the end of the 6th hour is the most important advantage of our study.

Early intervention is extremely important in bacterial groups such as *A baumannii*, which have multidrug resistance and limit the treatment options for hospital infections. The most important advantage of our study results is that the sensitivity result for colistin can be reported to the clinician on the same day as the identification. However, although all isolates included in the study were carbapenem-resistant, the low number of colistin-resistant isolates is a limitation of the study. Therefore, further studies are needed before this novel method can be used in routine laboratories.

Acknowledgments

This work was supported by the Akdeniz University Scientific Research Projects Coordination Unit (TSA-2020-5390). This study was presented in the Online Turkish Microbiology Symposium, December 25-27, 2020.

Conflict of Interest Disclosure

The authors have nothing to disclose.

REFERENCES

1. Albrecht MC, Griffith ME, Murray CK, et al. Impact of *Acinetobacter* infection on the mortality of burn patients [published correction appears in *J Am Coll Surg* 2007 Jan;204(1):191 Albrecht, Michael A (corrected to Albrecht, Michael C)]. *J Am Coll Surg.* 2006;203(4):546-550. doi:10.1016/j.jamcollsurg.2006.06.013
2. Wong D, Nielsen TB, Bonomo RA, Pantapalangkoor P, Luna B, Spellberg B. Clinical and pathophysiological overview of *Acinetobacter* infections: a century of challenges. *Clin Microbiol Rev.* 2017;30(1):409-447. doi:10.1128/CMR.00058-16
3. World Health Organization. WHO publishes a list of bacteria for which new antibiotics are urgently needed. 2017. Accessed October 14, 2023. https://www.who.int/news/item/27-02-2017-who-publishes-list-of-bacteria-for-which-new-antibiotics-are-urgently-needed
4. Shields RK, Paterson DL, Tamma PD. Navigating available treatment options for carbapenem-resistant *Acinetobacter baumannii-calcoaceticus* complex infections. *Clin Infect Dis.* 2023;76(suppl 2):S179-S193. doi:10.1093/cid/ciad094
5. Paul M, Carrara E, Retamar P, et al. European Society of Clinical Microbiology and Infectious Diseases (ESCMID) guidelines for the treatment of infections caused by multidrug-resistant Gram-negative bacilli (endorsed by European Society of Intensive Care Medicine). *Clin Microbiol Infect.* 2022;28(4):521-547. doi:10.1016/j.cmi.2021.11.025
6. Karlowsky JA, Hackel MA, McLeod SM, Miller AA. *In vitro* activity of sulbactam-durlobactam against global isolates of *Acinetobacter baumannii-calcoaceticus* complex collected from 2016 to 2021. *Antimicrob Agents Chemother.* 2022;66(9):e0078122. doi:10.1128/aac.00781-22
7. Chen Z, Chen Y, Fang Y, et al. Meta-analysis of colistin for the treatment of *Acinetobacter baumannii* infection. *Sci Rep.* 2015;5:17091. doi:10.1038/srep17091
8. CLSI. *Performance Standards for Antimicrobial Susceptibility Testing.* 29th ed. CLSI supplement M100. Clinical and Laboratory Standards Institute; 2019.
9. The European Committee on Antimicrobial Susceptibility Testing. *Breakpoint Tables for Interpretation of MICs and Zone Diameters. Version 9.0*; 2019. https://www.eucast.org/fileadmin/src/media/PDFs/EUCAST_files/Breakpoint_tables/v_13.1_Breakpoint_Tables.pdf
10. Coban AY. Rapid determination of methicillin resistance among *Staphylococcus aureus* clinical isolates by colorimetric methods [published correction appears in *J Clin Microbiol.* 2012;50(9):3148]. *J Clin Microbiol.* 2012;50(7):2191-2193. doi:10.1128/JCM.00471-12
11. Coban AY, Deveci A, Sunter AT, Palomino JC, Martin A. Resazurin microtiter assay for isoniazid, rifampicin, ethambutol and streptomycin resistance detection in *Mycobacterium tuberculosis*: updated meta-analysis. *Int J Mycobacteriol*. 2014;3(4):230-241. doi:10.1016/j.ijmyco.2014.09.002
12. Nordmann P, Jayol A, Poirel L. Rapid detection of polymyxin resistance in *Enterobacteriaceae*. *Emerg Infect Dis.* 2016;22(6):1038-1043. doi:10.3201/eid2206.151840
13. US FDA. *Guidance for Industry and FDA. Class II special Controls Guidance Document: Antimicrobial Susceptibility Test (AST) systems.* Center for Devices and Radiological Health, Food and Drug Administration, U.S. Department of Health and Human Services; 2009.
14. Temel A, Eraç B. A global threat: Acinetobacter baumannii infections, current condition in antimicrobial resistance and alternative treatment approaches. *Turk Hij Den Biyol Derg.* 2020;77(3):367-378.
15. Wunderink RG, Matsunaga Y, Ariyasu M, et al. Cefiderocol versus high-dose, extended-infusion meropenem for the treatment of Gram-negative nosocomial pneumonia (APEKS-NP): a randomised, double-blind, phase 3, non-inferiority trial. *Lancet Infect Dis.* 2021;21(2):213-225. doi:10.1016/S1473-3099(20)30731-3
16. Altarac DE, Isaacs R, Srinivasan S, et al. Efficacy and safety of sulbactam-durlobactam (SUL-DUR) versus colistin therapy in patients with *Acinetobacter baumannii-calcoaceticus* complex (ABC) infections: a global, randomised, active-controlled phase 3 trial (ATTACK). Abstract 02060. Presented at: 32nd ECCMID; Lisbon, Portugal; April 23-26, 2022.
17. Lescat M, Poirel L, Tinguely C, Nordmann P. A resazurin reduction-based assay for rapid detection of polymyxin resistance in *Acinetobacter baumannii* and *Pseudomonas aeruginosa*. *J Clin Microbiol.* 2019;57(3):e01563-e01518. doi:10.1128/JCM.01563-18
18. Jia H, Fang R, Lin J, et al. Evaluation of resazurin-based assay for rapid detection of polymyxin-resistant gram-negative bacteria. *BMC Microbiol.* 2020;20(1):7. doi:10.1186/s12866-019-1692-3

A comparison of staining methods for *Helicobacter pylori* in laparoscopic vertical sleeve gastrectomy resections

JoAnna Rudasill, MCP[1], Chelsea Peeler, MCP[1], Danielle Grant, MS[1], Cynthia Lazar, BS[2], Sheila L. Criswell, PhD[1]

[1]Department of Diagnostic and Health Sciences, University of Tennessee Health Science Center, Memphis, TN, US; [2]Department of Pathology, Methodist University Hospital, Memphis, TN, US. Corresponding author: Sheila Criswell; scriswel@uthsc.edu

Key words: Wright; alcian yellow toluidine blue; immunohistochemistry; sleeve

Abbreviations: AYTB, alcian yellow toluidine blue; IHC, immunohistochemistry; LSG, laparoscopic vertical sleeve gastrectomy

Laboratory Medicine 2024;55:386-390; https://doi.org/10.1093/labmed/lmad102

ABSTRACT

Background: *Helicobacter pylori* is an important public health concern due to its status as a carcinogenic bacterium. Well adapted to the acidic environment of the human stomach, the variety of strains and virulence factors of the organism when interacting with the host immune system creates an individualistic response. Although estimates suggest that approximately half of the global population is infected with *H pylori*, the majority of infected persons remain asymptomatic while harboring an increased risk of intestinal metaplasia and gastric cancers. Therefore, appropriate diagnostic testing protocols are imperative.

Methods: This study compared labeling methodologies, including Wright stain, alcian yellow toluidine blue (AYTB), and immunohistochemistry (IHC) on formalin-fixed paraffin-embedded stomach resections from sleeve gastrectomy patients, to detect *H pylori* infection.

Results: Although all 3 labeling methods evidenced similar specificity in *H pylori* detection, the IHC method was significantly more sensitive. However, the IHC cost per test was approximately 5-fold higher than that of the Wright or AYTB stains, and the technical time required per test was at least 6-fold that of Wright or AYTB.

Conclusion: Despite the higher cost per test, IHC is the most sensitive and preferred method for determination of *H pylori* infection.

Introduction

Helicobacter pylori is a gram-negative spiral-shaped bacterium that inhabits the gastric epithelium of its host. Approximately half the global population is infected by *H pylori*, with higher incidence in developing countries.[1] Bacterial colonization has a range of diverse effects on its host, with most patients demonstrating no or mild clinical symptoms, whereas a minority of patients develop gastroduodenal ulcers, chronic gastritis, gastric mucosa-associated lymphoid tissue lymphomas, or gastric adenocarcinoma.[2,3] Gastric adenocarcinoma is strongly associated with *H pylori* infection and was the fourth leading cause of cancer deaths in 2020,[4] providing the impetus for timely and accurate detection of the oncogenic bacterium. The mode of transmission of *H pylori* infection is most likely via oral/oral or fecal/oral routes between humans.[5] Infection typically occurs in early childhood, and the host remains colonized unless treated.[3] Studies have found high prevalence of *H pylori* in siblings and mothers of infected children, suggesting intrafamilial transmission. Additionally, higher rates of infection were seen in locations with poor infrastructure, a lack of sanitation, and overcrowding.[5]

Diagnostic methods for *H pylori* can be divided into invasive and noninvasive categories. Noninvasive testing includes urea breath tests, stool antigen testing, *Campylobacter*-like organism test, and serological testing. Urea breath tests and stool antigen testing have high sensitivity and specificity and are useful in initial diagnosis as well as determining whether treatment with antibiotic therapy was effective.[6] Invasive testing includes histology, rapid urease testing, and culture. These methods require endoscopy for sampling, making them more expensive, time-consuming, and requiring specialized staffing.[2] Although there are notable drawbacks to histology as a diagnostic method for *H pylori* infection, it is the gold standard and is the only method in which the degree of inflammation can be determined. Additionally, histology allows for the diagnosis of related conditions including intestinal metaplasia, atrophic gastritis, and cancer.[2]

Staining with H&E of gastric samples allows for the grading of inflammation but shows poor specificity and sensitivity for the diagnosis of *H pylori* infection, as the bacteria stain similarly to and are easily mistaken for the mucus secreted by the stomach neck cells.[2] Additional staining methods increase sensitivity in diagnosis of *H pylori* in these samples. The goal of this study was to compare 3 labeling methods for *H pylori* in gastric resections.

Methods

Laparoscopic vertical sleeve gastrectomy (LSG) is a type of bariatric surgery in which over half of the stomach is removed to assist in weight loss in obese individuals. We obtained 203 consecutive samples from 3 clinicians in a major metropolitan hospital system under institutional review board approval (No. 21-08515-XM from the University of Tennessee Health Science Center). All procedures performed in studies involving human participants were in accordance with the ethical standards of the institutional and/or national research committee and with the 1964 Helsinki declaration and its later amendments or comparable ethical standards. Three tissue samples, 10 mm × 3 mm, were excised from each resection. The fundus, body, and antrum were each equally sampled by extracting 1 sample from each resection end and 1 sample from the middle portion. The tissues were processed through formalin, increasing alcohol concentrations, xylene, and paraffin before final paraffin embedding.

The tissues were sectioned at 4 μm and stained with H&E for interpretation of histological features. For detection of *H pylori*, 3 staining methods were used and included Wright Romanowsky stain, alcian yellow toluidine blue (AYTB), and immunohistochemistry (IHC) assay with an anti-*H pylori* antibody. Prior to staining, all slides were deparaffinized using xylene and decreasing ethanol concentrations and then were hydrated with deionized water prior to undergoing the various staining procedures.

H&E Staining Procedure

Sections were placed in Surgipath SelecTech Hematoxylin 560 MX (3801576, Leica Biosystems) for 5 minutes, rinsed well in tap water for 1 minute, dipped in Select Acid Rinse (SL404, StatLab Medical Products) 3 to 4 times, then immediately transferred to running water for a 1-minute rinse. Next, the sections were agitated in Vintage Bluing (SL102, StatLab Medical Products) 30 times, rinsed with running tap water for 1 minute, dipped in 95% ethanol 10 times, and transferred to eosin (SL406, StatLab Medical Products) for 2 minutes and 15 seconds.

Alcian Yellow Toluidine Blue Staining Procedure

The tissue sections were oxidized in 1% periodic acid (P5463, Sigma Aldrich/Sigma Millipore) for 10 minutes, rinsed in tap water for 30 seconds, placed in 1% sodium metabisulfite (S244, Fisher Scientific) for 5 minutes, then placed in alcian yellow (KC3733, American MasterTech Scientific/StatLab Medical Products) for 10 minutes. The sections were then rinsed in tap water and placed into 20 mL 0.01% aqueous alkaline toluidine blue (T-161, Fisher Scientific) working reagent made basic with the addition of 30 μL 3% sodium hydroxide (AHS0626, American MasterTech Scientific/StatLab Medical Products) for 5 minutes, then rinsed for 60 seconds in running tap water.

Immunohistochemistry

Antigenic sites were decloaked 5 minutes at 120°C using a Biocare Decloaking Chamber (Biocare Medical) and Envision Flex Target Retrieval solution high pH (GV800/GV804 Dako/Agilent). After the antigen retrieval solution cooled to room temperature, sections were placed in 1X Envision Flex Wash buffer (DM831, Dako). All IHC steps were performed manually in a humidity chamber at room temperature using a Bond Polymer Refine Detection Kit (DS9800, Leica Biosystems) with buffer washes between each step. Kit peroxidase block was applied for 5 minutes followed by incubation with primary mouse monoclonal antibody to *H pylori* (NCL-L-Hpylori, Leica Biosystems), RRID:AB 563756, diluted 1:200 with Bond Primary Antibody Diluent (AR9352, Leica Biosystems) for 20 minutes. The detection kit post-primary and polymer reagents were applied each for 8 minutes prior to the diaminobenzidine color development step for 2 minutes. After a deionized water rinse, sections were stained with the kit hematoxylin for 5 minutes and then blued with buffer before a final deionized water rinse.

After all staining protocols, sections were dehydrated and cleared with alcohols and xylene then coverslipped. A control tissue positive for *H pylori* was placed on each slide closest to the label and investigators ensured appropriate staining on the control prior to tissue evaluation. Each microscope slide for *H pylori* detection was randomly numbered in a double-blinded method to prevent bias. The H&E slides were examined using an Olympus BX41 microscope (Olympus) with an Olympus DP71 digital microscope camera. Sample integrity was evaluated with H&E using the ×4 and ×10 objectives whereas detection of *H pylori* was performed with the ×40 objective. Images were captured using Olympus CellSens Standard software. The investigators were given a strict 2-minute time limit when evaluating each of the 3 tissue sections (6 minutes total) stained with Wright, AYTB, and IHC for *H pylori* to simulate the time realistically required by a practicing pathologist. Each investigator set a timer for 2 minutes at the onset of reviewing each tissue section. After the timer alarmed, the investigator made note of the findings, reset the timer, and reviewed the subsequent tissue section. The investigators did not attempt to detect *H pylori* with the H&E stain, as the organisms and mucus stain similarly. When interpretations differed among stain interpretation, the investigators resolved discrepancies together at a multihead microscope.

Results

Of the 203 patient samples evaluated for *H pylori*, 37 (18.2%) were positive, and 36 (97.3%) of the 37 were accompanied by moderate to marked chronic inflammation within the mucosal lamina propria. A comparison of the staining methods for *H pylori* demonstrated that the test sensitivity as measured per patient and per total tissue section was higher in sections stained using IHC as compared with that of AYTB or Wright stain (**FIGURE 1**, **TABLE 1**). However, the specificity for all 3 staining procedures was similar, all >97%. Three patient tissues were excluded from statistical analysis for sensitivity and specificity due to extreme rare organisms identified on all 3 staining methods. Each of these 3 patients demonstrated moderate to marked chronic inflammation in all 3 tissue sections, and the authors suggest that these instances may represent recently treated patients with rare residual viable or nonviable organisms and unresolved chronic inflammation. Interestingly, in each of the other 34 remaining cases positive for *H pylori*, all 3 tissue sections demonstrated the organism, suggesting that the entire greater curvature of the stomach was involved (**FIGURE 2**).

Discussion

Disease development due to infection with *H pylori* varies in type and severity and is influenced by both bacteria and host factors.[6] *H pylori* colonizes the gastric mucosa by binding to MUC1 produced by gastric epithelial cells and triggers inflammation by inducing the expression of cytokines and chemokines, notably CagA and VacA,[7] which attract

FIGURE 1. *Helicobacter pylori* **organisms as seen on H&E (A), Wright stain (B), alcian yellow toluidine blue stain (C), and immunohistochemistry (D). Arrows indicate organisms and arrowheads indicate intraluminal mucus and detritus that may be mistaken for organisms.**

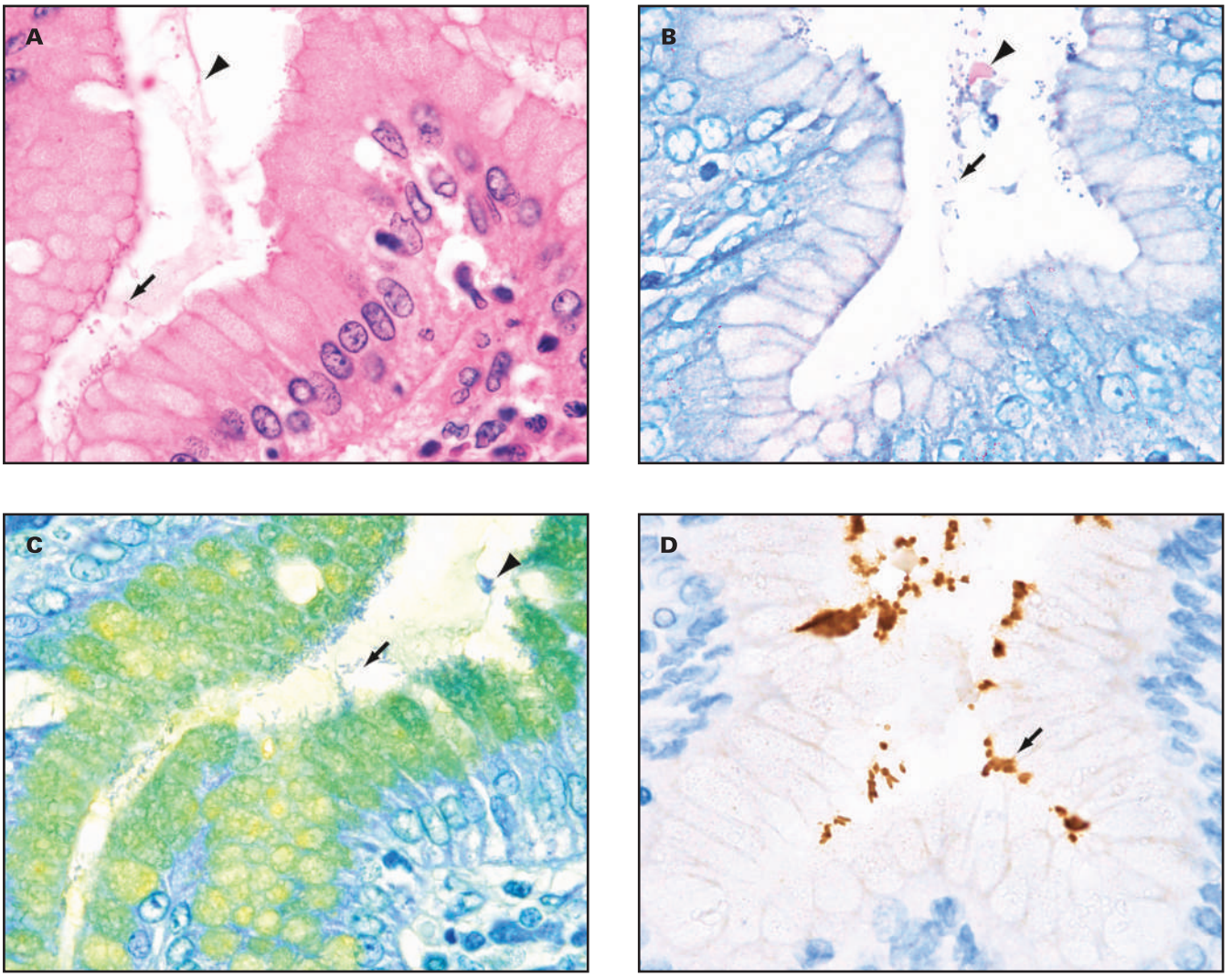

TABLE 1. Comparison of sensitivity and specificity of staining methods for *H pylori*

Method of labeling *H pylori*	Sensitivity by patient (n = 200), %	Specificity by patient (n = 200), %	Sensitivity by tissue section (n = 600), %	Specificity by tissue section (n = 600), %
Wright	81.0	98.2	85.0	98.8
Alcian yellow toluidine blue	69.3	96.5	68.9	97.8
Immunohistochemistry	94.4	96.0	96.2	97.1

neutrophils, lymphocytes, macrophages, and other immune cells.[3] Initial infection of persons in developed countries typically occurs during early childhood and persists until such time as eradication therapy is successfully performed or until the patient develops a gastric malignancy.[8,9] Eradication therapy consists of an antibiotic regimen coupled with proton pump inhibitors,[5,10] and with patient compliance, typically completely resolves infection. However, in regions of the world with poor sanitation or low income per capita, the recurrence rate of infection in adults ranges from 1.7% to 4.3%.[11] Explanations for recurrence include contamination of well water or agricultural irrigation water with fecal matter,[12] biofilms in the oral cavity providing a reservoir of *H pylori*,[5,13] inadequate dosage of antibiotics in the overweight population,[14] or noncompliance of patients with antibiotic therapy. Several studies describe practice protocols requiring all bariatric candidates to be tested for *H pylori* prior to surgery with verification of negative test results.[15-19] However, there frequently remains a low positivity rate postsurgery,[17,18] presumably due to the same risk factors indicated previously.[14]

The *H pylori* positivity rates in LSG specimens vary widely based on the patient population and range from 2.5% to 43.2%[15,17,18,20-25] which matches the current study value of 18.3%. Unfortunately, many studies

FIGURE 2. Laparoscopic vertical sleeve gastrectomy resection incorporating the entire greater curvature of the stomach to include the fundus (F), the body (B), and the antrum (A).

from the literature do not indicate what method was used to identify *H pylori*[15,20,26-29] or whether all specimens were histochemically stained and evaluated for *H pylori*[15,19,22,28] as opposed to only those cases that exhibited histologic characteristics suspicious for infection,[16,20,21] such as moderate to marked chronic inflammation. Indeed, in studies performed retrospectively over many years, there may have been multiple methods of *H pylori* detection used. The histologic examination procedure may also have evolved over time as LSG surgery increased in availability and popularity. Other studies did not indicate whether all submitted specimens were evaluated for *H pylori* or whether only those exhibiting chronic gastritis or other pathology seen on H&E were tested. Clearly, if only the specimens with chronic gastritis were tested, the results would skew the data to make *H pylori* and gastritis appear more co-dependent than if all specimens were tested.

A few studies indicated that a Giemsa Romanowsky stain,[17,22-24,30,31] H&E and IHC,[21,31] and Warthin-Starry[25,32] methods were performed to detect *H pylori*. In the current investigation, all stains demonstrated similar specificities, but IHC exhibited the highest sensitivity to identify *H pylori*. There are further advantages and disadvantages to each method. First, cost per test was <$5 for each Wright and AYTB stain and was approximately $25 for each IHC stain. However, the 3 investigators reviewing the *H pylori* preparations found that the IHC stain offered a slight advantage of contrast for *H pylori* evaluation (**FIGURE 1**). With the Wright stain, all organisms and tissue elements except mast cells and eosinophils stained a similar shade of blue, requiring identification based solely on morphological features. Although the AYTB stain did offer contrasting color of blue organisms against a yellow mucin background and therefore specifically highlighted the histological location to evaluate *H pylori* positivity, other tissue elements and cellular debris also stained blue, and when present in the lumen, needed to be differentiated from organisms. Additionally, the organisms occasionally did not absorb the toluidine blue stain adequately, causing false-negative results and sensitivities <70%. However, with the IHC assay, the organisms stained brown against the pale blue of all other tissue elements. The main disadvantages in using IHC include increased staining time (3 hours vs 15 minutes for Wright and 30 minutes for AYTB), the need for specialized reagents (high-quality, specific antibodies and reliable detection kits to prevent nonspecific background staining), and increased cost per test. As a further disadvantage to IHC, the use of inadequately buffered formalin can produce a formalin precipitate mimicking positive IHC labeling. Conversely, advantages to the IHC method are increased specificity for *H pylori* insofar that alternate normal flora are not identified and also the ease and reliability of interpretation. Whereas *H pylori* as visualized in the Wright or AYTB stains must be evaluated at ×40, often the organisms can be visualized at ×10 with IHC due to signal amplification. In treated patients, *H pylori* can appear more coccoid than rod-like, which may confound the observer when evaluating a Wright or AYTB stain, as it may appear as a different organism or luminal debris but which is nonetheless reliably identified by IHC.[2] The authors agree with previous reports that Romanowsky stains such as Wright or Giemsa are fast, reliable, economical, and particularly valuable in developing areas of the world,[2] but also stipulate that IHC was the most sensitive and easy to evaluate, as noted in findings from a previous study.[33]

Of 37 resections found to be positive for *H pylori*, 3 evidenced rare organisms in occasional tissue sections using the 3 staining methods. For these outlier cases, there were 18 observations for each stain (3 tissue sections × 2 independent reviews × 3 cases). Organisms were noted in 4 of 18 observations for the Wright stain, 9 of 18 observations for the AYTB stain, and 5 of 18 observations for the IHC stain. Although the AYTB method did allow for a greater percentage of organism identification in these select cases, all evaluators reviewed all sections after the identities were unblinded and the authors agree that those results are likely spurious because corresponding tissue sections on each stain demonstrated rare to no organisms. Although the authors did not have access to patient records, they suggest that these 3 cases likely represent recently treated *H pylori*-positive patients due to the rare organisms identified. It is unlikely that the infections represent new ones due to the marked chronic inflammation present. The remaining 34 (91.9%) of 37 patients positive for *H pylori* exhibited undisputed positivity in all 3 stomach regions, suggesting that the entire greater curvature of the stomach was colonized rather than only the lesser curvature or antrum. Other studies suggest that the upper body greater curvature is the best biopsy site to detect *H pylori* when other pathological processes, including atrophic gastritis, intestinal metaplasia, gastric ulcers, or adenocarcinoma, are present due to displacement of *H pylori*.[34,35]

Presurgical eradication of *H pylori* in LSG samples may not be necessary, as *H pylori* was not linked to postoperative complications, including staple line leak or hemorrhage.[18,20,22,25,32] Additionally, the resected specimen provides ample tissue for *H pylori* evaluation, allowing for diagnosis and treatment following LSG surgery. Moreover, most colonized stomach tissue is removed by surgery,[26] and 1 study determined that a high percentage of untreated patients undergoing LSG were negative for *H pylori* 3 months later, presumably due to the removal of all infected tissues.[31]

Conclusion

With most of the world infected with *H pylori*, the leading cause of gastric cancer, the requirement for reliable detection of infection is needed to ensure eradication. Although histochemical techniques including Wright and AYTB are fast and inexpensive, the most sensitive method for detecting *H pylori* histologically is IHC.

Acknowledgments

We thank the University of Tennessee Health Sciences Library Interlibrary Loan Staff, Wanda Booker-Wade, Paul Gahn, and Carolyn Polk for their assistance in procuring the required reference materials for our studies. We also thank the managers and histology scientists at Doctors Anatomic Pathology Services, St Bernards Healthcare, Methodist Le Bonheur Healthcare, Idexx, St Jude Children's Research Hospital, and University of Tennessee DermPath laboratory for their ongoing support of the histotechnology curriculum at the University of Tennessee Health Science Center.

Conflict of Interest Disclosure

The authors have nothing to disclose.

REFERENCES

1. Hooi J, Lai W, Ng W, Suen M. Global prevalence of *Helicobacter pylori* infection: systematic review and meta-analysis. *Gastroenterology.* 2017;153:420-429.
2. Lee J, Kim N. Diagnosis of *Helicobacter pylori* by invasive test: histology. *Ann Transl Med*. 2015;3(1):10.
3. White J, Winter J, Robinson K. Differential inflammatory response to *Helicobacter pylori* infection: etiology and clinical outcomes. *J Inflamm Res*. 2015;8:137-147.
4. World Health Organization. https://www.who.int/news-room/fact-sheets/detail/cancer. Accessed February 2023.
5. Goh K, Chan W, Shiota S, Yamaoka Y. Epidemiology of *Helicobacter pylori* infection and public health implications. *Helicobacter.* 2011;16(suppl 1):1-9. doi:10.1111/j.1523-5378.2011.00874.x
6. Suerbaum S, Michetti P. *Helicobacter pylori* infection. *N Engl J Med.* 2002;347(15):1175-1186. doi:10.1056/NEJMra020542
7. Gravina AG, Zagari RM, De Musis C, Romano L, Loguercio C, Romano M. *Helicobacter pylori* and extragastric diseases: a review. *World J Gastroenterol.* 2018;24(29):3204-3221. doi:10.3748/wjg.v24.i29.3204
8. Rowland M, Clyne M, Daly L, et al. Long-term follow-up of the incidence of *Helicobacter pylori*. *Clin Microbiol Infect.* 2018;24:980-984.
9. Ailloud F, Estibariz I, Suerbaum S. Evolved to vary: genome and epigenome variation in the human pathogen *Helicobacter pylori*. *FEMS Microbiol Rev.* 2021;45(1):fuaa042. doi:10.1093/femsre/fuaa042
10. Nagaraja V, Eslick GD. Evidence-based assessment of proton-pump inhibitors in *Helicobacter pylori* eradication: a systematic review. *World J Gastroenterol.* 2014;20(40):14527-14536. doi:10.3748/wjg.v20.i40.14527
11. Xue Y, Zhou L, Lu H, Liu J. Recurrence of *Helicobacter pylori* infection: incidence and influential factors. *Chin Med J (Engl).* 2019;132(7):765-771. doi:10.1097/cm9.0000000000000146
12. Farhadkhani M, Nikaeen M, Hassanzadeh A, Nikmanesh B. Potential transmission sources of *Helicobacter pylori* infection: detection of *H. pylori* in various environmental samples. *J Environ Health Sci Eng*. 2019;17(1):129-134. doi:10.1007/s40201-018-00333-y
13. Pataro AL, Cortelli SC, Abreu MH, et al. Frequency of periodontal pathogens and *Helicobacter pylori* in the mouths and stomachs of obese individuals submitted to bariatric surgery: a cross-sectional study. *J Appl Oral Sci*. 2016 May-Jun;24(3):229-238. doi:10.1590/1678-775720150534
14. Pintar T, Kaliterna N, Carli T. The need for a patient-tailored *Helicobacter pylori* eradication protocol prior to bariatric surgery. *J Int Med Res.* 2018;46(7):2696-2707. doi:10.1177/0300060518769543
15. Almazeedi S, Al-Sabah S, Al-Mulla A, et al. Gastric histopathologies in patients undergoing laparascopic sleeve gastrectomies. *Obes Surg.* 2013;23(3):314-319. doi:10.1007/s11695-012-0821-y
16. Ohanessian S, Rogers A, Karamchandani D. Spectrum of gastric histopathologies in severely obese American patients undergoing sleeve gastrectomy. *Obes Surg.* 2016;26:595-602.
17. Canil A, Iossa A, Termine P, Caporilli D, Petrozza V. Histopathology findings in patients undergoing laparoscopic sleeve gastrectomy. *Obes Surg.* 2018;28:1760-1765.
18. DiPalma A, Alhabdan S, Maeda A, et al. Preoperative *Helicobacter pylori* screening and treatment in patients undergoing laparascopic sleeve gastrectomy. *Obes Surg.* 2020;30:2816-2820.
19. Abeid A, Abeid SA, Nizri E, Kuriansky J, Lahat G, Dayan D. The association of *Helicobacter pylori*, eradication, and early complications of laparoscopic sleeve gastrectomy. *Obes Surg.* 2022;32(5):1617-1623. doi:10.1007/s11695-022-05996-z
20. Lauti M, Gormack S, Thomas J, Morrow J, Rahman H, MacCormick A. What does the excised stomach from sleeve gastrectomy tell us? *Obes Surg.* 2016;26:839-842.
21. Raess P, Baird-Howell M, Aggarwal R, Williams N, Furth E. Vertical sleeve gastrectomy specimens have a high prevalence of unexpected histopathologic findings requiring additional clinical management. *Surg Obes Relat Dis.* 2015;11:1020-1024.
22. AbdullGaffar B, Raman L, Khamas A, AlBadri F. Should we abandon routine microscopic examination in bariatric sleeve gastrectomy specimens? *Obes Surg.* 2016;26(1):105-110. doi:10.1007/s11695-015-1726-3
23. Turan G, Kocaöz S. *Helicobacter pylori* infection prevalence and histopathologic findings in laparoscopic sleeve gastrectomy. *Obes Surg.* 2019;29(11):3674-3679. doi:10.1007/s11695-019-04052-7
24. Sabbah N, Saoud C, Deeb M, Nasser S. *Helicobacter pylori* prevalence in laparoscopic sleeve gastrectomy specimen. *Gastroenterol Res Pract.* 2020:8843696. doi:10.1155/2020/8843696
25. Shanti H, Almajali N, Al-Shamaileh T, Samarah W, Mismar A, Obeidat F. *Helicobacter pylori* does not affect postoperative outcomes after sleeve gastrectomy. *Obes Surg.* 2017;27(5):1298-1301. doi:10.1007/s11695-016-2470-z
26. Hansen S, Pottorf B, Hollis H, Rogers J, Husain F. Is it necessary to perform full pathologic review of all gastric remnants following sleeve gastrectomy? *Am J Surg*. 2017;214(6):1151-1155. doi:10.1016/j.amjsurg.2017.06.029
27. Safaan T, Bashah M, Ansari W, Karam M. Histopathological changes in laparoscopic sleeve gastrectomy specimens: prevalence, risk factors, and value of routine histopathologic examination. *Obes Surg.* 2017;27:1741-1749.
28. Gonzalez-Heredia R, Tirado V, Patel N, Masrur M, Murphey M, Elli E. Is *Helicobacter pylori* associated with an increased complication rate after sleeve gastrectomy? *Bariatr Surg Pract Patient Care.* 2015;10(1):15-18. doi:10.1089/bari.2014.0045
29. Kopach P, Genega E, Shah S, Kim J, Suarez Y. The significance of histologic examination of gastrectomy specimens: a clinicopathologic study of 511 cases. *Surg Obes Relat Dis.* 2017;13:463-467.
30. Clapp B. Histopathologic findings in the resected specimen of a sleeve gastrectomy. *J Soc Laparoendosc Surg.* 2015;19(1):e2013.00259. doi:10.4293/JSLS.2013.00259
31. Keren D, Matter I, Rainis T, Goldstein O, Stermer E, Lavy A. Sleeve gastrectomy leads to *Helicobacter pylori* eradication. *Obes Surg.* 2009;19(6):751-756. doi:10.1007/s11695-008-9694-5
32. Albawardi A, Almarzooqi S, Torab F. *Helicobacter pylori* in sleeve gastrectomies: prevalence and rate of complications. *Int J Clin Exp Med.* 2013;6(2):140-143.
33. Ashton-Key M, Diss TC, Isaacson PG. Detection of *Helicobacter pylori* in gastric biopsy and resection specimens. *J Clin Pathol.* 1996;49(2):107-111. doi:10.1136/jcp.49.2.107
34. Kim CG, Choi IJ, Lee JY, et al. Biopsy site for detecting *Helicobacter pylori* infection in patients with gastric cancer. *J Gastroenterol Hepatol.* 2009;24(3):469-474. doi:10.1111/j.1440-1746.2008.05679.x
35. Enomoto H, Watanabe H, Nishikura K, Umezawa H, Asakura H. Topographic distribution of *Helicobacter pylori* in the resected stomach. *Eur J Gastroenterol Hepatol.* 1998;10(6):473-478. doi:10.1097/00042737-199806000-00007

CASE STUDY

A 6-year-old boy with an atypical liver neoplasm harboring a novel *RPS6KA3* variant

Daniel Bustamante, MD[1,2], *Jude Abadie, PhD*[1]

[1]Department of Pathology, Texas Tech University Health Sciences Center, El Paso, TX, [2]El Paso Children's Hospital, El Paso, TX. Corresponding author: jude.abadie@ttuhsc.edu

Key words: hepatocellular carcinoma, hepatoblastoma, *RPS6KA3* mutation, α-fetoprotein, analytical measurement range, hepatocellular malignant neoplasm not otherwise specified

Abbreviations: AMR, analytical measurement range; COG, Children's Oncology Group; HBL, hepatoblastoma; HCC, hepatocellular carcinoma; IHC, immunohistochemical; VAF, variant allele frequency; VUS, variant of unknown significance; HEMNOS, hepatocellular malignant neoplasm, not otherwise specified; RSK2, ribosomal S6 protein kinase-2

Laboratory Medicine 2024;55:391-393; https://doi.org/10.1093/labmed/lmad061

ABSTRACT

Pediatric hepatoblastoma (HBL) and hepatocellular carcinoma (HCC) are primary liver malignant neoplasms with 5-year event-free survival of >80% and <30%, respectively. In these patients, α-fetoprotein levels can guide surgical intervention and monitor disease progression. Although histology and immunohistochemical stains support diagnosis, genetic testing can elucidate mechanisms that drive pathogenesis. Pediatric HBL and HCC harbor well-characterized molecular signatures such as alterations in *CTNNB1*, *TERT*, and *AXIN1* that alter the Wnt/β-catenin pathway. Approximately 8% of individuals with HCC harbor *RPS6KA3* variants that appear with other gene mutations. Herein, we report a novel solitary pathogenic *RPS6KA3* variant finding in a 6-year-old boy whose final diagnosis was hepatocellular malignant neoplasm, not otherwise specified.

Clinical History

A 6-year-old boy, with 5 biological siblings and no significant personal or familial medical history, presented to the emergency department with onset of intermittent fevers and abdominal pain. A distended, tender abdomen was noted on examination. **FIGURE 1** illustrates a large (143.8 mm × 134.4 mm) lobulated liver mass on abdominal computed tomographic scan, suggestive of a primary malignant hepatic tumor. On admission, α-fetoprotein (AFP) results were recorded as being >52,000 ng/mL. An exact level was not obtained at that time because 52,000 ng/mL was equal to the analytical measurement range (AMR) of the laboratory, and the test was not validated for higher levels. An exact numerical AFP level was requested to support clinical management and for enrollment into a Children's Oncology Group (COG) protocol.

The preliminary diagnosis of hepatoblastoma (HBL) vs hepatocellular carcinoma (HCC) was more suspected when a reference laboratory, with a validated AMR for AFP as high as 900,000 ng/mL, reported a value >900,000 ng/mL (reference range, <10 ng/mL). AFP levels in patients with HCC typically do not reach the extremely elevated levels that are more common in HBL cases. One week after a difficult partial surgical resection, the AFP of the case patient decreased to 625,090 ng/mL, and then, 1 month after additional chemotherapy, to 2,400 ng/mL. No additional AFP levels were determined.

FIGURE 2 illustrates histologic findings from image-guided needle biopsies, revealing focal areas of immature-appearing hepatocytes arranged in sheets, nests, and acinar configurations. Extensive necrosis was present on a background of normal-appearing liver parenchyma. Immunohistochemical (IHC) stains demonstrated positivity for AFP and HepPar-1 (not shown). Although HepPar-1 antibodies can yield positive results in HBL, these markers are more sensitive and specific for HCC. IHC also tested positive for expression of β-catenin, a regulator of cell-to-cell adhesion and embryogenesis (**FIGURE 2A**), which is more consistent with HBL than HCC. The absence of reticulin fibers (**FIGURE 2B**) is consistent with HBL or HCC.

These morphologic findings, in conjunction with extremely elevated AFP, all supported the initial diagnosis of HBL. However, to mitigate the HepPar-1 findings, a pediatrics transplant facility provided a secondary pathology review, for which the report stated an unexpected diagnosis of HCC.

Molecular testing results were received after the aforementioned histology interpretation was reported. Next-generation sequencing (NGS), which surveyed almost 200 somatic genes, revealed a novel, truncating, likely pathogenic *RPS6KA3* variant (c.1530_1536del; p.F510L*fs*12*) on the X chromosome (ChrX:20185773-hg19; coverage = 233; variant allele frequency [VAF] = 62%). A *STAT5B* (c.637G>T; p.A213S) missense variant of unknown significance (VUS) was also reported (Chr17:40371774 NM_012448.3; coverage = 401; VAF = 22%). No other mutations were reported in the NGS panel, including variants in *CTNNB1*, *TERT*, or *AXIN1* known to harbor somatic mutations that occur in conjunction with *RPS6KA3* pathogenic variants in other cases of pediatric hepatic neoplasms.[1]

Molecular testing results were evaluated in the context of the tumor grade, which exceeded that of HBL, thus confirming the histologic absence of fetal and embryonal HBL. A further amendment to the diagnosis was made in conjunction with the consulting pathologist group. The revised final diagnosis was hepatocellular malignant neoplasm, not otherwise specified (HEMNOS). Consultation with the hematology-oncology service supported continuation of the COG protocol.

FIGURE 1. Computed tomography image showing dimensions (143.8 mm × 134.4 mm) of a large mass occupying most of the liver parenchyma, predominately in the right lobe, with extension into the caudate segment.

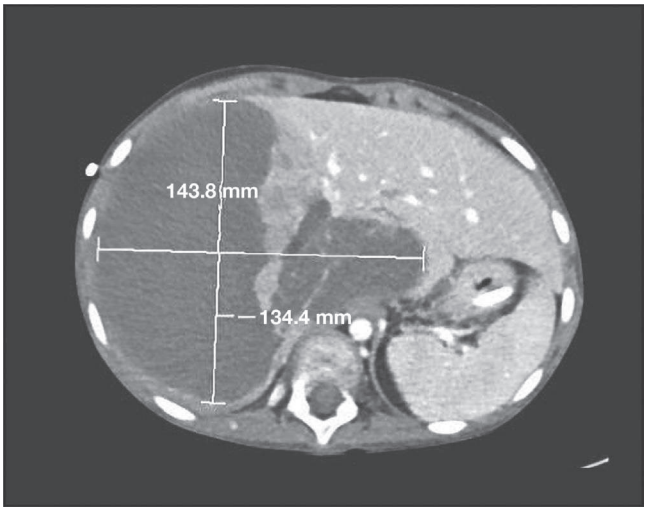

Discussion

AFP is used as a tumor marker to guide surgical intervention and monitor disease progression in pediatric patients with primary HBL and HCC. The 3-year and 5-year event-free survival rates in children with these tumors are >80% (HBL) and <30% (HCC).[1,2] Genetic testing can elucidate mechanisms driving pathogenesis in support of histology and IHC findings. *CTNNB1*, *TERT*, and *AXIN1* mutations altering the Wnt/β–catenin pathway are well-characterized and frequently occur in pediatric HBL and HCC cases.[3] Fewer than 10% of HCC cases harbor *RPS6KA3* variants that co-present with variants in the aforementioned genes.[3]

We report a novel, solitary *RPS6KA3* variant in a 6-year-old boy whose final diagnosis was HEMNOS after initially being diagnosed with HBL and subsequently with HCC. HEMNOS is a more recently described tumor associated with higher levels of AFP than HCC and which has complex histologic features shared between HBL and HCC.[4]

HBL usually affects pediatric populations between ages 6 months and 4 years. However, pediatric HCC mainly (~87%) affects older children and adolescents, with <15% affecting those younger than 5 years.[5] Primary pediatric hepatic cancer is rare, representing <2% of all pediatric cancers, and has a worldwide incidence of 2.3:1,000,000 in children and adolescents younger than 15 years old.[6]

HBL represents >70% of pediatric primary hepatic neoplasms, and HCC is more common than HBL in pediatric patients older than 10 years.[6] HBL rarely occurs in children older than 4 years, and HCC rarely occurs in children younger than 5 years. However, AFP levels, unlike in this case, are typically lower in HCC than HBL, with HCC having a poorer prognosis. HEMNOS is characterized as having high-risk clinical profiles but relatively favorable outcomes after chemotherapy and complete surgical resection.

A HEMNOS diagnosis is reserved for pediatric HCC tumors demonstrating varying morphologic characteristics and complex

FIGURE 2. Histologic findings. A, Trabecular pattern with cellular pleomorphism, nuclear vacuoles/inclusions, and numerous mitotic figures (×100). Epithelial neoplastic cells with hyperchromatic nuclei show higher nuclear-cytoplasmic ratios and exhibit eosinophilic and finely granular cytoplasm. B, Infiltrative neoplastic cells staining positive for β-catenin. Activated β-catenin normally drives cell-cycle progression and hepatic regeneration. Aberrant expression is associated with hepatoblastoma (HBL). C, Neoplastic population of cells testing positive for HepPar1, a monoclonal antibody that recognizes mitochondrial antigens of hepatocytes (this stain confirms hepatic origin). D, Reticulin staining that illustrates intact reticulin fibers between normal hepatocyte plates (left) but which is absent in neoplastic populations (right). The loss of reticulin staining in hepatic tissue supports a diagnosis of hepatocellular carcinoma; however, it does not differentiate it from HBL with a similar infiltrative pattern.

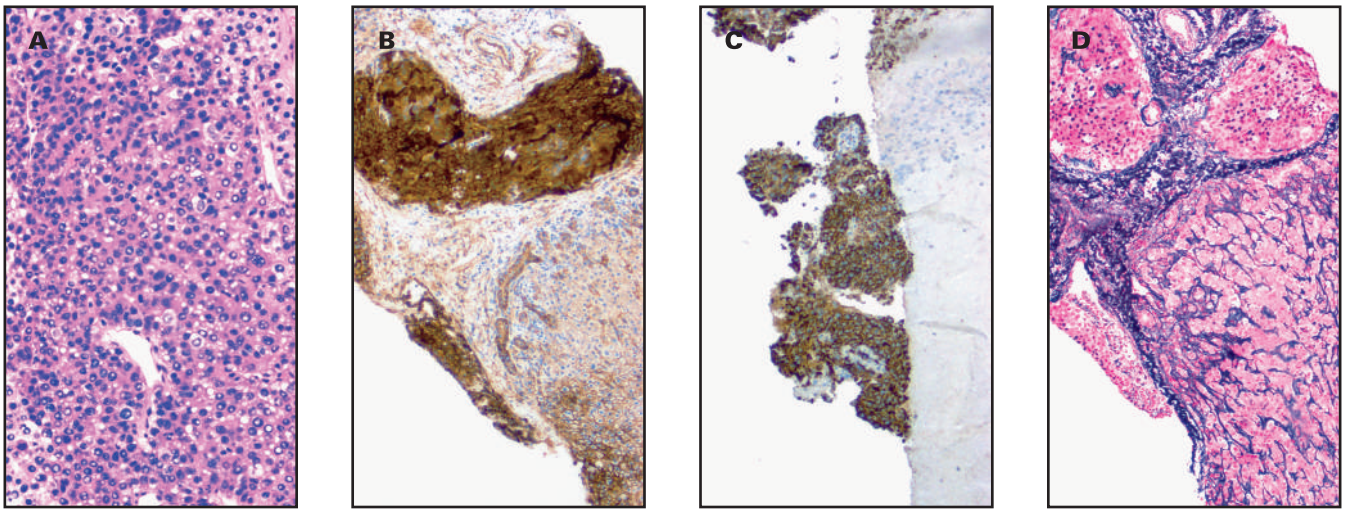

2024;55:391-393 | https://doi.org/10.1093/labmed/lmad061

histology consistent with HBL and HCC.[7] Although not a consideration in this case, HBL tumors occurring after chemotherapy can present with pleomorphic and anaplastic histology features similar to HCC.[5] To our knowledge, whether those tumors are HBL with HCC histologic morphology due to chemotherapeutic changes, HBLs with clonal progression, or HEMNOS has not been elucidated in the literature.

Because the canonical Wnt pathway can be activated in the absence of *CTNNB1* mutations, alterations of signaling pathways (eg, MAPK) and other gene variants (eg, *AXIN1*) have been implicated in β-catenin accumulation in hepatic tumorigenesis.[8] Nuclear positivity for β-catenin is not typical in HCC tumors, especially with markedly elevated levels of AFP. Further, *RPS6KA3* pathogenic variants have been described in approximately 8% of cases of HCC, HBL, and in HEMNOS, as observed in this case. However, they are usually found in conjunction with somatic gene mutations such as *AXIN1* and *CTNNB1*.[9] Other cases of HEMNOS should be evaluated for solitary *RPS6KA3*-truncating variants that may be associated with an aggressive clinical course. *RPS6KA3* encodes ribosomal S6 protein kinase-2 (RSK2) of the Ras/MAPK signaling pathway that is integral to cell proliferation, differentiation, and apoptosis.[9] Novel *RPS6KA3* variants inactivate RSK2; this novel frameshift mutation may be the molecular mechanism driving Wnt/β-catenin pathway alterations in the pathogenesis of this particular instance of HEMNOS.

AFP is a tumor marker that should be accurately measured to help differentiate diagnoses, guide therapy, and provide prognostic information among different hepatic cancers. This 70-kDa oncofetal glycoprotein is normally synthesized by the fetal liver and yolk sac, has considerable homology to albumin, and can be tested to diagnose and monitor HBL, HCC, and germ cell tumors.[1] When evaluated after liver resection or transplant, continuous elevated AFP levels often reflect a poor prognosis. Complete resection with adjuvant chemotherapy corresponds with significant AFP reduction and >80% survival rates in pediatric HBL cases.[10] However, irrespective of aggressive chemotherapy, 12-month survival rates are poor after resection of pediatric HCC tumors, especially when AFP levels are minimally decreased.

Laboratory Role in Diagnosis

In our case, AFP levels significantly decreased after partial resection and subsequent chemotherapy; however, the disease course remained aggressive. In cases when larger HCC tumors are difficult to completely resect, vascular chemoembolization may target micrometastases within liver parenchyma. Subsequently, recurrence monitoring can leverage molecular testing such as reverse transcription polymerase chain reaction to amplify mRNA from AFP production if micrometastatic lesions are present.[10]

Initial linearity validation studies for tumor markers such as AFP, whose levels can be extraordinarily elevated in various cancers, must be performed/established so that extended ranges can be reported for optimal patient management. When laboratories encounter tumor-marker specimens with AMRs higher than established levels, validation efforts should be conducted to extend AMRs for testing subsequent patient specimens.

It is essential to accurately interpret histology and IHC stains in the diagnosis of hepatocellular malignancies because overlapping morphology and staining characteristics may lead to an incorrect preliminary diagnosis and prognosis. Further, exploring genetic somatic variants in pediatric liver neoplasms may elucidate molecular signatures that can guide initial accurate identification of HBL, HCC, and HEMNOS. *RPS6KA3* variants, such as identified in this case, inactivate *RSK2*, which could be an important driver mutation in altering molecular mechanisms in the Wnt/β-catenin pathway, promoting the pathogenesis of HEMNOS.

Patient Follow-up

The patient had a 3.5-month hospitalization period after initial presentation, and he died 6.5 months after discharge (10.0 months after initial presentation). The case outcome would have remained unchanged if the nature of the *RPSK6A3* variant in the context of an HEMNOS diagnosis were initially identified. However, perhaps a quicker diagnosis of HEMNOS would have better facilitated patient management.

Conflict of Interest Disclosure

The authors have nothing to disclose.

REFERENCES

1. Haines K, Sarabia FS, Alvarez KR, et al. Characterization of pediatric hepatocellular carcinoma reveals genomic heterogeneity and diverse signaling pathway activation. *Pediatric Blood Cancer*. 2019;66(7):27745-27755.
2. Murawski M, Weeda VB, Maibach R, et al. Hepatocellular carcinoma in children: does modified platinum- and doxorubicin-based chemotherapy increase tumor resectability and change outcome? lessons learned from the SIOPEL 2 and 3 studies. *J Clin Oncol.* 2016;34(10):1050-1056. doi:10.1200/JCO.2014.60.2250
3. Khemlina G, Ikeda S, Kurzrock R. The biology of hepatocellular carcinoma: implications for genomic and immune therapies. *Mol Cancer.* 2017;3016(1):149. doi:10.1186/s12943-017-0712-x
4. Zhou S, Venkatramani R, Gupta S, et al. Hepatocellular malignant neoplasm, NOS: a clinicopathological study of 11 cases from a single institution. *Histopathology.* 2017;71(5):813-822. doi:10.1111/his.13297
5. Digiacomo G, Serra RP, Turrini E, et al. State of the art and perspectives in pediatric hepatocellular carcinoma. *Biochem Pharmacol.* 2023;207:115373-115373. doi:10.1016/j.bcp.2022.115373
6. Di Giuseppe G, Youlden DR, Aitken JF, Pole JD. Pediatric hepatic cancer incidence and survival: 30-year trends in Ontario, Canada; the United States; and Australia. *Cancer.* 2021;127(5):769-776.
7. Khanna R, Verma SK. Pediatric hepatocellular carcinoma. *World J Gastroenterol.* 2018;24(35):3980-3999. doi:10.3748/wjg.v24.i35.3980
8. Gao C, Wang Y, Broaddus R, Sun L, Xue F, Zhang W. Exon 3 mutations of *CTNNB1* drive tumorigenesis: a review. *Oncotarget*. 2017;9(4):5492-5508. doi:10.18632/oncotarget.23695
9. Johnston ME, Timchenko N. Molecular signatures of aggressive pediatric liver cancer. *Arch Stem Cell Ther*. 2021;2(1):1-4.
10. Minata M, Nishida N, Komeda T, et al. Postoperative detection of α-fetoprotein mRNA in blood as a predictor for metastatic recurrence of hepatocellular carcinoma. *J Gastroenterol Hepatol.* 2001;16(4):445-451. doi:10.1046/j.1440-1746.2001.02461.x

CORRECTION

Correction to: Diagnostic value of pleural effusion Krebs von den Lungen-6 in malignant pleural effusion of patients with non–small cell lung cancer

This is a correction to: Junjun Wang, Liqun Ling, Shuhui Chen, Lunan Chou, Yumin Wang, Lijuan Hu, Diagnostic value of pleural effusion Krebs von den Lungen-6 in malignant pleural effusion of patients with non–small cell lung cancer, *Laboratory Medicine*, 2023, lmad076, https://doi.org/10.1093/labmed/lmad076

In the originally published version of this manuscript, the corresponding author was identified as Junjun Wang (wym0577@163.com). The correct corresponding author is Lijuan Hu (hljsonya2012@163.com).

This error has been corrected online.